U.PORTO

DOUTORAMENTO

PROGRAMA GRADUADO EM ÁREAS DE BIOLOGIA BÁSICA E APLICADA

Epithelial Organization at Mitotic Exit

Mariana Osswald

D

2020

U.PORTO

Mariana Osswald. Epithelial Organization at Mitotic Exit

Epithelial Organization at Mitotic Exit

Mariana Osswald

D.ICBAS **2020**

SEDE ADMINISTRATIVA

INSTITUTO DE CIÊNCIAS BIOMÉDICAS ABEL SALAZAR

FACULDADE DE CIÊNCIAS

FACULDADE DE MEDICINA

MARIANA COSTA OSSWALD

EPITHELIAL ORGANIZATION AT MITOTIC EXIT

Tese de Candidatura ao grau de Doutor em Biologia Básica e Aplicada, apresentada aos Instituto de Ciências Biomédicas de Abel Salazar, Faculdade de Ciências e Faculdade de Medicina da Universidade do Porto.

Orientador – Doutor Eurico Morais de Sá
Categoria – Investigador Principal
Afiliação – Instituto de Investigação e Inovação em Saúde (i3S) da Universidade do Porto; Instituto de Biologia Molecular e Celular (IBMC) da Universidade do Porto

Coorientador – Professor Doutor Claudio Sunkel
Categoria – Professor Catedrático
Afiliação – Instituto de Ciências Biomédicas de Abel Salazar (ICBAS) da Universidade do Porto; Instituto de Investigação e Inovação em Saúde (i3S) da Universidade do Porto; Instituto de Biologia Molecular e Celular (IBMC) da Universidade do Porto

The work presented in this thesis was performed at the Epithelial Polarity and Cell Division (EPCD) group at the Institute for Research and Innovation in Health (i3S/IBMC) at the University of Porto under the supervision of Dr. Eurico Morais de Sá and the co-supervision of Prof. Claudio Sunkel.





Mariana Osswald was awarded a PhD fellowship (PD/BD/105746/2014) by the Graduate Program in Areas of Basic and Applied Biology (GABBA), a doctoral program from the Institute of Biomedical Sciences Abel Salazar (ICBAS), Faculty of Sciences (FCUP) and Faculty of Medicine (FMUP) from the University of Porto. This fellowship was funded by the Portuguese Foundation for Science and Technology (FCT). The research presented in this thesis was supported by a grant from the Portuguese Foundation for Science and Technology (FCT; PTDC/BEX-BCM/0432/2014) and a grant from NORTE2020 – Programa Operacional Regional do Norte (NORTE-01-0145-FEDER-000029).







ABSTRACT

Epithelial architecture relies on the apical-basal polarity machinery to create functionally distinct cortical domains to sustain essential epithelial functions. At the cellular level, polarity regulators distribute themselves asymmetrically into apical and basolateral plasma membrane domains to polarize epithelial cells and position cell-cell adhesive junctions. This machinery is critical to ensure epithelial integrity and, accordingly, loss of apical-basal polarity is known to disrupt epithelial architecture and is associated with developmental failure and disease. However, polarity proteins engage in a complex network of interactions so intricately connected to epithelial architecture, that it is generally difficult to interpret loss of function architecture phenotypes and ascribe them to a single specific cause. Furthermore, loss of polarity damages epithelia to such an extent that it obscures whether and how polarity proteins contribute to dynamic events in epithelia, such as cell division.

In this work, I explored optogenetic tools to inactivate apical-basal polarity acutely and address how apical-basal polarity guards the architecture of a proliferative epithelium. To this end, I used LARIAT, a previously reported optogenetic tool to cluster, sequester and inactivate GFP-tagged proteins in the seconds to minute range. I adapted LARIAT to *Drosophila* S2 cultured cells, where I compared the clustering efficiency of LARIAT variants and targeted the mitotic kinase Mps1 and the basolateral determinant Lgl to validate that LARIAT can be used to study cell division and polarity. Co-clustering analysis of Par6 and aPKC further confirmed that LARIAT can be repurposed to detect protein-protein interactions *in vivo*. To study how apical-basal polarity preserves epithelial architecture in a proliferative epithelium, I screened for the ability of LARIAT to inactivate polarity proteins in the *Drosophila* follicular epithelium. LARIAT efficiently clustered and inactivated apical polarity determinant aPKC, reproducing known epithelial architecture defects: gaps and multilayering. Live imaging revealed that epithelial gaps form by detachment of dividing and neighbouring cells. Strikingly, this was not due to loss of apical-basal polarity but rather to an increase in apical myosin and apical constriction. Accordingly, artificial induction of apical constriction through optogenetic recruitment of RhoGEF2 was sufficient to trigger the formation of gaps in the follicular epithelium. These results suggest a new role for aPKC in protecting epithelial integrity during proliferation through downregulation of apical contractility and show that unchecked apical constriction challenges the integrity of proliferative epithelia.

Altogether, in this work, I implemented optogenetic clustering tools to control target proteins with high temporal control and revealed a new role for aPKC in preserving epithelial integrity during proliferation, which is essential for proper epithelial architecture.

RESUMO

A polaridade é uma propriedade essencial de epitélios que lhes permite manterem uma organização assimétrica e exercerem funções especializadas, tais como absorção ou secreção. Esta assimetria é estabelecida por um conjunto conservado de proteínas de polaridade que se distribuem ao longo do eixo apical-basal para criar os domínios apical e basolateral e posicionar as adesões celulares que mantém a integridade dos epitélios. Por conseguinte, a perda de proteínas de polaridade leva ao aparecimento de falhas na organização epitelial que estão associadas a defeitos no desenvolvimento ou doença. No entanto, as proteínas de polaridade formam uma rede de interações com ligações complexas à organização epitelial, o que dificulta a compreensão das causas específicas que levam à perda de organização do tecido após perda de polaridade. Acresce ainda que os defeitos na organização epitelial causados pela perda de polaridade são de tal ordem, que dificultam a análise do contributo de proteínas de polaridade para eventos dinâmicos em epitélios, tais como divisão celular.

Neste trabalho, explorei a utilização de ferramentas de optogenética como um modo de inativar polaridade apical-basal de forma abrupta para estudar como é que a polaridade apical-basal mantém a organização de um epitélio proliferativo. Para isso, utilizei uma ferramenta de optogenética recente, chamada LARIAT, que permite agregar, sequestrar e inativar proteínas fundidas com GFP num curto espaço de tempo. Comecei por adaptar LARIAT para células S2 de *Drosophila* para comparar a capacidade de agregar de variantes de LARIAT. Em seguida, usei LARIAT para agregar a cinase mitótica Mps1 e a proteína de polaridade basolateral Lgl e, assim, validar que LARIAT pode ser utilizado para estudar mitose e polaridade. A análise da coagregação de Par6 e aPKC permitiu ainda verificar que é possível utilizar LARIAT para detetar interações entre proteínas *in vivo.* Para perceber como é que a polaridade apical-basal mantém a organização epitelial durante proliferação celular, comecei por testar se era possível inativar proteínas de polaridade específicas com LARIAT no epitélio folicular de *Drosophila.* A agregação da proteína de polaridade apical aPKC levou à sua inativação e aparecimento de defeitos na organização epitelial previamente associados à perda de aPKC: falhas de integridade e formação de massas desorganizadas de células. Uma análise temporal cuidada revelou que, após inativação de aPKC, a adesão entre células em divisão e células vizinhas falhava, levando à perda de integridade do epitélio. Surpreendentemente, este fenótipo não se deve à perda de polaridade apical-basal, mas sim a um aumento de miosina e constrição apicais. Uma vez que o aumento da contractilidade apical, através do recrutamento apical da RhoGEF2, se revelou suficiente para induzir falhas na integridade epitelial, estes resultados sugerem

que aPKC protege a integridade de epitélios através da diminuição da contractilidade apical e que constrição apical excessiva pode causar perda de integridade em epitélios proliferativos.

Em conclusão, durante esta tese, implementei ferramentas de optogenética para controlar a atividade de proteínas com elevada precisão temporal e descobri um novo papel para aPKC essencial para a integridade epitelial durante a divisão celular, e por conseguinte para preservar a organização epitelial.

AGRADECIMENTOS/ACKNOWLEDGEMENTS

Esta etapa não teria sido possível sem as muitas pessoas que me rodeiam e a quem, por isso, quero agradecer.

Ao Eurico, por ter aceitado ser meu orientador, pelo projecto espectacular que propôs, pelos desafios, pelas discussões científicas infindáveis que se seguiram, pelo tanto que aprendi, pelo entusiasmo e pela paciência, pela disponibilidade para *flights of imagination* (e não só) e pela ajuda com a aterragem (parafraseando a Professora Maria de Sousa), pelo encorajamento e pela confiança e por tantas outras coisas que ficam por agradecer.

Ao (Professor) Claudio, pelas fantásticas aulas de Biologia Molecular, que estão na origem de tudo o que se seguiu; por me ter recebido no melhor laboratório que conheço e onde vi a minha primeira divisão celular; pela cossupervisão e pela disponibilidade, pela curiosidade científica e pelo pragmatismo, pela confiança depositada e pela constante preocupação.

A todos os elementos do EPCD e do CDGS, presentes e passados, porque são eles que fazem o melhor laboratório; pelas muitas gargalhadas, pelas muitas conversas (científicas ou não), pela disponibilidade para ajudar, pela preocupação, por todas as atenções, por serem o *Happy Lab*.

Às muitas pessoas que marcaram a minha vida nestes anos, que se interessaram pelo meu percurso e que me ajudaram a crescer.

Aos meu amigos, por me terem ajudado a manter algum equilíbrio, pelos jantares, pelos jogos, pelas conversas mais profundas (e pelas menos profundas), por terem torcido por mim, por terem puxado por mim.

A toda a minha família, Osswalds, Costas e Condes, pela presença, pelo interesse, pelas perguntas, pelo apoio, pelos conselhos... pelas refeições.

Aos meus pais e aos meus irmãos, pela confiança inabalável, pela estabilidade, pela compreensão dos atrasos e ausências, por todo o incentivo e ajuda, por estarem sempre disponíveis, por se interessarem pelo estudo da mosca.

Ao Carlos, por estar sempre disponível, tanto na ciência como fora dela; por partilhar comigo os momentos altos e baixos, por me conhecer, pelo apoio incondicional, pelo entusiasmo e gosto pela ciência que são um exemplo para mim, pelas discussões científicas sempre estimulantes, por ser uma fonte de inspiração e força, pelos conselhos,

pelo optimismo e alegria contagiantes, pelos passeios, pelas músicas, pelos lanches, pelo muito que fica por dizer.

PREFACE AND LIST OF PUBLICATIONS

Most of the adventures recorded in this book really occurred; one or two were experiences of my own, the rest those of boys who were schoolmates of mine.

Mark Twain (1876), preface to *The Adventures of Tom Sawyer,* Hartford, CT: American Publishing Co.

All the adventures recorded here really occurred. While several were experiences of my own, some were not and, therefore, besides my supervisor Eurico Morais de Sá and my co-supervisor Claudio Sunkel, I must also thank Filipa Santos, André Carvalho and Ana Maria Carmo for their direct contribution to specific parts of the work; Nicolas Loyer and Jens Januschke for the work in the neuroepithelium; and Patrícia Grácio and Catarina Homem for the work in the neuroblast.

The main topic of this thesis is the coordination of epithelial apical-basal polarity with cell division to ensure the maintenance of epithelial tissue integrity. This thesis gathers relevant published and unpublished manuscripts, to which I contributed significantly while working at the Institute for Research and Innovation in Health (i3S/IBMC). The included manuscripts are properly identified and contain an initial statement detailing my contribution to the research described.

The chapters with experimental results are preceded by a general introduction to epithelial organization, apical-basal polarity and cell division. This includes a publication on the interplay between polarity, adhesion and cell division in epithelia (1). The experimental work is presented in the form of two manuscripts included as self-contained chapters with a brief introduction followed by methods, results, discussion and conclusion sections. The first manuscript has been published (2) and the second is being prepared for submission (3). I close my thesis with a concluding chapter where I extend the discussion of my main findings and their impact on our understanding of epithelial biology and cell polarity. Additionally, within the scope of this thesis, I also contributed to other publications (4-6). A brief overview of my contribution to these works is appended to this thesis.

Publications included in the main body of this thesis:

(1) Osswald M., Morais-de-Sá E. (2019) Dealing with apical-basal polarity and intercellular junctions: a multidimensional challenge for epithelial cell

division. Current Opinion in Cell Biology 60:75-83. doi.org/10.1016/j.ceb.2019.04.006

(2) Osswald M., Santos A.F., Morais-de-Sá E. (2019) Light-induced protein clustering for optogenetic interference and protein interaction analysis in Drosophila S2 cells. Biomolecules 9(2):61. doi.org/10.3390/biom9020061

(3) Osswald M., Barros-Carvalho A., Carmo A.M., Loyer N., Grácio P.C., Sunkel C.E., Homem C.C., Januschke J., Morais-de-Sá E. aPKC downregulates apical contractility to maintain shape and cohesion in proliferative *Drosophila* epithelia. (*in preparation*)

Other publications to which I contributed within the scope of this thesis:

(4) Moreira S., Osswald M.*, Ventura G.*, Gonçalves M., Sunkel C.E., Morais-de-Sá E. (2019) PP1-mediated dephosphorylation of Lgl controls apical-basal polarity. Cell Reports 26(2):293-301. *Equal contributions. doi.org/10.1016/j.celrep.2018.12.060

(5) Ventura G., Moreira S., Barros-Carvalho A., Osswald M., Morais-de-Sá E. (2020) Lgl cortical dynamics are independent of binding to the Scrib-Dlg complex but require Dlg-dependent restriction of aPKC. Development 147:dev186593. doi.org/10.1242/dev.186593

(6) Zeng J., Santos A.F., Mukadam A., Osswald M., Luptak J., Jacques D., Dickson C., Renner N., Johnson C., Vaysburd M., McEwan W. A., Morais-de-Sá E., Clift D., James L.C. (2021) Target-induced clustering activates Trim-Away of pathogens and proteins. Nat Struct Mol Biol. 28(3):278-289. doi.org/10.1038/s41594-021-00560-2

TABLE OF CONTENTS

ABSTRACT ..... **v**

RESUMO ..... **vii**

AGRADECIMENTOS/ACKNOWLEDGEMENTS ..... **ix**

PREFACE AND LIST OF PUBLICATIONS ..... **xi**

LIST OF FIGURES ..... **xxvii**

LIST OF TABLES ..... **xixix**

LIST OF ABBREVIATIONS ..... **xxxi**

PART I - GENERAL INTRODUCTION **1**

Chapter 1 - Epithelial polarity, morphology and integrity **3**

Historical perspective on epithelia: discovery of one of the main types of animal tissue 7

General organization of epithelial cells 9

Apical domain 9

Lateral domain and cell-cell junctions 11

Basal domain 13

The actomyosin network 14

Actomyosin network assembly and internal organization 15

Role of Rho GTPases in actomyosin regulation 16

RhoGTPase regulation 19

Actomyosin contractility and apical constriction 21

Adherens Junctions 23

E-cadherin/α-catenin/β-catenin complex 23

E-cadherin organization at adherens junctions 25

Epithelial Apical-Basal polarity 27

Apical-basal polarity is essential for development and homeostasis in metazoa 28

Apical-basal polarity in epithelia 31
The Crumbs complex in polarity and apical domain assembly 32
Par complex localization and aPKC activation 36
aPKC is a positive regulator of Crumbs and excludes basolateral determinants 39
The Scribble module restricts apical domain assembly 41
Apical and basolateral polarity proteins restrict Par3 to direct adherens junction localization, assembly and regulation 43
Polarity proteins regulate adherens junctions tension, remodelling and recycling 45
Polarity proteins regulate cell and tissue morphogenesis through actomyosin 48
Concluding remarks 50

Chapter 2 - Dealing with apical-basal polarity and intercellular junctions: a multidimensional challenge for epithelial cell division 51
Abstract 53
Introduction 53
Remodeling of apical-basal polarity at mitotic entry 54
Dealing with intercellular contacts at mitotic exit 56
Asymmetric furrow ingression along the apical-basal axis 57
A multicellular balance of forces controls epithelial cohesion and patterning 58
Preservation of a permeability barrier 60
Apical-basal polarization at mitotic exit 61
Concluding remarks 64

Chapter 3 - Aims and outline of approach and results 67

PART II - EXPERIMENTAL WORK 73

Chapter 4 - Light-induced protein clustering for optogenetic interference and protein interaction analysis in Drosophila S2 cells 75
Abstract 77
Introduction 78
Materials and Methods 80
Molecular biology 80
S2 cell culture, transfection and imaging 82

Immunofluorescence 83
Image Analysis 84
Results and Discussion 84
Generation and characterization of heat shock-inducible LARIAT modules in S2 cells 84
Interference with GFP-tagged proteins by optogenetic clustering 87
Analysis of protein-protein interactions via optogenetic co-clustering 91
Conclusions 92
Acknowledgments 93
Supplementary Material 93

Chapter 5 - aPKC downregulates apical contractility to maintain shape and cohesion in proliferative Drosophila epithelia 97
Abstract 100
Introduction 100
Materials and Methods 102
Drosophila genetics and stocks 102
Optogenetic experiments in the follicular epithelium 108
Fixation and stainings of egg chambers 109
Optogenetic experiment and immunofluorescence in neuroblasts 109
Imaging of fixed tissue 109
Live imaging 110
Protein extracts and Western blot 110
aPKC^{as4} allele inactivation 111
Quantifications, reproducibility and statistical analysis 111
Image preparation 115
Results 115
Optogenetic clustering inactivates aPKC with high temporal control 115
Acute aPKC inactivation leads to fast and stereotypical tissue disorganization 117
Cell division challenges tissue cohesion upon aPKC inhibition 119
Acute inactivation exposes the role of aPKC as a negative regulator of apical constriction 122
Balancing apicomedial actomyosin contractility in non-mitotic cells prevents excessive pulling forces on dividing cells 125
Persistent increase in apical contractility induces epithelial gaps 127
Discussion 129

Acknowledgments 132
Supplementary Material 133

Chapter 6 - General discussion and conclusion 139
Adaptation of optogenetic clustering tools for protein inactivation to Drosophila S2 cells 142
Optogenetic inactivation reveals that aPKC downregulates apical contractility to preserve epithelial integrity 144
Epithelial gaps form by detachment between dividing and neighbour cells..... 147
Cell division has to be coordinated with other force-generating events in epithelia 149
Mechanical constraints likely dictate the phenotypic outcome of aPKC inactivation 150
Conclusion 152

REFERENCES 153

APPENDIX 199
Contribution to additional publications 201
PP1-mediated dephosphorylation of Lgl controls apical-basal polarity..... 201
Lgl cortical dynamics are independent of binding to Dlg-Scrib complex but require Dlg dependent restriction of aPKC..... 203
Target-induced clustering activates Trim-Away of pathogens and proteins.. 206
References 207

LIST OF FIGURES

PART I – GENERAL INTRODUCTION

Chapter 1 – Epithelial polarity, morphology and integrity

Figure 1.1. Epithelial tissues can be classified according to cell shape, cell layers and the presence of specialized structures 8
Figure 1.2. Epithelial cells have distinct cortical domains and junctions organized along an apical-basal axis..... 10
Figure 1.3. Rho GTPases regulate actomyosin assembly and are, in turn, regulated by Rho GAPs and GEFs 19
Figure 1.4. Actomyosin pulses at the apical surface of epithelial cells lead to tissue folding. 22
Figure 1.5. E-cadherin/catenin complex. 24
Figure 1.6. E-cadherin complex organization at adherens junctions. 26
Figure 1.7. Apical-basal polarity in epithelial cells..... 33

Chapter 2 – Dealing with apical-basal polarity and intercellular junctions: a multidimensional challenge for epithelial cell division

Figure 2.1. Subcellular reorganization of apical-basal polarity regulators at mitotic entry in *Drosophila* epithelia.....55
Figure 2.2. Remodelling of adherens and occluding junctions during cell division. ... 59
Figure 2.3. Apical-basal polarization of epithelial cells at mitotic exit. 62

Chapter 3 – Aims and outline of approach and results

Figure 3.1. The *Drosophila* follicular epithelium. 71

PART II – EXPERIMENTAL WORK

Chapter 4 – Light-induced protein clustering for optogenetic interference and protein interaction analysis in Drosophila S2 cells

Figure 4.1.Schematic representation of LARIAT-mediated optogenetic clustering.... 79
Figure 4.2. Schematic representation of LARIAT plasmids for *Drosophila* S2 cells. . 81
Figure 4.3. A *Drosophila* S2 cell LARIAT toolbox. 85
Figure 4.4. LARIAT clusters do not affect bipolar spindle assembly and mitotic progression 88

Figure 4.5. GFP-Mps1 is efficiently trapped in LARIAT clusters. 89
Figure 4.6. High levels of LARIAT delocalize membrane-associated Lgl-GFP. 91
Figure 4.7. LARIAT detects aPKC and Par6 interaction in single cells 92
Supplementary Figure 4.S1. Laser intensity and LARIAT expression levels affect LARIAT clustering; related to Figure 4.4 94
Supplementary Figure 4.S2. Flag-tagged LARIAT clusters GFP; related to Figure 4.4. 95

Chapter 5 – aPKC downregulates apical contractility to maintain shape and cohesion in proliferative Drosophila epithelia

Figure 5.1. Optogenetic clustering inactivates aPKC and disrupts tissue architecture *in vivo* 116
Figure 5.2. aPKC inactivation leads to fast and stereotyped tissue disorganization in a proliferative epithelium 118
Figure 5.3. Cell division challenges tissue cohesion upon aPKC inactivation 121
Figure 5.4. aPKC inactivation induces apical constriction 123
Figure 5.5. Acute aPKC inhibition upregulates apical myosin II and contractility in different *Drosophila* epithelia 124
Figure 5.6. aPKC inactivation leads to excessive pulling forces on dividing cells 126
Figure 5.7. Increased apical contractility induces epithelial gaps 128
Supplementary Figure 5.S1; related to Figure 5.1. Optogenetic clustering disruptslocal release of aPKC substrates in the *Drosophila* follicular epithelium and neural stem cells 133
Supplementary Figure 5.S2; related to Figure 5.3. Cytokinesis completion is not required for tissue rupture upon aPKC inactivation 134
Supplementary Figure 5.S3; related to Figure 5.5. aPKC inhibition leads to increased apical myosin and tissue breaks in *Drosophila* epithelia 135

LIST OF TABLES

PART I – GENERAL INTRODUCTION

Chapter 1 – Epithelial polarity, morphology and integrity

Table 1 - 1. Polarity proteins in Drosophila and mammalian organisms..... 29

PART II – EXPERIMENTAL WORK

Chapter 4 – Light-induced protein clustering for optogenetic interference and protein interaction analysis in Drosophila S2 cells

Table 4 - 1. List of primers for molecular cloning. 82

Chapter 5 – aPKC downregulates apical contractility to maintain shape and cohesion in proliferative Drosophila epithelia

Table 5 - 1. List of *Drosophila melanogaster* transgenes and mutant alleles. 103

Table 5 - 2. Genotypes and light exposure details. 106

LIST OF ABBREVIATIONS

AJ	adherens junctions
aPKC	atypical protein kinase C
Baz	Bazooka
BH	basic and hydrophobic
CAM	cell adhesion molecule
CIB1	Cryptochrome-interacting bHLH
CIBN	CIB1 N-terminal
Crb	Crumbs
CRIB	Cdc42/Rac-interactive binding
CRY2	Cryptochrome 2
Dlg	Discs large
E-cad	Epithelial cadherin
EC	extracellular cadherin
ECM	extracellular matrix
EGF	epidermal growth-factor
ERM	Ezrin, Radixin and Moesin
GAP	GTPase activating protein
GDI	guanine nucleotide dissociation inhibitor
GEF	guanine nucleotide exchange factor
GUK	guanylate kinase
LAP	leucine-rich and PDZ
LARIAT	light-activated reversible inhibition by assembled trap
Lat A	Latrunculin A
Lgl	Lethal giant larvae
LmG	laminin-globular domain
LRR	leucine-rich repeats
ma	*macula adherens*
MAGUK	membrane-associated guanylate kinase
MP	multimerization protein
MPP5	multi-PDZ protein
MTOC	non-centrosomal microtubule-organizing center
Pals1	protein associatetd with lin seven-1
Par	partitioning defective

Patj	Pals1-associated tight junction protein
Pbl	Pebble
PDZ	PSD-95/Dlg/ZO-1
PHR	photolyase homology region
PI4P	phosphatidylinositol-(4)-phosphate
PIP_2	phosphatidylinositol-(4,5)-bisphosphate
PIP_3	phosphatidylinositol-(3,4,5)-trisphosphate
pmCIBN	plasma membrane anchored CIBN
PP1	protein phosphatase 1
PP2A	protein phosphatase 2A
RLC	myosin II regulatory light chain
S2	schneider 2
SAC	spindle assembly checkpoint
Scrib	Scribble
SH3	Src homology 3
Shg	shotgun
SJ	septate junctions
TAMP	tight junction-associated MARVEL protein
TJ	tight junctions
Trim21	Tripartite motif 21
tSJ	tricellular septate junctions
tTJ	tricellular tight junctions
Tum	Tumbleweed/RacGAP50C
V_HH	anti-GFP nanobody
WASP	Wiskott-Aldrich syndrome protein
WAVE	WASP verprolin homologous
za	*zonula adherens*
ZO	*zonula occludens*

PART I

GENERAL INTRODUCTION

CHAPTER 1

EPITHELIAL POLARITY, MORPHOLOGY AND INTEGRITY

Historical perspective on epithelia: discovery of one of the main types of animal tissue 7

General organization of epithelial cells 9

- Apical domain 9
- Lateral domain and cell-cell junctions 11
- Basal domain 13

The actomyosin network 14

- Actomyosin network assembly and internal organization 15
- Role of Rho GTPases in actomyosin regulation 16
- RhoGTPase regulation 19
- Actomyosin contractility and apical constriction 21

Adherens Junctions 23

- E-cadherin/α-catenin/β-catenin complex 23
- E-cadherin organization at adherens junctions 25

Epithelial apical-basal polarity 27

- Apical-basal polarity is essential for development and homeostasis in metazoa 28
- Apical-basal polarity in epithelia 31
- The Crumbs complex in polarity and apical domain assembly 32
- Par complex localization and aPKC activation 36
- aPKC is a positive regulator of Crumbs and excludes basolateral determinants 39
- The Scribble module restricts apical domain assembly 41
- Apical and basolateral polarity proteins restrict Par3 to direct adherens junction localization, assembly and regulation 43
- Polarity proteins regulate adherens junctions tension, remodelling and recycling 45
- Polarity proteins regulate cell and tissue morphogenesis through actomyosin 48

Concluding remarks 50

There are a lot of facts to be known in order to be a professional anything — lawyer, doctor, engineer, accountant, teacher. But with science there is one important difference. The facts serve mainly to access the ignorance… Scientists don't concentrate on what they know, which is considerable but minuscule, but rather on what they don't know… Science traffics in ignorance, cultivates it, and is driven by it. Mucking about in the unknown is an adventure.

Stuart Firestein (2012), *Ignorance: How it Drives Science*, Oxford University Press

At any given moment, inside the human body, a multitude of different biochemical reactions take place to sustain life. Nutrients are metabolized to release energy and intermediates that may serve as building blocks for cells; molecules are synthesized or broken down to recycle components; information to and from individual cells is conveyed through biochemical modifications; purposeful behavior emerges from sequences of biochemical reactions that trigger changes within cells. That so many different chemical reactions can take place within a cell or organism and create meaningful chains of events is made possible by compartmentalization. Compartments allow different biochemical environments to co-exist and to be independently regulated. Thus, they are key to the spatial control over metabolic processes and signaling pathways at the organism scale.

The importance of compartments in biology can be verified across scales, from single molecules to complex multicellular life forms. Individual compartments can be as small as an enzyme's active site that catalyzes a specific chemical reaction (Nurse, 2020). But macromolecules can also come together to form larger compartments (Diekmann and Pereira-Leal, 2013; Hyman et al., 2014; Murat et al., 2010). For instance among prokaryotes, some bacterial cells can assemble protein- or lipid-bound microcompartments dedicated to specific processes, such as the carboxysome or the magnetosome (Kerfeld et al., 2018; Murat et al., 2010). Eukaryotic cells, in turn, are characterized by a unique set of lipid-bound compartments, or organelles, optimized for different tasks. Mitochondria, for example, maintain specific metabolite concentrations, that are optimal for energy metabolism (Spinelli and Haigis, 2018), while lysosomes typically keep a low pH ideal for lysosomal enzymes to degrade macromolecules (Ballabio and Bonifacino, 2020). But compartments do not enable diversity and complexity only at the cellular level. At the supracellular scale, compartments within individual multicellular organisms enable more complex forms of regulated division of

labor and consequently their emergence was essential for the development and expansion of metazoan species.

Metazoan compartments were made possible by the appearance of a specific type of tissue: epithelia (Leys and Riesgo, 2012; Tyler, 2003). Epithelia are sheets of cells that can seal different compartments with distinct biochemical and physical properties (Jenkins and Tortora, 2013; Figure 1.1). They are the first type of tissue to appear during embryonic development and cover all surfaces of the vertebrate body, both internal and external. Thus, every substance that enters or leaves the body must do so by crossing an epithelium. As such, epithelia are the first line of defense of the body against physical, chemical or biological damage (e.g. epidermis). In addition, epithelia can perform a series of other functions that make them more than simple barriers able to separate and protect different compartments. Epithelia can select the substances they allow through, i.e. they can control the properties of compartments; they can perform a series of vectorial functions, including absorption (e.g. intestinal tract) and filtration (e.g. kidneys); they can themselves produce and secrete mucus, sweat or enzymes (e.g. parenchymal cells of glands); and they can provide specialized sensory surfaces (e.g. taste buds). Thus, epithelia are active players essential for development and homeostasis.

Epithelial functions rely on a specific internal organization of epithelial cells that underlies epithelial architecture. Although there is considerable variability across species and types of epithelia, there are conserved epithelial organization principles and molecular players that underlie the uniqueness of animal morphogenesis among multicellular organisms (Newman, 2016; Niklas et al., 2019). In this chapter, I will start by giving an overview of what defines epithelia and how epithelial cells are organized. Then I will focus on mechanisms that ensure epithelial architecture and integrity. In this context, I will discuss the apical actomyosin cytoskeleton, the adhesive junctions and apical-basal polarity. Adhesive junctions and the actomyosin cytoskeleton form a supracellular network that shapes and stabilizes epithelial tissues, guaranteeing epithelial integrity. Apical-basal polarity enables epithelial cells to behave assymmetrically and create internal compartments in an organism. After an overview of apical-basal polarity, I will focus in particular on how apical-basal polarity regulates epithelial organization through the adhesive junctions and the actomyosin cytoskeleton. Finally, in the following chapter, I will discuss how the adhesive and polarity machinery are regulated during epithelial cell division to maintain epithelial architecture and integrity in proliferative tissues.

HISTORICAL PERSPECTIVE ON EPITHELIA: DISCOVERY OF ONE OF THE MAIN TYPES OF ANIMAL TISSUE

The term epithelia was reportedly used for the first time in 1703 by Frederik Ruysch (1638-1731), a Dutch botanist famous for his techniques to preserve anatomical specimen. Upon dissecting a lip, Ruysch realized that it was covered by a thin layer, which he deemed different from the epidermis. He called this layer epithelia (Greek epi = on + thele = papillae; Lewis and Stöhr, 1913; Ruysch, 1703), in a reference to the underlying connective tissue evaginations, or papillae, present in the lip. Although the term epithelia was used sporadically during the following decades, it was not until the 1800s that it acquired its present meaning – a basic type of tissue – thanks to the work of Jacob Henle (1809-1885).

The use of the microscope to study different tissues led to an avalanche of discoveries in the 1800s. Ironically, the systematic study of tissues (i.e. the field of histology) is credited to have been started by a man known for his mistrust of microscopes, Marie François Xavier Bichat (1771-1802). Bichat was actually the first to use the word tissue to describe what he believed to be the indivisible units from which the body was made (Wilson, 2009). A surgeon and physician by training, Bichat became particularly interested in tissues when he realized that specific disease processes could frequently be traced back to specific types of tissues (Bynum, 2008). Consequently, he took an innovative approach to understand the human body and disease and dedicated most of his life to systematically characterize the composition of the body in terms of its tissues, which he ended up classifying into 21 different types, such as nervous, serous or muscular. In the following decades, it became clear that Bichat's tissues were still composites. The study of tissues under the microscope enabled numerous observations of cells, which led to the proposal of cell theory (Schleiden, 1838; Schwann, 1839). Generally attributed to Theodor Schwann (1810-1882) and Matthias Schleiden (1804-1881), cell theory placed the cell as the basic unit of life and posited that all organisms are communities of cells leading double lives: one as individuals and one as part of a whole. As such, all physiological and pathological behavior is a manifestation of the activity of cells and, to understand the body, one must focus on the power of individual cells. Cell theory translated into a new perspective from which to study tissues and by analyzing them in terms of how their cells are arranged, researchers were able to refine the classification system created by Bichat.

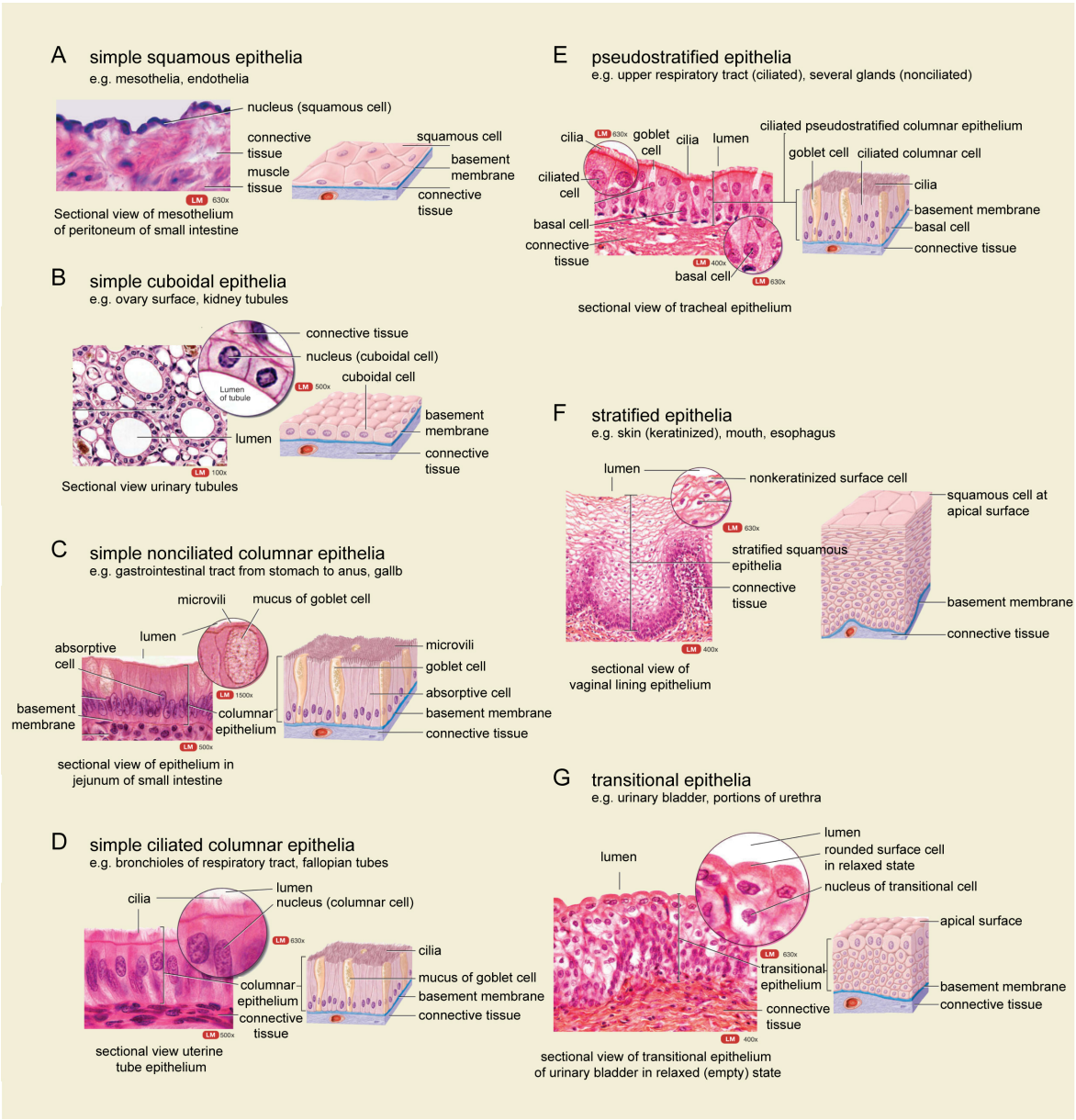


Figure 1.1. Epithelial tissues can be classified according to cell shape, cell layers and the presence of specialized structures. Examples of vertebrate epithelial tissues with different architetures. Epithelia can be classified as squamous (A), cuboidal (B) or columnar (C,D) for increasing height to width ratio of individual epithelial cells. Columnar cells contain more organelles, which makes them generally capable of higher levels of absorption and secretion. Epithelial cells can have apical specializations, such as microvili (B), that increase the absorptive surface area of the plasma membrane, or cilia (D), which can beat in unison to move mucus, foreign particles or oocytes, for example. Epithelia are also classified as simple (A-D) or stratified (F,G) depending on whether they have one or more cell layers respectively. Additionally, they are considered to be pseudostratified (E) when all cells are in contact with the basement membrane, but do not necessarily all extend to the apical surface of the epithelium. This leads to their nuclei being positioned at different distances from the basement membrane, which gives the impression of multiple layers. In transitional epithelia (G), cells can change their shape from cuboidal to squamous as the tissue stretches, without compromising epithelial integrity. Adapted from Jenkins and Tortora, 2013.

At around the same time as cell theory was proposed, Jacob Henle was working on the first detailed description of an epithelium from a cellular perspective (Henle, 1837). Henle noticed that the whole surface of an intestinal tract specimen was covered by a layer, which he determined to be densely packed with cells and free of blood vessels and nerve endings. Building on these findings, Henle recognized that, despite their diversity, all tissues covering body surfaces share similar morphological and functional characteristics, and thus all belong to the same system: they are all epithelial tissues (Kinne-Saffran and Kinne, 1994). Furthermore, current criteria to classify epithelia based on cell shape, the presence of specialized structures and amount of cell layers, can partially be traced back to Henle's work (Henle, 1841), although a full classification system was only developed later (Figure 1.1).

Over the following almost two centuries since Henle's work, researchers have published numerous findings on epithelial biology in development, homeostasis and disease. These have uncovered molecular structures (e.g. adherens junctions) and pathways (apical-basal polarity) shared by different epithelial tissues, that are key to support epithelial architecture and functions.

GENERAL ORGANIZATION OF EPITHELIAL CELLS

Epithelial layers are composed of cells polarized along an apical-basal axis. Simple epithelial cells typically have at least two segregated plasma domains with distinct lipid and protein compositions: an apical and a basolateral domain separated by epithelial cell-cell junctions (St Johnston and Ahringer, 2010; Figure 1.2). This apical-basal polarity is essential for the asymmetric organization of organelles, trafficking machinery and cytoskeleton and gives epithelia the ability to carry out vectorial functions essential for morphogenesis and homeostasis (Rodriguez-Boulan and Macara, 2014).

Apical domain

The apical domain of epithelial cells typically faces the exterior of the body, an internal cavity or the lumen of an organ and is defined by the accumulation of apical polarity determinants atypical protein kinase C (aPKC) and Crumbs (Assémat et al., 2008; St Johnston and Ahringer, 2010). At this surface, different epithelial cell types may form specialized structures that contribute to specific epithelial functions (Figure 1.1). For example, mammalian absorptive epithelia usually have a brush border of microvilli, finger-like actin-based

protrusions that increase the apical area for absorption (Sauvanet et al., 2015). Sensory cells may have stereocilia, which are actin-based structures, similar to microvilli, that contribute to hearing and balance through mechanosensing (McGrath et al., 2017). Another common apical structure, the cilium, is a microtubule-based protrusion, that can be adapted to perform very diverse functions, including to direct extracellular flow, sense extracellular cues or cell signaling (Gerdes et al., 2009; Spassky and Meunier, 2017). Below these structures and the plasma membrane lies the apical cortex, a supporting structure enriched in actin and spectrin filaments linked to the plasma membrane by ERM family proteins Ezrin, Radixin and Moesin (Fehon et al., 2010).

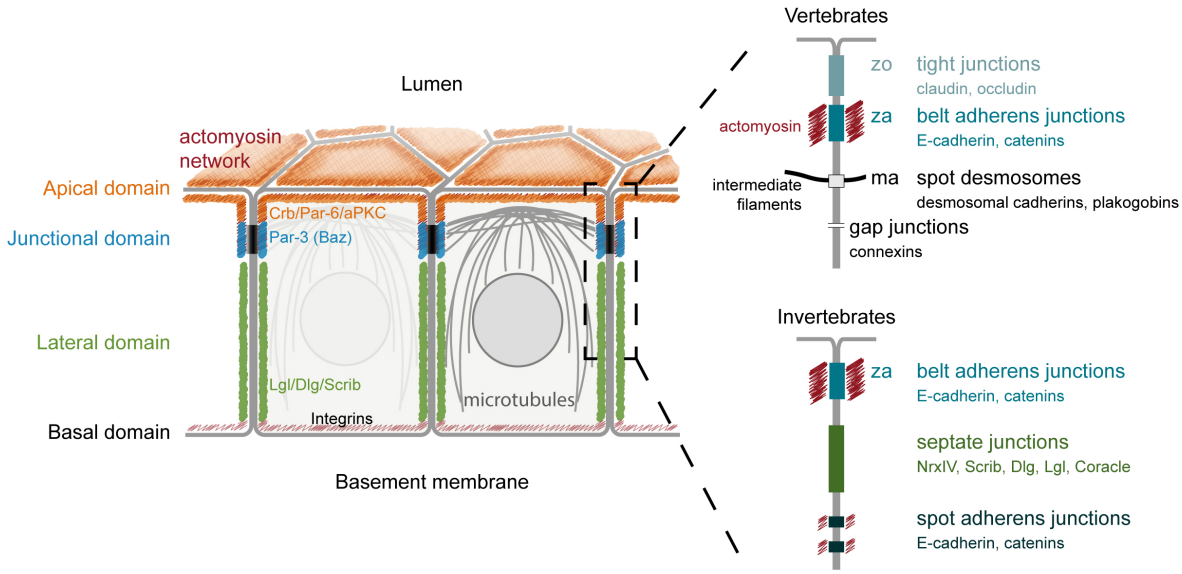


Figure 1.2. Epithelial cells have distinct cortical domains and junctions organized along an apical-basal axis. Epithelial cortical domains are defined by the accumulation of specific polarity determinants, including Crb, Par-6, aPKC, Par-3 (Baz in flies), Lgl, Dlg and Scrib, and enable epithelia to maintain their architecture and function properly. Additionally, epithelial cells form a series of junctions that connect them to each other along their lateral membrane. Vertebrate epithelial cells are connected to each other through occluding junctions, that form the *zonula occludens* (zo) and control epithelial permeability, and adherens junctions, that form the *zonula adherens* (za) and provide mechanical stability to epithelia. Below these apical junctions, vertebrate epithelial cells can also assemble demossomes, that form the *macula adherens* (ma) and provide additional mechanical stability, and gap junctions, that allow the passage of small molecules between cells. Invertebrate epithelial cells usually assemble septate junctions, a functional equivalent to the vertebrate occluding junction, below the *zonula adherens* and additional spot adherens junctions along the lateral membrane.

Lateral domain and cell-cell junctions

Just below the apical domain, at the apex of the lateral plasma membrane, epithelial cells assemble different types of cell-cell junctions with distinct structural morphologies, functions and molecular components. Initial electron microscopy studies of cell-cell junctions in different rat and guinea pig epithelia defined the *zonula occludens* (or tight junction), the *zonula adherens* (or adherens junctions) and the *macula adherens* (or desmosome; Farquhar and Palade, 1963; Figure 1.2). The latter was found to be specific to vertebrates. However, both the *zonula adherens* and *occludens* are essential for epithelial functions and can be found in vertebrates and invertebrates (Leys and Riesgo, 2012; Tyler, 2003). Over the past decades, the molecular organization of cell-cell junctions has been thoroughouly carachterized (reviewed in Franke, 2009; Horwitz, 2012): they are composed of transmembrane adhesion proteins that interact directly with each other through their extracellular domains. These interactions provide physical cohesion and mechanical stability to epithelial tissues and make them impermeable. The intracellular domain of transmembrane junction proteins indirectly links cell-cell junctions to the cytoskeleton, which regulates junctions and binds epithelial cells into a supracellular network. Additionally, epithelial cell-cell junctions integrate their barrier and adhesion function with other cellular processes, such as control of proliferation, by recruiting signaling molecules and regulators of gene expression involved in the Wnt and Hippo pathways among others (Garcia et al., 2018).

The most apical junction in vertebrates is the occluding tight junction. Its primary role is to serve as the paracellular diffusion barrier and selectively block solutes and ions from crossing epithelia. Additionally, tight junctions have been suggested to restrict phospholipid and transmembrane protein diffusion between the apical and the basolateral domains and thus help maintain their identity (Balda et al., 1996; Zihni et al., 2016). Morphologically, tight junctions are a network of sealing strands where the plasma membranes from neighbour cells are closely apposed. The most abundant transmembrane components are the members of the claudin family, which have been proposed to interact in *cis* at the plasma membrane to form the linear sealing strands. Furthermore, *trans* interactions between claudins on neighbour cells create the paracellular diffusion barrier and form charge- and size-selective pores of 4-8Å to control ion and water flux across epithelia (Suzuki et al., 2014; Tsukita et al., 2019). Additional transmembrane components – TAMPs (Tight junctions associated MARVEL proteins: occludin, tricellulin, MARVELD3) and Ig-like CAMs (Cell adhesion molecules: JAMs, CAR, angulin and ESAM) – are also important to maintain and regulate the permeability barrier, as well as to regulate the passage of larger solutes of up to 60Å across epithelia (Otani et al., 2019; Zihni et al., 2016). Transmembrane tight junction proteins recruit several adaptor and signaling proteins to the intracellular domain of tight junctions to regulate actomyosin, cell

polarity and signaling to the nucleus (Van Itallie and Anderson, 2014). The membrane-associated guanylate kinase (MAGUK) proteins *zonula occludens* (ZO-1, ZO-2, ZO-3), in particular, are important adaptors that loosely anchor the actin cytoskeleton to tight junctions to regulate junction architecture and stability and the passage of ions and solutes (Belardi et al., 2020; Citi, 2019).

The main anchoring junction in epithelia that senses, resists and responds to tensile forces at the cell-cell interface is the adherens junction (Lecuit and Yap, 2015; Mege and Ishiyama, 2017). Adherens junctions form belt-like cell-cell adhesion domains at the *zonula adherens*, characterized by an intercellular spacing of ~20nm. The main component of adherens junctions is the transmembrane protein E-cadherin, which binds in a homotypic fashion to E-cadherin on neighbour cells in a Ca^{2+}-dependent manner (Yoshida and Takeichi, 1982). The intracellular domain of E-cadherin indirectly recruits several proteins, including cell polarity and signaling molecules, such as Par-3/Baz and RhoGTPase regulators (Padmanabhan et al., 2015). But the key intracellular partners of E-cadherin are catenins, which, together with other actin binding proteins, anchor adherens junctions to bundles of actomyosin that run parallel to the plasma membrane. These interactions between adherens junctions and the actin cytoskeleton regulate junction behaviour, provide strong structural support for epithelial cells and create a coherent structural network that supports epithelial tissue morphology. Adherens junctions themselves and their connection to the actomyosin cytoskeleton are dynamic structures, which are extensively remodeled during morphogenesis (Guillot and Lecuit, 2013; Heisenberg and Bellaiche, 2013; Takeichi, 2014). It is this dynamic and responsive nature that confers epithelia the fluid-like properties that underlie the distinctive morphologies of metazoan organisms (Niklas et al., 2019).

Below tight and adherens junctions, the lateral cortex is defined by the accumulation of the Scribble polarity module (Assémat et al., 2008; St Johnston and Ahringer, 2010). Here, epithelial cells can form additional cell-cell junctions. Vertebrate epithelial cells frequently assemble desmosomes, an additional type of load-bearing junction, which can switch to a calcium independent hyperadhesion form and is able to absorb, sense and resist different kinds of stress, providing mechanical stability (Hatzfeld et al., 2017). Desmosomes are spot-like adhesion sites composed of desmosomal cadherins – desmoglein and desmocollin – connected to intermediate filaments through desmosomal plakins and armadillo proteins – desmoplakin, plakoglobin and plakophilin (Delva et al., 2009; Green et al., 2020). Although there are reports of spot-like adhesions in invertebrates, similar to desmosomes, they are linked to actin bundles rather than intermediate filaments and do not have desmosomal cadherins, which are vertebrate specific (Leys and Riesgo, 2012). Additionally, at their lateral

cell-cell interface, epithelial cells can also have gap junctions, a communication junction that allows the passage of ions and small molecules across cells (Mese et al., 2007).

The described junction organization is typical for vertebrate epithelial cells. However, invertebrate epithelial cells usually assemble a different type of occluding junction: the septate junctions (Banerjee et al., 2006). Septate junctions are functionally equivalent to tight junctions. However, they differ from tight junctions in their morphology and molecular composition: while they have some components in common, such as *Drosophila* claudins (Behr et al., 2003; Nelson et al., 2010; Wu et al., 2004), most components, including the transmembrane proteins Neuroglian and Neurexin (Baumgartner et al., 1996; Genova and Fehon, 2003; Izumi and Furuse, 2014), do not localize at vertebrate tight junctions. Additionally, their position relative to adherens junctions is usually different (Figure 1.2). While in vertebrate epithelia, tight junctions are closest to the luminal surface, in invertebrates the relative position of occluding and adherens junctions is generally inverted, with adherens junctions above septate junctions. However, there are exceptions to this even within the same organism. While most epithelial junctions described in *Drosophila* have a typical invertebrate organization, with belt adherens junctions on top of septate junctions, midgut epithelial cells only have spot adherens junctions below septate junctions (Chen et al., 2018; Tepass and Hartenstein, 1994).

Finally, it should be noted that although individual junctions were described as separate assemblies, components from different junctions can interact with each other to some extent. Some intracellular adaptors are able to bind to more than one type of junction: for example plakogobin (desmosome) and ZO-1 (tight junction) can also accumulate at adherens junctions (Green et al., 2019) and different junction components may even coalesce more fully in specific circumstances. For example, mammalian cardiomyocites assemble adherens junctions and desmosomal components into a mixed junction named *area composita* or intercellular disk that connects both to intermediate filaments and actomyosin and is believed to help sustain the increased stress of rhythmic heart beating (Borrmann et al., 2006; Li and Radice, 2010).

Basal domain

At the basal surface, epithelial cells can form integrin-based focal adhesions and hemidesmosomes that mediate cell-matrix attachments (Chastney et al., 2021). These junctions attach epithelial cells to the basement membrane, a thin extracellular matrix that supports the epithelium and serves as an anchoring interface to connective tissues. Integrins are transmembrane adhesion molecules that can recognize several components from the

extracellular matrix and transduce mechanical and chemical signals bidirectionaly across the plasma membrane. Similar to other adhesion molecules previously discussed, the intracellular domains of integrins recruit several intracellular proteins, that regulate integrin activation, mediate binding to the actin cytoskeleton or intermediate filaments and feed into signaling pathways that control cell behaviour and proliferation (Kechagia et al., 2019; Sun et al., 2019).

Different epithelia, both within the same and in different species, may display variations of the arrangement described, likely reflecting adaptations to specific functions. For instance, hepatocytes have a particular type of polarity where the apical domain faces a lumen formed at the lateral side of cells, between neighbour hepatocytes – the bile canaliculae (Treyer and Musch, 2013). Stratified epithelia such as the skin, in turn, are polarized along the whole structure and express different junctional components in different layers (Dias Gomes and Iden, 2021).

THE ACTOMYOSIN NETWORK

The actomyosin network is a meshwork of actin and non-muscle myosin II (myosin II) filaments critical to shape cells, control their mechanical properties, support different cellular structures and generate force to power dynamic behavior in cells and tissues across species (Agarwal and Zaidel-Bar, 2019; Chugh and Paluch, 2018; Stricker et al., 2010). Cells can assemble actomyosin networks with varying shapes and internal organization at different subcellular localizations and anchored to different structures, such as adherens junctions or the plasma membrane. Within these networks, myosin II can generate force by sliding and rearranging actin filaments. Actomyosin participates in crucial cellular functions, including transcription (Percipalle and Visa, 2006), vesicle trafficking (Masedunskas et al., 2011) and cell division (D'Avino et al., 2015), and controls critical aspects of epithelial cell biology, such as adherens junctions organization (Arnold et al., 2017) and remodeling (Pinheiro and Bellaiche, 2018), epithelial mechanical properties (Khalilgharibi et al., 2019), epithelial cell morphology and shape change (Heer and Martin, 2017). Additionally, epithelial cells can form supracellular actomyosin structures spanning multiple cells to drive cellular rearrangements during tissue elongation (Pare and Zallen, 2020) and apical constriction during epithelial invagination (Coravos and Martin, 2016), coordinate epithelial cell behavior during wound healing (Rothenberg and Fernandez-Gonzalez, 2019) and protect epithelia from stretch-induced damage (Duda et al., 2019).

In this section, I will summarize principles of actomyosin network assembly and how they relate to actin filament organization and function. Then I will focus on actomyosin regulation in particular by Rho GTPases and discuss how Rho GTPases themselves are regulated. Finally, I will touch briefly on how actomyosin and Rho GTPases dynamic behavior contributes to control cell and tissue shape, focusing on apical constriction.

Actomyosin network assembly and internal organization

Dozens of different actin binding proteins and regulators, including actin nucleators (e.g. Arp2/3 and formins), actin severing and disassembling enzymes (e.g. cofilin), actin cross-linkers (e.g. α-actinin) and motor proteins (e.g myosin II), cooperate in cells to assemble actomyosin networks with different architectures (Chugh and Paluch, 2018). Monomeric actin (globular or G-actin) assembles in a head-to-tail fashion into polarized actin filaments (filamentous or F-actin) with a barbed and a pointed end. This process can happen spontaneously but, in cells, it is mostly driven by actin nucleators (Campellone and Welch, 2010). Formins (e.g. Diaphanous in *Drosophila* and Diaphanous-related formins in vertebrates) add actin monomers to the fast-growing barbed end of an actin filament to create long unbranched actin filaments (Pruyne et al., 2002). Actin filament elongation by formins is restricted by capping proteins that bind to barbed ends and prevent formin-mediated elongation. Cells can generate new barbed ends amenable to formin-mediated elongation by severing pre-existing actin filaments to expose new uncapped ends (Carlsson, 2006). Additionally, the Arp2/3 complex can nucleate new actin filaments at the sides of pre-existing ones at a ~70° angle (Blanchoin et al., 2000). However, unlike formins, that remain linked to barbed ends during elongation, Arp2/3 remains at the pointed-end of the new filament and connects it to the side of the pre-existing filament, thus promoting the assembly of branched actin networks.

The activity of different actin nucleators is crucial to assemble networks characterized by branched, bundled or a meshwork-like organization of actin filaments (Skau and Waterman, 2015). Different actin filament arrangements have been associated with different cellular structures and processes: branched structures are typically associated with protrusive forces (e.g. lamellipodium formation) while bundled actin filaments generally produce contractile forces (e.g. cytokinetic ring constriction). However, actomyosin network architecture is not static. Network assembly and disassembly is a dynamic event that takes place in the seconds to minutes timescale, which enables quick changes in network architecture and output (Letort et al., 2015).

Dynamic actomyosin behavior produces force that can be harnessed by cells to drive different events. Cross-linked networks can generate force through actin filament assembly and disassembly, but the main process responsible for force generation is myosin II mediated sliding of actin filaments, which results predominantly in contractile forces and tension (Koenderink and Paluch, 2018). The motor protein myosin II is a hexamer of two heavy chains, two essential light chains and two myosin regulatory light chains (Vicente-Manzanares et al., 2009). The heavy chain mediates homodimerization through its C-terminal domain and binds to actin filaments through its N-terminal head domain. These two domains are connected by a neck region that binds the myosin light chain subunits of the complex. After myosin binds to an actin filament, an ATP-dependent conformation change drives a power stroke that enables myosin to walk on a filament towards its barbed end before releasing it. To be able to walk processively on actin filaments, nonmuscle myosin II homodimers assemble into bipolar minifilaments with a few myosin heads on each terminus (Fenix et al., 2016). Myosin minifilaments can bind simultaneously to different actin filaments and have been reported to create tension by cross-linking them (Ma et al., 2012). Depending on how actin filaments are oriented relative to each other, myosin movement towards their barbed ends can slide actin filaments, rearranging or disassembling actin networks and, thus, change their mechanical properties and/or produce force (Agarwal and Zaidel-Bar, 2019). *In vitro* assays with networks with specific actin filament arrangements have confirmed that the output of myosin II activity on actin filaments is dictated by network architecture (Ennomani et al., 2016; Reymann et al., 2012). Myosin II preferentially contracts antiparallel actin filaments, which results in networks with more anti-parallel filaments contracting more. Additionally, the position and amount of actin nucleation sites and crosslinkers also dictates the outcome of myosin II activity.

Role of Rho GTPases in actomyosin regulation

Several pathways regulate the activity of actin nucleators and myosin II through kinases, scaffolds and protein-protein interactions to control actomyosin in space and time (Zaidel-Bar et al., 2015). A recurrent theme in actomyosin regulation is the existence of central nodes that coordinate the localized activation and inactivation of a specific combination of actomyosin regulators to drive the local organization of networks with specific characteristics. Among these is the Rho family of small GTPases, in particular the conserved proteins Rho, Rac and Cdc42 (Hall, 1998). The Rho family of GTPases has at least 25 members in humans and Rho-like proteins have been found in all eukaryotic species examined so far (Hall, 2012). Initial experiments with constitutively active Rho GTPase mutants in fibroblasts revealed that Rho induces the assembly of contractile actin and myosin filaments to form stress fibers

(Ridley and Hall, 1992), Rac induces surface protrusions and membrane ruffling (lamellipodia; Ridley et al., 1992) and Cdc42 creates finger-like membrane protrusions (filopodia; Kozma et al., 1995; Nobes and Hall, 1995). Since then, Rho, Rac and Cdc42 have been found to function as central nodes that react to intracellular and extracellular cues and trigger the local assembly of actin networks with different architectures and different mechanical properties through the concerted regulation of different downstream effectors. Through actomyosin regulation, Rho GTPases control several processes, including cell shape, adherens junction formation and stability and cell migration (Agarwal and Zaidel-Bar, 2019; Lecuit et al., 2011; Ridley, 2015).

The ability of different Rho GTPases to drive the assembly of specific types of actomyosin networks has been linked to the regulation of different actin nucleators and myosin II (Figure 1.3A). Rho activity is associated with the assembly of contractile actomyosin networks through formin-mediated actin elongation and myosin II activation. One of the best-understood cases of formin activation is the Diaphanous-related formin mDia1 (Watanabe et al., 1997), which is kept in an inactive state through an auto-inhibitory interaction between its N- and C-terminal domains (Li and Higgs, 2003). This auto-inhibition is relieved by direct Rho binding to promote actin filament elongation (Otomo et al., 2005). Additionally, Rho promotes myosin II activity through Rho associated coiled-coil kinase (ROCK)-mediated phosphorylation of myosin regulatory light chain on two conserved residues (Ser19 and Thr18 in human myosin; Ser20 and Thr21 in *Drosophila*; Amano et al., 1996; Shewan et al., 2005). Unphosphorylated myosin II is kept inactive through an auto-inhibitory interaction where its tail domain bends on itself to block both minifilament assembly and the head domains (Craig et al., 1983; Jung et al., 2008; Scarff et al., 2020). Phosphorylation of the regulatory light chain relieves auto-inhibitory head-tail interaction, promotes minifilament assembly and enables processive walking on actin filaments. In addition to direct myosin II phosphorylation, ROCK also activates myosin II through inhibition of myosin phosphatase targeting subunit MYPT to prevent myosin dephosphorylation (Kimura et al., 1996). Unlike Rho, Cdc42 and Rac are able to promote Arp2/3-mediated branched actin nucleation through the nucleation promoting factors N-WASP (Wiskott-Aldrich syndrome protein; activated by Cdc42; Rohatgi et al., 1999) and WAVE (WASP verprolin homologous; activated by Rac; Eden et al., 2002).

The link initially established between Rho, Rac and Cdc42 and myosin II-dependent contractility or Arp2/3-mediated branched actin network provided a simple model to explain how different Rho GTPases control actomyosin-dependent processes. However, actomyosin regulation is more complex. Besides Rho, Rac and Cdc42 have also been reported to activate certain Diaphanous-related formins and contribute to contractility (Kuhn and Geyer, 2014). Similarly, myosin II can also be targeted by other kinases, including myosin light chain kinase (MLCK; activated by Ca2+), myotonia dystrophy-related Cdc42-binding kinase (MRCK; activated by Cdc42) and Citron kinase (activated by Rho) among others (Tan et al., 2008;

Totsukawa et al., 2000; Yamashiro et al., 2003). Additionally, a systematic literature review revealed close to 100 proteins reported to regulate actomyosin contractility (mainly through protein-protein interactions and activating or inhibitory phosphorylations) with extensive crosstalk and multiple links between upstream and downstream regulators (Zaidel-Bar et al., 2015). More than a single Rho GTPase can be active at similar subcellular sites (Machacek et al., 2009; Verboon and Parkhurst, 2015) and the same Rho GTPase can drive different events and activate different context-specific downstream regulators. Furthermore, other proteins and mechanical inputs can influence Rho GTPase activated effectors or cooperate with them to shape downstream events. A recent study in the *Drosophila* embryo using an optogenetic tool to activate Rho in the apical-medial region of epithelial cells highlighted the importance of cellular context in dictating the outcome of Rho GTPase activation (Rich et al., 2020). While Rho activation in ventral epithelial cells was able to recapitulate an early gastrulation during which anisotropic apical constriction induces tissue invagination, the same was not true for dorsal epithelial cells, where constriction was isotropic. The complexities of actomyosin regulation by Rho GTPases are also evident at adherens junctions, where structural components contribute to regulate actomyosin organization and function. Here, Rho, Rac and Cdc42 cooperate to assemble and regulate the underlying junctional actomyosin network. Rho activity has been shown to stabilize adherens junctions by inducing contractility and formin-mediated actin polymerization (Acharya et al., 2017). This correlates well with the bundled actin filament organization prevalent at adherens junctions (Indra et al., 2020). However, Arp2/3 activation by WAVE and N-WASP also contributes to actomyosin assembly at adherens junctions (Kovacs et al., 2011; Verma et al., 2012). Furthermore, adherens junctions components also recruit several other actin regulators, such as α-actinin, VASP, Zyxin or EPLIN (Kannan and Tang, 2015; Leerberg et al., 2014; Oldenburg et al., 2015; Taguchi et al., 2011), and it remains to be fully explored how all these players intersect in time and space to control actomyosin organization and function.

Finally, Rho GTPases also regulate other pathways independently of actomyosin, such as cell polarity (Etienne-Manneville and Hall, 2002), which may intersect with actomyosin regulation in specfic contexts. For example, in epithelial cells both actomyosin and cell polarity contribute to regulate adherens junctions (Diaz-Diaz et al., 2020).

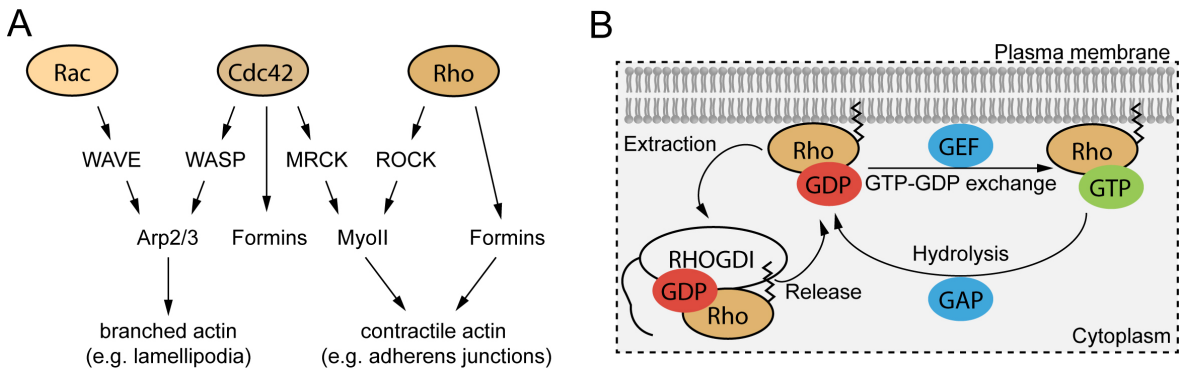


Figure 1.3. Rho GTPases regulate actomyosin assembly and are, in turn, regulated by Rho GAPs and GEFs. (A) Simplified schematic illustration of downstream effectors of Rho GTPases Rho, Rac and Cdc42. Activation of specific effectors leads to different downstream events. (B) Rho GTPase activity is spatially and temporally regulated by GEF, GAPs and GDIs.

RhoGTPase regulation

Rho GTPase activity has to be confined in space and time to ensure tight control over actomyosin networks and their dysregulation has been linked to neurological disorders and cancer progression (Aspenstrom, 2018; Boettner and Van Aelst, 2002). Generally, Rho GTPases are activated in response to a specific cue, such as ligand binding to a membrane receptor or mechanical stress, which promotes local membrane recruitment and/or activation of a specific Rho GTPase (Acharya et al., 2018; Kerridge et al., 2016; Manning and Rogers, 2014). Rho GTPases can be regulated through different types of molecular events, including post-translational modifications such as phosphorylation to change affinity for binding partners or prenylation to target Rho GTPases to membranes (Hodge and Ridley, 2016). However, the main mechanism that regulates Rho GTPase activity in cells is the control of their GTP/GDP bound state by guanine nucleotide exchange factors (GEFs) and GTPase activating proteins (GAPs; Figure 1.3B).

Small GTPases, including members of the Rho family, switch between an active GTP-bound conformation and an inactive GDP-bound conformation (Jaffe and Hall, 2005). Once activated by GTP-binding, GTPases bind and activate downstream effectors until GTP hydrolysis renders them inactive again. The inherent ability of GTPases to exchange GDP for GTP and hydrolyze GTP is extremely slow, so that their activation status is essentially controlled by the two groups of proteins that drive these two processes: GAPs and GEFs. GEFs promote GDP release, so it can be replaced by the more abundant GTP (Rossman et al., 2005). Consequently, GEFs activate Rho GTPases and promote effector binding. GAPs enhance the ability of Rho GTPases to hydrolyze GTP, leading to GTPase inactivation (Tcherkezian and Lamarche-Vane, 2007). Additionally, Rho GTPases can also be regulated

by guanine nucleotide dissociation inhibitors (GDIs; Garcia-Mata et al., 2011), which bind to Rho GTPases and conceal their prenyl groups to sequester Rho GTPases in the cytoplasm in a suppressed state.

The amount of RhoGAPs, GEFs and GDIs greatly outnumbers that of Rho GTPases: humans have 67 Rho GAPs (22 in *Drosophila*), 82 Rho GEFs (26 in *Drosophila*) and 3 Rho GDIs (1 in *Drosophila*). RhoGEFs can be classified into two different families, depending on the identity of their GEF catalytic domain: a Dbl homology domain or DOCK homology regions. RhoGAPs belong to a single family with a conserved RhoGAP domain. RhoGEF and RhoGAP domains are flanked by additional domains that regulate GTPase specificity, protein activity and subcellular localization (Cherfils and Zeghouf, 2013).

The subcellular distribution and concerted action of RhoGAPs, GEFs and GDIs regulates the activation of specific pools of Rho GTPases at different subcellular locations (Pertz, 2010). Consequently, the function of RhoGTPases is regulated by RhoGAPs, GEFs and GDIs expression in different tissues, by their subcellular localization, their specificity for one or more Rho GTPases and by their activity. RhoGAPs and GEFs themselves are regulated through protein-protein or protein-lipid interactions, binding of second messengers or post-translational modifications. These either promote GAP/GEF translocation to a specific compartment, relieve auto-inhibition by a flanking region which covers the small G protein binding site or induce allosteric changes in the catalytic domain (Bos et al., 2007). A recent systematic analysis of all human RhoGAPs and RhoGEFs confirmed that several are kept inactive through auto-inhibition, which has to be relieved for Rho GTPase activation (Muller et al., 2020). Interestingly, this study revealed a varying degree of Rho GTPase specificity for different RhoGAPs and GEFs with some of them being able to target more than one Rho GTPase. Additionally, some RhoGAPs and RhoGEFs were found to form complexes, which could enable coordinated regulation of downstream targets.

Current knowledge on how different RhoGAPs and GEFs regulate Rho GTPases *in vivo* stems mostly from studies of individual regulators, where the accumulation of specific RhoGEFs at subcellular locations was seen to trigger Rho GTPase activation to drive a downstream event, while RhoGAPs locally inactivate Rho GTPases. For example, in *Drosophila* epithelia, apical-medial accumulation of RhoGEF2 activates Rho locally to increase apical contractility, while a different RhoGEF, Cysts, promotes Rho activity at adherens junctions (Garcia De Las Bayonas et al., 2019; Kolsch et al., 2007; Silver et al., 2019). Rho GTPase activity can be ensured by simultaneous control of local GEF and GAP activity. For example, the centralspindlin complex has a nonmitotic role in Rho activation through recruitment of the RhoGEF Ect2 and inhibition of the local accumulation of p190RhoGAP in mammalian epithelial cell lines (Ratheesh et al., 2012). Thus, spatial control

over RhoGAP and RhoGEF subcellular localization and recruitment patterns Rho GTPase activity inside cells (Nakamura et al., 2017). Similarly, temporal control over their recruitment or activation at similar subcellular sites can lead to cycles of Rho GTPase activity. For example, in *Drosophila* epithelial cells, coordination of RhoGAP71E and RhoGEF2 at the apical-medial region controls Rho activity to elicit pulsatile actomyosin contractions during epithelial invagination (Mason et al., 2016).

Studies on the role of individual RhoGAPs and RhoGEFs in different processes have contributed significantly to our understanding of how Rho GTPase activity is regulated. Nevertheless, the role of several RhoGAPs and GEFs remains unknown. Furthermore, it remains to be fully explored how different RhoGAPs and RhoGEFs can drive different processes and how they cooperate to create patterns of Rho GTPase activity in space and time.

Actomyosin contractility and apical constriction

Pulsatile contractility seems to be an intrinsic characteristic of actomyosin networks in different cell types (Baird et al., 2017). This behaviour has been associated with local and transient accumulations of myosin II generally driven by oscillations in upstream regulators (Mason et al., 2016; Munjal et al., 2015) and can be harnessed to drive physical changes during morphogenesis (several reviews: Gorfinkiel, 2016; Heer and Martin, 2017; Miao and Blankenship, 2020; Siedlik and Nelson, 2015). Depending on actomyosin subcellular localization and its connection to cellular structures, pulsatile contractions can contract or shrink specific cellular domains and hereby adjust cell and tissue shape. Consequently, the pulsatile behaviour of actomyosin has been found to drive many morphogenetic events across species (Christodoulou and Skourides, 2015; He et al., 2010; Maitre et al., 2015; Martin et al., 2009; Pulido Companys et al., 2020; Rauzi et al., 2010; Roh-Johnson et al., 2012; Sherrard et al., 2010; Simoes et al., 2017; Solon et al., 2009). Among these, apical constriction stands out as a widely used process during morphogenesis throughout the animal kingdom.

During apical constriction, isotropic contractions at the apical-medial region of epithelial cells decrease apical cell size and cells become wedged. This process can occur in individual cells, as they leave an epithelium (Simoes et al., 2017), in small groups of cells (Roh-Johnson et al., 2012) or in a larger patch of tissue to promote tissue folding, for instance during tube formation (Christodoulou and Skourides, 2015; Martin et al., 2009). *Drosophila* embryos have been used extensively as a model to understand how pulsed actomyosin behavior triggers apical constriction and tissue deformations during presumptive mesoderm (Figure 1.4) and endoderm invagination (Martin et al., 2009; Sweeton et al., 1991), dorsal

closure (Hayes and Solon, 2017; Solon et al., 2009) and salivary gland tube formation (Sanchez-Corrales et al., 2018). In these systems, upstream signals have been found to trigger RhoGEF2-mediated Rho activation to drive pulsatile actomyosin contractions with concomitant apical area decrease (Azevedo et al., 2011; Dawes-Hoang et al., 2005; Kolsch et al., 2007; Martin et al., 2009; Nikolaidou and Barrett, 2004; Solon et al., 2009). Rho signaling activates actomyosin contractility through the coordinated activation of myosin II and F-actin assembly (Homem and Peifer, 2008; Mason et al., 2013).

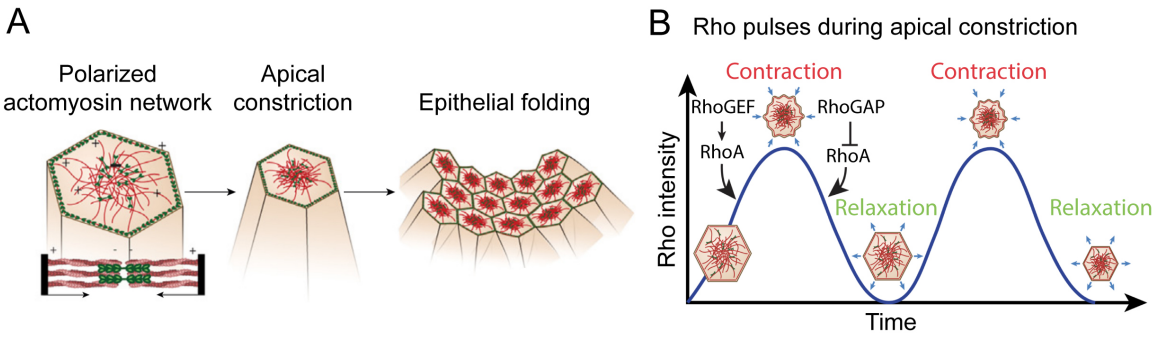


Figure 1.4. Actomyosin pulses at the apical surface of epithelial cells lead to tissue folding. (A) Presumptive mesoderm cells in *Drosophila* have a polarized medioapical actomyosin network, which constricts cells apically to fold the epithelium during ventral furrow formation. (B) This process is driven by pulses of actomyosin contractility controlled by oscillations in Rho activity. Adapted from Agarwal and Zaidel-Bar, 2019.

Apical constriction is driven in a ratchet-like manner by repeated cycles of Rho-mediated constriction and pauses to stabilize apical cell shape (Martin et al., 2009; Figure 1.4B). During ventral furrow formation, pulsatile actomyosin contractions have been shown to depend on the pulsatile accumulation of upstream regulators at the apical-medial region. Rho pulsates due to its sequential activation by RhoGEF2 and inactivation by RhoGAP71E (Mason et al., 2016). Downstream of Rho, Rok and myosin phosphatase also alternate at the apical-medial region, promoting myosin II pulsatile behavior and apical constriction (Vasquez et al., 2014). For apical constriction to promote coordinated tissue-scale deformations, cell-generated forces have to be transmitted across the epithelium through the physical linkage of the apical actomyosin network to adherens junctions (Dehapiot et al., 2020; Martin et al., 2010; Sawyer et al., 2009).

ADHERENS JUNCTIONS

Metazoan epithelia are deformable, responsive and cohesive. These characteristics stem from the adherens junctions: belt-like cell-cell adhesive structures positioned around epithelial cells at the apical-lateral interface (Newman, 2019). Adherens junctions are the main cell-cell adhesive junction, responsible for attaching epithelial cells to each other. They are essential to preserve epithelial integrity during development and homeostasis and their loss or deregulation has been associated with developmental disorders and disease (Jeanes et al., 2008; Vasioukhin, 2012).

Structurally, adherens junctions are dynamic assemblies of numerous proteins that co-operate to mediate cell-cell adhesion and link adhesion sites to the actomyosin cytoskeleton (Mege and Ishiyama, 2017). This organization implies that adherens junctions not only adhere epithelial cells to each other but also that: 1) they link the contractile actomyosin cortices from individual cells into a supracellular structure that provides mechanical stability to epithelia and ensures coherent behavior during morphogenesis; 2) they are ideally positioned to sense and propagate cell-generated forces and external mechanical inputs (e.g. blood flow) across epithelia to drive morphogenesis (Dorland and Huveneers, 2017; Lecuit et al., 2011; Martin et al., 2010; Roh-Johnson et al., 2012; Sawyer et al., 2009). Additionally, several components from adherens junctions undergo tension-dependent conformational changes to trigger downstream events ranging from cell adhesion reinforcement and actomyosin network remodeling to regulation of signaling pathways controlling cell fate, growth or proliferation (Angulo-Urarte et al., 2020; Pannekoek et al., 2019; Yap et al., 2018). Thus, adherens junctions are key hubs where mechanical inputs can be converted into biochemical signals to control cellular behavior and vice-versa. Adherens junctions themselves can be extensively remodeled in response to external or internal cues, which is essential to enable individual cells to slip past one another during morphogenesis without compromising epithelial integrity (Pinheiro and Bellaiche, 2018).

Here, I will focus on the internal organization of adherens junctions, their link to the actomyosin network and how they are assembled

E-cadherin/α-catenin/β-catenin complex

Cell-cell adhesion at adherens junctions is mediated by classical cadherins (Figure 1.5), a subgroup of the cadherin superfamily of transmembrane proteins (114 cadherin genes in the human genome, 17 in *Drosophila*). Cadherins are single pass transmembrane proteins that mediate homophilic, Ca^{2+}- dependent intercellular adhesion through an adhesive

ectodomain characterized by tandem extracellular cadherin (EC) repeats (Gul et al., 2017). Epithelial Cadherin (cadherin 1 (CDH1) in humans, *shotgun* (*shg*) in *Drosophila*) is the main cadherin type found in epithelial adherens junctions and its ectopic expression is enough to induce cell-cell junction formation in cells where they are otherwise absent (Chandran et al., 2021; Nagafuchi et al., 1987).

While the extracellular domain of E-cad mediates cell-cell adhesion through homophilic interactions, E-cadherin cytosolic tail is essential for adherens junction formation through recruitment of α-catenin and β-catenin (Nagafuchi and Takeichi, 1988; Ozawa et al., 1989). Together, they form the E-cadherin/α-catenin/β-catenin complex, the essential core of adherens junctions in different epithelia across metazoa (Cox et al., 1996; Kofron et al., 1997; Larue et al., 1994; Muller and Wieschaus, 1996; Tepass et al., 1996; Torres et al., 1997; Uemura et al., 1996). α-Catenin recruitment by β-catenin is particularly important to anchor E-cad to the actomyosin cytoskeleton through actin filament binding (Buckley et al., 2014). Additionally, as adherens junctions form, the cytosolic tail of E-cadherin, together with the associated catenins, recruits numerous proteins that form the cadherin adhesome and regulate cell-cell adhesion through control of adherens junction assembly, turnover, cytoskeletal anchoring and integration with intracellular signaling pathways (Guo et al., 2014; Toret et al., 2014; Van Itallie et al., 2014; Zaidel-Bar, 2013).

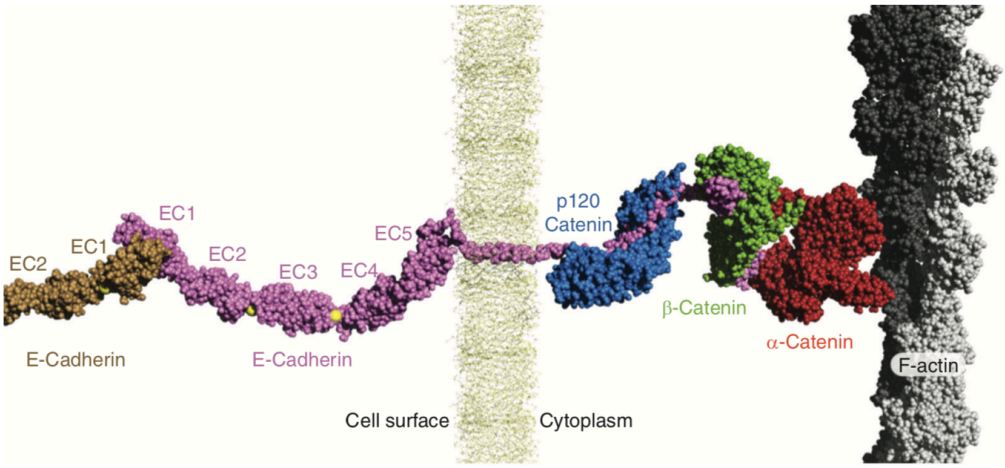


Figure 1.5. E-cadherin/catenin complex. Three-dimensional model of E-cadherin/catenin cell adhesion complex based on individual crystal structures (from Mege and Ishiyama, 2017).

E-cadherin organization at adherens junctions

Cadherin homophilic interactions and organization at adherens junctions are best understood for vertebrate classical cadherins (Brasch et al., 2012; Honig and Shapiro, 2020). Vertebrate classical cadherins, such as CDH1, have five extracellular EC repeats connected through Ca^{2+}-sensitive linkers (Figure 1.5). Ca^{2+} binding rigidifies the linker domains and triggers a conformational change in the cadherin ectodomain from a more globular arrangement to a slightly curved rod shape extending outward from the plasma membrane (Harrison et al., 2011; Pokutta et al., 1994). This conformational change promotes cadherin homophilic interactions in *trans* with cadherin molecules on the opposing cell surface through the membrane distal N-terminal region (Harrison et al., 2011; Vendome et al., 2011). X-ray crystallography has revealed two distinct *trans* interaction dimers for vertebrate classical cadherins. An interaction mediated by the linker region between the two N-terminal EC domains, EC1 and EC2, results in the formation of a so-called X-dimer (Nagar et al., 1996). This interaction mode has been proposed to function as an intermediate to a second and final configuration involving only the N-terminal EC1 repeat. In this configuration, two cadherins on opposing cell surfaces exchange a specific strand in their EC1 domains, forming a strand-swap dimer (Harrison et al., 2010; Shapiro et al., 1995). Vertebrate E-cadherins are proposed to assume a strand-swap dimer configuration to mediate cell adhesion at adherens junctions.

The ectodomain of E-cadherin has diverged significantly between vertebrates and invertebrates, which suggests that the molecular details of E-cadherin binding are likely to vary across species. While vertebrate classical cadherins only have five EC domains, classical cadherins in invertebrates can have varying amounts of EC repeats and additional distinct membrane proximal domains, such as epidermal growth-factor like (EGF-like) domains and laminin-globular domains (LmG; Gul et al., 2017). *Drosophila* E-cadherin has seven EC repeats, as well as additional membrane proximal EGF-like and a LmG domains. Deletion of E-cadherin domains in *Drosophila* revealed that the six N-terminal EC domains are sufficient and required to support adherens junction assembly and epithelial integrity (Haruta et al., 2010). Interestingly, structural analysis showed that invertebrate E-cadherin does not assume a rod shape upon Ca^{2+} binding, unlike the vertebrate one. Instead the N-terminal region bends on itself, due to Ca^{2+}-insensitive linkers between some EC domains, and homophilic interactions are likely mediated by domains EC2-EC4 (Jin et al., 2012; Nishiguchi et al., 2016).

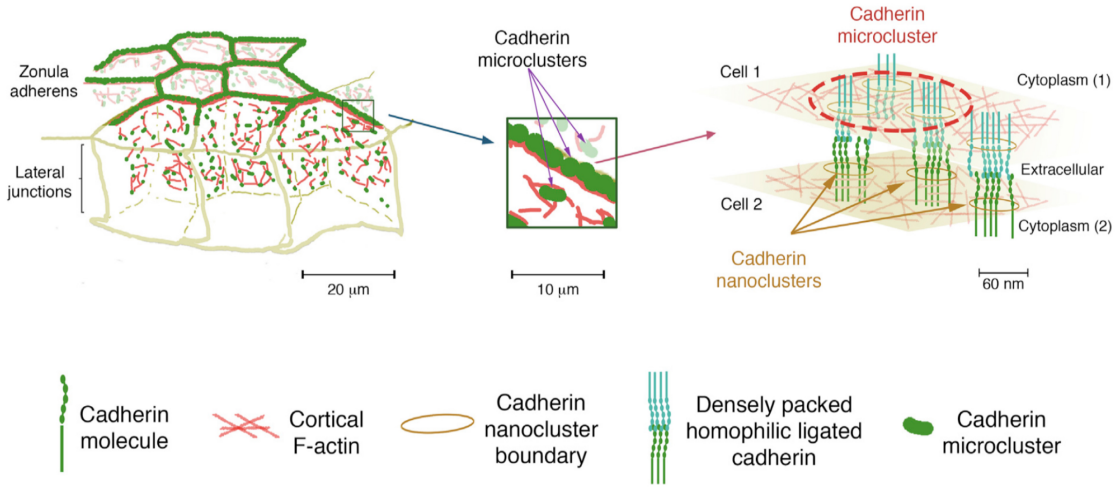


Figure 1.6. E-cadherin complex organization at adherens junctions. E-cadherin complex and cluster organization in epithelial cells at different scales (from Yap et al., 2015). E-cadherin aggregates in so-called nanoclusters, which in turn come together to form microclusters. Microclusters can be found more in a more dispersed manner along the lateral junction or more concentrated at the *zonula adherens*.

E-cadherin distribution at adherens junctions is not homogeneous (Figure 1.6). Confocal imaging of adherens junctions shows that E-cadherin-rich regions are interspersed with regions with little to no E-cadherin. A more detailed superresolution analysis revealed that both human and *Drosophila* E-cadherin organize themselves in nanoclusters of around ~50nm with varying E-cadherin densities at the plasma membrane of epithelial cells (Truong Quang et al., 2013; Wu et al., 2015; Figure 1.6). This organization has been proposed to allow comparatively weak short-lived interactions to co-operate and form stable adhesions (Yap et al., 2015). The details of how E-cadherin organizes itself into nanoclusters and how these nanoclusters come together at the apical-lateral border to form adherens junctions are not fully understood. However, considerable progress has been made to understand how E-cadherin ectodomain and intracellular binding partners contribute to adherens junctions assembly.

Structural analysis of vertebrate E-cadherin showed that it can engage simultaneously in a *trans* interaction to form a strand-swap dimer and in two additional *cis* interactions with other E-cadherin molecules on the same cell surface (Harrison et al., 2011). These interactions can drive purified E-cadherin extracellular domain to assemble a 2D lattice with an E-cadherin density compatible with the one observed in a subset of nanoclusters at adherens junctions (Harrison et al., 2011; Indra et al., 2018; Wu et al., 2015). This suggests a model, where adhesion is mediated by clusters of E-cadherin molecules immobilized through *cis* and *trans* interactions. Furthermore, *cis* interactions have been proposed to slow down additional E-cadherin molecules at the plasma membrane and to promote cluster growth

through accretion (Erami et al., 2015; Wu et al., 2010). A similar mechanism may exist in *Drosophila*, where *cis* interactions have also been found to promote E-cadherin lateral clustering and contribute to nanocluster assembly, even though E-cadherin assumes a different 3D conformation (Chandran et al., 2021). Interestingly, single E-cad molecule tracking in spot junctions of human A431 keratinocyte-like cells showed that individual E-cad molecules retain dynamic behavior with nanoclusters disassembling and E-cad reassembling into new nanoclusters while the junction itself remains globally stable (Indra et al., 2018). Thus, individual E-cadherin molecules or groups of molecules may behave more dynamically within adherens junctions than previously thought.

Nanocluster organization was further shown to depend on the cytoplasmic tail of E-cadherin and its intracellular binding partners, both in *Drosophila* and human cells (Chandran et al., 2021; Truong Quang et al., 2013; Wu et al., 2015). Interactions with actin in particular have been proposed to regulate E-cadherin behavior in multiple ways. Coupling to the dynamic actomyosin network has been proposed to drive E-cadherin packing into nanoclusters (Chandran et al., 2021), to prevent nanocluster fission or disassembly (Truong Quang et al., 2013), to act as a corral spatially restricting E-cadherin to nanocluster-sized regions (Wu et al., 2015), to drive E-cadherin higher order assembly and to stabilize it at adherens junctions (Buckley et al., 2014; Hong et al., 2013). E-cadherin can interact with actomyosin through several actin binding proteins and actomyosin regulators (Mege and Ishiyama, 2017). Specific interaction modes mediated by different proteins, as well as the local organization of the actomyosin network itself, are likely to regulate E-cadherin organization in different ways (Arnold et al., 2017).

EPITHELIAL APICAL-BASAL POLARITY

The emergence of cadherin-mediated cell-cell adhesion was essential for the development of multicellular animal tissues and consequently metazoan species. But it was the coordination of cell adhesion with the stable polarization of cell surfaces that allowed the development of metazoan species with interior spaces or lumens (Niklas and Newman, 2020). In epithelial cells, the asymmetric distribution of dedicated polarity proteins along an apical-basal axis (usually perpendicular to the tissue plane) dictates the polarization of the cytoskeleton, vesicle trafficking and cell surface specialized structures along this same axis (Rodriguez-Boulan and Macara, 2014b). This organization enable cells to perform different functions at distinct cell surfaces. The underlying molecular asymmetry, called apical-basal polarity, enables epithelial cells for example to restrict cell-cell adhesion to specific membrane

domains or absorb and secrete specific molecules at the apical or basal surface. Consequently, apical-basal polarity is essential to determine and sustain tissue architecture and function.

Here, I will focus on apical-basal polarity in metazoan epithelia and control of epithelial form. I will start by giving an overview of the importance of the apical-basal polarity machinery in metazoan species and then focus on epithelia and on the conserved set of core apical-basal polarity proteins. I will discuss how these interact and become polarized in epithelial cells in response to different cues, focusing in particular on apical polarity and the main polarity kinase in epithelia – aPKC. Finally, I will cover how polarity proteins control cell and tissue morphology through adherens junctions and actomyosin.

Apical-basal polarity is essential for development and homeostasis in metazoa

Cell polarity is not an epithelial or even metazoan specific feature, but rather a key feature of most cells that becomes apparent in the asymmetric arrangement of specific molecules along a transient or stable polarity axis and gives rise to asymmetries in form and function. In unicellular bacteria or eukaryotes, specific sets of molecules can create asymmetries that regulate cell growth and morphology, cell division and motility among other things (Chiou et al., 2017; Marshall, 2020; Treuner-Lange and Sogaard-Andersen, 2014). In plants and animals, molecular polarity machineries play important roles in a host of different cell and tissue-level processes that include cell and tissue morphogenesis, asymmetric cell division and differentiation, tissue growth and proliferation, cell migration, nutrient transport and pathogen defense (Butler and Wallingford, 2017; Campanale et al., 2017; Dettmer and Friml, 2011).

Cell polarization is generally mediated by dedicated polarity proteins. These become asymmetrically distributed in response to specific cues and, in turn, dictate the asymmetric organization of cellular structures to support cell morphology and function. Apical-basal polarity proteins are versatile regulators that polarize metazoan epithelial cells (St Johnston and Ahringer, 2010; Table 1.1), as well as other metazoan cell types, such as stem cells undergoing asymmetric cell division (Campanale et al., 2017; Inaba and Yamashita, 2012). Interestingly, apical-basal polarity proteins can support very different cell morphologies and functions, from neurons, that depend on a single polarized cortical domain to extend a single axon (Hakanen et al., 2019), to epithelial cells, that have at least three distinct polarized cortical domains along the apical-basal axis (St Johnston and Ahringer, 2010). The organization of different polarized systems depends on specific subsets of apical-basal

polarity proteins, as well as on the interactions between polarity proteins and cell type-specific proteins or structures.

Table 1.1. Polarity proteins in *Drosophila* and mammalian organisms.

Polarity complex	Protein	*Drosophila* orthologue	Mammalian paralogues	Mammalian gene name
Crumbs	Crumbs	Crumbs (Crb)	Crumbs1	CRB1
			Crumbs2	CRB2
			Crumbs3A, Crumbs3B	CRB3
	Pals1	Stardust (Sdt)	Pals1	MPP5
	PatJ	DPatj	PatJ	INADL
			MUPP1	MPDZ
	Lin7	Lin7	Lin7a	MALS-1/Veli-1
			Lin7b	MALS-2/Veli-2
			Lin7c	MALS-3/Veli-3
Par	Par6	Par6	Par6A (Par6C)	PARD6A
			Par6B	PARD6B
			Par6G	PARD6G
	aPKC	aPKC	aPKCζ	PRKCZ
			aPKCλ/ι	PRKCI
	Par3	Bazooka (Baz)	Par3A	PARD3A
			Par3B (PAR3L)	PARD3B
Scribble	Scribble	Scribble (Scrib)	Scribble	SCRIB
			Lano	LRRC1
			Densin/LAP1	LRRC7
	Dlg	Dlg	DLG1/SAP97	DLG1
			DLG2/PSD93	DLG2
			DLG3/SAP102	DLG3
			DLG4/SAP90	DLG4
			DLG5/P-dlg	DLG5
	Lgl	Lgl	LGL1/Hugl-1	LLGL1
			LGL2/Hgl	LLGL2
Additional polarity proteins	Par1	Par1	Par1a	MARK3
			Par1b	MARK2
			Par1c	MARK1
			Par1d	MARK4
	Par4	Lkb1	LKB1	STK11
	Par5	Par5	14-3-3	YWHA(x)
	Yurt	Yurt	Lulu/YMO1	EPB41L5
			Lulu2/EHM2	EPB41L4B

The core components of the apical-basal molecular machinery were first identified in genetic screens for genes that affect budding in *S. cerevisiae*, asymmetric division of the one cell *C. elegans* embryo or embryonic development in *D. melanogaster* (Adams et al., 1990; Bilder and Perrimon, 2000; Kemphues et al., 1988b; Tepass et al., 1990; reviewed in Assemat et al., 2008; Margolis and Borg, 2005). These proteins were found to be conserved regulators of polarity in metazoan species (Table 1.1). In the *C. elegans* zygote, PAR proteins specify the anterior-posterior body axis by segregating to opposite cortical domains after fertilization and promoting the asymmetric segregation of cell content (Gubieda et al., 2020; Hoege and Hyman, 2013). Polarity proteins also specify the anterior-posterior axis in the *Drosophila* oocyte and regulate embryonic development from the very early stages onwards through polarization of *Drosophila* epithelia (Bastock and St Johnston, 2008; St Johnston and Ahringer, 2010). Similarly, apical-basal polarity emerges early in mammalian development during embryo compaction and regulates further development through tissue polarization (White et al., 2017). Furthermore, apical-basal polarity proteins also contribute to development and homeostasis in metazoa through control of asymmetric cell division and cell fate determination (e.g. trophectoderm specification, neuroepithelia or skin; White et al., 2017; Yamashita et al., 2010), regulation of single or collective cell migration (e.g. wound healing or T-cell migration; Krummel and Macara, 2006; Mayor and Etienne-Manneville, 2016), control of cell and tissue form and function (e.g. neurons or epithelia; Hakanen et al., 2019; Roignot et al., 2013) and regulation of growth and proliferation (Elbediwy et al., 2016; McCaffrey and Macara, 2012).

Due to their extensive involvement in metazoan developmental and homeostatic processes, it is not surprising that apical-basal polarity proteins are generally essential for life in vertebrates and invertebrates. Their discovery in model organisms was predicated on their loss causing extensive developmental problems. In vertebrate models and humans, polarity proteins have also been linked to developmental defects and disease, such as inflammatory bowel disease or retinopathies (Charrier et al., 2015; Dauber et al., 2013; Hirose et al., 2006; Mehalow et al., 2003; Murdoch et al., 2003; Stoll et al., 2004; Whiteman et al., 2014). Furthemore, in *Drosophila* epithelia, loss of polarity was found to trigger overproliferation and loss of tissue architecture, accompanied by changes in transcription profile, which suggested polarity proteins function as tumor suppressors (Bilder, 2004; Bilder et al., 2000; Bunker et al., 2015; Gateff, 1978). As expected, in human and mice models, disruption of epithelial polarity was found to be an early hallmark of many epithelial cancers linked to loss of tissue architecture (Halaoui and McCaffrey, 2015; Halaoui et al., 2017; McCaffrey et al., 2012). Additionally, loss of polarity proteins has been found to contribute to tumourigenesis and metastasis (Banks et al., 2012; Halaoui et al., 2017; Iden et al., 2012; Jung et al., 2019;

Rothenberg et al., 2010; Vorhagen et al., 2018; Xue et al., 2013; Zen et al., 2009; Zhan et al., 2008). However, polarity proteins regulate other processes relevant for tumorigenesis, including cell migration, cell survival and proliferation. And while enforcing tissue architecture is expected to suppress tumour formation, upregulation of growth, survival or migration may have the opposite effect. Accordingly, some vertebrate orthologues of polarity proteins have been found to contribute to tumor development in specific contexts (Iden et al., 2012; Regala et al., 2005; Vorhagen et al., 2018). Thus, the causal relationship between loss of polarity and tumorigenesis has been more difficult to dissect in vertebrates due to the involvement of polarity in multiple processes, as well as the existence of multiple vertebrate orthologues for polarity proteins (Table 1.1; discussed in Fomicheva et al., 2020; Halaoui and McCaffrey, 2015; Saito et al., 2018).

Apical-basal polarity in epithelia

Apical-basal polarity relies on the asymmetric accumulation of polarity proteins at the cell cortex or plasma membrane. In simple epithelia, the accumulation of polarity proteins at specific cortical domains along the apical-basal axis defines at least three distinct cortical domains: 1) the apical domain is defined by the accumulation of members of the Crumbs complex (Crumbs, Patj, Pals1, Lin7) together with aPKC, Par6 and Cdc42; 2) the junctional domain by the accumulation of Par3 and 3) the basolateral domain by the Scribble module (Scribble, Dlg, Lgl) and Par1 (Figure 1.7A; Rodriguez-Boulan and Macara, 2014; St Johnston and Ahringer, 2010). The subcellular localization of the different apical-basal polarity proteins together with findings on their genetic and biochemical interactions led to most of them being grouped into the functionally distinct apical Par (aPKC, Par6 and Par3) and Crumbs complexes and the basolateral Scribble module (Assemat et al., 2008). An additional polarity module composed by Yurt, Coracle, Neurexin-IV and Na+,K+-ATPase was later identified through negative genetic interactions with Crumbs to support basolateral membrane identity (Laprise et al., 2009). Furthermore, a recently published analysis of the polarized *Drosophila* midgut epithelium revealed that these cells polarize independently of most known apical-basal polarity regulators except for integrins, suggesting that additional polarity proteins still have to be discovered (Chen et al., 2018).

The asymmetric distribution of apical-basal polarity proteins relies on mutual antagonism. Early studies in *Drosophila* indicated that the apical Crumbs and lateral Scribble complexes were able to antagonize each other to create distinct cortical domains (Bilder et al., 2003; Tanentzapf and Tepass, 2003). Accordingly, in the absence of apical polarity proteins, basolateral proteins spread to the apical domain and, conversely, loss of basolateral

identity extends the apical domain (Wodarz et al., 2000; Rolls et al., 2003; Hutterer et al., 2004; Harris and Tepass, 2008; Franz and Riechmann, 2010; Fletcher et al., 2012). Modelling approaches further suggested that mutual antagonism by itself is not sufficient for two distinct cortical domains to emerge and indicated that this also relies on cooperation or positive feedback between polarity determinants from the same domain (Fletcher et al., 2012; Goehring et al., 2011; McCusker, 2020). Thus, the current model suggests that epithelial cell polarization is a self-organizing system where apical polarity proteins exclude basolateral determinants through mutual antagonism and co-operate with each other to define the apical domain (Figure 1.7A). Together, polarized polarity proteins regulate epithelial cell shape and function through polarized reorganization of the microtubule and actomyosin networks (Raman et al., 2018), regulation of RhoGTPase activity (Etienne-Manneville and Hall, 2002; Ngok et al., 2014), polarization of vesicle trafficking and membrane phospholipids (Eaton and Martin-Belmonte, 2014; Krahn, 2020; Shivas et al., 2010; van et al., 2020) and regulation of E-cadherin distribution and stability (Harris and Tepass, 2010). Polarization of these structures, in turn, reinforces the localization of polarity proteins creating positive feedback loops that ensure stable cell polarity. Additionally, polarity proteins can link tissue architecture to the control of growth, proliferation and differentiation through the regulation of signaling pathways such as Hippo (Elbediwy et al., 2016; McCaffrey and Macara, 2012).

And how do apical-basal polarity proteins perform their functions? The majority of apical-basal polarity proteins do not have intrinsic catalytic activity. Instead, they work through protein-protein interactions to assemble scaffolds for localized signaling and control of cellular structures. Accordingly, polarity proteins have multiple protein interaction domains that enable them to create extensive interaction networks (Brajenovic et al., 2004; Pires and Boxem, 2018; Riga et al., 2020; Stephens et al., 2018; Tan et al., 2020). Among these interaction domains, PDZ (PSD-95/Dlg/ZO-1) domains are recurrent in cell polarity and often found in tandem repeats in polarity proteins. PDZ domains are relatively promiscuous interaction domains that bind predominantly to short C-terminal motifs, although they can also recognize internal motifs or dimerize. The presence of multiple PDZ domains, as well as other domains, enables polarity proteins to recruit several interactors to distinct cortical domains and polarize cells.

The Crumbs complex in polarity and apical domain assembly

Members of the Crumbs complex are conserved polarity determinants that accumulate at the apical domain of different metazoan epithelia to regulate apical-basal polarity, junction formation and stability, vesicle trafficking, apical surface specializations and the apical cytoskeleton (Margolis, 2018; Rodriguez-Boulan and Macara, 2014; St Johnston and

Ahringer, 2010). Crumbs is a transmembrane protein initially identified as an asymmetrically localized regulator of epithelia in *Drosophila* (Tepass et al., 1990). Its loss was found to prevent apical domain formation and disrupt epithelial organization, while its overexpression expanded the apical domain (Fletcher et al., 2012; Lemmers et al., 2004; Roh et al., 2003; Wodarz et al., 1995). Crumbs extracellular domain is able to interact in *trans*. This interaction has been proposed to contribute to Crumbs localization (Fletcher et al., 2012; Letizia et al., 2013; Roper, 2012). Crumbs intracellular domain is a small (37 aminoacid-long) highly conserved sequence that contains two protein-protein interaction motifs: a membrane proximal FERM (band 4.1/ezrin/radixin/moesin)-binding domain and a C-terminal PDZ-binding motif composed of four aminoacids (Izaddoost et al., 2002; Klebes and Knust, 2000). These domains mediate Crumbs functions through interaction with several proteins.

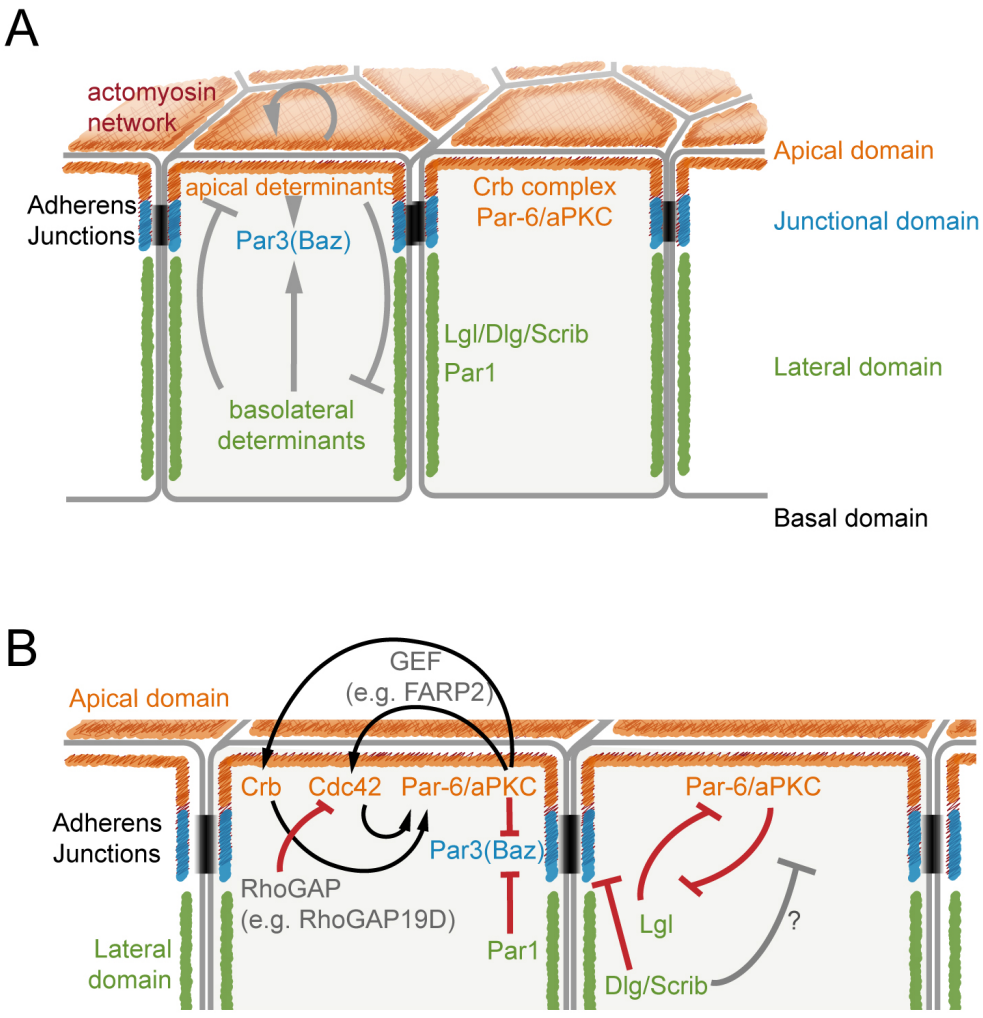


Figure 1.7. Apical-basal polarity in epithelial cells. (A) Simple epithelial cells are polarized along an apical-basal axis with distinct cortical domains defined by the accumulation of specific apical (Crb complex, Par6 and aPKC), basolateral (Scrib module and Par1) and junctional (Par3) polarity determinants. Apical-basal polarization is a self-organized system that relies on mutual antagonism between apical and basolateral polarity determinants and positive feedback between apical determinants. (B) Illustration of specific antagonistic or cooperative interactions

between polarity determinants. Crb and Cdc42 promote apical Par6-aPKC activity and/or localization, while aPKC in turn, promotes apical Crb and Cdc42 function. Cdc42 activity itself is restricted by additional mechanisms to ensure proper polarization. Additionally, Par6-aPKC engage in mutual antagonistic interactions with Lgl and together with Par1 restrict Par3(Baz) localization to the junctional domain. Scrib module components Dlg and Scrib also contribute to adherens junction formation and prevent apical extension through unknown mechanisms.

The FERM-binding domain enables Crumbs to interact with several FERM proteins, including βH-spectrin and ERM proteins, such as Moesin (Medina et al., 2002). These connect the cell membrane to the underlying actin cytoskeleton and serve as scaffolds for cell signalling (Fehon et al., 2010; Liem, 2016). Consequently, they provide a link between cell polarity, the apical cytoskeleton and apical domain morphogenesis. Accordingly, loss of Crumbs3 in mouse epithelia causes defects in microvili formation and apical membrane blebs (Charrier et al., 2015; Whiteman et al., 2014). Furthermore, Crumbs interaction with Moesin has also been suggested to contribute to Crumbs localization and dynamic behavior (Aguilar-Aragon et al., 2020; Bajur et al., 2019; Fletcher et al., 2012) and to regulate cell shape and the actomyosin network during morphogenesis in flies (Flores-Benitez and Knust, 2015; Klose et al., 2013; Letizia et al., 2011; Salis et al., 2017). The Crumbs FERM-binding domain also binds directly to the upstream Hippo pathway regulator Expanded and recruits it to the apical domain of epithelial cells to regulate cell proliferation (Chen et al., 2010; Grzeschik et al., 2010; Ling et al., 2010). Accordingly, loss of Crumbs upregulated Hippo pathway targets and induced overproliferation in flies. Additionally, the FERM-binding domain also binds to the FERM protein Yurt, which has been proposed to function as a negative regulator of Crumbs (Laprise et al., 2006).

The Crumbs PDZ-binding motif mediates Crumbs complex formation by binding to Pals1 (protein associatetd with lin seven-1, also known as multi-PDZ protein MPP5; Stardust in *Drosophila*; Bachmann et al., 2001; Hong et al., 2001; Hurd et al., 2003; Klebes and Knust, 2000). Pals1 is a MAGUK protein, with a PDZ, a Src homology 3 (SH3) and a guanylate kinase (GUK) domains, all required to bind Crumbs with high affinity (Koch et al., 2016; Li et al., 2014). Pals1 is an adaptor that connects Crumbs simultaneously to Patj (Pals1-associated tight junction protein) and Lin-7 through its two N-terminal L27 domains (Roh et al., 2002). PatJ, in turn, is a scaffold protein with multiple PDZ domains that can interact with tight junction proteins and possibly scaffold their assembly (Adachi et al., 2009; Michel et al., 2005). Accordingly, in vertebrates, the Crumbs complex is particularly enriched at the apical margin immediately above tight junctions (Makarova et al., 2003; Shin et al., 2005; Tan et al., 2020) and loss of Crumbs affects tight junction formation (Shin et al., 2005; Straight et al., 2004), while induction of Crumbs expression can trigger tight-junction formation (Fogg et al., 2005). In vertebrate cell lines, Patj also binds to Angiomotin, which targets RICH1, a Cdc42 GAP, to

tight junctions. These proteins are both required for Crumbs-mediated tight junction maintenance (Wells et al., 2006).

The Crumbs PDZ-binding motif is essential for cell polarity, not only through Pals1 binding, but also through interaction with the Par complex. To specify the apical domain in epithelial cells, Crumbs recruits the apical polarity kinase aPKC and its adaptor Par6 to the apical domain and promotes their activity (Figure 1.7B; Hayase et al., 2013; Hurd et al., 2003; Morais-de-Sa et al., 2010; Nunes de Almeida et al., 2019; Schluter et al., 2009; Sherrard and Fehon, 2015; Walther and Pichaud, 2010). Several direct interactions between members of Crumbs and Par complexes have been reported, which could mediate aPKC and Par6 apical recruitment, including between Par6 and Pals1 or Patj (Hayase et al., 2013; Hutterer et al., 2004; Krahn et al., 2010; Nam and Choi, 2003; Penkert et al., 2004; Wang et al., 2004). However, Par6 can also interact directly with the Crumbs PDZ-binding motif (Dong et al., 2020; Lemmers et al., 2004; Whitney et al., 2016) and at least in some contexts, Crumbs-dependent aPKC activity does not require Pals1 (Nunes de Almeida et al., 2019; Walther and Pichaud, 2010). Thus, it remains unknown whether and how other members of the Crumbs complex contribute to aPKC-mediated apical domain formation.

Interactions between the Crumbs and Par complexes enable them to cooperate in the specification of apical polarity. Moreover, Crumbs can also promote apical identity through regulation of Rho GTPase activity and membrane phospholipid composition. In vertebrate cells, Ezrin, an ERM protein that binds to Crumbs, recruits the GEF Dbl3 to the apical domain to activate the apical determinant Cdc42 and promote apical identity (Zihni et al., 2014). Furthermore, in *Drosophila* embryos, Crumbs has been shown to promote apical domain identity through a mutually antagonistic relationship with basolateral Rac1 and the PIP_3 producing PI3K (Chartier et al., 2011). In polarized epithelial cells, the basolateral membrane is typically enriched in PIP_3 and the apical membrane in PIP_2. Interestingly, ectopic insertion of PIP_3 at the apical surface or PIP_2 at the basolateral surface of MDCK cysts was sufficient to recruit polarity proteins from the opposing domain (Gassama-Diagne et al., 2006; Martin-Belmonte et al., 2007), indicating that membrane composition feeds back into cell polarity. Thus, Crumbs also ontributes to cell polarity through membrane phospholipid asymmetry. Additionally, in *Drosophila* salivary glands, Crumbs has also been shown to regulate apical phospholipid composition through lipid phosphatases Pten and OCRL (Lattner et al., 2019). Moreover, Crumbs also directs apical secretion (Lattner et al., 2019). Since Crumbs itself is also targeted to the apical domain by dynein-mediated transport (Aguilar-Aragon et al., 2020; Li et al., 2008), this may provide a positive feedback loop to maintain the apical domain. Thus, vesicle trafficking and membrane phospholipids also contribute to Crumbs-mediated cell polarization, although the exact molecular mechanisms remain unclear.

Through its many interactors, Crumbs regulates cell polarity, apical morphogenesis and cell proliferation. Interestingly, loss of Crumbs or its binding partners does not affect all epithelia to the same extent even within the same species (Penalva and Mirouse, 2012; Tepass and Knust, 1990). This suggests that different epithelia can be more or less dependent on specific Crumbs functions, and therefore interactors, for example to assemble specialized apical domains (e.g. photoreceptors; Pellikka et al., 2002; Pichaud, 2018) or maintain apical-basal polarity in epithelia undergoing extensive cell remodelling during morphogenetic events (Campbell et al., 2009). However, we still do not know how different Crumbs interactors and functions are coordinated in space and time to support epithelial functions. It will be interesting to know the extent to which Crumbs engages with different interactors simultaneously, how stable these protein assemblies are and how essential or redundant different interactions are. A crystal structure of Crumbs3 cytosolic tail bound to Moesin, shows that binding to Moesin through the FERM domain and to Pals1 through the PDZ-binding domain cannot happen simultaneously (Wei et al., 2015), suggesting that Crumbs engages in mutually exclusive interactions. Accordingly, in the *Drosophila* follicular epithelium, Crumbs colocalizes with aPKC and Moesin in different regions of the apical domain (Sherrard and Fehon, 2015) and super-resolution imaging of apical polarity determinants in vertebrate epithelia revealed that Crumbs3 shows little association with Patj-Pals1 or aPKC-Par6 (Mangeol et al., 2020). This suggests that the apical domain of epithelial cells is not homogeneous and subsets of Crumbs and its interactors likely mediate specific functions at distinct subcellular apical domains.

Par complex localization and aPKC activation

The Par (Partitioning defective) proteins Par3 (Bazooka in *Drosophila*) and Par6 were initially identified in a genetic screen for maternal effect lethal mutations that disrupted early asymmetries in the *C. elegans* embryo (Kemphues et al., 1988a; Kemphues et al., 1988b). Together with aPKC, they form the conserved Par complex essential for apical domain identity in epithelial cells (Horikoshi et al., 2009; Hung and Kemphues, 1999; Hutterer et al., 2004; Izumi et al., 1998; Martin-Belmonte et al., 2007; Suzuki et al., 2001; Tabuse et al., 1998). Additionally, members of the Par complex are also involved in tight junction and adherens junction assembly (Harris and Peifer, 2007; Suzuki et al., 2001; Totong et al., 2007), spindle orientation (Dias Gomes et al., 2019; Hao et al., 2010), and regulation of cell survival and tissue growth (Ahmed and Macara, 2017; Grzeschik et al., 2010; Warner et al., 2010).

aPKC is the main apical polarity kinase (Hong, 2018). It is a serine/threonine kinase that belongs to the PKC family (Steinberg, 2008). However, unlike other PKCs, which are regulated by phospholipid binding and Ca^{2+}, aPKC is generally regulated by protein-protein

interactions. aPKC has a pseudosubstrate domain that inhibits its own C-terminal kinase domain (Zhang et al., 2014). An N-terminal PB1 domain interacts directly with a similar domain on Par6 (Joberty et al., 2000; Li et al., 2010; Lin et al., 2000; Qiu et al., 2000). Par6 functions as a stable binding partner and adaptor that mediates most physical interactions to localize aPKC and controls its kinase activity. In addition to the aPKC-binding domain, Par6 also has a Cdc42/Rac-interactive binding (CRIB) domain, that binds to the apical regulator Cdc42, and a single PDZ binding domain, that can bind members of the Crumbs complex and Par3 (Li et al., 2010). Par3 is a scaffold with an N-terminal oligomerization domain (Feng et al., 2007; Zhang et al., 2013), three PDZ domains, a phospholipid binding domain (Claret et al., 2014; Krahn et al., 2010; Wu et al., 2007) and an aPKC binding domain that binds to the aPKC kinase domain (Suzuki et al., 2001). Thus, aPKC, Par6 and Par3 can interact directly with each other to form the Par complex.

In vertebrate and invertebrate models, Par3 has been found to target aPKC and Par6 to the apical domain (Franz and Riechmann, 2010; Harris and Peifer, 2005; Horikoshi et al., 2009). But, after initial recruitment, Par3 is not found to colocalize with Par6 and aPKC in epithelia: while Par3 accumulates at apical junctions, aPKC and Par6 are at the apical domain (Mangeol et al., 2020; St Johnston and Ahringer, 2010; Tan et al., 2020). This separation of Par3 from Par6-aPKC depends on aPKC activity. aPKC phosphorylates Par3 on its conserved aPKC binding domain at Ser827 (Figure 1.7; Ser980 in *Drosophila*; Morais-de-Sa et al., 2010; Nagai-Tamai et al., 2002; Walther and Pichaud, 2010). This phosphorylation disrupts the interaction between aPKC and Par3. However, this is not sufficient to separate Par3 from aPKC and Par6, presumably due to the interaction between Par6 and Par3 PDZ domains. Crumbs PDZ-binding motif was shown to compete with Par3 for Par6-aPKC and consequently the specific presence of Crumbs in epithelial cells releases Par3 from the apical Par complex(Morais-de-Sa et al., 2010). Additionally, Par6 interaction with active Cdc42 is also required for this process *in vivo* (Nunes de Almeida et al., 2019; Walther and Pichaud, 2010). Structural and biochemical studies showed that Cdc42 binding to the Par6 CRIB domain allosterically regulates the affinity of the PDZ domain for Par6 binding partners (Peterson et al., 2004; Whitney et al., 2011). Interestingly, Cdc42 specifically enhances Par6 binding to Crumbs C-terminal PDZ-binding motif, but not to the internal Par6 PDZ-binding motif of Pals1 (Hutterer et al., 2004; Penkert et al., 2004; Whitney et al., 2016), suggesting that Cdc42 can direct Par6 to specific binding partners and may help Crumbs outcompete Par3. Additionally, Cdc42 has also been reported to separate aPKC-Par6 from junctional Par3 through an MRCK-dependent increase in apical actomyosin contractility (Zihni et al., 2017).

Modulation of Par3 affinity for aPKC has also been suggested to regulate Par complex disassembly. Par3 has been proposed to function as both a substrate and an inhibitor of aPKC (David et al., 2013; Rodriguez et al., 2017). A structural analysis of vertebrate aPKC bound to

the aPKC binding domain of Par3 suggested that the aPKC phosphorylation site is flanked by two conserved regions that bind with high affinity to aPKC and enable it to function as an inhibitor (Soriano et al., 2016). Consequently, modulation of Par3-aPKC binding affinity was proposed to turn Par3 from an inhibitor to a good substrate. However, it remains unclear whether and how Par3-aPKC affinity could be regulated *in vivo* (Holly and Prehoda, 2019). Alternative interaction domains may also contribute to regulate the Par3-Par6-aPKC complex. A recent study identified a novel conserved C-terminal PDZ-binding domain in aPKC that interacts directly with Par3 PDZ2 (Holly et al., 2020). This interaction is not disrupted by aPKC phosphorylation and consequently is proposed to mediate the formation of a stable complex. However, its relevance in epithelial cells is unknown. A similar conserved motif was identified on the C-terminus of Par6 and found to interact with Par3 (Renschler et al., 2018). But, although this motif contributes to Par6 localization in the *Drosophila* embryonic epithelium, its deletion did not compromise embryo viability and the relevance of this interaction in epithelial cells remains unclear. Curiously, analysis of recent Par3 mutant alleles in *Drosophila* suggested that Par3 is not essential for apical-basal polarization in the *Drosophila* follicular epithelium and consequently that redundant pathways may target Par6-aPKC to the apical domain (Shahab et al., 2015).

Besides regulation of aPKC localization, Par6, Cdc42 and Crumbs have also been proposed to regulate aPKC activity. *In vitro* assays with purified components suggested that Par6 binding inhibits aPKC activity (Atwood et al., 2007; Joberty et al., 2000; Lin et al., 2000; Qiu et al., 2000; Yamanaka et al., 2001). Additional binding of Cdc42 to Par6 was shown to be essential to relieve Par6 inhibition and promote aPKC activation *in vitro*. However, Par6 is known to bind potential aPKC inhibitors, such as Par3 and Lgl (Hutterer et al., 2004; Soriano et al., 2016; Wirtz-Peitz et al., 2008; Yamanaka et al., 2006), that may have been co-purified from cells in these assays. Paradoxically, Par6 binding has also been suggested to activate aPKC in a Cdc42-independent manner through allosteric conformational changes that displace the aPKC pseudosubstrate domain and relieve aPKC auto-inhibition (Graybill et al., 2012). A recent study in mammalian HEK293 and *Drosophila* cells identified a polybasic domain within aPKC's pseudosubstrate domain capable of binding to membrane phospholipids PIP and PIP_2 (Dong et al., 2020). When Par6 or its aPKC binding domain were co-expressed with aPKC in cells, this polybasic domain targeted aPKC to the plasma membrane, suggesting that Par6 does displace the pseudosubstrate domain independently of Cdc42. However, phosphorylation of a known aPKC substrate, Lgl, in cells further required the co-expression of Crumbs, suggesting that pseudosubstrate displacement is not enough to activate aPKC. Thus, further biochemical and structural studies are required to understand how Par6, Cdc42 and Crumbs regulate aPKC activation.

Since Cdc42 is able to promote aPKC activity through its proper localization and/or activation, it is essential that Cdc42 activity itself is spatially controlled in epithelial cells along the apical-basal axis. Cdc42 activity itself can be spatially regulated by RhoGAPs and RhoGEFs (see section on RhoGTPase regulation). In vertebrate epithelial cells, apical ERM protein Ezrin activates Cdc42 through its GEF Dbl3 (Zihni et al., 2014). Additionally, apical recruitment of Tuba also contributes to apical Cdc42 activity in Caco-2 cells and MDCK cysts (Bryant et al., 2010; Otani et al., 2006; Qin et al., 2010). In *Drosophila*, RhoGAP19D was recently identified as a Cdc42 GAP that accumulates at the lateral cell membrane and prevents apical domain expansion by restricting Cdc42 and downtream aPKC-Par6 activation (Fic et al., 2021).

aPKC is a positive regulator of Crumbs and excludes basolateral determinants

Establishment of polarized cortical domains relies on the ability of apical and basolateral polarity proteins to mutually antagonize each other. Accordingly, loss of aPKC or related apical polarity proteins leads to loss of apical domain identity and spreading of the basolateral domain, while constitutive aPKC activity extends the apical domain and suppresses basolateral identity in vertebrates and invertebrates (Chalmers et al., 2005; Fletcher et al., 2012; Franz and Riechmann, 2010; Grifoni et al., 2007; Hutterer et al., 2004; Rolls et al., 2003; Wodarz et al., 2000). However, our understanding of how apical and basolateral polarity protein functions are integrated at the molecular level to polarize epithelial cells remains incomplete, notwithstanding the well-documented mutually antagonistic relationship between aPKC and the basolateral determinant Lgl (Figure 1.7B). aPKC contributes to cell polarization by phosphorylating downstream targets to reinforce apical domain identity and exclude basolateral polarity determinants. In particular, aPKC is proposed to antagonize basolateral identity through Lgl, one of the best characterized substrates of aPKC. aPKC phosphorylates Lgl to exclude it from the apical domain and restrict it to the basolateral domain (Hutterer et al., 2004; Plant et al., 2003; Yamanaka et al., 2003). Consequently, in its absence, Lgl extends apically. Lgl localization to the plasma membrane depends on electrostatic interactions between the highly positive polybasic (also called basic and hydrophobic) domain and negatively charged phosphoinositides (Bailey and Prehoda, 2015; Dong et al., 2015; Heo et al., 2006). aPKC phosphorylation sites on Lgl are concentrated in the polybasic domain and phosphorylation of three serines in this region is sufficient to disrupt electrostatic interactions with plasma membrane phosphoinositides, effectively impairing cortical recruitment of Lgl (Almagor et al., 2019; Bailey and Prehoda, 2015; Dong et

al., 2015). This mechanism enables aPKC to inhibit Lgl-mediated basolateral domain expansion. However, it remains unclear how additional Scribble module components are excluded from the apical domain. aPKC can also phosphorylate Dlg, but the impact of this phosphorylation in epithelial cells is unclear (Golub et al., 2017; Lu et al., 2021). Interestingly, phosphorylation of the same sites on Lgl has been shown to promote binding of an Lgl peptide to vertebrate Dlg4, suggesting that aPKC may modulate interactions between members of the Scribble module (Zhu et al., 2014). In addition to Lgl, aPKC activity also excludes Par1, another basolateral determinant. Phosphorylation of Par1 by aPKC promotes 14-3-3 binding and displaces it from the cortex, restricting Par1 activity (Doerflinger et al., 2010; Hurov et al., 2004; Kusakabe and Nishida, 2004; Suzuki et al., 2004).

aPKC activity has also been proposed to reinforce apical domain identity through Crumbs, although the precise mechanism remains unclear (Figure 1.7B). aPKC phosphorylates Crumbs FERM domain in vitro and these phosphorylation sites were reported to contribute to Crumbs apical localization and epithelial organization in flies (Fletcher et al., 2012; Sotillos et al., 2004), possibly by modulating Crumbs binding to specific partners (Wei et al., 2015). However, recent analysis of phosphomimetic and phosphodefective Crumbs mutants knocked into the endogenous *crumbs* locus in flies indicates that Crumbs phosphorylation by aPKC is not required for viability, fertility or apical-basal organization (Cao et al., 2017). Consequently, the relevance of Crumbs phosphorylation under physiological conditions remains unclear. But aPKC may also regulate Crumbs functions through phosphorylation of Crumbs interactors. aPKC can phosphorylate and negatively regulate Yurt (Gamblin et al., 2014; Nakajima and Tanoue, 2011). This has been suggested to impair Yurt oligomerization and interaction with Crumbs (Gamblin et al., 2018). In turn, Yurt also antagonizes aPKC to restrict apical domain expansion (Gamblin et al., 2014). Furthermore, aPKC can also promote apical identity through localized Cdc42 activity. In human epithelial cell lines, aPKCι phosphorylates the Cdc42 GEF FARP2, to activate Cdc42 locally and promote cell polarity (Elbediwy et al., 2019). In addition, aPKC may also promote the accumulation of Cdc42 GEFs indirectly through Ezrin (Wald et al., 2008; Zihni et al., 2014).

Curiously, analysis of aPKC hypomorphic alleles in *Drosophila* suggested that aPKC kinase activity is not absolutely essential in the *Drosophila* follicular epithelium, unlike in other epithelia and that redundant mechanisms may exist to compensate for loss of aPKC (Kim et al., 2009). A recent screen of Cdc42 effectors suggested that Pak1 may compensate for loss of aPKC and phosphorylate aPKC substrates (Aguilar-Aragon et al., 2018). However, Pak1 does not accumulate asymmetrically at the apical domain and it remains unclear how its activity is coordinated with aPKC.

The Scribble module restricts apical domain assembly

The basolateral domain of epithelial cells is characterized by the accumulation of the conserved Scribble module components: Scribble, Lethal giant larvae (Lgl) and Discs large (Dlg). Loss of these proteins in *Drosophila* embryos impairs epithelial polarization and leads to overproliferation, which suggested that they are tumor suppressors (Bilder, 2004; Bilder et al., 2000; Bilder and Perrimon, 2000; Gateff, 1978). During cellularization in *Drosophila* embryos they are recruited to the lateral membrane, where they are required to exclude apical polarity determinants and promote the coalescence of spot adherens junctions into the apical belt-like junctions (Bonello and Peifer, 2019). Additionally, Dlg and Scribble also localize at and are required to assemble septate and tricellular junctions (Sharifkhodaei et al., 2019; Zeitler et al., 2004). The similar phenotypes observed upon loss of Lgl, Dlg or Scribble, their complete or partial colocalization and interdependency for proper localization and function suggested that they function in the same pathway to antagonize apical polarity determinants and led to them being grouped into the Scribble module or complex.

In vertebrates, Scribble module components also localize at the basolateral domain, overlapping with adherens junctions (Laprise et al., 2004; Metais et al., 2005; Navarro et al., 2005; Qin et al., 2005; Yamanaka et al., 2006; Yamanaka et al., 2003). Loss of Scribble components is associated with defects in junction formation and stability. However, their depletion frequently leads to milder effects in cell polarity, likely due to the existence of multiple paralogues that may compensate for each other (Table 1.1). Accordingly, a recent study showed that vertebrate Scribble functions redundantly with two related proteins, Erbin and Lano (Choi et al., 2019). In human DLD1 cells, any of these three proteins was sufficient to support cell polarity, while loss of all three resulted in loss of polarity with aPKC, Par6, Pals1 and Lgl mislocalization.

Scribble, Dlg and Lgl have multiple protein interaction domains (Bonello and Peifer, 2019; Stephens et al., 2018). Scribble, together with Erbin and Lano, belongs to the leucine-rich and PDZ (LAP) family of proteins. All LAP proteins have an N-terminal leucine-rich repeats (LRR) domain and LAP-specific domain that are sufficient to target Scribble to the basolateral domain and rescue cell polarity (Albertson et al., 2004; Choi et al., 2019; Legouis et al., 2003; Zeitler et al., 2004). Consistent with this, these domains are sufficient for the formation of a Dlg-Scrib complex in the *Drosophila* follicular epithelium (Ventura et al., 2020). Additionally, Scribble also has four PDZ domains that are associated with targeting to septate junction formation and their assembly (Albertson et al., 2004; Sharifkhodaei et al., 2019; Zeitler et al., 2004) and a palmytoilation motif (Chen et al., 2016). Vertebrate Scribble also associates with ZO-2, suggesting that it may also play a role in vertebrate tight junctions (Metais et al., 2005).

Additionally, vertebrate Scribble C-terminus also contains a spectrin binding motif (Boeda and Etienne-Manneville, 2015). Dlg is a member of the MAGUK family of proteins that contains three N-terminal PDZ domains, followed by an SH3 domain and a C-terminus GUK domain. Lgl has several WD40 repeats, which form a double β-propeller domain that usually acts as a protein interaction scaffold (Schapira et al., 2017). Despite the evidence that Scribble, Dlg and Lgl are interdependent and function as part of a module to promote basolateral identity and restrict apical polarity, there is limited indication that they function as a stable ternary complex in epithelial cells. Dlg can interact indirectly with Scribble through Guk-holder (Mathew et al., 2002), but Guk-holder appears to be dispensable for epithelial polarity (Khoury and Bilder, 2020; Lu et al., 2021). Dlg can also interact with an Lgl peptide *in vitro* (Zhu et al., 2014). Additionally, Lgl can interact with the Scribble LAP-specific domain (Abedrabbo and Ravid, 2020; Choi et al., 2019). However, the relevance of these interactions *in vivo* is unclear.

Scribble module targeting to the basolateral domain and septate junctions is not well understood. Scribble and Dlg appear to consistently function upstream of Lgl to promote its cortical localization both in vertebrates and invertebrates. However, recent work suggested that Lgl cortical localization is not promoted by direct binding but instead by their role to prevent ectopic phosphorylation of Lgl in the lateral domain (Khoury and Bilder, 2020; Ventura et al., 2020). Moreover, the hierarchy of Scrib module components seems to vary in distinct cell types. In the *Drosophila* midgut, Scribble is essential to recruit both Dlg and Lgl to septate junctions (Chen et al., 2018), while in the *Drosophila* embryonic and follicular epithelia Dlg is suggested to be upstream of Scrib and promote its recruitment to the basolateral membrane (Bilder et al., 2000; Khoury and Bilder, 2020; Ventura et al., 2020). In the latter, Dlg recruitment to the cell cortex was recently shown to be mediated by a polybasic domain in the Dlg SH3 domain that is able to interact with membrane PIP_2 and PI4P (Lu et al., 2021). This interaction cooperates with the Dlg PDZ domains to promote robust cortical localization.

The Scribble module is believed to prevent apical domain expansion through Lgl-mediated Par complex inhibition in vertebrates and invertebrates (Hutterer et al., 2004; Yamanaka et al., 2006; Yamanaka et al., 2003). Lgl can bind to Par6 and aPKC to form a complex separate from Par3 (Betschinger et al., 2003; Wirtz-Peitz et al., 2008; Yamanaka et al., 2003). This complex is robustly detected in co-immunoprecipitations. In addition, Lgl depletion leads to increased interaction of aPKC with Par3 and Cdc42 (Yamanaka et al., 2006). Furthermore, Lgl binding has been shown to inhibit aPKC activity *in vitro* (Atwood and Prehoda, 2009). This suggests a model in which Lgl competes with Par3 and Cdc42 for Par6-aPKC binding and restrains aPKC activity through the formation of an inactive complex. Upon activation, aPKC phosphorylates Lgl and releases itself from Lgl (Graybill et al., 2012). Alternatively, Lgl may simply compete with other aPKC substrates and in this way decrease

their phosphorylation by aPKC. In addition to Par6-aPKC inhibition by Lgl, basolateral proteins have also been suggested to promote Crumbs recycling from the lateral cortex to the apical domain in *Drosophila* (Fletcher et al., 2012), possibly through Scribble-mediated regulation of retromer and cargo sorting (de Vreede et al., 2014). In *C. elegans* Scribble has also been proposed to regulate protein trafficking through a somewhat different mechanism that involves Rab10-mediated endocytic recycling (Liu et al., 2018), but further work is required to understand how Scribble may contribute to cell polarity through vesicle trafficking. Additionally, aPKC levels are downregulated by the *Drosophila* E3 ligase Slimb (Morais-de-Sa et al., 2014; Skwarek et al., 2014), however it is unclear whether Slimb intersects with the Scribble module.

Apical and basolateral polarity proteins restrict Par3 to direct adherens junction localization, assembly and regulation

Par3 accumulates at the junctional domain to localize and regulate adherens junctions. Analysis of *Drosophila* embryo development revealed that Par3 functions as a landmark for adherens junction localization. During cellularization, Par3 accumulates at the prospective junctional domain independently of E-cadherin and directs the assembly of adherens junctions (Harris and Peifer, 2004; McGill et al., 2009). In the absence of Par3, small E-cadherin clusters fail to localize properly and do not expand into belt-like adherens junctions that encircle epithelial cells at the apex of their lateral membrane, similar to *C. elegans* (Achilleos et al., 2010). Later in development, during germband extension, ROCK (Rok in *Drosophila*) phosphorylates Par3 to exclude it from shrinking adherens junctions and planar polarize β-catenin *(Simoes et al., 2010)*. Adherens junctions, in turn, can also shift position and recruit Par3 (Weng and Wieschaus, 2017), suggesting that they also control Par3. This may involve a direct interaction between Par3 and Echinoid or β-catenin (Wei et al., 2005). Cdc42 effector Pak4 (p21-activated kinase), Canoe (*Drosophila* Afadin) and Polychaetoid (*Drosophila* ZO-1) also accumulate at adherens junctions and promote Par3 localization and junction stability (Manning et al., 2019; Walther et al., 2018; Walther et al., 2016). However, it is unknown if these proteins mediate Par3 localization at adherens junctions directly. Furthermore, in vertebrate epithelia, Par3 has been found to associate directly with nectins and tight junction components, such as JAMs, to promote tight and adherens junction assembly (Ebnet et al., 2001; Itoh et al., 2001; Ooshio et al., 2007; Takekuni et al., 2003).

Par3 has to be specifically targeted to the apical-lateral border to ensure that junctions form at the correct location (Figure 1.7B). In *Drosophila* epithelia, ectopic Baz accumulation has been shown to be sufficient to recruit the E-cadherin/catenin complex (Morais-de-Sa et al., 2010; Walther and Pichaud, 2010). Par3 localization at the junctional domain depends on

its ability to oligomerize and to bind phospholipids, in particular PIP_2 (Benton and St Johnston, 2003; Claret et al., 2014; Feng et al., 2007; Krahn et al., 2010; Kullmann and Krahn, 2018; McKinley et al., 2012; Mizuno et al., 2003). In the *C. elegans* one cell embryo, Par3 oligomers become polarized through advection associated to polarized cortical actomyosin flows (Dickinson et al., 2017; Goehring et al., 2011; Rodriguez et al., 2017). However, in epithelial cells it remains unclear if Par3 oligomerization and membrane association are required to target Par3 or to retain it at the junctional domain. Additional Par3 protein interaction domains have also been suggested to contribute to Par3 localization (McKinley et al., 2012).

Apical and basolateral polarity are both essential to position Par3 correctly along the apical-basal axis. At the apical domain, aPKC phosphorylates Par3 to release it from the Par complex and restrict its localization. Par3 phosphorylation disrupts binding to aPKC (Morais-de-Sa et al., 2010; Walther and Pichaud, 2010) and Stardust (Krahn et al., 2010) and promotes Par3 junctional accumulation. Accordingly, phosphodefective Par3 (BazS980A) was shown to accumulate at the apical domain of *Drosophila* epithelia and promote apical junction assembly (Morais-de-Sa et al., 2010; Walther and Pichaud, 2010). Par3 basolateral exclusion is driven by microtubule-dependent transport and the conserved basolateral kinase Par1. At the basolateral domain, Par1 phosphorylates Par3 to promote 14-3-3 binding and inhibit Par3 oligomerization and interaction with aPKC (Benton and St Johnston, 2003; Hurd et al., 2003). Accordingly, phosphodefective Par3 (BazS151A, S1085A) forms clusters at the basolateral domain of epithelial cells (Benton and St Johnston, 2003) and loss of Par1 results in E-cadherin accumulation at the basolateral surface of the *Drosophila* embryo (Bayraktar et al., 2006). Interestingly, aPKC also colocalizes with ectopic Par3 accumulations at the basolateral side, suggesting that Par1 may also phosphorylate Par3 to restrict apical domain identity. Additionally, Par3 was also found to be transported from the basal to apical region in a dynein-dependent manner along microtubules (Harris and Peifer, 2005; McKinley and Harris, 2012). Par1 also promotes Par3 polarization through microtubule-dependent transport, possibly through microtubule organization (Doerflinger et al., 2003) or endocytosis (Jouette et al., 2019). This has been proposed to trigger a positive feedback loop that promotes microtubule-dependent Par3 polarization and Par3-dependent centrosome polarization (Jiang et al., 2015; Schmoranzer et al., 2009). Interestingly, Par1 levels can be modulated to regulate adherens junction position along the apical-basal axis and control morphogenesis. During *Drosophila* dorsal fold formation, decreased Par1 activity causes a basal shift in adherens junction position in specific cells while neighbour cells maintain adherens junctions apically (Wang et al., 2012). This difference in junction position between neighbour cells results in fold formation.

Additional mechanisms are believed to spatially restrict adherens junctions, due to the mild phenotype associated with Par1 mutants (Doerflinger et al., 2003). A recent study in the

Drosophila embryo, reports a new role for Scribble and Dlg in preventing Par3 accumulation at the basolateral domain (Bonello et al., 2019). During cellularization, Scrib and Dlg were found to accumulate at adherens junctions upstream of Par3, exclude Par3 from the basolateral domain and contribute to adherens junctions assembly. Dlg depletion resulted in Par1 mislocalization. However, Par1 loss was found to only partially mimic the loss of Scrib or Dlg phenotype, suggesting an additional role for Scrib and Dlg in junction assembly.

At the junctional domain, Par3 promotes E-cadherin/catenin nanocluster organization (Truong Quang et al., 2013) and adherens junction assembly (Harris and Peifer, 2004; McGill et al., 2009). This involves regulation of the underlying actomyosin cytoskeleton. In the *Drosophila* embryo, Par3 recruits the synaptotagmin-like PIP_2-binding Bitesize to adherens junctions (Pilot et al., 2006). Bitesize, in turn, recruits Moesin to promote actin belt organization and stabilize adherens junctions. In vertebrate epithelia, Par3 also binds to the Rac GEF Tiam1 to downregulate local Rac1 activity (Chen and Macara, 2005; Mertens et al., 2005) and interacts with Lim kinase 2 to enhance cofilin-mediated actin severing (Chen and Macara, 2006). Furthermore, Par3 functions as a scaffold to dock the exocyst complex and target E-cadherin exocytosis (Ahmed and Macara, 2017).

Par3 may also contribute to regulate adherens junctions through protein dephosphorylation. Par3 itself is dephosphorylated by PP1 and PP2A and may contribute to target them to junctions to regulate additional adherens junction components (Krahn et al., 2009; Traweger et al., 2008; Yamashita et al., 2020). Furthermore, Par3 also binds to Pten (Feng et al., 2008), which may regulate binding of junctions components and create a positive feedback loop to promote Par3 localization through its phospholipid binding domain.

Polarity proteins regulate adherens junction tension, remodelling and recycling

Adherens junctions are dynamic assemblies that integrate and balance mechanical forces and readjust themselves to maintain tissue integrity. Increasing evidence indicates that polarity proteins not only position adherens junctions along the apical-basal axis through Par3, but also promote the assembly and regulate the continuous belt-like *zonula adherens* through endocytosis and actomyosin regulation (Coopman and Djiane, 2016). Accordingly, E-cadherin and β-catenin display different dynamics in polarized versus unpolarized epithelial cells (Huang et al., 2011).

Crumbs and PatJ have been shown to regulate junctional actomyosin through Rho activation both in vertebrates and invertebrates. In MDCK cultured cells, the Crumbs complex recruits p114RhoGEF, a Rho activator, to the apical junctions (Loie et al., 2015; Nakajima and

Tanoue, 2011; Terry et al., 2011). Here, the vertebrate Yurt homolog, Lulu2, activates p114RhoGEF to promote junctional actomyosin assembly. Similarly, in the *Drosophila* embryo, PatJ and Par3 interact with the p114RhoGEF homolog Cysts to promote junctional myosin accumulation downstream of Crumbs through Rho activity (Silver et al., 2019). Additionaly *Drosophila* Patj was shown to associate with myosin phosphatase, and suggested to inhibit it to increase myosin phosphorylation and junctional tension (Sen et al., 2012). Interestingly, the Cdc24-aPKC axis of apical polarity has been shown to downregulate junctional tension in vertebrates and invertebrates (Warner and Longmore, 2009a; Zihni et al., 2017). In vertebrate cultured cells this may be mediated by Yurt phosphorylation to prevent p114RhoGEF activation (Nakajima and Tanoue, 2011). Additionally, Willin, a vertebrate FERM protein, was found to cooperate with Par3 to recruit aPKC to adherens junctions to downregulate junctional ROCK (Ishiuchi and Takeichi, 2011). aPKC was shown to phosphorylate ROCK near a membrane binding domain and impair ROCK recruiment to adherens junctions. Downregulation of aPKC led to a reduction in apical surface area, consistent with previous observations that aPKC counteracts myosin II-dependent centripetal contraction of circumferential actomyosin (Kishikawa et al., 2008). These results show that the Crumbs complex and aPKC regulate junctional tension antagonistically. However, how their activities are coordinated to ensure proper junction assembly and integrity is unknown.

Interestingly, Crumbs has also been associated with increased E-cadherin dynamics in morphogenetically active tissues (Bajur et al., 2019) and downregulation of ROCK activity (Roper, 2012). During development, neighbour epithelial cells can increase junctional actomyosin at specific boundaries and create what appears to be a supracellular actomyosin cable. This type of actomyosin structure can define tissue boundaries and contribute to morphogenetic events such as tissue invagination both in vertebrates and invertebrates (Roper, 2013). In *Drosophila*, myosin II accumulates at cell-cell junctions in a complementary pattern to Crumbs and aPKC where the actomyosin cable assembles (Roper, 2012) and the anisotropy in Crumbs localization was found to trigger actomyosin cable assembly. This was proposed to be mediated by aPKC inhibition of ROCK and a similar mechanism was suggested to regulate a Crumbs-dependent epithelial-to-mesenchymal transition during mouse gastrulation (Ramkumar et al., 2016). A recent study reports that actomyosin cable assembly depends on the increased stability of ROCK at the junctions that are free of Crumbs (Sidor et al., 2020). However, *in vitro* assays indicate that at least in *Drosophila* the Cdc42 effector Pak1, and not aPKC, phosphorylates ROCK. This does not impair ROCK accumulation at junctions but leads to increased ROCK dynamics at junctions positive for Crumbs and drives anisotropic accumulation of ROCK at specific junctions that lack Crumbs. This provides a simple mechanism for actomyosin planar polarization. It would be interesting

to know if this mechanism also contributes to ROCK-Par3 planar polarization during cell rearrangements (Simoes et al., 2010).

In addition to junctional tension, apical polarity also appears to have a conserved role in the regulation of E-cadherin complex endocytosis (Balklava et al., 2007). In the *Drosophila* pupal thorax epithelium loss of Par6-aPKC or Cdc42 function leads to defective internalization of E- cadherin and loss of E-cadherin homogeneous distribution at adherens junctions (Georgiou et al., 2008; Leibfried et al., 2008). Here, Cdc42 and Par6-aPKC were found to promote endocytosis through Cip4 and WASP. Dysregulation of Cip4 and WASP was found to result in the formation of long tubular structures consistent with blocked vesicle scission (Fricke et al., 2009), supporting a model whereby Cdc42 promotes E-cadherin vesicle scission by WASP and Cip4 in a Par6-aPKC-dependent manner. In turn, junctional Rho was found to prevent E-cadherin endocytosis (Warner and Longmore, 2009b). Curiously, in vertebrate cultured cells, aPKC was also suggested to antagonize E-cadherin mediated endocytosis by downregulating p120-catenin interaction with Numb (Sato et al., 2011), suggesting that aPKC may play context-specific roles.

In addition to apical polarity proteins, the basolateral Scribble complex also regulates adherens junction stability (Navarro et al., 2005; Qin et al., 2005). In MDCK cells Scribble has been shown to prevent E-cadherin endocytosis and regulate internal sorting of E-cadherin vesicles (Lohia et al., 2012). In part, this may be related to apical protein antagonism by Scribble. However, in vertebrate cultured cells, Scribble was recently shown to have a more direct role in junction stabilization through direct interaction and recruitment of DLC3, a RhoGEF, and of SGEF, a RhoGAP, to adherens junctions (Awadia et al., 2019; Hendrick et al., 2016). Additionally, in mouse neural stem cells, Lgl was recently reported to bind to N-cadherin cytosolic tail and promotes its internalization (Jossin et al., 2017).

Recent data supports a bigger role for polarity proteins in junction regulation during development and homeostasis that goes beyond simple positioning. Apical and basolateral polarity proteins are able to regulate E-cadherin trafficking, which contributes to the maintenance of adherens junctions and could also contribute to adherens junctions remodelling during development. Furthermore, cell polarity also contributes to regulate tension at adherens junctions, which is essential to balance forces at cell-cell contacts and stabilize adherens junctions. Additionally, apical polarity also plays an instructive role in directing junctional tension asymmetries during morphogenetic events.

Polarity proteins regulate cell and tissue morphogenesis through actomyosin

Epithelial cells and tissues are shaped through the concerted regulation of the cell cytoskeleton and actomyosin-dependent forces. In epithelial cells polarity proteins regulate the cell cytoskeleton to direct the asymmetric position of specific cell structures, such as the apical cytoskeleton, which is anchored and regulated by the apical Crumbs and Par complexes. Polarity proteins may also regulate the shape of specific cell structures. For example the Crumbs complex is essential for microvili assembly in vertebrate intestinal cells (Charrier et al., 2015; Whiteman et al., 2014); aPKC controls the assembly of motile cilia in sea urchin embryos (Pruliere et al., 2011); aPKC and Lgl antagonistically regulate myosin II to regulate the length of microridges in the zebrafish epidermis (Raman et al., 2016). Additionally, polarity proteins can regulate cell contractility at different subcellular locations (Zihni et al., 2017) to control cell mechanics (Dias Gomes et al., 2019) and, as is becoming increasingly clear, to change cell and tissue shape for instance through apical constriction.

Several morphogenetic processes rely on constriction of the apical surface, including gastrulation, tube formation and wound healing. In *Drosophila* embryos an opening over the dorsal epithelium called amnioserosa is closed by the epidermis in a process called dorsal closure. During this process, the actomyosin cytoskeleton of the amnioserosa cells pulsates at the apical-medial surface to drive apical cell constriction and promote dorsal closure (Pasakarnis et al., 2016; Solon et al., 2009). Par3 and Par6-aPKC were found to accumulate cyclically in the apical-medial surface of the amnioserosa to drive pulsatile contractions (David et al., 2010). Par6-aPKC was found to accumulate with increasing actomyosin and downregulate actomyosin contractility to promote a pause in contraction, while Par3 has been proposed to antagonize aPKC to promote contractile pulse duration (David et al., 2013). This suggested a model, according to which Par proteins create a negative feedback loop to create oscillations in apical actomyosin accumulation and drive ratcheted contractions (Durney et al., 2018). How aPKC downregulates apical contractility during apical constriction remains unclear. In vertebrate cells, aPKC can inhibit ROCK directly at adherens junctions (Nakajima and Tanoue, 2011), however this does not appear to be the case in *Drosophila* (Sidor et al., 2020). Additionally, aPKC may also contribute to actomyosin regulation and slow down filament assembly by direct myosin II phosphorylation (Even-Faitelson and Ravid, 2006), Lgl or Par1 antagonism (Hava et al., 2009; Majumder et al., 2012) or Rho inactivation through a Rho GAP (Zhang and Macara, 2008).

During *C. elegans* gastrulation, two epithelial cells constrict apically to become internalized and give rise to the endoderm. During this process, Cdc42 was found to drive apical contractility through accumulation of MRCK (Marston et al., 2016), suggesting that

apical polarity may also actively promote apical constriction. Interestingly, Crumbs can have different effects on apical constriction. In *Drosophila*, Crumbs overexpression triggers onset of apical constriction and loss of Crumbs causes defective dorsal closure and trachea invagination (Harden et al., 2002; Letizia et al., 2011), suggesting that Crumbs can promote apical contractility. However, during dorsal closure, Crumbs was found to associate with Moesin to downregulate Rho-mediated contractility and brake constriction (Flores-Benitez and Knust, 2015). Although it remains unclear how Crumbs regulates apical constriction, it is possible that Crumbs regulates it in opposite ways depending on its binding partner: association with Moesin may prevent apical constriction, while Yurt promotes it (Flores-Benitez and Knust, 2015; Loie et al., 2015; Nakajima and Tanoue, 2010; Salis et al., 2017). Additionally, another Crumbs binding partner, βH-spectrin, was recently shown to regulate ratcheted apical constriction, possibly through regulation of apical actomyosin network connectivity (Krueger et al., 2020). How Crumbs partners are selected remains unknown, however it could involve aPKC activity (Biehler et al., 2021; Gamblin et al., 2014; Wei et al., 2015).

Polarity proteins define an apical-basal axis that polarizes cellular structures and can also be used to direct transient asymmetric accumulation of contractile actomyosin networks. Furthermore, polarity proteins play a more direct role in controling these asymmetrically positioned contractile networks through mechanisms that frequently involve Rho GTPase regulation. This can likely regulate cell shape in homeostasis through force balance or tip the scales and promote cell shape change. Apical Par6-aPKC is generally associated with decreased Rho-mediated contractility, both at junctions and at the apical-medial region, while the Crumbs complex appears to play a more variable role, promoting or preventing Rho activity. Additionally, interplay between apical and basolateral polarity complexes and actomyosin regulation can also contribute to morphogenesis (Weng and Wieschaus, 2017). Deregulation of polarity-actomyosin interactions leads to tissue organization defects that may be relevant not only during development, but also in disease. Accordingly, in biopsies from patients with inflammatory bowel disease there is a significant correlation between local inflammation, decreased aPKC activity and increased amounts of myosin IIA (Wald et al., 2011) and in a TNFα-mediated inflammation cellular model, constitutive aPKC activation rescued myosin IIA levels (Mashukova et al., 2011). Additionally, characterization of the development of human breast lesions leading to carcinoma, showed an association between loss of Par6, decreased contractility and lumen collapse (Halaoui et al., 2017).

CONCLUDING REMARKS

Epithelial architecture is essential for epithelial functions during development and homeostasis. Epithelial cell shape and consequently epithelial morphology is controlled by adherens junctions and the actomyosin cytoskeleton. Additionally, apical-basal polarity proteins define an apical-basal axis to polarize the cell surface, cytoskeleton and organelles. Thus, apical-basal axis is fundamental to orient cells in space, not unlike a cellular compass. Moreover, increasing experimental evidence shows that apical-basal polarity controls epithelial cell morphology through mechanisms that go beyond definition of the apical-basal polarity axis. Apical-basal polarity proteins are directly involved in the assembly and dynamic regulation of adherens junctions and contribute to regulate the actomyosin cytoskeleton at different cell surfaces. This interplay between apical-basal polarity, actomyosin and adherens junctions in epithelial cells has been shown to contribute to morphogenesis and homeostasis in specific contexts. However, the molecular mechanisms are frequently not fully understood, at least in part because interfering with polarity proteins results in pleiotropic effects on epithelia. Furthermore, the involvement of apical-basal polarity in the control of epithelial cell morphology and morphogenesis is likely to be much more widespread. Thus, much remains to be explored to understand how apical-basal polarity may contribute to development and homeostasis in different epithelia through the dynamic regulation of cellular structures and key cellular and tissue-level events, such as cell division or tissue folding.

CHAPTER 2

DEALING WITH APICAL-BASAL POLARITY AND INTERCELLULAR JUNCTIONS: A MULTIDIMENSIONAL CHALLENGE FOR EPITHELIAL CELL DIVISION

Abstract 53

Introduction 53

Remodeling of apical-basal polarity at mitotic entry 54

Dealing with intercellular contacts at mitotic exit 56

- Asymmetric furrow ingression along the apical-basal axis 57
- A multicellular balance of forces controls epithelial cohesion and patterning 58
- Preservation of a permeability barrier 60

Apical-basal polarization at mitotic exit 61

Concluding remarks 64

This manuscript was published in Current Opinion in Cell Biology in 2019 (vol. 60 p.75-83). I created all figures, wrote the original draft of the final section on how epithelial cells become polarized at mitotic exit and reviewed and edited the manuscript together with my supervisor Eurico Morais de Sá. It is included in my thesis as an introdution to current knowledge on the coordination between cell division and apical-basal organization in epithelia.

DEALING WITH APICAL-BASAL POLARITY AND INTERCELLULAR JUNCTIONS: A MULTIDIMENSIONAL CHALLENGE FOR EPITHELIAL CELL DIVISION

Mariana Osswald[1,2] and Eurico Morais-de-Sá[1,2,3]

1. Instituto de Biologia Molecular e Celular, Universidade do Porto, Porto, Portugal
2. Epithelial Polarity and Cell Division group, Instituto de Investigação e Inovação em Saúde (i3S), Universidade do Porto, Porto
3. corresponding author: eurico.sa@ibmc.up.pt
   i3S – Instituto de Investigação e Inovação em Saúde
   Rua Alfredo Allen, 208, 4200 – 135 Porto
   Tel: +351 226074921

ABSTRACT

Epithelial cell division is essential to shape developing tissues and for the homeostasis of adult organs. However, the mechanical and biochemical reorganization of dividing cells represents a major challenge to the integrity and architecture of the epithelial barrier. Here, we portray recent findings from a variety of model organisms that revealed how apical–basal polarity and intercellular adhesion are modulated during cell division to maintain a permeability barrier and to transmit epithelial organization to daughter cells. This demands not only that dividing and neighboring cells remodel their adhesion and contractility, but also cell cycle-dependent regulation of apical–basal polarity in the dividing cell. Additionally, mitotic structures, such as the midbody, provide spatial cues to enforce epithelial cell organization.

INTRODUCTION

Epithelial tissues are the 'bouncers' of multicellular life, forming sheets of cells that shape tissues and compartmentalize our organs. Within them, adherens (AJ) and occluding junctions (tight junctions (TJ) in vertebrates; septate junctions (SJ) in invertebrates) link

epithelial cells and regulate paracellular diffusion, respectively (Lecuit and Yap, 2015; Zihni et al., 2016). The epithelial barrier and other specialized functions, such as gut secretion and absorption, have long been known to require a polarized cellular organization, which positions intercellular junctions along the apical–basal axis of epithelial tissues (Farquhar and Palade, 1963). Research in the last decades has uncovered how the apical–basal polarity machinery polarizes epithelial physiology and renders a distinct cytoskeletal and functional organization to different plasma membrane domains through conserved proteins, including the apical aPKC-Par and Crumbs complexes and the basolateral Lgl-Dlg-Scrib module (Flores-Benitez and Knust, 2016; Rodriguez-Boulan and Macara, 2014; Figure 2.1). Apical–basal organization is at an apparent steady-state during interphase, but progression through mitosis demands dynamic readjustments in epithelial architecture. For example, cell adhesion to the extracellular matrix (ECM) must be modulated, an aspect extensively studied in epithelial cell culture (Taneja et al., 2019). Nevertheless, although *in vivo* studies have provided insight into the coordination between polarity and asymmetric cell division (Venkei and Yamashita, 2018), there is a knowledge gap regarding how symmetrically dividing epithelial cells integrate mechanical and biochemical cues during development and tissue homeostasis. Here, we review recent studies in model organisms showing that cell division imposes a reorganization of apical–basal polarity and intercellular adhesion. The emerging picture suggests not only that this preserves the epithelial barrier during proliferation, but also that it shapes morphogenesis and propagates cellular asymmetries to daughter cells.

REMODELING OF APICAL-BASAL POLARITY AT MITOTIC ENTRY

During mitotic entry, reorganization of the actomyosin cytoskeleton rounds cells and reduces their basal contacts with the ECM. Cell culture work linked the mitotic kinase Cdk1 to the regulation of integrin-mediated adhesion during the cell cycle (Jones et al., 2018), but it remains unknown how ECM attachment is modulated *in vivo*. Nevertheless, recent *in vivo* studies dissected the reorganization of apical–basal polarity in symmetrically dividing cells, and revealed its significance for cell shape change and tissue morphogenesis.

Apical polarity regulators adjust their localization during mitosis in various *Drosophila* tissues (Figure 2.1). Bazooka (Par-3) decreases markedly in the apical region of mitotic cells in the *Drosophila* imaginal discs and in the follicular epithelium, where similar behavior was observed for aPKC and Par-6 (Bergstralh et al., 2013; Morais-de-Sa and Sunkel, 2013; Ragkousi et al., 2017). In the follicular epithelium, both aPKC and Par-6 accumulate in the cytoplasm and are redistributed along the cortex (Carvalho et al., 2015; Morais-de-Sa and

Sunkel, 2013). Furthermore, aPKC, Par-6 and the RhoGTPase Cdc42 also extend along the lateral cortex during symmetric divisions in the pupal notum, a monolayered epithelium in the *Drosophila* dorsal thorax (Rosa et al., 2015). Here, they act together with the RhoGTPase exchange factor Pebble (Pbl, human ECT2) to promote mitotic rounding through the formin Diaphanous, which induces isotropic organization of the actin cytoskeleton. How does the cell cycle control the redistribution of apical determinants? Pbl ectopic expression displaces aPKC to the lateral domain even in interphasic cells (Rosa et al., 2015), suggesting that Pbl release from the nucleus during prophase can trigger the redistribution of apical determinants. Interestingly, the mitotic kinase Polo/PLK-1 was shown to phosphorylate the PAR-3 oligomerization domain to modulate the localization and stoichiometry of the aPKC-Par complex in the *Caenorhabditis elegans* zygote (Dickinson et al., 2017). Although these phosphorylation sites are not conserved in *Drosophila* Baz or human Par-3, this hints at multiple links between cell cycle control and apical–basal polarity.

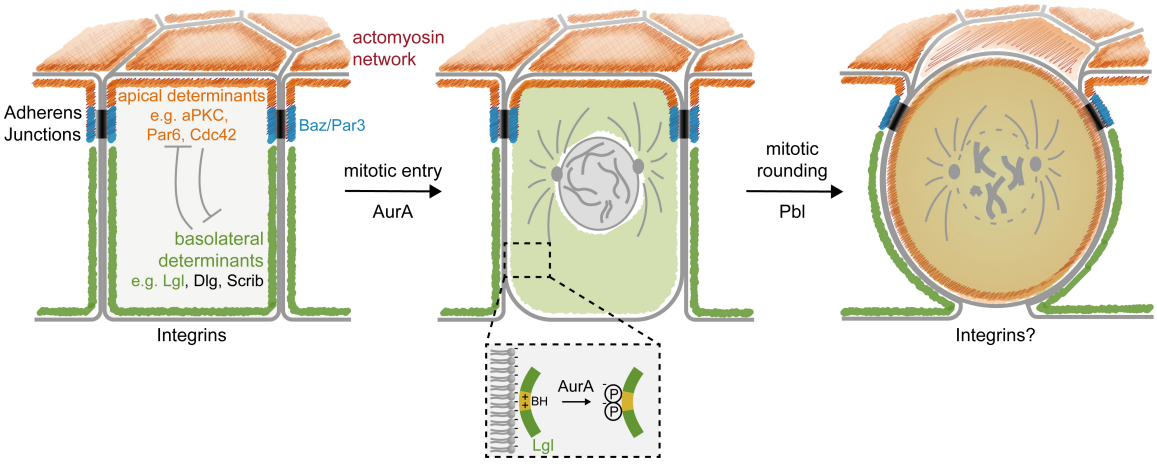


Figure 2.1. Subcellular reorganization of apical-basal polarity regulators at mitotic entry in *Drosophila* epithelia. During interphase, asymmetric distribution of polarity proteins polarizes epithelial cells along an apical-basal axis. Apical polarity components, such as the Par-6-aPKC complex and Cdc42 (orange), exclude basolateral determinants Lgl (green), Dlg and Scrib to the opposite cell side and vice-versa. Baz, the *Drosophila* Par-3 homolog, positions adherens junctions (AJs) between the apical and basolateral domain. In Drosophila epithelia, cell cycle events reshape apical-basal polarization in the dividing cell. At mitotic entry, Aurora A phosphorylates Lgl in a basic and hydrophobic (BH) domain to reduce its affinity to negatively charged phospholipids and release Lgl from the cortex. Pbl release from the nucleus is coordinated with the redistribution of apical determinants aPKC, Par-6 and Cdc42 to change the actomyosin cytoskeleton (red) into an isotropic stiff mesh that rounds cells. Additionally, Baz disappears from apical contacts at least in some epithelia. It is unclear how dividing epithelial cells adjust integrin-mediated ECM adhesion.

Apical depolarization could also result from the redistribution of the basolateral determinant Lgl, an aPKC-Par-6 antagonist. At the G2-M transition, Aurora A becomes active

and phosphorylates Lgl in two serines (S656 and S664) within a basic and hydrophobic (BH) domain (Bell et al., 2015; Carvalho et al., 2015). This reduces Lgl's affinity to plasma membrane phosphoinositides and releases it from the cortex (Bailey and Prehoda, 2015; Dong et al., 2015; Figure 2.1). The other basolateral determinants Scrib and Dlg do not follow Lgl cytoplasmic reallocation, but rather stay in the cortex to orient planar cell division (Bergstralh et al., 2013; Nakajima et al., 2013). In fact, cortical Dlg recruits Pins (LGN in mammals) to transmit cortical pulling forces to astral microtubules and align the spindle in the *Drosophila* follicular epithelium and in the chick neuroepithelium (Bergstralh et al., 2013; Saadaoui et al., 2014). In contrast, Lgl cortical retention disrupts mitotic spindle orientation in follicle cells (Bell et al., 2015; Carvalho et al., 2015). Since Lgl and LGN/Pins bind to the same motif within the Guanylate kinase domain of Dlg (Saadaoui et al., 2014; Zhu et al., 2014), the current interpretation is that Lgl is released from the cortex so it cannot compete with Pins for Dlg binding (Bell et al., 2015; Carvalho et al., 2015). However, this regulatory mechanism cannot be generalized as mitotic spindles orient independently of Pins and Dlg in some *Drosophila* tissues (Bergstralh et al., 2016; Bosveld et al., 2016).

Live imaging analysis of the sea anemone *Nematostella vectensis* has also shown that the apical polarity markers Par-6 and Par-3 are transiently lost during the synchronous cell divisions of the primary embryonic epithelium (Ragkousi et al., 2017). Apical polarity loss is not associated with oscillations in Lgl localization and it does not require Aurora activity, but it depends on Cdk1 and embryonic de-compaction. However, it is still unclear whether delocalization of apical proteins is driven directly by active Cdk1 or if it is an indirect outcome of partial intercellular detachment during mitosis-associated embryonic decompaction. Blocking embryo compaction, for example using constitutively active Moesin^{T562E}, disrupts the localization of Par-6 to apical intercellular contacts. This suggests that the mechanical reorganization of the cortex associated with cell rounding remodels polarity. Interestingly, mitotic cell rounding destabilizes intercellular contacts specifically in the central blastoderm of zebrafish embryos, but not in the margin, where increased contractility resists contact loss (Petridou et al., 2018). These distinct responses within the same tissue make it a potential system to address if and how disassembly of cell-cell contacts during mitotic rounding is spatially linked to apical polarity reorganization.

DEALING WITH INTERCELLULAR CONTACTS AT MITOTIC EXIT

Electron microscopy studies in human and mouse epithelial tissues initially suggested that dividing cells preserve intercellular adhesion (Baker and Garrod, 1993; Jinguji and

Ishikawa, 1992). Live imaging with fluorescent markers in a variety of vertebrate and invertebrate epithelial tissues has now reinforced this conclusion, but it has also highlighted that adhesion is locally modulated during cytokinesis. Indeed, polarized intercellular adhesion makes epithelial cytokinesis unique because it forces dividing cells and their neighbours into a mechanical interplay to regulate the cohesion and integrity of the epithelial barrier and to control epithelial packing during morphogenesis.

Asymmetric furrow ingression along the apical-basal axis

During cytokinesis a contractile actomyosin ring constricts until a narrow microtubule-rich bridge, termed midbody, forms between the daughter cells (Green et al., 2012). One almost universal feature of epithelial cytokinesis is that the furrow ingresses asymmetrically from the basal to the apical side (Bourdages et al., 2014; Founounou et al., 2013; Guillot and Lecuit, 2013; Herszterg et al., 2013; Higashi et al., 2016; Kosodo et al., 2008; Morais-de-Sa and Sunkel, 2013; for review Herszterg et al., 2014; Thieleke-Matos et al., 2017). This positions the midbody in the vicinity of the apical junctional complexes, where it then propagates tissue organization (see below). In *Drosophila* embryonic and follicular epithelium, cytokinesis asymmetry depends on the position of AJs close to the apical side, where they resist actomyosin ring constriction (Guillot and Lecuit, 2013; Morais-de-Sa and Sunkel, 2013). Although vertebrate AJs sit on the opposite side of occluding junctions, polarized intercellular contacts are still critical for asymmetric furrowing in vertebrate cells, as single cells dissociated from mouse small intestine organoids change to symmetric ring constriction (McKinley et al., 2018). Moreover, TJs maintain close contact with the cytokinetic ring in frog and mammalian epithelia and could therefore regulate the asymmetry of cytokinesis in vertebrates (Higashi et al., 2016; Jinguji and Ishikawa, 1992). Recent work indicates that TJs relieve tension on AJs in *Xenopus* embryos and, accordingly, loss of the TJ component Zonula Occludens-1 (ZO-1) increases AJ resistance to ring constriction (Hatte et al., 2018). Besides apical constraints, asymmetric cytokinesis may also be driven by higher contractility in the basal part of the ring due to myosin accumulation (Herszterg et al., 2013), and may require lowering of focal adhesion-dependent attachment to the ECM, which opposes apical-directed ingression in polarized MDCK cysts (Taneja et al., 2016).

A multicellular balance of forces controls epithelial cohesion and patterning

During cytokinesis, diverse mechanisms adjust adhesion and contractility at the ingressing membranes to pattern the epithelial tissue while maintaining cohesiveness. In the *Xenopus* gastrula epithelium, dividing cells reinforce intercellular adhesion next to the ring through Vinculin recruitment and AJ stabilization (Higashi et al., 2016; Figure 2.2A). The current model for junction strengthening predicts that tension unfolds α-Catenin, which then exposes vinculin binding sites (Higashi et al., 2016; Kim et al., 2015; Yao et al., 2014). Intriguingly, FLIM microscopy with an E-Cadherin (E-cad) FRET-based tension sensor in *Xenopus* embryos did not detect an increase in tension at the ingressing membranes or tension differences in dividing cells (Herbomel et al., 2017), which suggests that ring constriction is insufficient to change E-Cad conformation. The TJ component ZO-1 may also participate in mechanotransduction during cytokinesis since its levels increase at the beginning of cleavage furrow ingression (Higashi et al., 2016), it stretches in response to actomyosin-dependent forces (Spadaro et al., 2017), and it relieves tension at the AJs (Hatte et al., 2018). Further studies are nevertheless required to advance our mechanistic understanding and to identify in which developmental context which organisms reinforce junctions to preserve epithelial integrity during cytokinesis.

In contrast to *Xenopus*, in *Drosophila* tissues E-Cad-based AJs ultimately reduce in response to the force produced by ring constriction (Founounou et al., 2013; Guillot and Lecuit, 2013; Herszterg et al., 2013; Morais-de-Sa and Sunkel, 2013). How ring pulling forces are transduced into remodeling of adhesion and contractility was recently elucidated through a combination of genetic and laser ablation experiments in the *Drosophila* pupal notum and biophysical modelling of E-cad and actomyosin dynamics (Pinheiro et al., 2017; Figure 2.2B Adherens Junctions plane). In this tissue, ring constriction elongates the ingressing junction, which is sufficient to dilute E-cad and thus reduce AJ adhesion (Pinheiro et al., 2017). In turn, the local decrease of E-cad linked actomyosin triggers self-organized actomyosin flows that accumulate myosin in the neighbouring cell at the base of the invagination (Pinheiro et al., 2017). This pool of myosin sets the length of the future daughter-daughter AJ by providing cortical tension to maintain cell membranes tightly packed until a wave of midbody-linked Arp2/3- and Rac-dependent F-actin polymerization removes neighbouring membranes and establishes a daughter-daughter interface (Herszterg et al., 2013).

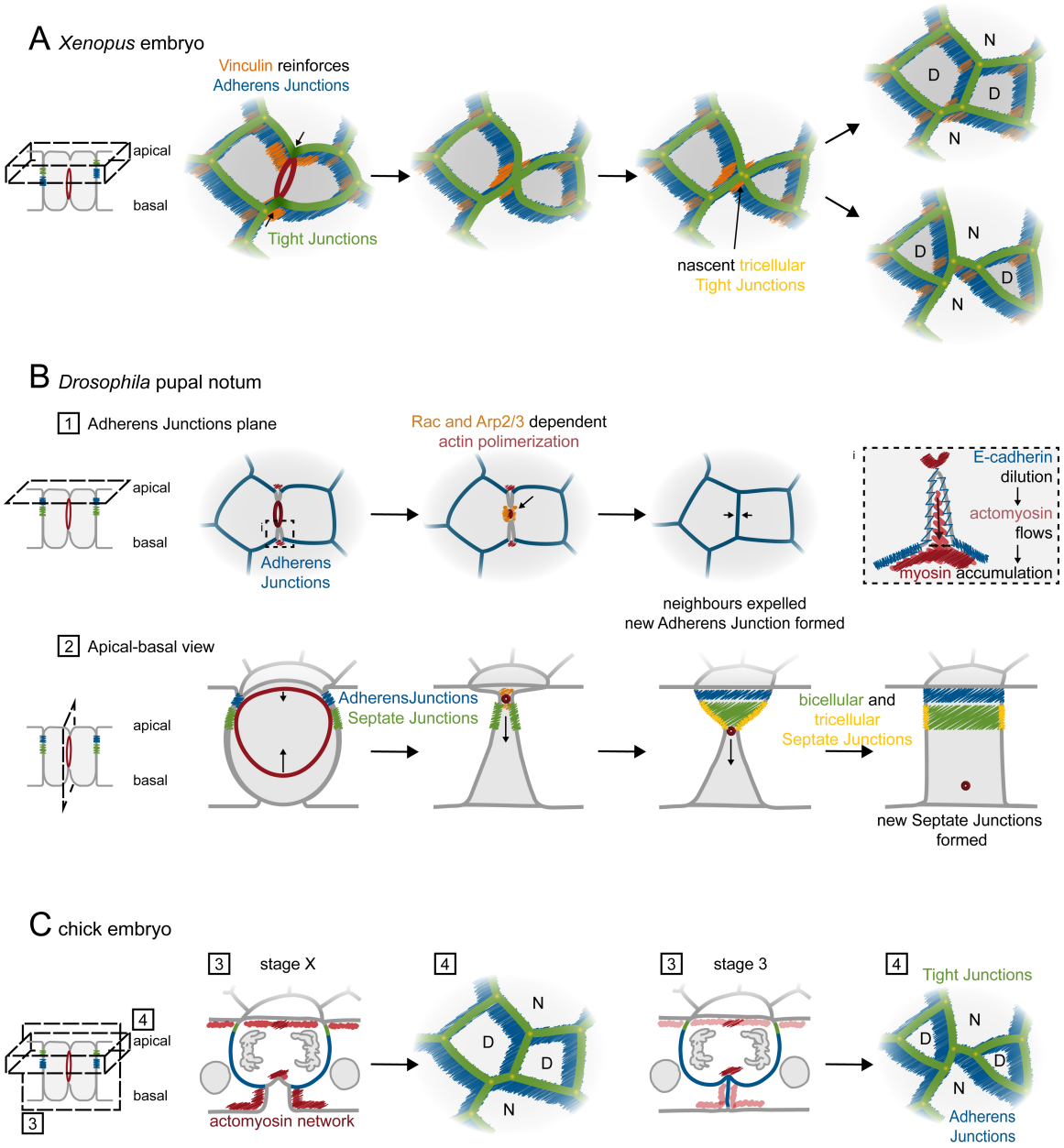


Figure 2.2. Remodelling of adherens and occluding junctions during cell division. Schematic representation of AJs (blue) and occluding junctions (green) remodeling during cytokinesis in the *Xenopus* gastrula (A), in the *Drosophila* pupal notum (B) and in chick embryos (C). In the *Xenopus* gastrula, ring pulling forces reinforce adhesion locally between dividing and neighbouring cells by stabilizing AJ components through Vinculin (orange) recruitment to the ingressing membranes (arrows). After ring constriction, tricellular tight junctions (yellow) form at the new 4-cell contact, which eventually resolves, as a new cellular interface forms either between the two new daughter cells (D) or the contacting neighbouring cells (N). (B) Cytokinesis events in the *Drosophila* pupal notum are represented at the AJ plane (1) and along the apical-basal axis (2). Cytokinesis dilutes E-cadherin-based AJs at the ingressing membranes as they elongate. This triggers actomyosin flows (red) in the neighbouring cell from the ring contacting membrane to the base of the invagination, where myosin (dark red) accumulates. Myosin accumulation in the neighbours keeps the cells packed until a burst of Rac and Arp2/3-dependent actin polymerization (orange) around the midbody promotes AJ formation between the daughter cells. *Drosophila* occluding junctions, the septate junctions (SJs), are positioned below the AJs. Asymmetric ring constriction positions the midbody between the AJ and SJ level (2). The midbody then descends as the new bicellular (green)

and tricellular SJ (yellow) form right above it. SJ formation allows final disentanglement of the 4-cell contact around the midbody and stabilization of a daughter-daughter interface along the apical-basal axis. (C) Actomyosin contractility controls basal to apical neighbouring cell intercalation between daughter cells during chick development. Prior to gastrulation, high actomyosin contractility (dark red) in epithelial cells prevents neighbouring cells from establishing contact below dividing cells. This ensures that daughter cells are kept in contact. Low actomyosin contractility (light red) during gastrulation allows neighbouring cells to form E-cadherin-based adhesions below the dividing cell, which promote neighbouring cell intercalation.

The aforementioned mechanism could generally be used to keep daughter cells in contact. However, intercalation of neighbouring cells between daughter cells intersperses cell lineages and plays a role in morphogenesis during mouse (Lau et al., 2015; McKinley et al., 2018; Packard et al., 2013), chick (Firmino et al., 2016) and frog (Higashi et al., 2016) development. Geometric properties, such as size and aspect ratio, are critical determinants of neighbouring cell intercalation (Carroll et al., 2017; McKinley et al., 2018). Light sheet microscopy in mouse small intestine organoids indicated that elongated height facilitates neighbouring cell insertion in the basolateral region below apically displaced dividing cells (McKinley et al., 2018). Accordingly, cell division coupled interspersion is restricted to regions of the mouse embryo with a high aspect ratio (McKinley et al., 2018). Interestingly, in chick development, high actomyosin accumulation at the basolateral side of neighbouring cells was shown to prevent them from establishing contact below the dividing cell and thus ensure the formation of a daughter-daughter interface prior to gastrulation (Firmino et al., 2016). In this system, actomyosin contractility seems to be globally modulated during development, and it is unclear whether a mechanosensitive mechanism controls local responses to cell division. Nevertheless, these findings demonstrate how modulating contractility and contact with neighbouring cells leads to distinct tissue topology (Figure 2.2C). Furthermore, they underline the importance of adhesion and contractility also at the basolateral region, where they are likely to play other roles, such as ensuring the reintegration of cells that divide out of the epithelial plane (Bergstralh et al., 2015; Packard et al., 2013).

Preservation of a permeability barrier

Cell division challenges the permeability barrier since it requires occluding junctions to accommodate major shape changes and localized tensile forces. How this barrier is kept during cytokinesis has been recently characterized in the *Xenopus* gastrula and in the *Drosophila* pupal notum, where the functionally analogous occluding junctions are maintained during cell division (Daniel et al., 2018; Higashi et al., 2016; Wang et al., 2018). These studies

defined that resolving the 4-cell structure connecting dividing and neighbouring cells around the midbody is a critical step controlling the establishment of new occluding junctions, and so it is not surprising that the midbody is initially positioned just below AJs in invertebrates and apical to AJs in vertebrates. In the pupal notum, SJs are formed between daughter cells through *de novo* SJ assembly in the apical to basal direction, which displaces the midbody basally while it remains enclosed by the pre-existing SJ (Daniel et al., 2018; Wang et al., 2018; Figure 2.2B apical-basal view). During this period Gliotactin and Anakonda form the tricellular SJ (tSJ) at the attachment site between dividing and neighbouring cells to enable the disentanglement of the midbody from neighbouring cell membranes (Wang et al., 2018). It is worth noting that abscission is completed basally, but midbody movement does not require essential regulators of abscission, including Alix and the ESCRT-III component Shrb (Daniel et al., 2018; Wang et al., 2018).

Despite the lack of conservation between tSJ and tricellular TJ (tTJ) components, the core tTJ components Angulin-1 and Tricellulin are also recruited to vertices formed between the midbody and the ingressed neighbouring cells in *Xenopus* embryos (Higashi et al., 2016; Figure 2.2A). This defines the new tTJ position, and precedes the formation of a short bicellular TJ interface between neighbouring cells, which can either be stabilized or remodelled to establish a daughter-daughter interface. Studies in *Xenopus* embryo provided the best characterization of barrier function preservation during cell division, showing that fluorescent tracers do not cross the proliferative tissue (Higashi et al., 2016). However, an ultrasensitive method for detection of local breaches in the epithelial barrier, ZnUMBA, unveiled that TJs are often compromised in response to acute forces (Stephenson et al., 2019), such as those associated with cell division. Nevertheless, localized Rho activity is anticipated to rapidly restore barrier function by concentrating ZO-1 and Occludin in the damaged region through local actin-polymerization and ROCK-dependent increase of junction contractility (Stephenson et al., 2019).

APICAL-BASAL POLARIZATION AT MITOTIC EXIT

Different cell types, ranging from neurons to chondrocytes, polarize at the end of cell division (Feldman and Priess, 2012; Li et al., 2018; Moreira et al., 2019; Pollarolo et al., 2011). Epithelial apical-basal polarization entails the reallocation of polarity proteins and the polarization *de novo* of the interface generated by cytokinesis. Pre-existing cues maintained during cell division may facilitate daughter cell polarization, such as proposed for planar cell polarity (Heck and Devenport, 2017). Here, we focus on evidence showing that apical-basal

polarization at mitotic exit is temporally coordinated by cell cycle regulators, and spatially regulated by the midbody and centrosomes (Figure 2.3).

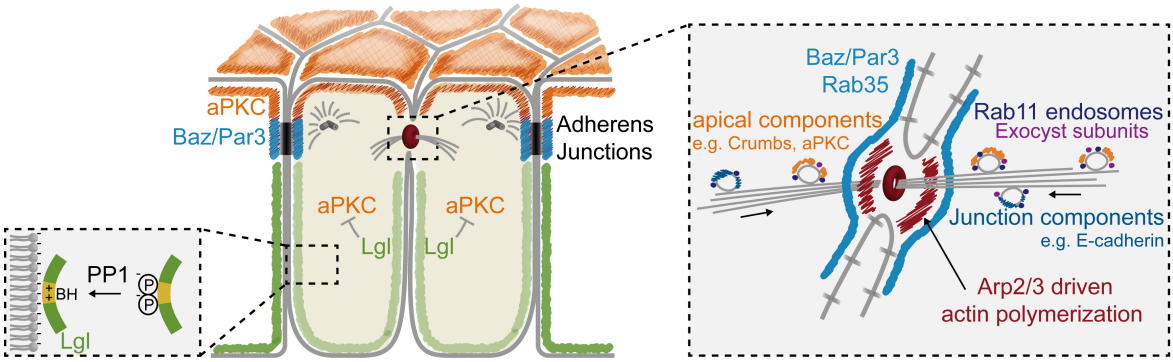


Figure 2.3. Apical-basal polarization of epithelial cells at mitotic exit. In *Drosophila* epithelia, PP1 phosphatase dephosphorylates Lgl basic and hydrophobic (BH) domain to time its cortical relocalization with mitotic exit. Lgl accumulation re-establishes the basolateral domain (green) and prevents the accumulation of aPKC at this site. Additional putative mechanisms that may contribute to apical-basal polarization at mitotic exit in intact epithelia are depicted. The midbody at the new cellular interface and the apically positioned centrosomes, in particular, may provide important spatial cues. Arp2/3-dependent actin polymerization is spatially oriented by the midbody in *Drosophila* epithelia, whereas the midbody directs vesicle trafficking of apical (orange) and AJ (blue) components in Rab11 endosomes positive for exocyst subunits in cultured epithelial cells. In proliferative epithelia, similar vesicles may be anchored and fused to the membrane through binding of vesicle components to Baz/Par-3, Rab35 or other molecules present at the target site.

Recent work in *Drosophila* epithelia shows that PP1 phosphatase times apical-basal repolarization with mitotic exit through Lgl regulation (Moreira et al., 2019). PP1 dephosphorylates Lgl in the aPKC/Aurora phosphorylation sites to increase the affinity of the BH domain to the plasma membrane, thereby promoting its cortical localization. This mechanism is particularly critical at mitotic exit when all Lgl is in the phosphorylated and cytoplasmic form and must be reloaded to the cortex to repress the accumulation of aPKC in the lateral side of the new interface formed between daughter cells (Moreira et al., 2019). CDK1 is therefore central to the regulation of apical-basal polarity during mitosis, since it represses PP1 activity until mitotic exit (Wu et al., 2009). Lgl dephosphorylation relies on a canonical RVxF PP1-binding motif that is highly conserved in metazoans but not in *S. cerevisiae* SRO7, which also lacks the phosphorylatable BH domain (Dong et al., 2015). Thus, these motifs may have co-evolved as a module to control membrane association. It would be interesting to know if PP1 also targets other polarity regulators at mitotic exit. aPKC-mediated phosphorylation of Baz/Par-3 releases aPKC from the inhibitory binding of Par-3 while enabling Par-3/Baz localization to AJs (Morais-de-Sa et al., 2010; Soriano et al., 2016), and

work in vertebrate cells indicates that PP1 also reverses this phosphorylation (Traweger et al., 2008).

The apically positioned midbody has emerged as a major spatial regulator of apical-basal organization. Findings in *Drosophila* epithelia revealed a burst of Rac and Arp2/3-dependent actin polymerization around the midbody that defines the length and position of the new apical daughter-daughter interface (Herszterg et al., 2013; Morais-de-Sa and Sunkel, 2013). It is not clear how Rac-dependent actin polymerization is locally activated or how the midbody contributes to epithelial apical-basal polarization *in vivo*. However, ectopic formation of the apical lumen occurs when the midbody is mispositioned in mammalian 3D cell culture (Lujan et al., 2016), where extensive work places the midbody and its associated microtubules as a hub for directed vesicle trafficking of polarity proteins (reviewed in Fremont and Echard, 2018; Roman-Fernandez and Bryant, 2016). During MDCK cyst formation, apical proteins travel in Rab11 and FIP5 positive endosomes to the apical membrane initiation site (AMIS) at the end of the first cell division. Recent work reports that Arp2/3 also concentrates around the midbody in mammalian cells, where Rac1-dependent actin polymerization facilitates targeting of apical endosomes to define the AMIS and to promote TJ formation (Mangan et al., 2016). Apical vesicles are captured at the AMIS through the interaction between tight junction component Cingulin and FIP5 (Mangan et al., 2016) and by binding of activated Rab35 and the lumen regulator Podxl (Klinkert et al., 2016). Another essential link between the midbody, trafficking and polarization is Par-3, which accumulates at the cleavage furrow or midbody, and is one of the initial factors promoting apical lumen and TJ formation in different systems (Bryant et al., 2010; Buckley et al., 2013; Wang et al., 2014). Moreover, it has recently been shown to dock the exocyst at TJs and promote protein delivery (Ahmed and Macara, 2017). Interestingly, recent findings in *Arabidopsis thaliana* show that plant cell polarization also relies on vesicle trafficking to the new daughter-daughter interface (Glanc et al., 2018), indicating that this is a widespread strategy to link cytokinesis with polarization.

The final midbody destination *in vivo* is tailored to fit epithelial-specific purposes. For example, midbody asymmetric inheritance defines cell fate in the zebrafish neuroepithelium (Pollarolo et al., 2011), whereas in *Drosophila* the midbody moves basally to coordinate cell division with the maintenance of the permeability barrier (Daniel et al., 2018; Wang et al., 2018), and in MDCK cells it migrates towards the centrosome to promote ciliogenesis (Bernabe-Rubio et al., 2016). A recent preprint reports that after the terminal divisions of the *C.elegans* embryo, the midbody migrates from a central position between daughter cells to the apical membrane, where it contributes to *de novo* polarization during the formation of the gut and pharynx lumen (Bai et al., 2018). This also involves protein delivery by the midbody as the α-Catenin orthologue, HMP-1, travels together with Aurora B (AIR-2) and Rab11 to the

apical surface, where they persist after the remainder ring components have been internalized (Bai et al., 2018).

As epithelial cells exit mitosis, centrosomes are often positioned apically where they can dictate microtubule organization. In the last division of *C.elegans* gut precursors, centrosomes migrate together with PAR-3 and PAR-6 to transfer the microtubule nucleators γ-tubulin and CeGrip-1 to the apical membrane, where the latter generates a non-centrosomal microtubule-organizing center (MTOC; Feldman and Priess, 2012). Centrosome localization is also associated with apical-basal polarity in mouse development as centrosomes reposition towards ECM adhesions during epithelial-to-mesenchymal transition (Burute et al., 2017), but the mechanistic understanding of how the centrosome could mediate apical-basal polarization in epithelia is limited. Recent findings in *Drosophila* embryonic epithelium identified a Par1-promoted positive feedback loop between centrosomes and Par-3/Baz that drives isotropic distribution of Par-3/Baz at the AJ level (Jiang et al., 2015). Flies can however develop to adults without centrioles (Basto et al., 2006), and so microtubule organization by non-centrosomal MTOCs may be sufficient to coordinate apical-basal polarization in *Drosophila*. Interestingly, despite the absence of centrosomes during early mouse embryogenesis, it was shown that the intercellular bridge recruits the non-centrosomal microtubule organizer CAMSAP3 to generate microtubule tracks for Rab11 and dynein-mediated transport of E-cad (Zenker et al., 2017).

CONCLUDING REMARKS

Recent advances highlight that the cell-cycle dependent regulation of kinase and phosphatase activities is re-purposed as a temporal input to remodel apical-basal polarity in proliferative epithelia. These cell-intrinsic mechanisms add to a multidimensional coordination of adhesion and contractility between dividing and neighbouring cells during cytokinesis, which not only maintains mechanical cohesion and barrier function, but also actively patterns the epithelial tissue and localizes spatial cues to propagate apical-basal organization. Although we are only scratching the surface on the coordination between polarity, adhesion and epithelial cell division, it is already clear that mechanisms are often specifically fitted to particular biological contexts, and so further analysis is needed to elucidate the functional and molecular basis for divergencies. Another direction will be dissecting how apical-basal reorganization impacts cellular processes that maintain genome stability, such as chromosome segregation, whose fidelity has been linked to tissue architecture (Knouse et al., 2018). Thus, interrogating epithelial cell division at the organism level is fertile land for

epithelial biology, which will thrive with the advances in optogenetics and *in vivo* mechanical manipulation.

CHAPTER 3

AIMS AND OUTLINE OF APPROACH AND RESULTS

Mann tracht, un Gott lacht.
Man plans, and God laughs.
Yiddish proverb

Epithelial functions and architecture depend on apical-basal polarity (Chapter 1). Accordingly, loss of apical-basal polarity leads to gross defects in tissue architecture, which are associated with developmental failure and disease (Bilder et al., 2000; Forteza et al., 2016; Halaoui et al., 2017; Horne-Badovinac et al., 2001; McCaffrey et al., 2012; Muller and Wieschaus, 1996; Rolls et al., 2003; Tepass et al., 1990). However, polarity proteins engage in a complex network of interactions, so intricately connected to epithelial architecture, that it is generally difficult to interpret loss of function architecture phenotypes and ascribe to them a single specific cause. Furthermore, loss of polarity disrupts epithelia to such an extent that it becomes complicated to study further contributions of polarity proteins to dynamic events in epithelia, such as cell division.

A series of studies revealed an interplay between apical-basal polarity and cell division (reviewed in Chapter 2). As cells go into mitosis, apical and basolateral determinants redistribute inside the cell to enable mitotic rounding and ensure proper spindle orientation (Bell et al., 2015; Bergstralh et al., 2013; Carvalho et al., 2015; Morais-de-Sa and Sunkel, 2013; Rosa et al., 2015). Additionally, epithelial organization also shapes cell division. Epithelial cytokinesis involves an interplay between dividing and neighbour cells and proceeds assymmetrically from the basal to the apical domain due to the apical junctions that constrain the contractile ring (Firmino et al., 2016; Founounou et al., 2013; Guillot and Lecuit, 2013; Herszterg et al., 2013; Morais-de-Sa and Sunkel, 2013; Pinheiro et al., 2017). Apical-directed cytokinesis positions the midbody close to the apical side, where it has been suggested to act as a cue for adherens junction formation between the two new daughter cells (Herszterg et al., 2013; Morais-de-Sa and Sunkel, 2013). These studies highlighted a plastic behaviour of apical-basal polarity to accommodate epithelial cell division and exposed that cell division in epithelia requires adaptations to conform with epithelial cell morphology. This interplay between morphology, apical-basal polarity and cell division is likely to be more extensive, as cell division involves extensive changes in cell shape and cellular organization (Green et al., 2012; Morgan, 2007; Taubenberger et al., 2020), throughout which, dividing epithelial cells should, in principle, stay connected to their neighbours to maintain the permeability barrier intact. However, further addressing how apical-basal polarity contributes to epithelial cell

division is made difficult by the gross defects in epithelial organization upon disruption of apical-basal polarity with conventional tools for RNAi-mediated depletion or gene knock-out. This highlights a need for tools to inactivate polarity with high spatiotemporal control.

Optogenetics is particularly well-suited to address the need for high spatiotemporal control in model organisms, since it was initially developed precisely for this purpose to study intact neuronal circuits in living animals (Rost et al., 2017). Optogenetics relies on genetically encoded light-sensitive protein modules to enable control over biochemical circuits in living cells with light (Tischer and Weiner, 2014). In the past 15 years, several classes of light-sensitive proteins found in all kingdoms of life have been repurposed as optogenetic tools to study very diverse processes. Generically, these tools have been used to uncage a sterically blocked active site or domain (Guntas et al., 2015; Strickland et al., 2012; Zhou et al., 2017), induce clustering (Bugaj et al., 2013; Lee et al., 2014; Taslimi et al., 2014) or trigger recruitment to specific subcellular localizations through light-induced dimerization (Guntas et al., 2015; Kennedy et al., 2010; Strickland et al., 2012). Non-neuronal optogenetic tools have recently been successfully introduced in model organisms (Hartmann et al., 2020; Johnson and Toettcher, 2019). However, here they have mostly been used to trigger protein activity with light.

In this work I aimed to 1) establish optogenetic tools to address the matter of temporal control over apical-basal polarity activity and inactivate polarity proteins acutely. Furthermore I also aimed to 2) use these tools to address how apical-basal polarity guards the architecture of epithelia during proliferation. To this end, I used light-activated rerversible inhibition by assembled trap (LARIAT), a previously reported optogenetic tool to cluster, sequester and inactivate GFP-tagged proteins in the seconds to minute range. I started by adapting LARIAT to *Drosophila* S2 cells (Chapter 4). In this system, I compared the clustering efficiency of different LARIAT variants to determine an optimal clustering tool. Furthermore, I also validated that LARIAT can be used to study mitosis and polarity, by verifying that clusters themselves did not affect progression through mitosis and testing the ability of LARIAT to interfere with mitotic kinase Mps1 and polarity determinant Lgl. LARIAT was also confirmed to detect protein-protein interactions *live* through analysis of Par6 and aPKC co-clustering as a proof of concept. Finally, I also combined LARIAT clustering with the E3 Ligase Trim21 to develop an optogenetic tool for acute protein degradation (Appendix).

To study apical-basal polarity in a proliferative epithelium, I used the *Drosophila* follicular epithelium (Figure 3.1). The *Drosophila* follicular epithelium is a widely used model to study polarity, cell division and morphogenesis (Aguilar-Aragon et al., 2020; Bergstralh et al., 2013; Carvalho et al., 2015; Chen et al., 2019; Finegan et al., 2019; Morais-de-Sa and Sunkel, 2013; Tanentzapf et al., 2000). It is an adult epithelium that emerges through mesenchymal to epithelial transition to protect the developing germline (King, 1970). During

oogenesis in *Drosophila,* individual egg chambers are formed by 16 germ cells that are enveloped by the shell-like follicular epithelium as they go through 14 developmental stages (reviewed in Bastock and St Johnston, 2008; Bilder and Haigo, 2012; He et al., 2010). During the initial stages 2 to 6, the follicular epithelium proliferates to accompany the growth of the germline. After stage 6, the follicular epithelium stops proliferating and continues growing through endoreplication and cell growth. The follicular epithelium is a simple monolayer where the apical surface faces the germline it surrounds and the basal domain faces an outer basement membrane. During the proliferative stages, epithelial cells have no septate junctions, which are only formed later after stage 9. Importantly, for the purpose of this work, *Drosophila* egg chambers can be cultured *ex vivo* (Cetera et al., 2016; Manning and Starz-Gaiano, 2015; Peters and Berg, 2016). Furthermore, their round morphology makes them ideal for direct visualization of the epithelium both along the apical basal axis (imaging of a midsagittal cross-section) or along the planar axis (imaging of a surface cross-section).

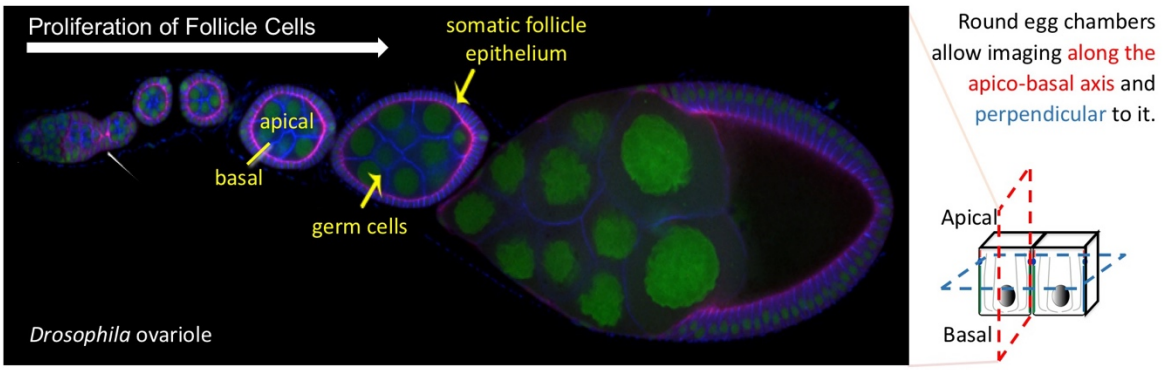


Figure 3.1. The *Drosophila* follicular epithelium. A single ovariole is composed by a string of individual egg chambers in different developmental stages. In each egg chamber, the polarized follicular epithelium envelops the growing germline (adapted from a figure prepared by Eurico Morais de Sá).

To study how apical-basal polarity preserves epithelial architecture during proliferation, I first tested whether LARIAT could inactivate polarity proteins in the *Drosophila* follicular epithelium (Appendix). Inactivation of the apical polarity determinant aPKC with LARIAT reproduced the formation of known architecture defects: epithelial gaps and multilayering. A detailed analysis of gap formation, revealed that these appear through detachment of dividing and neighbour cells due to an increase in apical constriction. A different optogenetic tool to increase apical contractility through acute recruitment of RhoGEF2 to the apical surface confirmed that increased apical constriction challenges epithelial integrity during proliferation. Altogether, the results suggest a new role for aPKC in protecting epithelial integrity during proliferation through downregulation of apical constriction.

PART II

EXPERIMENTAL WORK

CHAPTER 4

LIGHT-INDUCED PROTEIN CLUSTERING FOR OPTOGENETIC INTERFERENCE AND PROTEIN INTERACTION ANALYSIS IN *DROSOPHILA* S2 CELLS

Abstract 77

Introduction 78

Materials and Methods 80

- Molecular biology 80
- S2 cell culture, transfection and imaging 82
- Immunofluorescence 83
- Image Analysis 84

Results and Discussion 84

- Generation and characterization of LARIAT modules in S2 cells 84
- Interference with GFP-tagged proteins by optogenetic clustering 87
- Analysis of protein-protein interactions via optogenetic co-clustering 91

Conclusions 92

Acknowledgments 93

Supplementary Material 93

The manuscript here included was published in Biomolecules in 2019 (vol. 9 iss. 2 article 61). Together with Eurico Morais de Sá, I designed the project and experiments. I performed most experiments, analyzed the data and prepared the figures for the manuscript. Ana Filipa Santos, a master student in the group, cloned Par6-RFP and executed and quantified the protein-protein interaction experiments presented in Figure 4 – 7. I wrote the original draft together with Eurico Morais de Sá and participed in reviewing and editing the final manuscript.

Hobbes: Watcha doin'?
Calvin: I'm seeing if it's hot enough to fry an egg on the sidewalk.
Hobbes: I guess it isn't.
Calvin: Ugh, what a mess. (starts running) C'mon I'll bet it's hotter on the car dash!
Bill Watterson (2nd Sep 1992), Calvin and Hobbes

LIGHT-INDUCED PROTEIN CLUSTERING FOR OPTOGENETIC INTERFERENCE AND PROTEIN INTERACTION ANALYSIS IN *DROSOPHILA* S2 CELLS

Mariana Osswald[1,2], A. Filipa Santos[1,2] and Eurico Morais-de-Sá[1,2,3]

1. Instituto de Biologia Molecular e Celular, Universidade do Porto, Porto, Portugal
2. Epithelial Polarity and Cell Division group, Instituto de Investigação e Inovação em Saúde (i3S), Universidade do Porto, Porto
3. corresponding author: eurico.sa@ibmc.up.pt
   i3S – Instituto de Investigação e Inovação em Saúde
   Rua Alfredo Allen, 208, 4200 – 135 Porto
   Tel: +351 226074921

ABSTRACT

Drosophila S2 cells are a simple and powerful system commonly used in cell biology, since they are well suited for high resolution microscopy and RNAi-mediated depletion. However, understanding dynamic processes, such as cell division, also requires methodology to interfere with protein function with high spatiotemporal control. Here, we

report the adaptation of an optogenetic tool to *Drosophila* S2 cells. Light activated reversible inhibition by assembled trap (LARIAT) relies on the rapid light-dependent heterodimerization between CRY2 and CIB1 to form large protein clusters. An anti-GFP nanobody fused with CRY2 allows this method to quickly trap any GFP-tagged protein in these light-induced protein clusters. We evaluated clustering kinetics in response to light for different LARIAT modules, and showed the ability of GFP-LARIAT to cluster and inactivate the mitotic protein Mps1 and to disrupt the membrane localization of the polarity regulator Lgl. Moreover, we validated light-induced co-clustering assays to assess protein-protein interactions in S2 cells. In conclusion, GFP-based LARIAT is a versatile tool to answer different biological questions, as it enables probing of dynamic processes and protein-protein interactions with high spatiotemporal resolution in *Drosophila* S2 cells.

INTRODUCTION

Understanding the mechanisms that control the dynamic behavior of most cell biology processes requires an experimental setup that enables detailed visualization with high resolution microscopy and which is amenable to genetic manipulation. *Drosophila* Schneider 2 (S2) cells have long been recognized as a powerful cell culture model to study the underlying mechanisms controlling cell division, being particularly well-suited for high-throughput RNA interference screens via double-stranded RNAs (Bettencourt-Dias et al., 2004; Goshima et al., 2007; Heigwer et al., 2018; Moutinho-Pereira et al., 2010; Rogers and Rogers, 2008). Moreover, S2 cells provide a reduced system for the molecular dissection at the cell autonomous level of processes that require reorganization of the cytoskeleton and the plasma membrane in a particular axis, such as cell motility, cell polarity and oriented cell division, complementing findings that are difficult to untangle in the complexity of the organism (Carvalho et al., 2015; Johnston et al., 2009; Ribeiro et al., 2014). Importantly, investigation of these very dynamic cellular processes requires progression from established genetic approaches to methodologies that perturb protein function with high spatial and temporal control. Temporal control can be achieved through chemical inhibition, but this lacks spatial resolution, reversibility and shows common off-target effects. Thus, the advances in optogenetic tools that enable rapid modulation of protein activity with light have been critical to provide unprecedented spatiotemporal control over dynamic cellular processes (Guglielmi et al., 2016; Liu and Tucker, 2017), and are likely to bring fruitful times for cell biologists.

Light-Activated Reversible Inhibition by Assembled Trap (LARIAT) was developed in mammalian cells to manipulate protein function through light-inducible and reversible

formation of multimeric protein clusters (Lee et al., 2014). This tool combines the photoreceptor Cryptochrome 2 (CRY2) with Cryptochrome-interacting bHLH (CIB1) oligomers. CRY2 forms both homo-oligomers and heterodimers with CIB1 within seconds of blue-light exposure (Kennedy et al., 2010). This was coupled with a fusion between CIB1 and the multimerization domain of CaMKIIα to drive the formation of large clusters (Figure 4.1). In addition, CRY2 fused with an anti-GFP nanobody sequesters GFP-tagged proteins in the light-induced clusters in a reversible manner (Lee et al., 2014). LARIAT is therefore a versatile tool that has been exploited in mammalian cells to disrupt a variety of pathways, including Rho GTPase signaling, the microtubule cytoskeleton and membrane trafficking (Lee et al., 2014; Nguyen et al., 2016), as well as cell adhesion and actomyosin contractility in *Drosophila* tissues (Qin et al., 2018; Qin et al., 2017). However, these approaches have yet to be implemented in *Drosophila* cell culture models. (Moreira et al., 2019)

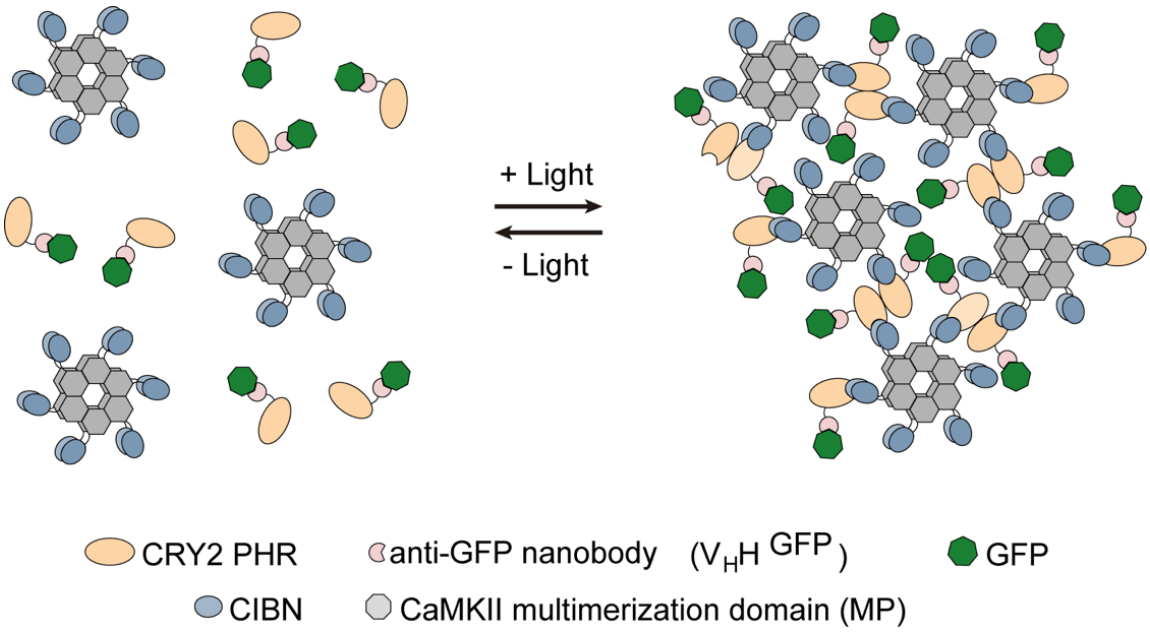


Figure 4.1.Schematic representation of LARIAT-mediated optogenetic clustering. LARIAT enables optogenetic clustering of target proteins to interfere with their function and probe interactions. CIB1 N-terminal (CIBN) fused with the multimerization domain from CaMKIIα (MP) forms dodecamers in the cytoplasm. CRY2 photolyase homology region (PHR) is fused with an anti-GFP nanobody that binds specifically to GFP-tagged proteins. Blue light triggers CRY2 oligomerization and binding to CIBN and consequently the formation of clusters to trap GFP-tagged proteins. In the dark, CRY2 reverts spontaneously to its ground state and clusters disassemble.

Here, we adapted optogenetic clustering to *Drosophila* S2 cells, generating an inducible module for expression of the LARIAT components. To validate LARIAT as a tool to study cell division in S2 cells, we provide an example of application showing that LARIAT

can be used to trap and inactivate the key regulator of mitotic fidelity Mps1. Moreover, we evaluated the potential of LARIAT in S2 cells for the molecular dissection of other processes associated with cell division, such as the regulation of cortical polarity. Both asymmetric stem cell division (Betschinger et al., 2003; Peng et al., 2000) and mitotic spindle orientation in some epithelial tissues (Bell et al., 2015; Carvalho et al., 2015; Guilgur et al., 2012; Hao et al., 2010) rely on the dynamic control of two conserved regulators of cortical polarity, the aPKC complex and Lgl. We thus monitored the ability of LARIAT to delocalize the membrane-associated protein Lgl, and to determine protein interactions within the aPKC complex in living cells. Hence, this study provides a new tool that expands the power of *Drosophila* S2 cells as a model for spatiotemporal investigation of mechanisms controlling cell division and cell polarity, two highly dynamic and interconnected processes, whose proper understanding demands ability to interfere with protein function and to evaluate protein interactions with high temporal control.

MATERIALS AND METHODS

Molecular biology

We cloned all LARIAT modules (Figure 4.2), aPKC, aPKCΔN and Par6 into *Drosophila* Gateway vectors. We started by inserting them into pENTR through FastCloning (Li et al., 2011a) with the respective primers (indicated in Table 4.1). We amplified CIB1 N-terminal (CIBN; amino acids 1-170) fused with mCerulean and the oligomerization domain from CaMKIIα (amino acids 315-478) from pCMV-CIB1-mCerulean-MP (Addgene plasmid #58366) (Lee et al., 2014), CRY2 photolyase homology region (amino acids 1-498) fused with an anti-GFP nanobody (V_HH) from pCMV-SNAP-CRY2-VHH(GFP) (Addgene plasmid #58370) (Lee et al., 2014) and aPKC, aPKCΔN (amino acids 180-606) and Par6 from their respective cDNAs (BDGP *Drosophila* Gold collection). After PCR amplification with Phusion Polymerase (NEB), we destroyed template DNA with DpnI (NEB) and transformed chemically competent TOP10 *E.coli* cells with the insert and pENTR PCR mixes. To generate pENTR-CIBN-MP, we removed mCerulean from pENTR-CIBN-mCerulean-MP through restriction with AgeI (NEB) and BspEI (NEB). pENTR-CRY2olig(E490G)-V_HH was generated through site-directed mutagenesis as in FastCloning (Li et al., 2011a; Table 4.1). Then, we recombined aPKC and aPKCΔN into pHGW, Par6 into pHWR, CIBN constructs into pHW and CRY2 constructs into pHRW through LR Clonase II (Thermo Fisher)-mediated recombination.

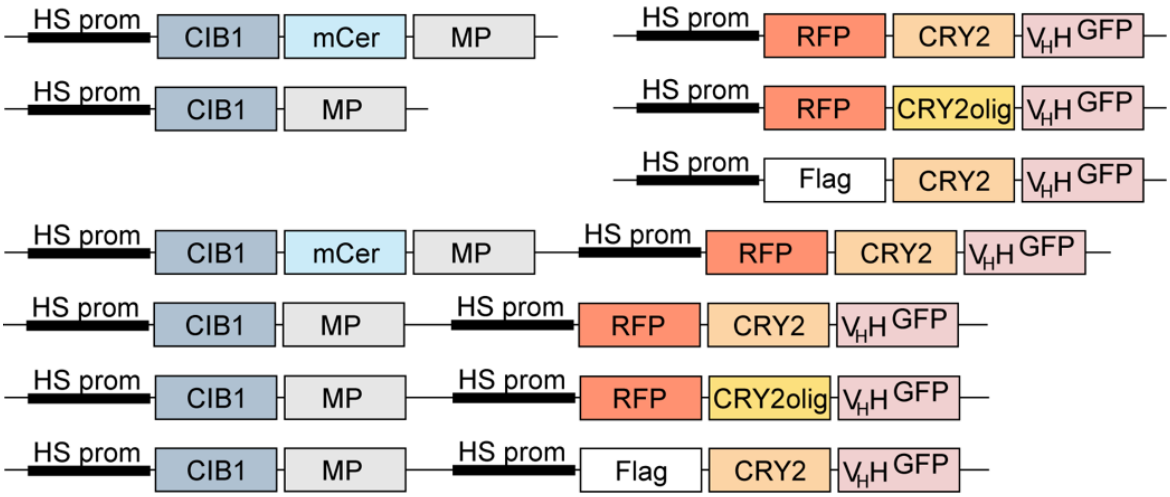


Figure 4.2. Schematic representation of LARIAT plasmids for *Drosophila* S2 cells. LARIAT modules were cloned downstream of the Hsp70 promoter. Untagged and mCerulean-tagged CIB1 N-terminal (CIBN) are fused with the multimerization domain from CaMKIIα (MP). Flag- or RFP-tagged CRY2 photolyase homology region are fused with an anti-GFP nanobody (VHHGFP). CRY2olig has enhanced oligomerization ability due to a single point mutation - E490G. Different CRY2 and CIBN expression cassettes were combined in the same vectors for efficient co-expression.

For S2 cell transfection, we joined CIBN and CRY2 constructs in the same plasmid through Circular Polymerase Extension Cloning (CPEC) (Quan and Tian, 2011). To this end, we created fragments with overlapping extremities through amplification with Gateway primers (Table 4.1) of RFP-tagged CRY2 constructs, including promoter and terminator regions, and both pHW-CIBN plasmids. CIBN and CRY2 fragments were combined through overlap annealing and Phusion DNA polymerase (NEB)-mediated extension. To create a non-fluorescent LARIAT plasmid, we recombined CRY2-V_HH into pHFW harboring an additional AfeI restriction site before the Hsp70 promoter created through site-directed mutagenesis. Then, the CRY2-V_HH expression cassette was excised with AfeI (NEB) and PvuI (NEB) and inserted into pHW-CIBN-MP previously linearized with PmeI (NEB) and PvuI (NEB). All expression plasmids were sequenced prior to *Drosophila* S2 cell transfection and will be made available through Addgene. pHWG-Lgl (Carvalho et al., 2015), mCherry-α-Tubulin (Goshima et al., 2007) and pMT-EGFP-Mps1 and pMT-EGFP (Conde et al., 2013) have been described previously.

Table 4.1. List of primers for molecular cloning.

Purpose	Primer Name	Primer Sequence (5' – 3')
pENTR insertion	CIBN-mCer-MP Fw	GCTGCTCCATTTACAATGAATGGAGCTATAGGAG
	CIBN-mCer-MP Rv	AGCGCGTCCACCTTTTCAATGGGGCAGGACG
	CRY2-V_HH Fw	GCTGCTCCATTTACAATGGACAAAAAGACCATC
	CRY2-V_HH Rv	AGCGCGTCCACCTTTTTAGCTGGAGACGGTGAC
	aPKC Fw	GCTGCTCCATTTACAATGCAGAAAATGCCCTC
	aPKC/aPKCΔN Rv	AGCGCGTCCACCTTTGACGCAATCCTCCAGAG
	aPKC ΔN Fw	GCTGCTCCATTTACAATGAAGCTGTTGGTGCACAAG
	Par6 Fw	GCTGCTCCATTTACAATGTCGAAGAACAAGATAAACAC
	Par6 Rv	AGCGCGTCCACCTTTCAAATGCAGCACTCCATC
	pENTR Fw	AAAGGTGGACGCGCTGACCCAGCTTTCTT
	pENTR Rv	TGTAAATGGAGCAGCCGCGGAGC
mutagenesis	CRY2olig E490G Fw	GATCTCTCGCACTCGGGGCGCCCAGATTATG
	CRY2olig E490G Rv	CGAGTGCGAGAGATCGCTTTAG
	Gateway AfeI Fw	GAGTCAGTGAGCGAGCACGTGGAAGAGCGCTCAATACGC
	Gateway AfeI Rv	CTCGCTCACTGACTCGCTGCGCTC
CPEC	Gateway CIBN Fw	TCCCGTTTGCGGCATTTTGCCTTC
	Gateway CIBN Rv	GGCGCTCAATAAGGGCGACACGGA
	Gateway CRY2 Fw	CCCTTATTGAGCGCCCAATACGCAAAC
	Gateway CRY2 Rv	AATGCCGCAAACGGGATCCAGACATGATAAG

S2 cell culture, transfection and imaging

Drosophila S2-DGRC cells (*Drosophila* Genomics Resource Center - DGRC) were cultured at 25°C in Schneider's Insect medium (Sigma-Aldrich) supplemented with 10% fetal bovine serum. We used Effectene Transfection Reagent (QIAGEN) according to the manufacturer's instruction to transiently transfect S2 cells with the plasmids indicated for the experiments in each figure. After transfection, cells were incubated in the dark, but no measure was taken to limit light exposure during cell manipulation prior to LARIAT expression. We induced expression of all Hsp70 promoter controlled constructs by incubating the cells at 37°C for 45 minutes at least 6 hours prior to imaging and of the GFP-Mps1 or GFP construct with 100μM $CuSO_4$ at least 12 hours prior to imaging. After LARIAT expression was induced, we kept cells in the dark and used a 593 nm LED light (Super

Bright LEDs) during manipulation when necessary. For imaging, we seeded S2 cells on glass-bottom dishes (MatTek Corporation) coated with Concanavalin A (for experiments in Figure 4.3, Figure 4.4 and Figure 4.5) or poly-L-lysine (for experiments in Figure 4.6 and Figure 4.7). Cells were imaged between day 2 and day 7 post-transfection with an Andor XD Revolution Spinning Disk Confocal system equipped with two solid state lasers – 488nm and 561nm -, an iXonEM+ DU-897 EMCCD camera and a Yokogawa CSU-22 unit built on an inverted Olympus IX81 microscope with a PLAPON 60x/NA 1.42 or a UPLSAPO 100x/NA 1.40 objective. Cells for mitotic timing experiments were imaged in a Nikon TE2000 microscope equipped with a modified Yokogawa CSU-X1 unit (Solamere Technology), an FW-1000 filter-wheel (ASI) and an iXon+ DU897 EM-CCD (Andor) and controlled by NIS-Elements via a DAC board (National Instruments, PCI-6733). Excitation by two sapphire lasers at 488nm and 561nm respectively was controlled by an acousto-optic tunable filer (Gooche&Housego, model R64040-150). We used an oil-immersion 60x 1.4NA Plan-Apo DIC CFI (Nikon, VC series). All live-imaging experiments were performed at controlled temperature of 25°C.

Immunofluorescence

The Flag tagged CRY2 was validated through immunofluorescence. *Drosophila* S2 cells were transiently transfected with pMT-EGFP and pH-CIBN-MP-HF-CRY2-V_HH(GFP) with Effectene Transfection Reagent (QIAGEN). To induce clustering, cells were exposed to a 472nm LED light (Super Bright LEDs) prior to fixation. 10^5 cells were then centrifuged onto slides for 5 min at 1000 rpm (Cytospin2, Shandon), fixed with 3.7% formaldehyde (Sigma-Aldrich) in PHEM (60mM PIPES, 25mM HEPES, Ph 7.0, 10mM EGTA, 4mM Mg_2SO_4) for 12 min and permeabilized with 0.5% Triton X-100 (Sigma-Aldrich) in PBS three times for 5 minutes each. Fixed cells were blocked for 1 hour with 10% FBS diluted in PBS-0.05% Tween-20 (Sigma) and afterwards incubated overnight at 4°C with mouse anti-Flag (1:250, M2 clone, Sigma-Aldrich) diluted in blocking solution. Subsequently, cells were washed three times with PBS-0.05% Tween20 and incubated for 1 hour at room temperature with anti-mouse Alexa 647 (1:1000, Invitrogen) diluted in blocking solution. After washing three times with PBS-0.05% Tween20, slides were mounted with Vectashield Mounting Medium with DAPI (Vector Laboratories). Slides were imaged with a LEICA TCS SP5 II laser scanning confocal microscope (Leica Microsystems).

Image Analysis

Image sequences were assembled and analyzed using Fiji/ImageJ (Schindelin et al., 2012). To quantify protein clustering, we calculated the coefficient of variation in the cytoplasm (region of interest (ROI) over 40μm^2 in size). Briefly, we measured standard deviation of fluorescence intensity in the ROI and divided it by the mean fluorescence intensity in the same region corrected for background signal. Then, we normalized the coefficient of variation to its mean value before cluster formation and plotted it through time with GraphPad Prism 8. To determine how long it takes to revert to 50% and 10% of maximal clustering in Supplementary Figure 4.S1, clustering curves were smoothed with a moving average. For the experiments in Figure 4.4 and Figure 4.5, mitotic timing was determined as the time between nuclear envelope breakdown (NEB, defined as the first frame where tubulin signal is present inside the nuclear area) and anaphase onset (AO, defined as the first frame where movement toward opposite sides by both spindle halves can be seen). To determine which cells expressed LARIAT constructs, we measured clustering in the first three time points after clustering stimulation through GFP or GFP-Mps1 coefficient of variation. We measured GFP-Mps1, Lgl-GFP and RFP-CRY2 relative expression levels by extracting average fluorescence intensity in the cell and correcting for background signal. Fluorescence intensity profiles along lines were obtained with the Plot Profile tool from Fiji. Kymographs were made by stacking the indicated line ROIs from every timepoint sequentially.

RESULTS AND DISCUSSION

Generation and characterization of heat shock-inducible LARIAT modules in S2 cells

To build a toolbox for interference with protein function through optogenetic clustering in *Drosophila* S2 cells, we adapted LARIAT from a set of constructs previously developed for human cells (Lee et al., 2014). We cloned CIB1 N-terminal (CIBN) fused with a multimeric protein (MP; the oligomerization domain from CaMKIIα) and CRY2 photolyase homology region (PHR) into a single plasmid to ensure constant relative amounts of CIBN and CRY2 in transfected cells (Figure 4.2). CRY2 fusion with an anti-GFP nanobody (VHH) allows clustering of GFP-tagged proteins without additional cloning. Finally, we used an inducible Hsp70 promoter to allow temporal control over LARIAT expression, which obviates the need to limit light exposure during cell culture.

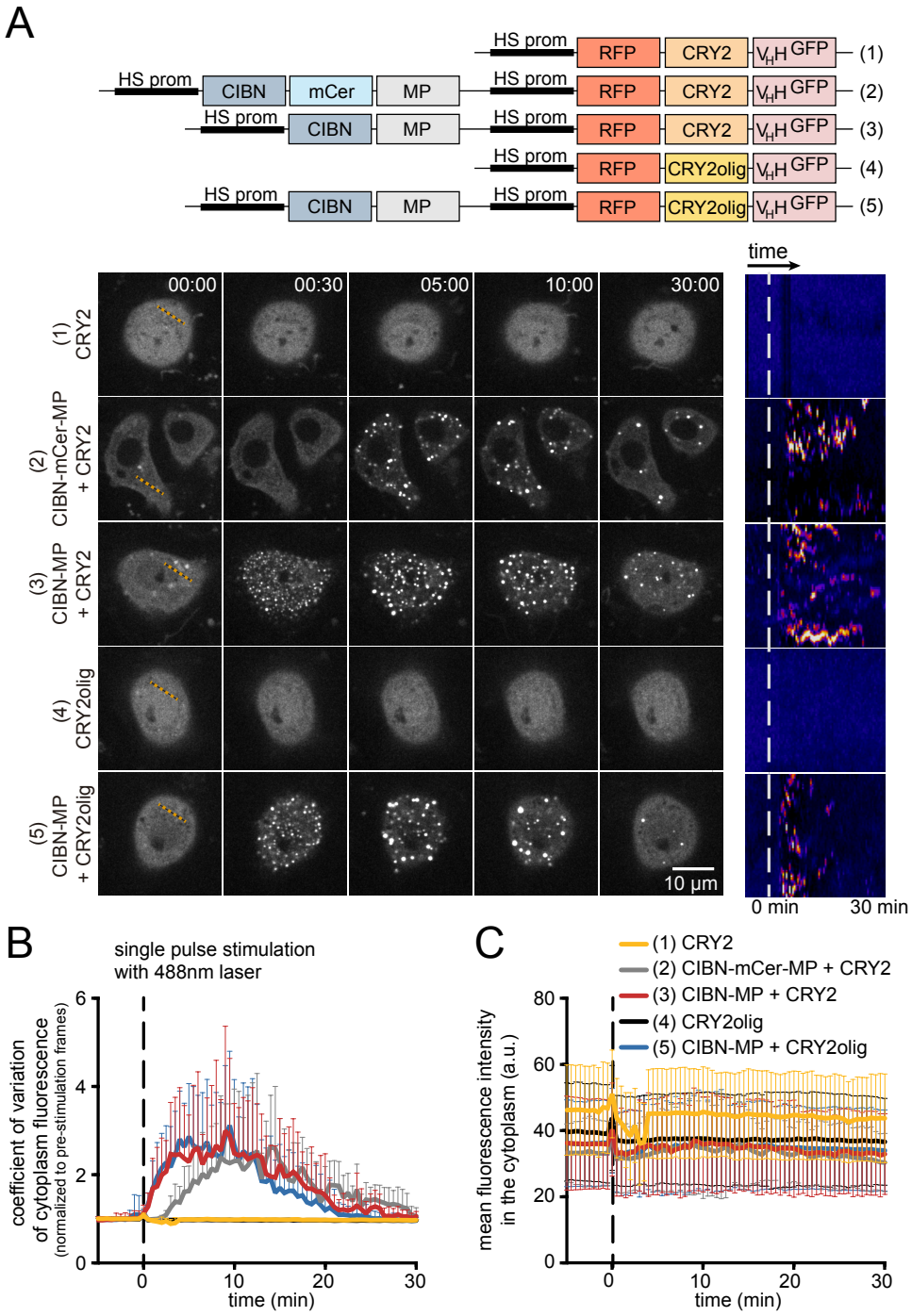


Figure 4.3. A *Drosophila* S2 cell LARIAT toolbox. (A) Representative timepoints and z-sections of *Drosophila* S2 cells expressing the indicated LARIAT modules. Transfected cells were kept in the dark prior to live-imaging. Pseudo-colored kymographs made along the orange dashed lines represent cluster formation and disassembly after stimulation with a 488 nm laser set to 1mW laser power for 300 msec at minute 0 (white dashed line). (B) Clustering was quantified with the coefficient of variation of cytoplasm fluorescence and (C) mean fluorescence intensity was plotted along time. Graphs display mean ± s.d. n(CRY2) = 9 cells; n(CIBN-mCer-MP+CRY2) = 5 cells; n(CIBN-MP+CRY2) = 15 cells; n(CRY2olig) = 10 cells; n(CIBN-MP+CRY2olig) = 13 cells.

In *Drosophila* S2 cells, CRY2 clustered with CIBN-MP in under 30 seconds after a single pulse stimulation with a 488 nm laser (construct 3 in Figure 4.3A, Supplementary Movie 3 - 1), a similar timeframe to the one for human cells (Lee et al., 2014). Cluster size increased during about 5 minutes upon the pulse of light and then disassembled spontaneously within around 30 minutes with no protein degradation (Figure 4.3A, C). Clustering sequesters RFP-CRY2 in puncta and disrupts fluorescence homogeneity in the cytoplasm. Thus, we evaluated clustering kinetics by measuring fluorescence heterogeneity with the coefficient of variation of RFP-CRY2 fluorescence (standard deviation normalized to average intensity). This allowed us to quantitatively compare the kinetics of cluster assembly and reversibility in different imaging conditions and for different optogenetic modules (Figure 4.3B). Interestingly, the reversion half-life is longer in S2 cells (t1/2 = 17.5; Supplementary Figure 4.S1C) when compared with human cells, where LARIAT-induced clusters return to diffusive state within 10 minutes in the dark (t1/2 ~ 5.7 min) (Lee et al., 2014). Modulation of laser intensity controls the extent of CRY2/CIBN clustering in S2 cells (Supplementary Figure 4.S1A), as previously observed in mammalian cells (Lee et al., 2014). However, we observed longer reversion periods in S2 cells (t1/2 = 16; Figure A1D) even using very low laser intensity, for which protein clusters are barely detected. Since S2 cell experiments are performed at lower temperature (25°C), this difference may be related to an effect of temperature in the rate of CRY2-CIBN complex formation or disassembly, as previously proposed (Li et al., 2011b).

The clustering efficiency of different CRY2 variants has also been correlated with their expression levels (Park et al., 2017; Taslimi et al., 2014). Accordingly, we observed faster kinetics of LARIAT-mediated clustering for cells expressing higher levels of RFP-CRY2/CIBN (Supplementary Figure 4.S1B). Thus, to enable comparison between the different LARIAT modules (constructs 2,3,5 in Figure 4.3A), we restricted the analysis to cells within a range of equivalent expression of LARIAT components measured by RFP fluorescence (Figure 4.3C). Removal of the mCerulean tag from CIBN increased clustering for the same expression levels and light stimulation conditions (Figuer 4.3A, B), suggesting that mCerulean could be partially blocking CRY2 binding to CIBN. Given that mCerulean is a β barrel with its N- and C-termini sticking out from the same side (Ormo et al., 1996), we speculate that fusion with mCerulean positions CIBN towards the inside of the oligomer, partially obstructing access of CRY2 to CIBN.

In mammalian cells, CRY2 oligomerization by itself was shown to cluster target proteins (Bugaj et al., 2013). However, when expressed by themselves in our assay, we did not detect clustering with either CRY2 or CRY2olig, a CRY2 variant with enhanced oligomerization ability due to the point mutation E490G (Duan et al., 2017; Taslimi et al., 2014; Figure 4.3). This could result from lower expression levels of CRY2 variants driven

by the inducible heat-shock promoter relatively to the strong constitutive expression induced in mammalian cells by the CMV promoter. Interestingly, when co-expressed with CIBN-MP in S2 cells, CRY2olig did not cluster more efficiently than wild-type CRY2 and the clusters disassembled faster (Figure 4.3), indicating that this LARIAT module should be considered for experiments that require faster reversibility of protein interference. Altogether, these experiments highlight the potential of adjusting expression levels and laser intensity to control clustering kinetics and also suggest that LARIAT clustering can be fine-tuned by modulating CRY2 propensity to oligomerize. It would be interesting to test the effect of CRY2clust (Park et al., 2017), CRY2low (Duan et al., 2017) and other variants that affect photocycle kinetics (Taslimi et al., 2016) on LARIAT, as they will enable further modulation of cluster assembly and stability.

Interference with GFP-tagged proteins by optogenetic clustering

The presence of LARIAT clusters does not affect mammalian cell viability (Lee et al., 2014). We therefore proceeded to evaluate the potential of GFP-based LARIAT to dissect mitotic processes. We started by testing if the presence of protein clusters by themselves could interfere with mitotic progression and spindle organization. With that purpose, we generated LARIAT constructs where the RFP-tag for CRY2 was replaced by a FLAG tag to enable proper visualization of microtubule organization using mCherry-tubulin, while co-expression of GFP was used to validate cluster formation (Supplementary Figure 4.S2). Formation of light-induced protein clusters enables the assembly of normal bipolar spindles and does not interfere with the time from nuclear envelope breakdown to anaphase onset (Figure 4.4). This suggests that the formation of CRY2-CIBN clusters does not affect mitotic spindle assembly or chromosome congression at the metaphase plate, as any defects on these processes would introduce significant delays in mitotic exit.

As a proof of concept that LARIAT can be used to dissect cell divison in *Drosophila* S2 cells, we then tested the ability of GFP-based LARIAT to sequester and inactivate the mitotic kinase Mps1. Mps1 is a conserved upstream regulator of the Spindle Assembly Checkpoint (SAC), a molecular mechanism that ensures chromosome segregation fidelity during mitosis by preventing chromatid separation until all chromosomes are properly attached to opposite spindle poles (Pachis and Kops, 2018; Weiss and Winey, 1996). Upon mitotic entry, Mps1 accumulates at the kinetochores to promote SAC signaling (Abrieu et al., 2001; Stucke et al., 2002). When co-expressed with LARIAT, Mps1-GFP rapidly clustered during mitosis upon blue light exposure (Figure 4.5A). Mps1-GFP signal decreased in the cytoplasm and increased at RFP-CRY2-VHH puncta, indicating that Mps1-

GFP was efficiently trapped in the optogenetic clusters (Figure 4.5B). As cells reach metaphase, Mps1 must be removed from kinetochores and inactivated to enable anaphase onset (Hiruma et al., 2015; Jelluma et al., 2010; Ji et al., 2015; Moura et al., 2017). Accordingly, high overexpression levels of Mps1 leads to persistent SAC signaling that blocks cells in mitosis during a prolonged period of time (Conde et al., 2013 and Figure 4.5C). Importantly, light-induced clustering of Mps1-GFP is sufficient to revert this phenotype (Figure 4.5C), indicating that efficient optogenetic trapping of Mps1 leads to inactivation.

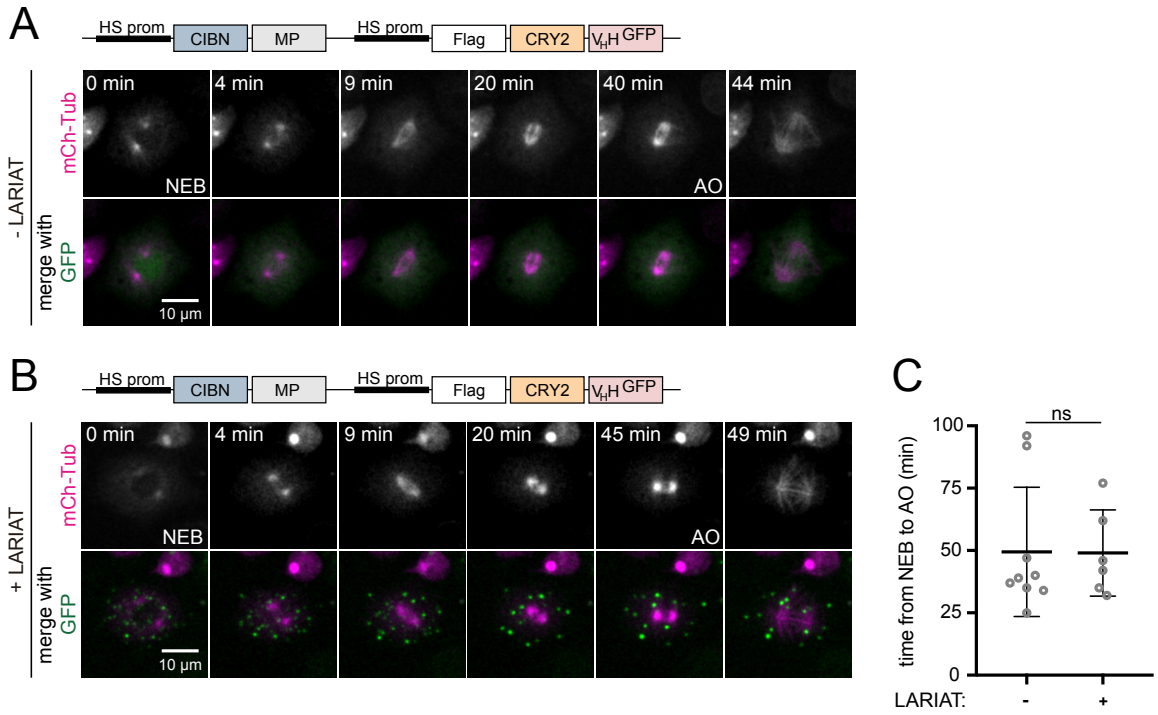


Figure 4.4. LARIAT clusters do not affect bipolar spindle assembly and mitotic progression. Clustering effect on mitotic progression was analyzed through live-imaging of *Drosophila* S2 cells expressing GFP, mCherry-α-Tubulin (A) alone and co-transfected with CIBN-MP and Flag-CRY2-VHH (B). The 488 nm laser used to image GFP triggered clustering since prophase. LARIAT expression was confirmed by measuring GFP coefficient of variation in the first three frames of each movie. (C) Graph shows average mitotic timing ± s.d. Mitotic timing is defined as the time it takes for a cell to progress from nuclear envelope breakdown (NEB) to anaphase onset (AO).

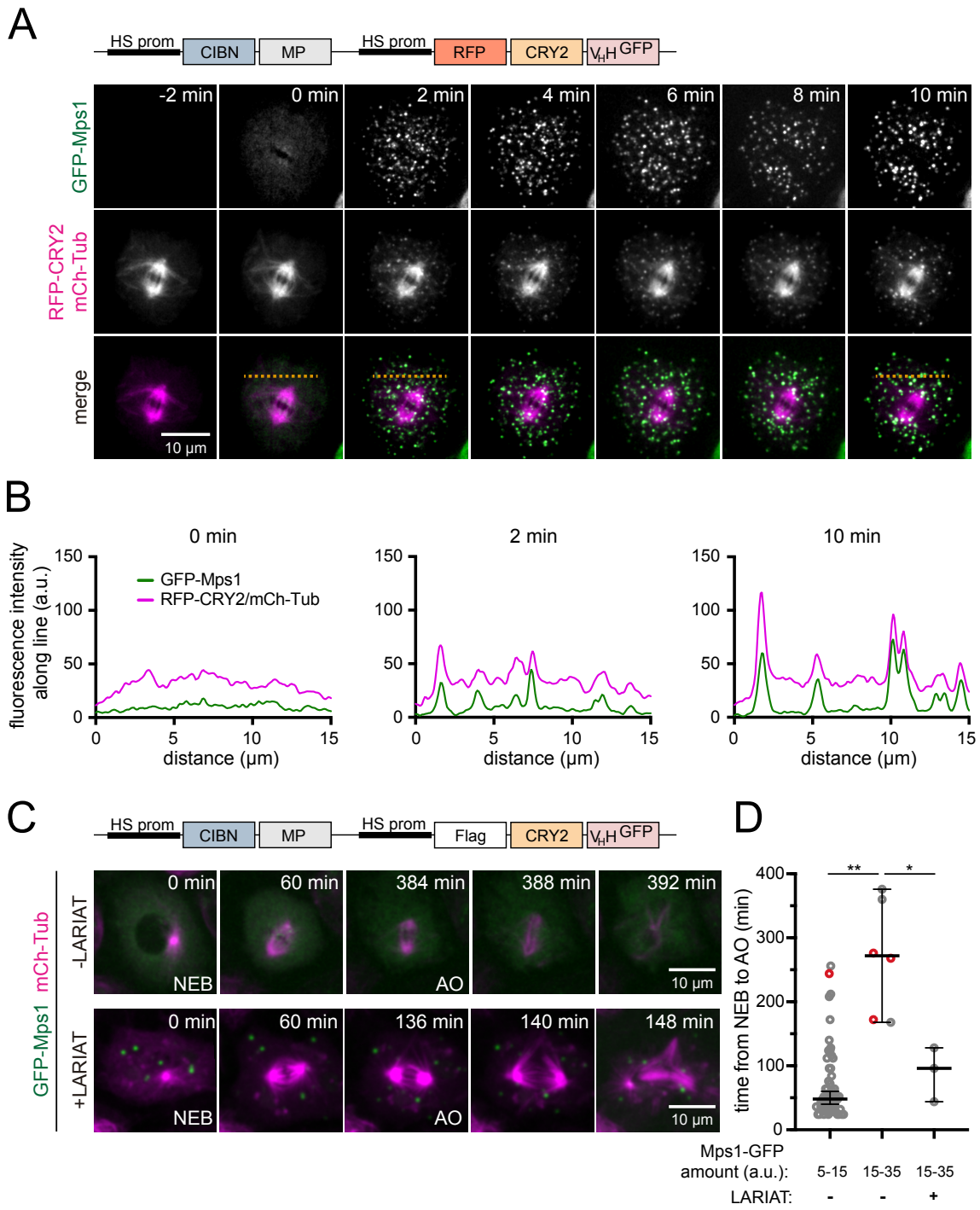


Figure 4.5. GFP-Mps1 is efficiently trapped in LARIAT clusters. Clustering was analyzed through live-imaging of *Drosophila* S2 cells expressing GFP-Mps1, mCherry-α-Tubulin, CIBN-MP and RFP-CRY2-VHH. The 488 nm laser used to image GFP-Mps1 from timepoint 0 onwards triggered clustering. (A) Representative stills and (B) intensity profiles for GFP-Mps1 and RFP-CRY2-VHH/mCherry-α-Tubulin along the orange dashed line are shown. (C) Representative stills of GFP-Mps1, mCherry-α-Tubulin, CIBN-MP and Flag-CRY2-VHH transfected cells analyzed through live-imaging during cell division. (D) Graph shows median mitotic timing ± 95% confidence interval. Mitotic timing is defined as the time it takes for a cell to progress from nuclear envelope breakdown (NEB) to anaphase onset (AO). GFP-Mps1 levels were determined by measuring GFP fluorescence in the cell cytoplasm in the first frame and LARIAT clustering was confirmed by measuring GFP-Mps1 coefficient

of variation in the first three frames of each movie. Red circles in the graph represent cells that did not exit mitosis during the time they were imaged.

We also determined the ability of GFP-based LARIAT to disrupt the localization of proteins associated with the plasma membrane and the underlying cortex, and which could play a role in processes associated with cell division. To this end, we analyzed Lgl, whose subcellular distribution controls the segregation of cell fate determinants during asymmetric cell division (Betschinger et al., 2003; Ohshiro et al., 2000; Peng et al., 2000; Wirtz-Peitz et al., 2008) and is tightly regulated to enable proper mitotic spindle orientation in *Drosophila* epithelial tissues (Bell et al., 2015; Carvalho et al., 2015). Lgl localizes at the cell cortex mainly through association with plasma membrane phosphoinositides (Bailey and Prehoda, 2015; Dong et al., 2015), although it also interacts with the actomyosin cytoskeleton (Betschinger et al., 2003; Strand et al., 1994). Lgl cortical localization is reproduced in *Drosophila* S2 cells, which have previously been used to dissect the molecular mechanisms controlling Lgl regulation and function (Betschinger et al., 2003; Carvalho et al., 2015). Thus, we tested if we could disrupt Lgl-GFP localization with LARIAT. Prior to clustering stimulation, RFP-CRY2-VHH accumulated at the cell cortex indicating that the GFP-nanobody recruited CRY2 to the same subcellular regions as Lgl-GFP (Figure 4.6A). Blue light exposure led to immediate cluster formation, which ultimately resulted in Lgl-GFP removal from the cortex (Figure 4.6A, A' and movie S2). However, light-induced disruption of Lgl localization failed for a significant number of cells. We found that efficient removal of Lgl from the cortex requires high levels of RFP-CRY2 relative to Lgl-GFP (Figure 4.5B, B', C), which highlights the importance of expressing LARIAT modules in excess of the target protein. This can be ensured by keeping target proteins at endogenous levels, for example using GFP knock-in lines easily generated through CRISPR/Cas9 in *Drosophila* S2 cells (Kunzelmann et al., 2016).

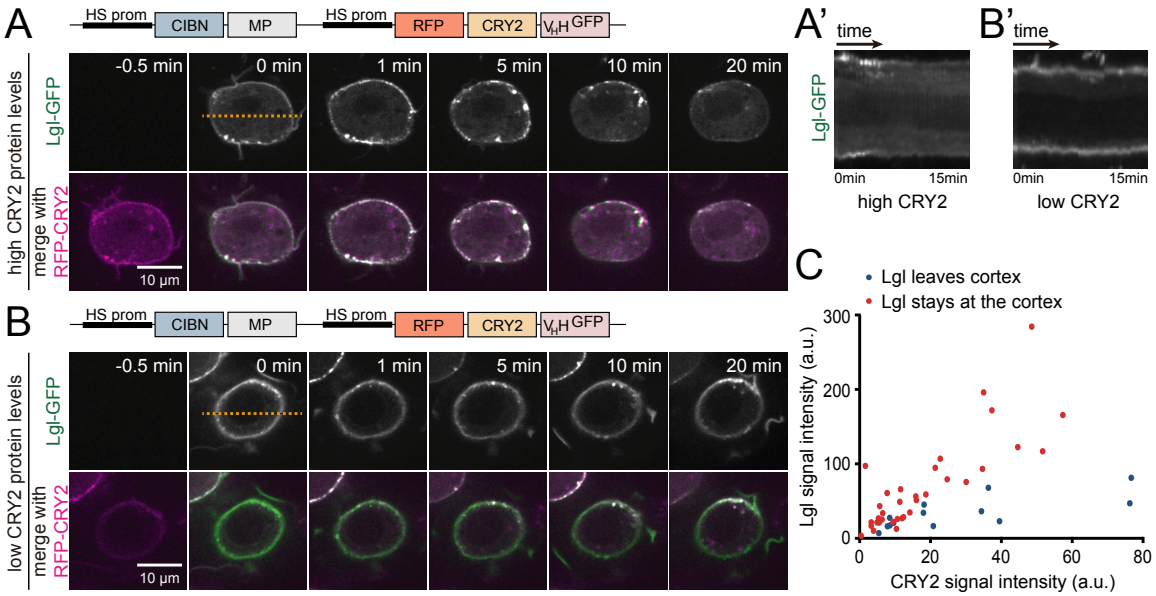


Figure 4.6. High levels of LARIAT delocalize membrane-associated Lgl-GFP. (A, B) Representative timepoints and (A', B') respective kymographs of *Drosophila* S2 cells transiently transfected with Lgl-GFP, CIBN-MP and RFP-CRY2-VHH expressing (A, A') higher or (B, B') lower levels of CRY2 relative to Lgl. (C) Dispersion plot for average Lgl-GFP and RFP-CRY2-VHH signal intensity in cells in which Lgl left (blue) or remained in (red) the cortex after clustering. Each dot represents a single cell.

Analysis of protein-protein interactions via optogenetic co-clustering

CRY2olig has previously been applied as a tool to measure protein interactions by evaluating recruitment of binding partners to light-induced clusters of target proteins (Taslimi et al., 2014). This system requires the production of constructs to tag any new "bait" protein with CRY2olig. We evaluated if we could use GFP-based LARIAT to probe interactions between GFP tagged proteins, for which there are many constructs available, and putative binding partners co-expressed with a different fluorescent tag or detected using antibodies in fixed tissue. As a proof of concept, we evaluated if this system could detect the formation of the aPKC/Par-6 complex, which regulates cortical polarity during asymmetric cell division (Betschinger et al., 2003; Wirtz-Peitz et al., 2008). aPKC-Par-6 interaction is mediated by heterodimerization between the N-terminal PB1 (Phox and Bem1) domains of aPKC and Par6 (Hirano et al., 2005; Joberty et al., 2000; Suzuki et al., 2001). Upon blue-light stimulation, Par6-RFP redistributed rapidly and colocalized with the GFP-aPKC clusters, confirming that the two proteins interact with high-affinity (Figure 4.7A, B). Importantly, the LARIAT system can be used for structure-function analysis, as removing the N-terminal region with the PB1 domain of aPKC (GFP-aPKCΔN) was sufficient to fully abolish the localization of Par6-RFP in the optogenetic clusters (Figure 4.7C, D). Thus, this

is a particularly useful approach in *Drosophila* S2 cells to complement current well-established biochemical methodology to identify protein interactions. Most importantly, detection of protein interactions with LARIAT allows live examination of interactions at the single cell level, which enables precise analysis during specific periods of the cell cycle. Furthermore, it can also be used to dissect the effect of pharmacological manipulation of signaling pathways or cytoskeleton organization on protein interactions.

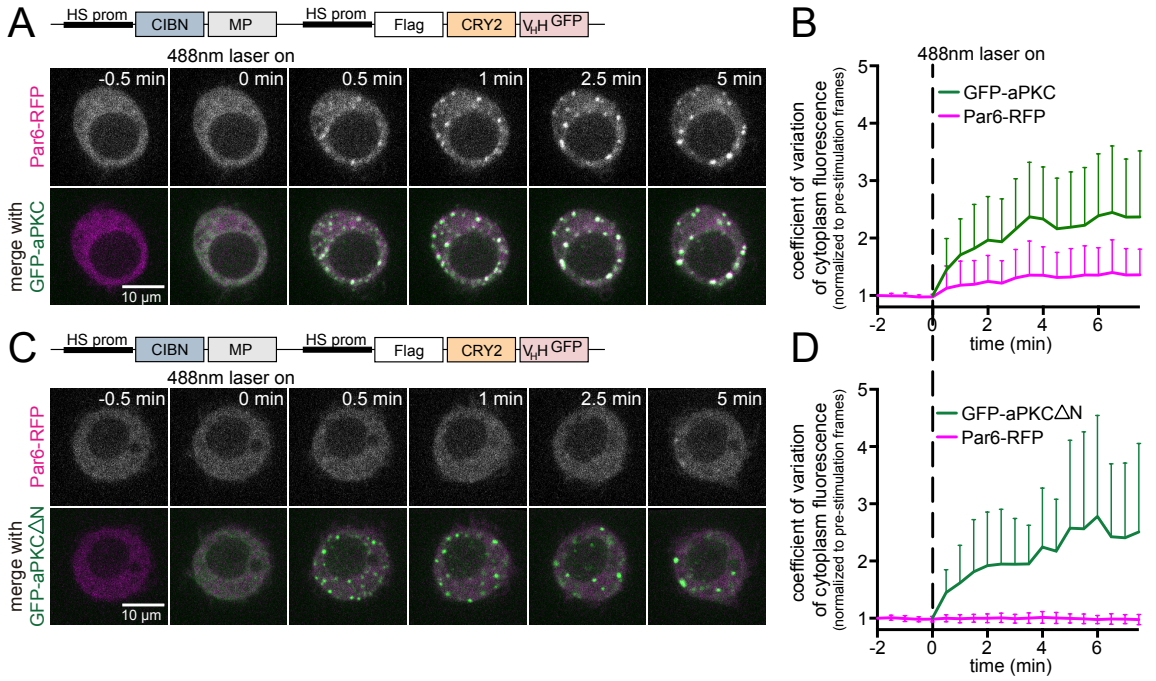


Figure 4.7. LARIAT detects aPKC and Par6 interaction in single cells. Representative timepoints of *Drosophila* S2 cells expressing Par6-RFP, CIBN-MP, Flag-CRY2-VHH and (A) GFP-aPKC or (C) GFP-aPKCΔN. (B, D) Par6-RFP and (B) GFP-aPKC or (D) GFP-aPKCΔN clustering is represented by the coefficient of variation of cytoplasm fluorescence. Graphs display mean ± s.d. n ≥ 15 cells for each condition.

CONCLUSIONS

In this work, we generated optogenetic modules to study protein function and interactions in *Drosophila* S2 cells. *Drosophila* LARIAT allows light-controlled clustering of proteins at the single cell level, which can be used to interfere with protein localization and function in S2 cells. This is particularly useful for proteins involved in multiple processes, whose depletion leads to pleiotropic phenotypes. Furthermore, we also expand the application of LARIAT to probe for protein interactions. Since this is done at the single cell level through live imaging, it can be used to test protein interactions at specific phases of

the cell cycle. Finally, comparison of different LARIAT variants provides relevant information to guide the generation of new optogenetic modules, and our data suggests that tweaking CRY2 oligomerization properties may produce LARIAT modules with faster reversibility. This would provide even tighter temporal control over protein function.

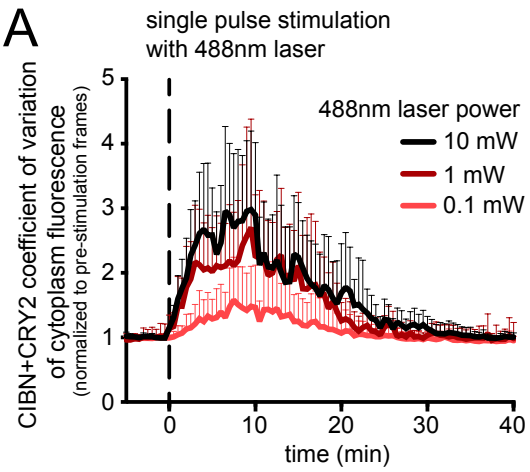
ACKNOWLEDGMENTS

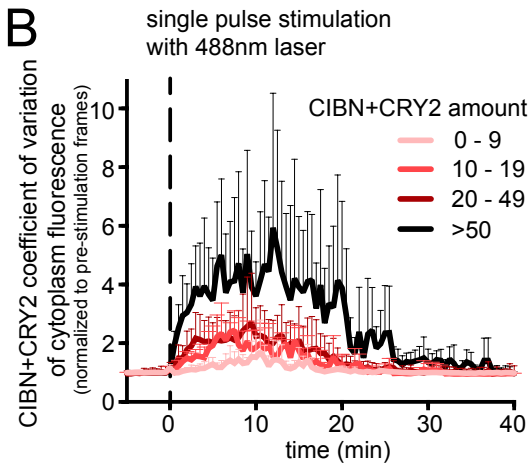
We thank the Claudio Sunkel Laboratory for the Mps1-GFP plasmid and the Hélder Maiato Laboratory for access to the Nikon TE2000 microscope.

SUPPLEMENTARY MATERIAL

Supplementary Movie 4.1: A *Drosophila* S2 cell LARIAT toolbox; related to Figure 4.4.

Supplementary Movie 4.2: LARIAT-mediated clustering causes Lgl to leave the cortex in *Drosophila* S2 cells; related to Figure 4.6.





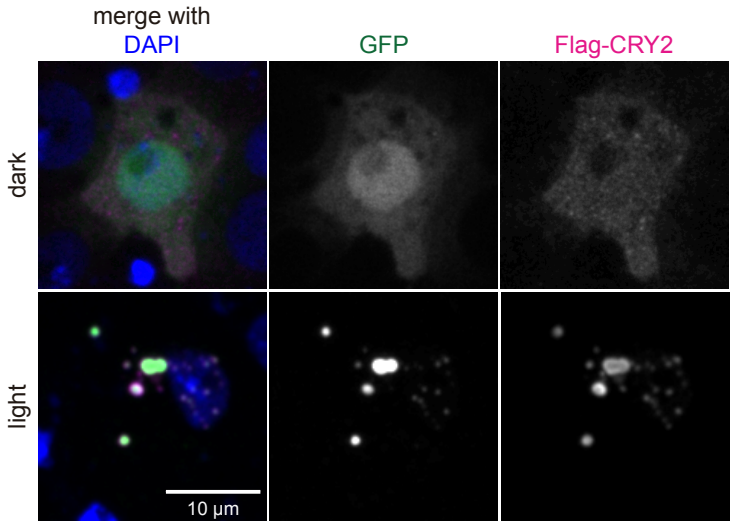
C

	time after cluster stimulation (min)	
clusters disassembled	50%	90%
LARIAT constructs		
CRY2	-	-
CIBN-mCer-MP + CRY2	20.0	30.5
CIBN-MP + CRY2	17.5	26.0
CRY2olig	-	-
CIBN-MP + CRY2olig	14.0	21.5

D

	time after cluster stimulation (min)	
clusters disassembled	50%	90%
CIBN-MP + CRY2 - varying expression levels (a.u.)		
0 - 9	15.0	22.5
10-19	15.5	23.0
20-49	17.5	23.5
>50	20.0	30.5
CIBN-MP + CRY2 - varying 488nm laser power		
0.1 mW	16.0	22.0
1 mW	17.5	23.5
10 mW	16.5	27.5

Supplementary Figure 4.S1. Laser intensity and LARIAT expression levels affect LARIAT clustering; related to Figure 4.4. *Drosophila* S2 cells expressing CIBN-MP and RFP-CRY2-VHH were analyzed through live-imaging. (A) LARIAT clustering was stimulated with a 488 nm laser set to the indicated laser power for 300 msec at minute 0. Clustering was quantified with the coefficient of variation of cytoplasm fluorescence. Graph displays mean ± s.d. n>10 cells expressing between 20-49 relative amount of CIBN-MP + RFP-CRY2-VHH for each laser condition. (B) Cells exposed to 1 mW 488nm laser power in (A) were grouped according to CIBN-MP and RFP-CRY2-VHH expression level measured through average fluorescence intensity in the cytoplasm in the frames prior to clustering stimulation. Graph displays mean ± s.d. n(0-9) = 4 cells; n(10-19) = 4 cells; n(20-49) = 12 cells; n(50+) = 4 cells. Timepoint at which clustering reversal reaches 50% and 90% of maximum clustering was estimated after smoothing curves plotted in Figure 4.4B (C) and here in A and B (D).



Supplementary Figure 4.S2. Flag-tagged LARIAT clusters GFP; related to Figure 4.4. *Drosophila* S2 cells expressing GFP, CIBN-MP and Flag-CRY2-VHH incubated in the dark or exposed to a 472nm LED light to stimulate clustering were stained for Flag.

CHAPTER 5

aPKC DOWNREGULATES APICAL CONTRACTILITY TO MAINTAIN SHAPE AND COHESION IN PROLIFERATIVE *DROSOPHILA* EPITHELIA

Abstract 100

Introduction 100

Materials and Methods 102

Drosophila genetics and stocks 102

Optogenetic experiments in the follicular epithelium 108

Fixation and stainings of egg chambers 109

Optogenetic experiment and immunofluorescence in neuroblasts 109

Imaging of fixed tissue 109

Live imaging 110

Protein extracts and Western blot 110

aPKC^{as4} allele inactivation 111

Quantifications, reproducibility and statistical analysis 111

Image preparation 115

Results 115

Optogenetic clustering inactivates aPKC with high temporal control 115

Acute aPKC inactivation leads to fast and stereotypical tissue disorganization 117

Cell division challenges tissue cohesion upon aPKC inhibition 119

Acute inactivation exposes the role of aPKC as a negative regulator of apical constriction 122

Balancing apicomedial actomyosin contractility in non-mitotic cells prevents excessive pulling forces on dividing cells 125

Persistent increase in apical contractility induces epithelial gaps 127

Discussion 129

Acknowledgments 132

Supplementary Material 133

This manuscript included in this chapter is being prepared for submission. Together with Eurico Morais de Sá, I designed the project and experiments. I performed most experiments and analyzed most data. André Carvalho, a master student, helped with the experiments to verify that blue light could permeate the abdomen of the fly (Figure 5.1B), contributed to the initial characterization of gap formation (Figure 5.2A,B,E, 5.3B, 5.4A) and performed the Western in Figure 5.1C and the movies and analysis in Figure 5.6D-H. Ana Maria Carmo quantified epithelial defects in one independent experiment of aPKC LARIAT (Figure 5.2B-G) and in one independent experiment of aPKC LARIAT in tum RNAi (Figure 5.3F). Ana Maria Carmo also imaged cell division in tum depleted epithelial cells (Supplementary Figure 5.S2A,B). Nicolas Loyer did the experiments in the neuroepithelium (Figure 5.5C-E, Supplementary Figure 5.S3B) and the movie in Supplementary Figure 5.S3C. Patrícia Grácio did the experiment in neuroblasts (Supplementary Figure 5.S1B,C). Eurico Morais de Sá collected the movies in Figures 5.3C, 5.6A,B and Supplementary Figure 5.S2A. I prepared the figures together with my supervisor and I wrote the figure legends and materials and methods. Eurico Morais-de-Sá wrote the remaining original draft, which I helped to review

That's funny.

Alexander Fleming (1928), when he noticed the lysis of the staphylococci.

aPKC DOWNREGULATES APICAL CONTRACTILITY TO MAINTAIN SHAPE AND COHESION IN PROLIFERATIVE *DROSOPHILA* EPITHELIA

Mariana Osswald[1,2], André Barros-Carvalho[1,2], Ana M Carmo[1,2], Nicolas Loyer[3], Patricia C. Grácio[4]; Claudio E Sunkel[1,2], Catarina C Homem[4], Jens Januschke[3] and Eurico Morais-de-Sá[1,2,5,*]

1. Instituto de Biologia Molecular e Celular, Universidade do Porto, Porto, Portugal.
2. Instituto de Investigação e Inovação em Saúde (i3S), Universidade do Porto, Porto,
3. Cell and Developmental Biology, School of Life Sciences, University of Dundee, Dow Street, Dundee, DD5 1EH UK
4. iNOVA4Health, CEDOC, NOVA Medical School, NMS, Universidade Nova de Lisboa, Lisbon, Portugal.
5. Lead contact

* correspondence: eurico.sa@ibmc.up.pt

i3S – Instituto de Investigação e Inovação em Saúde

Rua Alfredo Allen, 208, 4200 – 135 Porto

Tel: +351 226074921

ABSTRACT

Apical-basal polarity is an essential epithelial trait controlled by the conserved PAR-aPKC polarity network. Deregulation of polarity proteins disrupts tissue organization but the underlying mechanism is often unclear due to functional pleiotropy. Here we used optogenetics and chemical-genetics for fast inactivation of *Drosophila* aPKC to disentangle the primary cellular responses that disrupt epithelial and neuroepithelial architecture. Live imaging revealed epithelial gaps form quickly by detachment of dividing and neighbour cells in the proliferative follicular epithelum. Instead of polarity loss, we show that this phenotype results from increased apical constriction in non-mitotic cells, which pull on mitotic cells to trigger detachment. Accordingly, induction of apical constriction by light-induced recruitment of RhoGEF2 to the apical side induces tissue rupture. Our work highlights aPKC as a key negative regulator of apical contractility in multiple tissues and shows that unbalanced apical constriction threatens tissue cohesion in proliferative epithelia.

Highlights

- Optogenetic clustering disrupts aPKC function in vivo with high temporal control
- aPKC inactivation leads to intercellular detachment next to dividing cells
- aPKC downregulates apical contractility in multiple Drosophila tissues
- Persistent apical constriction challenges cohesion in proliferative tissue

INTRODUCTION

Cell polarity is a defining feature of epithelial function. Apical-basal asymmetry ensures the polarized localization of intercellular junctions to form a cohesive epithelial barrier at the organ surface. Epithelial architecture is also tightly regulated by the distribution of actomyosin driven forces at the apical, basal and junctional level (Munjal and Lecuit, 2014; Takeichi, 2014). This organization often displays plasticity to drive shape change during morphogenesis, growth or homeostatic events that require mitotic proliferation and cell death. Whereas this raises the importance of the dynamic modulation of polarity cues to build and maintain the three-dimensional structure of an organ, how polarity regulators direct actomyosin contractility to orient cell deformation, and the impact of these functions in tissue architecture remain open questions.

Conserved apical-basal polarity regulators, such as the apical PAR complex (Cdc42-Par-6-aPKC), the Crumbs complex (Crb-Sdt-PatJ), and the basolateral proteins Dlg, Lgl and Scrib, generate apical-basal asymmetry through their accumulation at specific cortical domains (Rodriguez-Boulan and Macara, 2014; St Johnston and Ahringer, 2010). Apical-basal polarization positions belt-like adherens junctions (AJ) at the apical-lateral border where they mechanically link neighbouring cells. It is thus not surprising that polarity disruption induces epithelial disorganization during animal development or as part of disease progression (Bilder et al., 2000; Chalmers et al., 2005; Fomicheva et al., 2020; Halaoui et al., 2017; Horne-Badovinac et al., 2001; Imai et al., 2006; Wodarz et al., 2000). However, the potentially pleiotropic effects of polarity loss often make the molecular basis of each phenotype uncertain. Moreover, on top of contributing to localize and regulate adhesion, polarity proteins regulate cell fate, cell division orientation, actomyosin contractility and microtubule dynamics (Dias Gomes et al., 2019; Etienne-Manneville and Hall, 2001; Franco and Carmena, 2019; Hao et al., 2010; Harris and Peifer, 2007; Iden et al., 2012; Ishiuchi and Takeichi, 2011; Jung et al., 2019; Korotkevich et al., 2017; Niessen et al., 2013). Thus, understanding the basis of epithelial architecture phenotypes at the organism level demands interference with protein function with high temporal control.

aPKC is indisputably the most studied kinase regulating animal cell polarity (Hong, 2018). A large body of work revealed its central role in apical-basal polarization by phosphorylating a number of polarity proteins, including Baz/Par3, Lgl, Par-1, Yurt and Crb. Phosphorylation regulates local cortical binding through the modulation of multivalent protein interactions and homo-oligomerization (Gamblin et al., 2018; Goransson et al., 2006; Krahn et al., 2010; Morais-de-Sa et al., 2010; Suzuki et al., 2004), or simply by reducing electrostatic interactions with plasma membrane phospholipids (Bailey and Prehoda, 2015; Dong et al., 2015). Other aPKC targets are not core polarity proteins. For example, in mammalian cells, phosphorylation of Rho-associated coiled-coil-containing kinase (ROCK, *Drosophila* Rok) represses the localization of this non-muscle myosin activator in apical junctions, inhibiting constriction to ensure regularity of apical surface size (Ishiuchi and Takeichi, 2011; Matsuzawa et al., 2021). Moreover, aPKC shows a dynamic cyclic distribution to the apicomedial area in the *Drosophila* embryonic amnioserosa, where it acts as a negative regulator of actomyosin networks to control pulsatile apical constriction and drive ratcheted contraction (David et al., 2010; Durney et al., 2018). Although the aPKC substrate involved in amnisoserosa contraction is unknown, these findings suggest that local aPKC enrichment is transduced into the spatial regulation of actomyosin-dependent cell deformation. Interestingly, aPKC function is also integrated with actomyosin reorganization during cell division. Cortical distribution of aPKC-Par6-CDC42 contributes to the assembly of an isotropic actomyosin cortex during mitotic rounding in the *Drosophila*

notum (Rosa et al., 2015). This is consistent with the lateral redistribution of aPKC-Par6 in mouse and sea anemone blastomeres and the fly follicular epithelium (Morais-de-Sa and Sunkel, 2013; Ragkousi et al., 2017; Rosa et al., 2015; Zenker et al., 2018), and adds to the plethora of potential functional outputs associated with aPKC phenotypes.

The monolayered follicular epithelium that encloses the *Drosophila* female germline has been explored as a tractable system to study the impact of apical-basal polarity regulators in tissue architecture. Loss of function of basolateral and apical regulators induces the formation of multilayered tissue (Bilder et al., 2000; Tanentzapf et al., 2000), whereas some apical polarity mutants, such as *crb* and *apkc*, also produce large gaps in epithelial integrity (Guilgur et al., 2012; Kim et al., 2009; Tanentzapf et al., 2000). These distinct outcomes suggest individual roles whose proper understanding demands temporally-controlled inactivation. By combining optogenetics with chemical inhibition, we characterized the progressive development of tissue disorganization and disentangled the importance of aPKC in the regulation of actomyosin contractility from its role in polarity. We show that epithelial gaps form specifically in proliferative tissue and that they arise by detachment of dividing and neighbour cells. Unexpectadly, this phenotype stems not from the role of aPKC in apical-basal polarity but from its role as a repressor of apicomedial actomyosin networks in non-mitotic cells. Upon aPKC inactivation, non-mitotic cells hypercontract and pull on dividing cells until adhesions give way. Accordingly, optogenetic induction of apical constriction by local recruitment of RhoGEF2 phenocopies aPKC inactivation. Hence, our work reveals the importance of keeping apical contractility in check during proliferation since unbalanced constriction poses a challenge to tissue integrity during proliferation-mediated growth of an epithelial shell.

MATERIALS AND METHODS

Drosophila genetics and stocks

Drosophila melanogaster stocks (Table 5.1) were kept on standard fly food at 18°C or 25°C. To inactivate apical polarity in epithelial cells, we combined GFP-tagged aPKC in its endogenous locus (Chen et al., 2018) with *tj-Gal4* or *GR1-Gal4* to drive *UAS-LARIAT* expression (Qin et al., 2017) in the follicular epithelium. Additionally, we used the ATP analog-sensitive allele *aPKC^{as4}* (Hannaford et al., 2019). *pnt-Gal4* was used to drive *UAS-LARIAT* expression in type II neuroblasts. For the conditional expression of UAS constructs in the follicular epithelium, crosses were set up at 18°C. After eclosion, adult offspring were

transferred to 29°C to drive expression of UAS constructs. Expression of all UAS constructs in the follicular epithelium was induced for 1 day at 29°C, except for optogenetic RhoGEF2 membrane recruitment (Figure 7B-D), which was induced for 2-3 days at 29°C. For co-expression of LARIAT with other UAS constructs, we used temperature-sensitive *Gal80^{ts}* to fully suppress premature Gal4-UAS driven transcription prior to temperature shift to 29°C. To express LARIAT in clones, we generated *Gal80* clones through FLP/FRT-mediated recombination (Xu and Rubin, 1993). These crosses were kept at 25°C, protected from light and heat shocks were performed at 37°C for 2 hours 2-3 times. Standard *Drosophila* methods were used to generate the different genotypes (Table 5.2).

Table 5.1. List of *Drosophila melanogaster* transgenes and mutant alleles.

Drosophila stocks and description	Stock origin
par-6^{D226} P{w$^+$, par-6>Par-6::GFP} To analyze Par-6 localization at endogenous levels. A genomic fragment encompassing the *par-6* gene with EGFP at the 3' terminus of the CDS (cloned in a pCaSpeR vector) rescues the *par-6^{D226}* null allele (P-element imprecise excision deleted the *par-6* promoter, start codon and sequence corresponding to the first 121 aminoacids, as well as the ubiquitin conjugating enzyme gene *CG8188*).	J. Knoblich (Wirtz-Peitz et al., 2008)
aPKC>GFP::aPKC; aPKC endogenously tagged with EGFP fused to its N-terminus through CRISPR/Cas9.	D. St Johnston (Chen et al., 2018)
lgl>lgl::mCherry *lgl* genomic rescue construct with mCherry at the 3' terminus of the CDS inserted into the *lgl* locus through genomic engineering[1].	Y. Hong (Dong et al., 2015)
shg>shg::GFP Endogenously tagged *Drosophila* E-cad (*shg*). *shg* genomic rescue construct with GFP inserted into the *shg* locus through genomic engineering[1].	Y. Hong (Huang et al., 2009)
shg>shg::3xmKate2/CyO^{GFP}; Endogenously tagged *Drosophila* E-cad (*shg*). *shg* rescue construct with three tandem mKate2 or GFP tags inserted into the *shg* locus through genomic engineering[1].	Y. Bellaïche (Pinheiro et al., 2017)
P{w$^+$=PTT-GC}zip[CC01626]/SM6a; *Drosophila* non-muscle myosin II heavy chain – Zip – tagged endogenously through a YFP containing P-element insertion (from the Carnegie protein trap library) was used to follow myosin II localization.	Bloomington Stock Center (#51564) (Buszczak et al., 2007)

P{w$^+$, *sqh>sqh::3xmKate2}/CyO;* P{w$^+$, *sqh>sqh::3xmKate2}/TM6, Tb* *Drosophila* non-muscle myosin II regulatory light chain – Sqh – tagged with three tandem mKate2 repeats in a pCaSpeR-based *sqh* rescue construct and inserted in chromosome II or III was used to follow myosin II localization.	Y. Bellaïche (Pinheiro et al., 2017)
P{w$^+$, *his2Av>his2Av::mRFP}/MKRS* mRFP inserted in a genomic fragment encompassing the Histone 2A variant gene *his2Av* (cloned in a pCaSpeR vector).	C. Lehner (Pandey et al., 2005)
P{w$^+$, *UASt>V_HH(GFP)::SNAP::CRY2(PHR)::P2A::CIBN::MP*} LARIAT constructs: CRY2 PHR domain fused to SNAPtag and a GFP nanobody (V_HH) and N-terminal CIB domain (residues 1-170) fused to the CaMKIIα multimerization domain (MP) expressed from a single construct with the help of a P2A self-cleaving peptide (cloned in a pUASt vector; inserted in chromosomes II and III).	X. Wang (Qin et al., 2017)
P{w$^+$, *UASp>pmCIBN*}/FM6 N-terminal CIB domain (residues 1-170) fused to CAAX membrane targeting sequence from human Kras4B (cloned in pPW vector; under Gal4-UAS control).	S. de Renzis (Guglielmi et al., 2015)
P{w$^+$, *UASp>CRY2::OCRL*}/FM7 CRY2 PHR domain fused to the *Drosophila* inositol polyphosphate 5-phosphatase OCRL (cloned in pPW vector; under Gal4-UAS control).	S. de Renzis (Guglielmi et al., 2015)
P{w$^+$, *UASp>PatJ::CIBN::pmGFP*}/CyO PatJ fused to N-terminal CIB domain (residues 1-170) and membrane targeted GFP fused to human Kras4B CAAX (cloned in pPW vector; under Gal4-UAS control).	S. de Renzis (Krueger et al., 2018)
P{w$^+$, UASp> *RhoGEF2::CRY2::mCherry*}/TM3,Ser Catalytic DHPH domain of RhoGEF2 fused to CRY2 PHR domain and tagged with mCherry (cloned in pPW vector; under Gal4-UAS control).	S. de Renzis (Izquierdo et al., 2018)
P{w$^+$, UASp> *RhoGEF2::CRY2*}/TM3,Ser Catalytic DHPH domain of RhoGEF2 fused to CRY2 PHR domain (cloned in pPW vector; under Gal4-UAS control).	S. de Renzis (Izquierdo et al., 2018)
P{y$^+$ v$^+$, *UAS>mCherry*.VALIUM10}attP2 mCherry under Gal4-UAS control (cloned in a VALIUM10 vector).	Bloomington Stock Center (#35787)
P{y$^+$ v$^+$, *UAS>tum RNAi*.VALIUM10}attP2 Tum RNAi under Gal4-UAS control (cloned in a VALIUM10 vector; from the TRiP collection).	Bloomington Stock Center (#28982)
P{w$^+$, UASp> *UASp>sqh^{E20E21}*}	Bloomington Stock Center (#64411)

Phosphomimetic myosin II regulatory light chain, sqh T20E, S21E, under Gal4-UAS control was used to increase myosin II activity.	
P{w$^+$, UASp> *UASp>sqh^{A20A21}*} Non-phosphporylatable myosin II regulatory light chain, sqh T20A, S21A, under Gal4-UAS control was used to decrease myosin II activity.	Bloomington Stock Center (#64114)
P{w$^+$, UASp>*T7::RhoGEF2*} RhoGEF2 with an N-terminal T7 tag under Gal4-UAS control was used to increase Rho activity.	Bloomington Stock Center (#9386)
*P{w$^+$=GawB}NP1624/*CyO*;* Also known as TJ-Gal4: Gal4 enhancer trap line where Gal4 is under regulation of *traffic jam* regulatory sequences. Used to express Gal4 and drive UAS construct expression in the follicular epithelium.	DGRC stock #104055 (Olivieri et al., 2010)
*P{w$^+$=GawB}GR1/*TM6B, Tb Also known as GR1-Gal4: Gal4 enhancer trap line where Gal4 is under regulation of unknown regulatory sequences that drive Gal4 and consequently UAS construct expression in the follicular epithelium.	T. Schüpbach (Gupta and Schupbach, 2003)
P{w$^+$, tubP>Gal80^{ts}} Temperature-sensitive Gal80 under regulation of the αTub84B promotor. Used to suppress Gal4-UAS construct expression under 29ºC.	Bloomington Stock Center (#7018)
P{w$^+$, ubi>nlsRFP} w* P{ry$^+$, hs>Flp}12 P{ry$^+$, neoFRT}19A For FLP/FRT-mediated generation of clones.	Bloomington Stock Center (#31418)
P{ry$^+$, hs>Flp}1 P{w$^+$, tubP>Gal80} w* P{ry$^+$, neoFRT}19A For FLP/FRT-mediated generation of clones.	Bloomington Stock Center (#5133)
P{lacW}aPKC^{k06403}/CyO aPKC null allele obtained by insertional mutagenesis of a P-element construct.	E. Knust (Wodarz et al., 2000)
aPKC^{as4} ATP analog-sensitive aPKC allele (I342A and T405A mutations introduced through CRISPR/Cas9).	J. Januschke (Hannaford et al., 2019)
aPKC^{as4}::mScarlet ATP analog-sensitive aPKC allele tagged with mScarlet-I	J. Januschke

[1] Genomic engineering: ends out gene targeting to replace the target gene with an attP site through homologous recombination followed by ϕC31-mediated DNA integration.

Table 5.2. Genotypes and light exposure details. *Drosophila* genotype for each figure panel. When applicable, optogenetic experiment details are indicated: whether optogenetic system was activated by exposing flies or dissected ovaries cultured *ex vivo* to blue light and how long samples were exposed to blue light. For live imaging experiments, optogenetic system was only activated after image acquisition started.

Genotype		Optogenetic system activation details
Figure 5.1		
B	*UAS>pmCIBN/UAS>CRY2::OCRL; tj>Gal4, ubi>pH::mCh/+;*	Flies – 2 days
C	*w^{1118};;* *; tj>Gal4 GFP::aPKC/GFP::aPKC;* *; tj>Gal4 GFP::aPKC/GFP::aPKC; UAS>LARIAT/* *; tj>Gal4 GFP::aPKC/+; UAS>LARIAT/* *; tj>Gal4 GFP::aPKC/$aPKC^{k06403}$; UAS>LARIAT/*	dark
D	*; GFP::aPKC; GR1>Gal4/UAS>LARIAT* *; GFP::aPKC/+; GR1>Gal4/UAS>LARIAT*	Flies – 2 days
E	*; tj>Gal4 GFP::aPKC/GFP::aPKC; (Control)* *; tj>Gal4 GFP::aPKC/GFP::aPKC; UAS>LARIAT/* *; tj>Gal4 GFP::aPKC/+; UAS>LARIAT/* *; tj>Gal4 GFP::aPKC/$aPKC^{k06403}$; UAS>LARIAT/*	Flies – 1 day
Figure 5.2		
A	*; tj>Gal4 GFP::aPKC/GFP::aPKC; H2A::RFP/UAS>LARIAT*	Live imaging
B, E	*; GFP::aPKC; GR1>Gal4/UAS>LARIAT*	Flies – 0, 2, 4, 6 or 12 hours
C-D, F-G	*; tj>Gal4 GFP::aPKC/GFP::aPKC; UAS>LARIAT/+*	Flies – 0, 2, 4, 6 or 12 hours
H, I, J	*; $aPKC^{as4}$;*	-
Figure 5.3		
A	*; tj>Gal4 GFP::aPKC/GFP::aPKC; sqh::mKate2x3/UAS>LARIAT*	Live imaging
B	*; tj>Gal4 GFP::aPKC/GFP::aPKC; UAS>LARIAT/+*	Live imaging
C	*; tj>Gal4 GFP::aPKC/GFP::aPKC; H2A::RFP/UAS>LARIAT*	Live imaging
D, E	*; tj>Gal4 GFP::aPKC/GFP::aPKC; + (Control)* *; tj>Gal4 GFP::aPKC/GFP::aPKC; UAS>LARIAT/+*	Ovaries *ex vivo* – 2 hours
F	*; tj>Gal4 GFP::aPKC/GFP::aPKC; UAS>LARIAT/UAS>mCh (Control)* *; tj>Gal4 GFP::aPKC/GFP::aPKC; UAS>LARIAT; $Gal80^{ts}$/UAS>tum RNAi*	Flies – 2 hours
Figure 5.4		

A	*; tj>Gal4 GFP::aPKC/ Lgl::mCherry GFP::aPKC; UAS>LARIAT/+* *; tj>Gal4 GFP::aPKC/GFP::aPKC E-cad::mKate2x3; UAS>LARIAT/+*	Live imaging
B-D	*; tj>Gal4 GFP::aPKC/GFP::aPKC; sqh::mKate2x3/UAS>LARIAT*	Live imaging
E	*ubi::nlsRFP hsFlp FRT19A /hsFlp tub>Gal80 FRT19A; tj>Gal4 GFP::aPKC/GFP::aPKC UAS>LARIAT; +* LARIAT expressing cells are marked by bright RFP signal (two nlsRFP copies) and GFP::aPKC clustering.	Live imaging
Figure 5.5		
A, B	*; $aPKC^{as4}$ /$aPKC^{k06403}$ E-cad-3xGFP; sqh::mKate2x3/+*	-
C	*; $aPKC^{as4}$::mScarlet;*	-
D-E	*; $aPKC^{as4}$::mScarlet Zip::GFP;*	
Figure 5.6		
A	*; tj>Gal4 GFP::aPKC/GFP::aPKC*	-
B	*; tj>Gal4 GFP::aPKC/GFP::aPKC; sqh::mKate2x3/+*	-
C	*; tj>Gal4 GFP::aPKC/GFP::aPKC; sqh::mKate2x3/UAS>LARIAT*	Live imaging
D-F	*; tj>Gal4 GFP::aPKC/GFP::aPKC E-cad::mKate2x3; (Control)* *; tj>Gal4 GFP::aPKC/GFP::aPKC E-cad::mKate2x3; UAS>LARIAT/+*	Live imaging
Figure 5.7		
A	*; tj>Gal4 GFP::aPKC/GFP::aPKC UAS>LARIAT; $Gal80^{ts}$/UAS>mCh (Control)* *; tj>Gal4 GFP::aPKC/GFP::aPKC UAS>LARIAT; $Gal80^{ts}$ /UAS>Sqh^{E20E21}* *; tj>Gal4 GFP::aPKC/GFP::aPKC UAS>LARIAT; $Gal80^{ts}$ /UAS>Sqh^{A20A21}* *; tj>Gal4 GFP::aPKC/GFP::aPKC UAS>LARIAT; $Gal80^{ts}$ /UAS>RhoGEF2*	Flies – 2 hours
B	*; tj>Gal4/UAS>PatJ::CIBN::pmGFP; UAS>RhoGEF2::CRY2::mCherry/+*	Live imaging
C	*; tj>Gal4/UAS>PatJ::CIBN::pmGFP; UAS>RhoGEF2::CRY2 /Sqh::mKate2x3*	Live imaging
C-F	*; tj>Gal4/UAS>PatJ::CIBN::pmGFP; UAS>RhoGEF2::CRY2::mCherry/+*	Flies – 2 hours
Supplementary Figure 5.S1		
A	*; tj>Gal4 GFP::aPKC/GFP::aPKC Lgl::RFP; UAS>LARIAT/+*	Flies – 1 day
B, C	*; GFP::aPKC/GFP::aPKC; pnt>GAL4/MKRS (Control)* *; GFP::aPKC UAS>LARIAT/GFP::aPKC; pnt>GAL4/MKRS*	Larvae – 1 hour

Supplementary Figure 5.S2		
A	*; tj>Gal4 E-cad::GFP sqh::mKate2x3/+; Gal80^{ts}/UAS>tum RNAi* *; tj>Gal4 E-cad::GFP sqh::mKate2x3/+;*	-
B	*; tj>Gal4 GFP::aPKC/GFP::aPKC UAS>LARIAT; sqh::mKate2x3/UAS>tum RNAi*	Live imaging
C	*; GFP::aPKC;* *; tj>Gal4 GFP::aPKC/GFP::aPKC; UAS>LARIAT/+*	Ovaries *ex vivo* – 2 hours
D	*; tj>Gal4 GFP::aPKC/GFP::aPKC;* *; tj>Gal4 GFP::aPKC/GFP::aPKC; UAS>LARIAT/+*	Ovaries *ex vivo* – 2 hours
Supplementary Figure 5.S3		
A	par6^{D226} Par-6::GFP/+; aPKC^{as4}; sqh::mKate2x3/+	-
B	; aPKC^{as4}::mScarlet;	-
C	; aPKC^{as4}::mScarlet/aPKC^{as4}::mScarlet Zip::GFP;	-

Optogenetic experiments in the follicular epithelium

For optogenetic experiments in the follicular epithelium, adult flies were selected 1-3 days after eclosion and transferred to 29ºC to drive UAS construct expression. To avoid unintended optogenetic system activation by light, fly vials were kept inside cardboard boxes or wrapped in aluminum foil and handled in a dark room from this point forward. For *in vivo* optogenetic experiments, flies were exposed to blue light for the indicated periods of time (Table 5.1) by placing vials at approximately 8 cm from a 472nm LED (SuperBrightLEDs; GU5.3 MR16; 300 lumens). Control flies from each genotype were kept in the dark and dissected in a dark room with a 593nm LED light source (SuperBrightLEDs; GU5.3 MR16; 300 lumens) to avoid triggering CIBN-CRY2 interaction. For *ex vivo* optogenetic experiments, ovaries were dissected in a dark room in *ex vivo* culture medium (Schneider's medium (Sigma-Aldrich) supplemented with 10% FBS (fetal bovine serum, heat inactivated; Thermo Fisher) and 200 μg/uL insulin (Sigma-Aldrich)). Afterwards, ovaries were transferred to new *ex vivo* culture medium, ovarioles were partially separated and exposed to blue light for 2 hours in 24-well-plates using the same setup as for whole flies. When indicated, specific drugs or DMSO (for control samples) were added 15 minutes before exposure to blue light: MG132 (Calbiochem; 20 μM) to inhibit the proteasome and prevent anaphase onset; colchicine (Sigma-Aldrich; 30 μM) to depolymerize microtubules and block cells in mitosis; Binucleine-2 (Sigma-Aldrich; 20 μM or 40 μM) to inhibit Aurora B; and Latrunculin A to disrupt the actin cytoskeleton (Sigma Aldrich; 5 μg/mL). All drug solutions were prepared in DMSO, except for Colchicine, which was dissolved in ethanol.

Control ovaries from each condition were left in the dark for the same time period. Flies and ovaries cultured *ex vivo* were at room temperature during blue light exposure. For live imaging, ovaries were dissected in a dark room and CIBN-CRY2 interaction was only triggered with the 488 nm laser used for GFP-tagged protein image acquisition.

Fixation and stainings of egg chambers

Drosophila ovaries were dissected in Schneider's medium (Sigma-Aldrich) supplemented with 10% FBS (fetal bovine serum, heat inactivated; Thermo Fisher) and washed once with PBT (PBS + 0.05% Tween 20 (Sigma-Aldrich)) before fixation in 4% paraformaldehyde solution (in PBS with 0.2% Tween 20 (Sigma-Aldrich)) for 20 min. For F-actin staining, Phalloidin-FITC or Phalloidin-TRITC (Sigma-Aldrich) was added to the fixative solution at 1 μg/mL and incubation time was increased to 30 min. After washing 3 times for 10 min with PBT, samples were mounted with Vectashield with DAPI (Vector Laboratories).

Optogenetic experiment and immunofluorescence in neuroblasts

Following a 12h egg-laying period, control and LARIAT embryos were kept in the dark until wandering L3 larvae (wL3) stage. wL3 of both conditions were exposed to light for 1h. Brains were then dissected in PBS 1x, fixed in 4% paraformaldehyde for 20 min at room temperature and washed three times with PBST (0.1% Triton X-100 in 1x PBS). Brains were blocked with 1% normal goat serum in 0.1% PBST for at least 20 min at room temperature and incubated overnight at 4°C with rabbit anti-Miranda (1:2000, non commercial) and mouse monoclonal anti-phospho-Histone H3 (pH3) Ser10 (1:1000, Cell Signalling, 9706), diluted in blocking solution. Afterwards, brains were washed three times, blocked for 20 min and incubated for 2h at room temperature with secondary antibodies Alexa Fluor 647-conjugated goat anti-mouse and Alexa Fluor 568-conjugated goat anti-rabbit (Invitrogen), used at 1:1000. Finally, brains were mounted in Aqua Polymount (Polysciences, Inc).

Imaging of fixed tissue

Images of *Drosophila* fixed egg chambers were collected with a 1.1 NA/40x water or 1.30 NA/63x glycerine objectives on an inverted laser scanning confocal microscope

Leica TCS SP5 II (Leica Microsystems) or 1.20 NA/63x objective on an inverted laser scanning confocal microscope Leica SP8 (Leica Microsystems). To score epithelial defects, images for egg chamber staging were collected with a 10x objective on a Zeiss Axio Imager Z1 microscope (Carl Zeiss, Germany) or a Zeiss Axio Imager Z1 Apotome microscope (Carl Zeiss, Germany). Epithelial defects (epithelial gaps and/or multilayering) were detected with a 20x or 40x Oil objective. Images from *Drosophila* larvae brains were acquired with a Zeiss LSM880 confocal microscope (Zeiss).

Live imaging

For live imaging of *Drosophila* egg chambers, individual ovarioles were dissected in *ex vivo* culture medium (Schneider's medium (Sigma-Aldrich) supplemented with 10% FBS (fetal bovine serum, heat inactivated; Thermo Fisher) and 200 μg/uL insulin (Sigma-Aldrich)) and the enveloping muscle removed as previously described (Morais-de-Sa and Sunkel, 2013). Ovarioles were transferred to new culture medium and imaged on coverslips or glass bottom dishes (MatTek; No 1.5) with an Andor XD Revolution Spinning Disk Confocal system equipped with two solid state lasers – 488nm and 561nm -, an iXonEM+ DU-897 EMCCD camera and a Yokogawa CSU-22 unit built on an inverted Olympus IX81 microscope with a PLAPON 60x/NA 1.42 or a UPLSAPO 100x/NA 1.40 objective using iQ software (Andor). For Figure 5.2B and C, ovarioles were stained with CellMask Orange Plasma membrane Stain (ThermoFisher; diluted 1:10 000 in culture medium) for 15 minutes and washed twice with culture medium before imaging. Live imaging was performed at 25ºC. When indicated, the actin cytoskeleton was disrupted with 5 μg/mL of Latrunculin A (Sigma-Aldrich) added at least 15 minutes before imaging. We collected z-stacks of 3-12 serial optical sections separated by 0.5-1 μm at 30s to 1min time intervals. Midsagittal egg chamber cross-sections were used to image the follicular epithelium along the apical-basal axis and z-stacks at the surface of the egg chamber to cross-section the follicular epithelium along the apical-basal axis.

Protein extracts and Western blot

To confirm endogenous and GFP::aPKC levels in the different genotypes used for optogenetic aPKC inactivation (Figure 5.1E), we prepared protein extracts from *Drosophila* ovaries from at least 15 flies per genotype dissected in a dark room. Dissected *Drosophila* ovaries were transferred to lysis buffer (150mM KCl, 75mM HEPES pH 7.5, 1.5 mM EGTA,

1.5mM $MgCl_2$, 15% glycerol, 0.1% NP-40, 1x protease inhibitors cocktail (Roche) and 1x phosphatase inhibitors cocktail 3 (Sigma-Aldrich)), frozen in liquid nitrogen, thawed and then disrupted through sonication. We clarified lysates through two consecutive centrifugations at 14000 rpm for 10 min at 4°C. Protein concentration was determined with NanoDrop 1000 Spectrophotometer (Thermo Fisher). Samples were then resolved through SDS-PAGE and transferred to a nitrocellulose membrane using the iBlot Dry Blotting System (Invitrogen) for Western blotting. Protein transference was confirmed by Ponceau staining (0.25% Ponceau S in 40% methanol and 15% acetic acid). The membranes were blocked for 2 h at room temperature with 5% dry milk prepared in PBT and incubated overnight at 4°C with the primary antibodies (rabbit anti-aPKC 1:2000 (c-20, Santa Cruz Biotech) and mouse anti-α-Tubulin 1:10 000 (DM1A, Sigma-Aldrich)) diluted in PBT + 1% dry milk. After washing three times for 10 min with PBT, membranes were incubated with the secondary antibodies conjugated with horseradish peroxidase (Amersham) for 1 h at room temperature according to the manufacturer's instructions. After washing again three times for 10 min with PBT, blots were developed with ECL Chemiluminescent Detection System (Amersham) according to the manufacturer's instructions and revealed with a ChemiDoc XRS+ (BioRad).

aPKC^{as4} allele inactivation

For epithelial defect analysis in the follicular epithelium, *Drosophila* ovaries from aPKC^{as4} flies (prepared as previously described in the optogenetic experiments section) were cultured *ex vivo* for 2 hours in the presence of the ATP analog 1NA-PP1 (Calbiochem; prepared in DMSO) at the indicated concentration before fixation. DMSO was added to control samples. For live imaging of egg chambers and larval neuroepithelium, the indicated concentration of 1NA-PP1 or DMSO was added to the culture medium at the indicated timing.

Quantifications, reproducibility and statistical analysis

Image processing and quantifications were done with FIJI (Schindelin et al., 2012). Statistical analysis and graphs were done in GraphPad Prism 8 (GraphPad Software Inc., La Jolla, CA, USA), except when otherwise indicated.

Epithelial defects analysis: To evaluate epithelial architecture, we scored the amount of egg chambers at specific developmental stages with one or more epithelial gaps,

one or more multilayering events or both. We determined the developmental stage of egg chambers by measuring their area in midsagittal cross-sections, as a proxy for size. To define the size intervals corresponding to each developmental stage, we staged GFP::aPKC control egg chambers according to phenotypic characteristics, as in Jia *et al*., (Jia et al., 2016), and correlated their stage with their size. We scored epithelial defects (epithelial gaps and/or multilayering) and their position (anterior, posterior, dorsal-ventral) by inspecting midsagittal cross-sections of egg chambers: for LARIAT experiments, egg chambers were stained with DAPI (DNA) and Phalloidin (F-actin); for optogenetic RhoGEF2 membrane recruitment, egg chambers were stained with DAPI (DNA) and PatJ-CIBN-pmGFP and RhoGEF2-CRY2-mCherry fluorescence was used. For the initial analysis of aPKC inactivation with LARIAT (Figure 5.1E), results from 3 independent experiments (≥ 8 flies per condition) were summed up in a single contingency table and the graph shows the relative amount of egg chambers (stages 3 to 8) with each type of defect found. For statistical analysis, epithelial defects and/or multilayering were grouped in a single defect category and Fisher's exact test with Bonferroni correction for multiple comparison was used. Additionally, we used Chi-square to test if the incidence of different types of defects (epithelial gaps, multilayering or both) was statistically different between samples. For other experiments, graphs show mean percentage of egg chambers with the indicated type of defect ± standard deviation (SD). The percentage of defects obtained for each independent experiment (≥ 8 flies per condition per independent experiment) are represented as individual data points in the graphs. Total amount of egg chambers scored for each analysis is indicated in the respective graph. To ensure consistent UAS-LARIAT expression levels, only proliferative stages 4 to 6 or non-proliferative stages 7 and 8 were included in subsequent analyses. We used Fisher's exact test, with Bonferroni correction for multiple comparisons when necessary, to test contingency tables comparing sum counts of egg chambers with one or more epithelial gaps vs no gap. To compare the frequency of epithelial gap and multilayering formation at the anterior, posterior and dorsal-ventral regions, we analyzed how many of the epithelial gaps and multilayering events detected upon aPKC clustering in proliferative and non-proliferative egg chambers and upon $aPKC^{as4}$ inactivation in proliferative egg chambers were at these different regions (the respective graphs are shown in Figure 5.2D, G and J).

Miranda asymmetry in neuroblasts: The distribution of Miranda along the membrane of dividing NBs (pH3 positive) was analysed. To extract Miranda intensity profile, that is, the intensity of Miranda (I_M) along the length of the cell membrane (L), we proceeded as in (Rodriguez et al., 2017) with minor changes: we used a 30-pixel wide stripe to delineate the membrane; profile extraction was initiated in the basal membrane section, so

that L<50% correspond to basal Miranda intensity values. In the end, Miranda intensity (I_M) was plotted as a function of percentage of membrane length (L). To obtain the asymmetry index (ASI) for Miranda, Basal (B) and Apical (A) intensities were calculated as the area under the Miranda intensity plot (I_M) for the basal (L ≤50%) and apical (L>50%) sections of the membrane. Absolute ASI values were calculated as in (Hannaford et al., 2019) with the following formula:

$$\frac{B - A}{2(B + A)}$$

ASI values were then normalized relative to control mean so that, an ASI of 1 represents normal asymmetry and lower values (~0) indicate loss of asymmetry. As *pnt*-GAL4 only drives LARIAT expression in type II neuroblasts, only this subtype was considered in all calculations. Statistical analysis was performed using Prism 6 (GraphPad Software Inc., La Jolla, CA, USA), mean ± SD are depicted and individual ASI values represented (normalized to control mean). Statistical significance of the difference of means was calculated using unpaired *t*-test and considered significant when $p < 0.05$.

Apical myosin II in the follicular epithelium: To quantify apical accumulation of myosin II after aPKC inactivation, we measured sqh-3xmKate2 fluorescence intensity at the apical domain of follicular epithelial cells in single plane midsagittal cross-sections of egg chambers acquired during live imaging. For each egg chamber, 4 regions of interest (ROIs), each one encompassing the apical domain of at least 4 cells in the dorsal, ventral, anterior and posterior regions, were manually defined and tracked through time. Mean apical fluorescence intensity (AFI) for each timepoint was extracted from raw movie datasets, corrected for mean cytoplasm fluorescence intensity (CFI; average value measured for each timepoint in 3 follicular epithelial cells) and normalized to the corrected fluorescence intensity before aPKC inactivation ($AFI_{initial}$-$CFI_{initial}$) as follows:

$$\frac{AFI - CFI}{AFI_{initial} - CFI_{initial}}$$

For aPKC LARIAT experiments, $AFI_{initial}$-$CFI_{initial}$ corresponds to the AFI-CFI value at min 0 (when optogenetic clustering is triggered). For $aPKC^{as4}$ experiments $AFI_{initial}$-$CFI_{initial}$ was obtained by averaging AFI-CFI for the 5 frames before aPKC inactivation with 1NA-PP1 at min 0. Whenever, an epithelial gap started forming at a particular region, quantification at that same region was stopped.

Egg chamber circularity: To assess egg chamber deformation after aPKC inactivation, we measured egg chamber circularity in single plane midsagittal cross-sections of sqh-3xmKate2 egg chambers acquired during live imaging. The apical surface of the

follicular epithelium was manually segmented and circularity (4π(area/perimeter^2)) was measured. Egg chamber circularity was only quantified while no epithelial defect appeared.

Apical surface area and myosin II in the neuroepithelium: To measure apical surface contraction in the neuroepithelium upon aPKC^{as4} inactivation with 1NA-PP1 , the ROI edges were manually tracked as red dots using aPKC^{as}-mScarlet signal to detect apical cell edges. These dots were then connected using a steerable filter for line detection. The resulting shape was then filled and dilated (blue mask in Figure 5.5C) to approximate the area to measure. Apical area was normalized to its initial value at min 0. To measure myosin II intensity at the apicomedial region and apical junctions after aPKC^{as4} inactivation with 1NA-PP1, apical junctions were segmented using aPKC^{as}-mScarlet signal. aPKC signal to noise ratio was increased by a steerable filter detecting lines and a junctional mask (as the one shown in Figure 5.5E) was generated by thresholding. The mask for the apicomedial region was generated by inverting and contracting the junctional mask. Myosin II intensity was obtained by extracting average Zip-YFP intensity with these masks and normalizing to junctional intensity before aPKC inactivation at min -2.

Apical area in interphase and mitotic cells in the follicular epithelium: To evaluate apical constriction in interphase cells and pulling forces on mitotic cells, we measured epithelial cell area in cross-sections at the junctional level of the follicular epithelium acquired during live imaging. For each egg chamber, we plotted the mean apical area quantified from 4 interphase cells (not adjacent to each other) that were manually segmented using E-cad-3xmKate2. Surface area was normalized to the initial mean value, obtained by averaging the corresponding cell area for the 3 frames before aPKC clustering (from min -2 to 0). To analyze the effect of tissue rupture on the speed of apical constriction, the aPKC LARIAT measurements from Figure 5.6E were plotted as a function of time relative to tissue rupture (new min 0) in Figure 5.6F. Linear regression was used to evaluate the difference in constriction rate before and after rupture. A similar procedure was used to segment mitotic cells where aPKC was clustered at least 10 min before anaphase onset and no more than 10 min before mitotic entry in egg chambers where no epithelial gaps were visible. Anaphase onset was defined as the first frame of cell elongation (determined through E-cad-3xmKate2 signal at the lateral cortex) as a proxy for the spindle pulling sister chromatids apart. Mitotic entry was defined as the first frame of visible mitotic rounding in a lateral cortex cross-section. Mean cell area was normalized to the corresponding cell area 9 min before anaphase onset.

Image preparation

Representative images were processed and prepared using FIJI. Representative midsagittal images from egg chambers are from a single optical section or 2-3 plane maximum projection. Surface images from egg chambers are maximum projections of all optical sections covering the epithelial domain of interest. When necessary, movies were registered with the FIJI plugin *StackReg* (EPFL; Biomedical Imaging Group), to correct for whole egg chamber movement during live imaging; and a Gaussian Blur or Gaussian Blur 3D filter was applied to remove random noise.

RESULTS

Optogenetic clustering inactivates aPKC with high temporal control

We employed an optogenetic clustering tool – light activated reversible inhibition by assembled trap (LARIAT) – to inactivate aPKC in the *Drosophila* follicular epithelium *in vivo* and with high temporal control (Figure 5.1A). LARIAT clustering is triggered when blue light promotes the interaction of CRY2 with CIBN fused with a multimerization domain (Lee et al., 2014). To validate if trasmission of light across the abdomen is sufficient to trigger CRY2-CIB interaction in the *Drosophila* ovary, we used a CRY2-CIB module that recruits the 5-phosphatase OCRL to the pasma membrane, where it converts PI(4,5)P2 to PI(4)P (Guglielmi et al., 2015). Exposure to blue light of flies expressing CRY2-OCRL and membrane anchored CIBN (pmCIBN) in the follicular epithelium induces multilayered tissue (Figure 5.1B), as previously observed with mutations that disrupt membrane PI(4,5)P2 (Devergne et al., 2014). Thus, optogenetic manipulation can be used to interfere with protein function in the *Drosophila* ovary in living flies.

To interfere with aPKC function, we used flies expressing endogenously GFP-tagged aPKC and CRY2 fused to a GFP nanobody, which recruits GFP-aPKC to LARIAT clusters upon light-exposure (Figure 5.1A, Figure 5.1C). GFP-aPKC formed clustered puncta in the follicular epithelium after exposure to blue-light (24h) of flies expressing UAS-LARIAT (UAS-V_HH::CRY2-P2A- CIBN::MP) driven by GAL4 in follicle cells (Figure 5.1D). The follicular epithelium showed both gaps in epithelial integrity and multilayering (Figure 5.1D and 1E). The presence of one untagged allele prevents the appearance of defects (Figure 5.1D and 5.1E), indicating that clustering produces loss of function phenotypes rescued by the wild-type allele. To test if LARIAT-mediated clustering resulted in kinase inactivation, we evaluated the localization of aPKC substrates, Lgl and Miranda, whose

membrane localization is repressed by phosphorylation (Bailey and Prehoda, 2015). As antecipated in a context of kinase inactivation, Lgl extended apically upon optogenetic clustering of aPKC in follicle cells (Supplementary Figure 5.S1A). Likewise, aPKC clustering induced mislocalization of cell fate determinant Miranda during asymmetric division in *Drosophila* neural stem cells (Supplementary Figure 5.S1B-S1C). Taken together, these results show that LARIAT-mediated clustering enables temporally controlled inactivation of aPKC and is widely applicable in cell polarity studies.

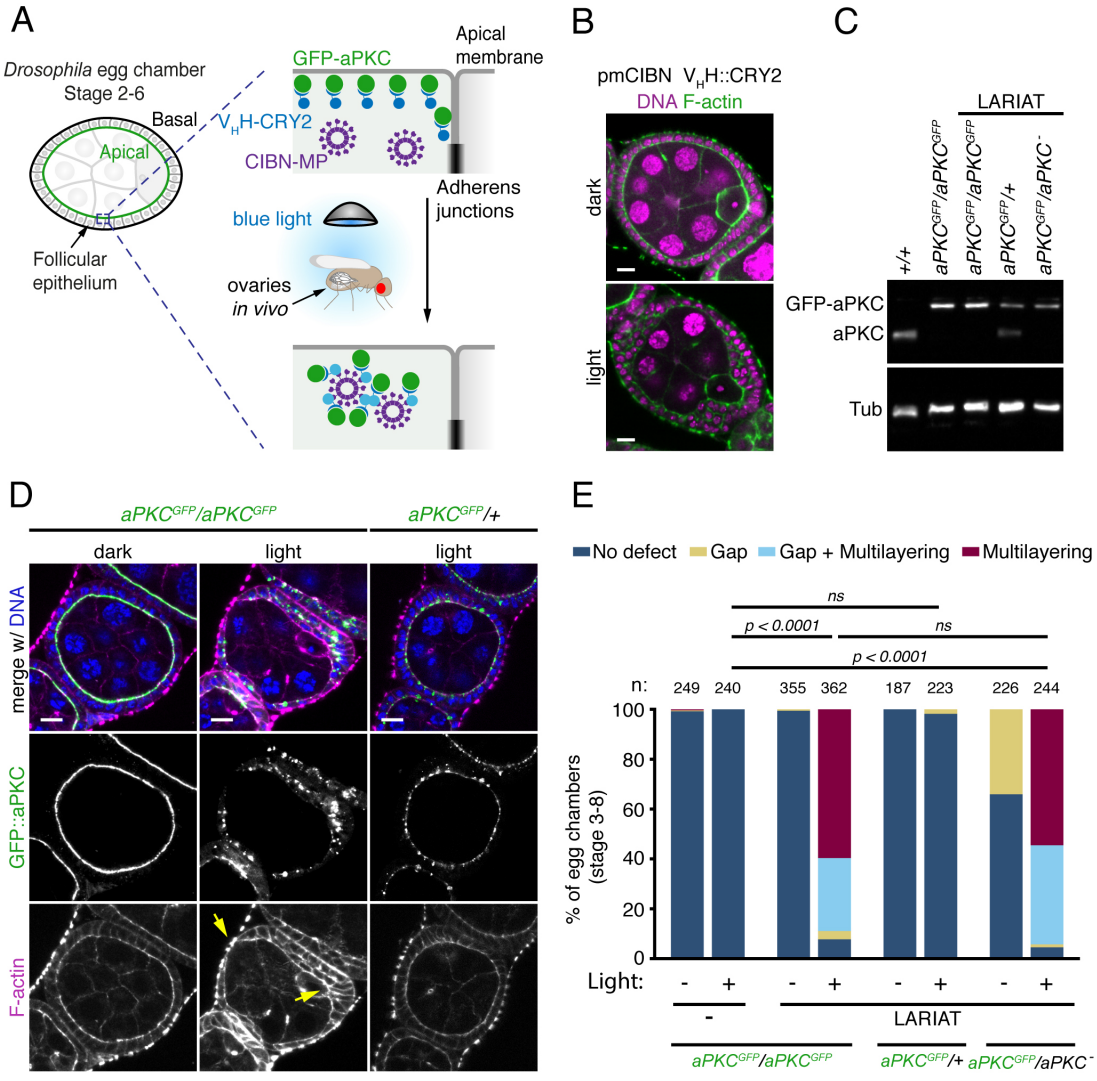


Figure 5.1. Optogenetic clustering inactivates aPKC and disrupts tissue architecture *in vivo*. (A) Schematic representation of optogenetic aPKC inactivation strategy. LARIAT (V_HH::CRY2 and CIBN::MP) was expressed in the follicular epithelium of *Drosophila* egg chambers. Endogenously tagged GFP::aPKC is targeted by CRY2 fused with a GFP nanobody (V_HH). Exposing flies to blue light triggers CRY2 binding to CIBN fused with a multimerization domain (MP) and clusters GFP::aPKC. **(B)** Midsagittal images of egg chambers from flies expressing membrane tethered pmCIBN and CRY2::OCRL in the follicular epithelium and exposed to blue light for 48 hours to trigger OCRL membrane recruitment prior to egg chamber fixation and staining for F-actin (green) and DNA (magenta) to label nuclei. Control flies were kept in the dark. **(C)** Western blot shows protein level for untagged and GFP::aPKC in ovaries for the indicated genotypes. α-Tubulin was used as loading control. **(D)**

GFP::aPKC was clustered as in (A) for 48 hours before egg chambers were fixed and stained for F-actin (magenta) and DNA (blue). Control flies were kept in the dark. Flies were either homozygous or heterozygous for endogenously-tagged *GFP::aPKC*. Arrows point to epithelial gap and multilayering in midsagittal views. **(E)** Frequency of epithelial gaps and multilayering in egg chambers (stages 3 to 8) from flies with the indicated combinations of wild-type, GFP::aPKC or $aPKC^{k06403}$ null allele after 24 hours blue light exposure (n = total amount of egg chambers scored). LARIAT was expressed in the follicular epithelium when indicated. Control flies were kept in the dark. Fisher's exact test was used to compare incidence of defects between different samples (ns, not significant); Chi-square to compare incidence of different defects between GFP::aPKC homozygous and GFP::aPKC/$aPKC^{k06403}$ flies. Scale bars: 10 μm.

Acute aPKC inactivation leads to fast and stereotypical tissue disorganization

To characterize how tissue architecture is lost after aPKC inactivation, we clustered GFP-aPKC in egg chambers cultured *ex vivo*. Live imaging shows GFP-aPKC starts to cluster within seconds of blue-light induction until aPKC becomes fully redistributed in large clusters initially formed in the apical domain (Figure 5.2A and Movie 5.S1). Intriguingly, whereas multilayering is the most frequent phenotype after a day of light exposure (Figure 5.1E), gaps are the earliest defect observed during the initial period of optogenetic clustering (Figure 5.2A and Movie 5.S1). We have thus dissected the progressive development of tissue disorganization by exposing flies to blue light for different periods of time, and we separated the phenotypic quantification between proliferative (developmental stages 4 to 6) and non-proliferative epithelia (developmental stages 7 and 8). This allowed us to confirm that gaps are the most prevalent phenotype within 2 hours of aPKC inactivation (~50% in proliferative stages - Figure 5.2B and 2C), which is consistent with their early appearance in *ex vivo* imaging. Moreover, this analysis revealed epithelial gaps are specifically generated in the proliferative stages and during the initial period of aPKC inactivation as its prevalence progressively declines (Figure 5.2E and 5.2F). In contrast, gap frequency increases from 2h to 6h of light exposure in non-proliferative developmental stages. Since egg chambers in late proliferative stages (5 and 6) are expected to transition to non-proliferative stage 7 within this timeframe, this increase suggests that gaps are generated in proliferative tissue and maintained as egg chambers continue developing. Multilayering also initiates in proliferative stages, and becomes frequent after 4h of aPKC inactivation in both proliferative (~20% at 2h; ~85% at 4h; 95% at 6h) and non-proliferative stages (0% at 2h; ~25% at 4h; ~85% at 6h). Thus, both defects are largely originated in proliferative stages, with gaps appear specifically during the initial phase of aPKC clustering.

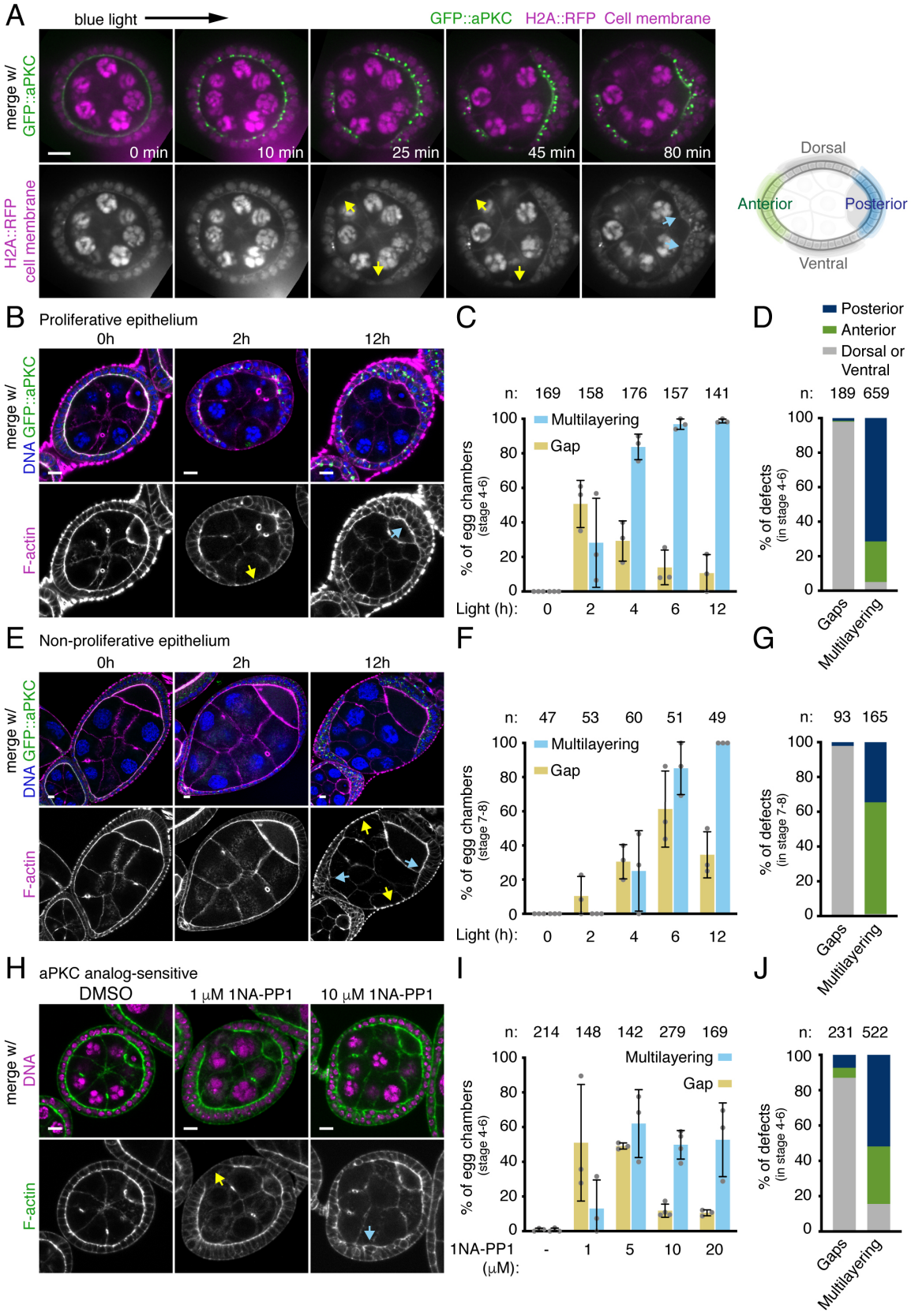


Figure 5.2. aPKC inactivation leads to fast and stereotyped tissue disorganization in a proliferative epithelium. (A) Time-lapse midsagittal images of an egg chamber expressing LARIAT (in the follicular epithelium), GFP::aPKC (green) and H2A::RFP (magenta) show epithelial gaps (yellow arrows) and multilayering (blue arrows). Imaging with 488nm laser triggered LARIAT clustering from min 0 onwards.

Schematic representation of egg chamber regions (right). **(B-G)** Representative midsagittal images and epithelial defect quantification in proliferative (stages 4-6; B-D) and non-proliferative (stages 7-8; E-G) GFP::aPKC (green) homozygous egg chambers expressing LARIAT and stained for F-actin (magenta) and DNA (blue). Flies were exposed to blue light for the indicated time before ovary fixation. **(H-J)** Representative midsagittal images and epithelial defect quantification in proliferative aPKC^{as4} egg chambers treated with the indicated concentrations of 1NA-PP1 *ex vivo* to inactivate aPKC for 2 hours prior to fixation and staining for F-actin (green) and DNA (magenta). Frequency (C, F, I) and position (D, G, J) of epithelial gaps (yellow arrows) and multilayering (blue arrows) was scored in midsagittal cross-sections. (C, F, I) Graphs show mean ± SD; grey data points represent percentage from independent experiments; n = total amount of egg chambers scored (D, G, J) Graphs show the spatial distribution of all defects scored in C, F, I; n = total amount of epithelial gaps or multilayering events. Scale bars: 10 μm.

The different phenotypic outcome in the initial period of light exposure could be explained by incomplete aPKC inactivation during the period when clusters are first assembled. To test this hypothesis, we used an *aPKC allele* (aPKC^{as4}) engineered for inhibiton with ATP analogues (Hannaford et al., 2019) to evaluate the specific phenotypic impact of a range of aPKC inhibition levels. *aPKC^{as4}* ovaries cultured for 2 h with 1μM of 1NA-PP1, which *in vitro* reduces aPKC activity to ~15% (Hannaford et al., 2019), had predominantly epithelial gaps (~50% gaps vs 10% multilayering). However, increased drug concentrations led to frequent multilayering while preventing the appearence of epithelial gaps (Figure 5.2I and 5.2J). Thus, gaps in epithelial integrity are associated specifically with partial aPKC inactivation, whereas multilayering arises by strong loss of aPKC function. It is worth noting that the two phenotypes are not mutually exclusive (Figure 5.1E) and are commonly observed in different positions of the egg chamber (Figure 5.2D, 5.2G and 2J).

Cell division challenges tissue cohesion upon aPKC inhibition

Failure in germline encapsulation (Tanentzapf et al., 2000) or a long-term arrest in cell proliferation (Berns et al., 2014; Borreguero-Munoz et al., 2019) are possible causes of epithelial gaps. These interpretations are however not compatible with gaps appearing in less than 30 minutes upon light exposure. To characterize how epithelial tissue is disrupted we induced optogenetic clustering of aPKC in egg chambers cultured *ex vivo*. Live-imaging in midsagital sections using Sqh-mKate2, a tagged version of non-muscle myosin II regulatory light chain (MyoII-RLC) that labels the actomyosin cortex, enables identification of dividing follicle cells, where myosin is redistributed from the apical side to the whole cortex. This shows that epithelial gaps appear next to dividing cells and rapidly expand (Figure 5.3A and Movie 5.S2). Moreover, imaging at the surface of the egg chamber

with a plasma membrane marker confirms the appearance of gaps between dividing cells and its neighbors (Figure 5.3B and Movie 5.S3). These findings are consistent with the predominant appearance of gaps in proliferative stages and suggest that they result from a challenge that cell division represents to intercellular attachment.

Dividing cells require local remodelling of adherens junctions and must coordinate cell separation during cytokinetic ring constriction with the maintenance of tissue cohesion (Osswald and Morais-de-Sa, 2019; Pinheiro et al., 2017; Ragkousi and Gibson, 2014). The observation that gaps quickly expand indicates that tissue tension may play a role by pulling apart dividing and neighboring cells. To test the significante of mechanical forces in the generation of epithelial gaps, we disrupted the actin cytoskeleton with Latrunculin A (Lat A). Time-lapse imaging with chromosome and membrane markers indeed shows that Lat A treatment enables nuclear separation and fully blocks membrane ingression during cytokinesis while maintaining epithelial attachment in the context of aPKC clustering (Figure 5.3C and Movie 5.S4). Accordingly, treatment of egg chambers with Lat A prior to aPKC clustering prevented the formation of epithelial gaps (Figure 5.3D and 5.3E). Thus, actomyosin-dependent force is necessary for tissue rupture upon aPKC inactivation.

Disruption of the actin cytoskeleton blocks global tissue tension and also prevents ring constriction. To test the relevance of cytokinesis, we performed optogenetic inactivation of aPKC in follicle cells depleted of Tumbleweed/RacGAP50C (Tum), a component of the centralspindlin complex that controls the assembly of the cytokinetic ring (Mishima et al., 2002). We confirmed that Tum RNAi induced cytokinesis failure as visualized by imaging with Sqh-mKate2 and E-CAD-GFP (Supplementary Figure 5.S2A). However, live imaging showed gaps are still formed in the epithelial layer next to dividing cells after optogenetic inactivation of aPKC (Supplementary Figure 5.S2B). In fact, Tum RNAi does not restore tissue integrity upon 2h of optogenetic inactivation of aPKC (Figure 5.3F and 5.S2B). We further tested the significance of cytokinesis by inducing acute mitotic arrest or cytokinesis failure before aPKC inactivation. Treatment with the microtubule-depolymerizing drug Colchicine or inhibition of Cyclin B degradation using the proteasome inhibitor MG132 are well-established approaches to block cells in mitosis, whereas inhibition of Aurora B with binucleine 2 disrupts cytokinetic ring assembly (Smurnyy et al., 2010). However, none of these treatments were able to restore tissue integrity (Supplementary Figure 5.S2C, 5.S2D). We thus conclude that the presence of dividing cells provides a weak spot for tissue disruption regardless of cytokinesis completion.

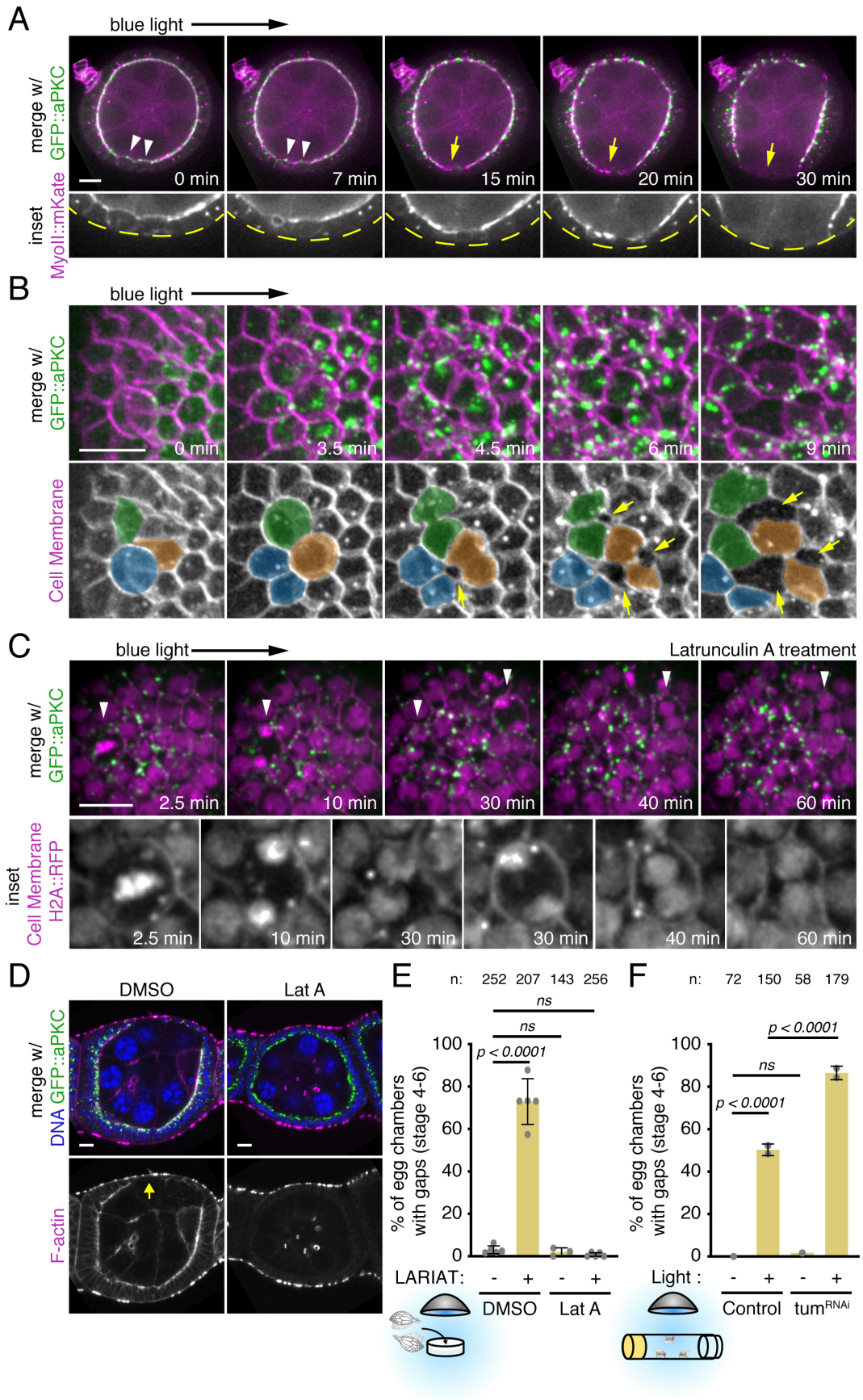


Figure 5.3. Cell division challenges tissue cohesion upon aPKC inactivation. (A, B, C) Time-lapse images of egg chambers expressing LARIAT, GFP::aPKC (green) and either (A; midsagittal view) MyoII(sqh)::mKate2

(magenta) or (B; surface view) stained with membrane marker (magenta) alone or (C; surface view) together with H2A::RFP (magenta). Imaging with 488nm laser clustered aPKC from min 0 onwards. (A) Epithelial gap (yellow arrow) forms where cells divided (white arrowheads); dashed line delineates egg chamber in MyoII(sqh) inset. (B) Epithelial gaps (yellow arrow) form adjacent to dividing cells (coloured). (C) Actin was disrupted with Latrunculin A (LatA) before LARIAT clustering. Insets show dividing cells (arrowheads). **(D)** Representative midsagittal images and **(E)** quantification of epithelial gaps in proliferative follicular epithelium expressing GFP::aPKC (green) and LARIAT stained for F-actin (magenta) and DNA (blue). Actin was disrupted prior to blue light exposure *ex-vivo* for 2 hours. Epithelial gaps (yellow arrow) were scored in the presence or absence of LARIAT. **(F)** Epithelial gaps were scored in control and Tum RNAi egg chambers from GFP::aPKC LARIAT flies exposed to blue light for 2 hours. Graphs show mean ± SD; grey data point represent percentage from independent experiments; n = total amount of egg chambers scored; Fisher's exact test was used (ns, not significant); Scale bars: 10 μm.

Acute inactivation exposes the role of aPKC as a negative regulator of apical constriction

To identify the primary cellular effect that underlies gap formation we analysed the immediate impact of optogenetic clustering on polarity, adhesion and the actomyosin cytoskeleton. Live imaging shows Lgl-mCherry and E-CAD-mKate continue enriched at the lateral membrane and the apical junctions respectively during the initial period of clustering, and are only affected where rupture occurs (Figure 5.4A and Movie 5.S5). Since actomyosin-dependent force is necessary for rupture, we further analysed the response of apical Myosin. Sqh-mKate2 fluorescence increases at the apical side since the first minutes of optogenetic clustering (Figure 5.4B, 5.4C). This myosin accumulation is associated with tissue deformation, evaluated by a change in the circularity of the whole apical surface of intact follicular epithelia prior to any rupture (Figure 5.4D). The change observed at the tissue scale could be driven by simultaneous alterations in the apical area of individual cells. Accordingly, mosaic tissue with clonal expression of UAS-LARIAT shows that optogenetic clustering induces constriction of the apical area specifically in the expressing patch, suggesting a cell autonomous effect of aPKC clustering (Figure 5.4E and Movie 5.S6). Altogether, we concluded that misregulation of the apical actomyosin cytoskeleton and apical domain deformation is the primary effect observed upon optogenetic aPKC inactivation.

We next used chemical inhibition of aPKC as an alternative strategy to test if acute inhibition uncovered the primary effect of aPKC on apical contractility. Treatment of *aPKC*^{as4} egg chambers with low concentrations of inhibitor (1μM 1NA-PP1) leads to a quick increase of apical myosin, which persist at high levels in regions of the follicular epithelium where gaps are absent (Figure 5.5A and 5.5B). Higher concentration of 1NA-PP1 (10 μM)

induces a more transient increase of apical myosin, which peaks before 20 minutes after drug treatment (Figure 5.5A and 5.5B). This is consistent with the timing of polarity loss visualized by disappearence of apical Par-6 around 20 min after addition of the same concentration of 1NA-PP1 (Hannaford et al., 2019). The prolonged increase of apical myosin for weak aPKC inhibition may reflect the perdurance of apical polarity as live imaging shows that GFP-Par-6 remains properly positioned in regions with an intact monolayer during the initial period of inactivation (Supplementary Figure 5.S3A). We conclude that acute inactivation of aPKC enables the dissection of the primary impact of aPKC function in downregulation of apical contractility prior to polarity loss.

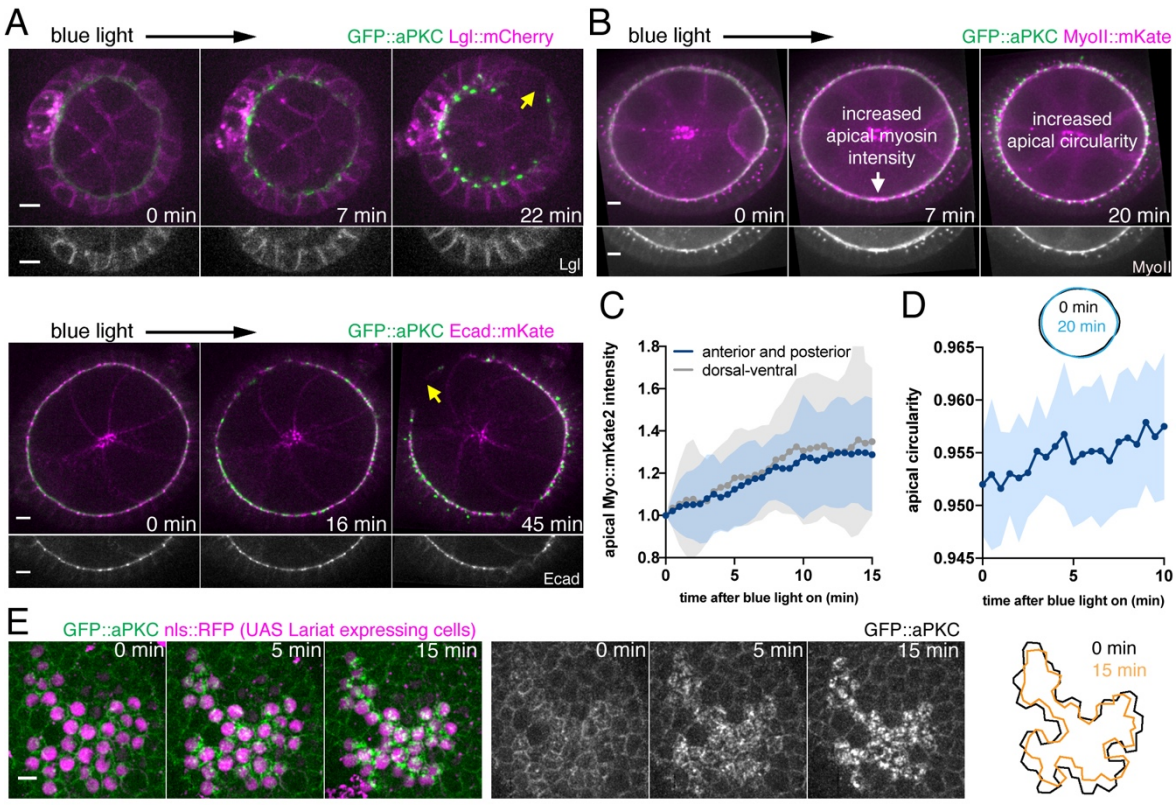


Figure 5.4. aPKC inactivation induces apical constriction. (A, B) Time-lapse midsagittal images of egg chambers expressing LARIAT, GFP::aPKC (green) and either (A top) Lgl-mCherry, (A bottom) E-cad::mKate2 or (B) MyoII(sqh)::mKate2 (shown in magenta and in insets). Imaging with 488 nm laser triggered aPKC clustering from min 0 onwards. (A) Yellow arrows indicate epithelial gap formation. **(C)** MyoII(sqh) accumulation at the apical surface after aPKC clustering was measured at the anterior/posterior (AP) and dorsal/ventral (DV) regions, corrected for cytoplasm intensity and normalized its initial value at min 0 (n ≥ 96 AP and ≥ 96 DV cells from 12 egg chambers). **(D)** Egg chamber circularity was measured at the apical surface of the follicular epithelium (n = 10 egg chambers). **(E)** Time-lapse surface images of GFP::aPKC follicular epithelium cells with mosaic LARIAT expression (marked by nls::RFP in magenta). Imaging with 488 nm laser triggered aPKC clustering and apical domain constriction in LARIAT-expressing cells. Overlayed masks for LARIAT expressing clone at min 0 and 15 (right). Graphs show mean ± 95% SD. Scale bars: 5 μm.

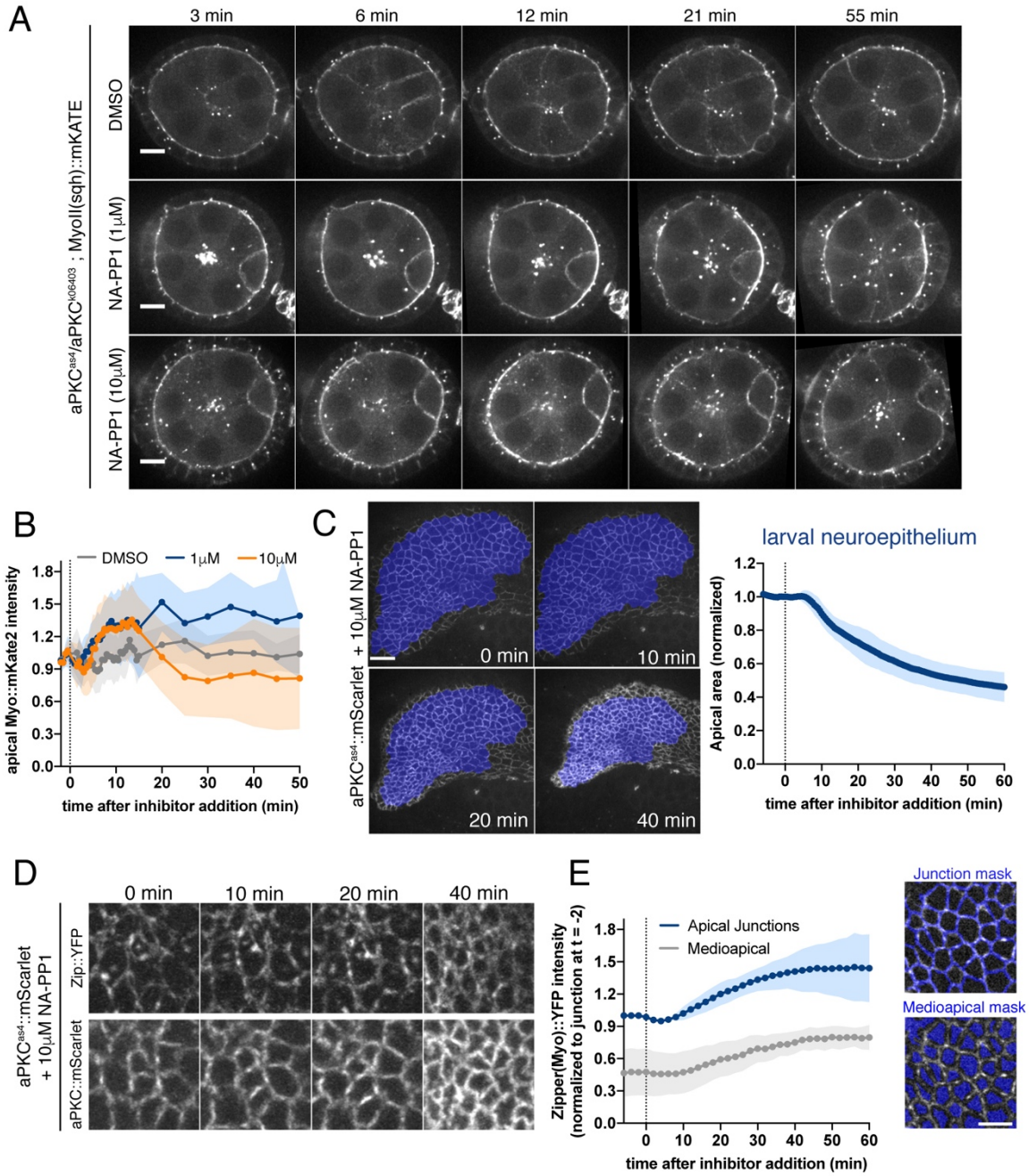


Figure 5.5. Acute aPKC inhibition upregulates apical myosin II and contractility in different *Drosophila* epithelia. (A) Time-lapse midsagittal images of *aPKC^{as4}/aPKC^{k06403}* egg chambers expressing MyoII(sqh)::mKate2. The indicated concentrations of 1NA-PP1 were added at timepoint 0. **(B)** MyoII(sqh) intensity at the apical surface was corrected for cytoplasm intensity and normalized to average intensity prior to aPKC inhibition (n ≥ 32 cells from ≥ 2 egg chambers per condition). **(C)** Contraction of an *aPKC^{as4}::mScarlet* larval brain neuroepithelium following the addition of 10 μM 1NA-PP1 at min 0. Graph (right) shows average apical area (blue mask) of aPKC^{as4}-mScarlet larval brain neuroepithelial cells following the addition of 10 μM 1NA-PP1 normalized to its initial value at min 0 (n = 10 neuroepithelia with an average of 157 cells, across 5 independent experiments). **(D)** Close-up of an aPKC^{as4}::mScarlet, non-muscle myosin II heavy chain MyoII(zip)::YFP larval brain following addition of 10 μM 1NA-PP1 **(E)** MyoII(zip) intensity at the apical junctions and medioapical region (quantification masks on the right) was normalized to junction intensity at -2 min (n = 4 neuroepithelia with ≥ 108 cells). Graphs show mean ± SD. Scale bar: 10 μm (A,C); 5 μm (E)

To determine if downregulation of apical contractility is a general mechanical role for aPKC, we analysed the response of the *Drosophila* neuroepithelium to acute inhibition. Genetic interefence suggested that aPKC is necessary to activate apical contractility by maintaining the apical localization of myosin in neuropithelial cells of the *Drosophila* optic lobe (Franco and Carmena, 2019). By performing live imaging of *aPKC*^{as4}::mScarlett brains we could acutely inhibit aPKC to directly follow the primary impact in apical shape and myosin accumulation. These experiments showed a global contraction of the neuroepithelium initiated within 10 minutes of inhibitor addition (Figure 5.5C and 5.S7). Although global apical contraction did not produce large tissue rupture, we frequently observed local loss of the apical contact next to dividing cells (50%, n=16, 9 brains, Supplementary Figure 5.S3B). Furthermore, apical contraction is associated with an increase in the mean intensity of junctional and medioapical myosin (Figure 5.5D and Figure 5.5E). Thus, downregulation of apical contraction is a primary role for aPKC in distinct epithelial tissues.

Balancing apicomedial actomyosin contractility in non-mitotic cells prevents excessive pulling forces on dividing cells

Myosin is normally enriched at both the junctional level and medioapical surface of follicle cells, where it drives pulses of apical constriction (Alegot et al., 2018). Although GFP-aPKC largely accumulates at the apical intercellular contacts, it also displays a smaller dynamic medioapical pool that accompanies cycles of myosin accumulation (Figure 5.6A,B and Movie 5.S8). Therefore, we investigated the impact of aPKC inactivation on each actomyosin pool through live imaging of Sqh-mKate2 at the egg chamber's surface. Strikingly, myosin rapidly accumulates at the medioapical level upon optogenetic or chemical inactivation of aPKC (Figure 5.6C, Supplementary Figure 5.S3C, Movie 5.S9). The accumulation of myosin at the apical surface only occurs in interphase cells due to reversion of apical actomyosin accumulation at mitotic entry as part of the transition to an isotropic cortex (Ko et al., 2020; Ramanathan et al., 2015; Rosa et al., 2015). In fact, aPKC normally extends along the cortex during mitosis in follicle cells (Figure 5.6A; (Morais-de-Sa and Sunkel, 2013), and its clustering does not affect the reversal of apical myosin accumulation when cells enter mitosis (Figure 5.6C, arrow). Thus, aPKC antagonizes apicomedial actomyosin networks specifically in non-mitotic follicle cells.

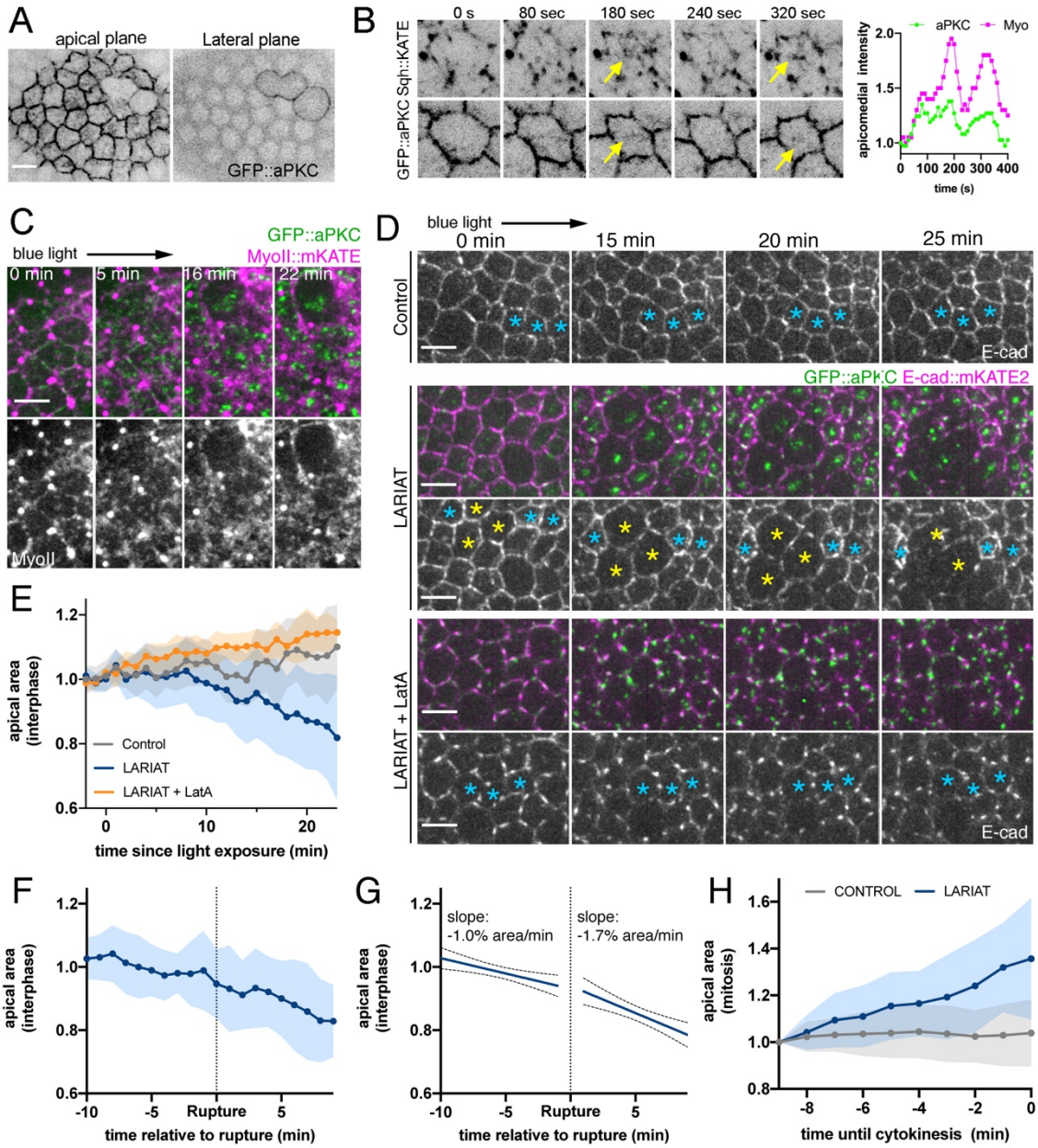


Figure 5.6. aPKC inactivation leads to excessive pulling forces on dividing cells. (A) GFP::aPKC in the follicular epithelium at the apical surface (left) and at the lateral cortex (right). **(B)** Live-imaging of GFP::aPKC and MyoII(sqh)::mKate2 at the apical surface of a follicle cell shows dynamic accumulation at the apicomedial region (arrows). Graph shows the normalized and background subtracted mean pixel intensity of GFP::aPKC and MyoII(sqh)::mKate2 measured in the medioapical region of this cell using a circular 2.5μm diameter ROI (right). **(C, D)** Live imaging of GFP::aPKC (green) LARIAT in the follicular epithelium with either (C) MyoII(sqh)::mKate2 or (D) E-cad::mKate2 in magenta (surface view). Imaging with the 488 nm laser triggered aPKC clustering from min 0 onwards. (C) After GFP::aPKC clustering, MyoII(sqh)::mKate2 accumulates at the apicomedial region, except the in dividing cell (yellow arrow). (D) Asterisks indicate dividing (yellow) and non-dividing (blue) cells. Control did not express LARIAT (top). Lat A was added prior to aPKC clustering (bottom). **(E)** Apical surface area in non-dividing cells was measured at the junction level and normalized to the mean value before clustering ($n \geq 7$ egg chambers per condition). **(F)** Graph shows LARIAT dataset from (E) re-aligned in time relative to epithelial gap formation. **(G)** Linear regression before and after rupture shows apical constriction accelerates after tissue detachment. **(H)** Apical surface area in dividing cells measured at the

junction level and normalized to 9 min prior to anaphase onset (n = 23 cells from 5 egg chambers (Control) and 21 cells from 13 egg chambers (LARIAT). Graphs show mean ± SD Scale bars: 5 μm

We then imaged E-cad-mKate2 to measure the impact of optogenetic aPKC inactivation on the apical surface area. The apical area of interphase cells decreases since the initial period of clustering, but constriction accelerates at the onset of tissue rupture (Figure 5.6D-G). This suggests that the continuous attachment in the closed system formed by the follicular monolayer opposes apical deformation until gaps are formed. Cell deformation is driven by actomyosin-dependent forces, as disruption of the actin cytoskeleton with Lat A prevents the reduction of the apical area upon optogenetic clustering of aPKC (Figure 5.6D and 5.6F and and Movie 5.S10). This suggests that the primary cause of tissue deformation and loss of cohesion is the mechanical challenge produced by actomyosin reorganization in the apical cortex.

Reversion of apical constriction in mitotic cells can induce local relaxation of the apical cortex (Godard et al., 2020; Ko et al., 2020), and so we hypothesized that hypercontraction in neighbouring cells could produce excessive pulling in dividing cells. We analysed the variation of the apical cell area measured at the level of the AJ in cells that entered mitosis during the initial period of light-exposure (<10 min). Optogenetic clustering induces increased expansion of the apical domain prior to anaphase onset indicating that mitotic cells are pulled and stretched by the surrounding hypercontractile tissue until detachment (Figure 5.6H and Movie 5.S10). Hence, aPKC inactivation leads to unbalanced contractility in proliferative tissue, which favours detachment next to dividing cells.

Persistent increase in apical contractility induces epithelial gaps

Our data suggests that aPKC inhibition causes apical actomyosin contraction in non-dividing cells, which breaks attachment next to dividing cells. To directly test the significance of increased apical constriction, we interfered with actomyosin contractility by overexpression of unphosphorylatable (sqhAA) or phosphomimetic (sqhEE) versions of the myosin-RLC, which respectively reduce and increase contractility when forming bipolar filaments with wild-type myosin-RLC (Beach et al., 2014; Kasza et al., 2014; Munjal et al., 2015; Vasquez et al., 2016). SqhAA overexpression restores epithelial integrity, whereas overexpression of SqhEE has the opposite outcome during optogenetic inactivation of aPKC (Figure 5.7A), further supporting that the increase of apical contractility is the driver of cell detachment. Moreover, overexpression of RhoGEF2, which activates RhoGTPase-dependent medioapical contractility during *Drosophila* embryogenesis (Garcia De Las

Bayonas et al., 2019; Mason et al., 2016), also increases the frequency of proliferative egg chambers that display gaps after 2h of light induced clustering (Figure 5.7A).

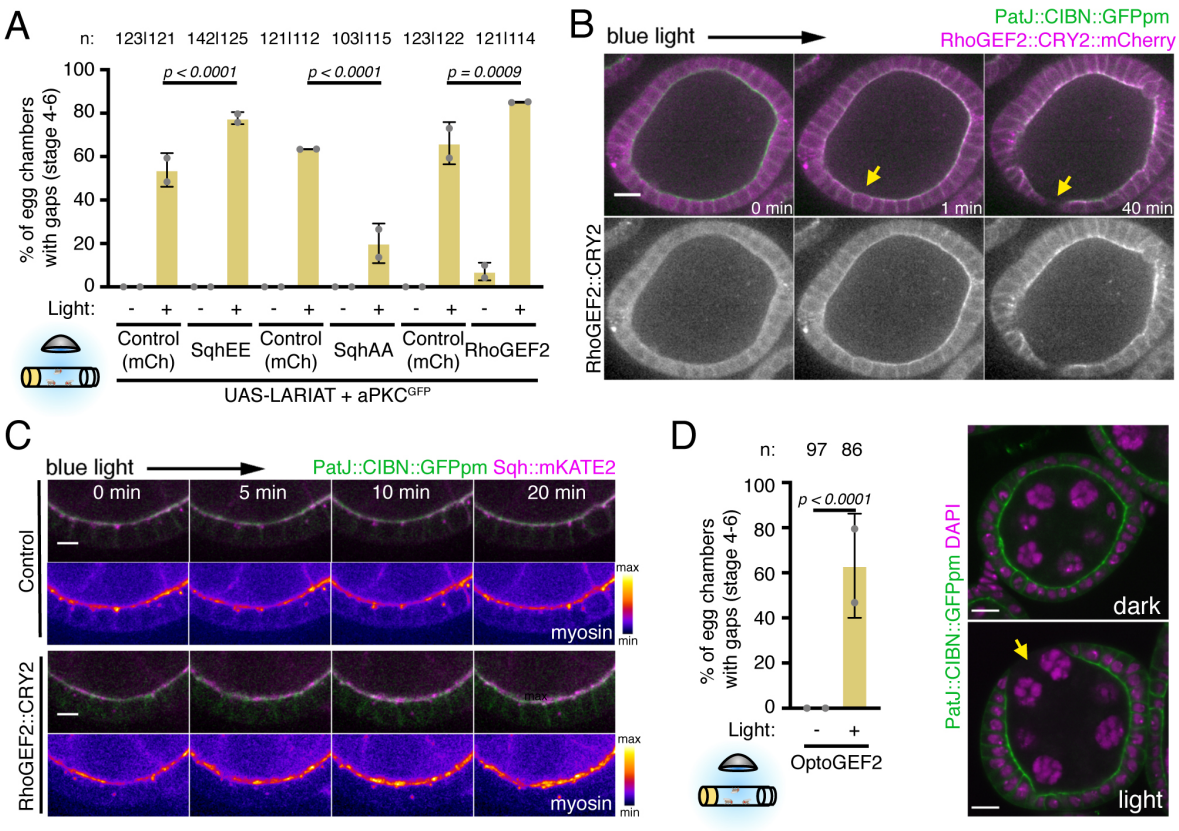


Figure 5.7. Increased apical contractility induces epithelial gaps. (A) Epithelial gaps in stages 4 to 6 were scored upon overexpression of mCherry (Control), Sqh^{E20E21} (SqhEE), Sqh^{A20A21} (SqhAA) or RhoGEF2 in the follicular epithelium of GFP::aPKC LARIAT flies. Flies were exposed to blue light for 2 hours prior to fixation. Control flies were left in the dark. **(B)** Live imaging of egg chamber expressing apical membrane targeted PatJ::CIBN::pmGFP (green) and RhoGEF2::CRY2::mCherry (magenta) in the follicular epithelium (midsagittal view). Imaging with 488 nm laser targeted RhoGEF2 to the apical domain from timepoint 0 onwards. Yellow arrow denotes gap formation in a region with a dividing cell **(C)** Time-lapse images of the follicular epithelium expressing PatJ::CIBN::pmGFP (green), RhoGEF2::CRY2 and MyoII(sqh)::mKate2 (magenta; midsagittal view). Pseudo-colored MyoII(sqh)::mKate2 panel shows its increase at the apical surface after RhoGEF2 apical recruitment. **(D)** Representative midsagittal images (right) and epithelial gap (yellow arrow) quantification (left) in egg chambers (stages 4 to 6) from flies expressing PatJ::CIBN::pmGFP (green) and RhoGEF2::CRY2::mCherry exposed to blue light for 2 hours prior to fixation and staining for DNA (magenta). Control flies were left in the dark. Graphs show mean ± SD; grey data points represent independent experiments; n = total amount of egg chambers scored; Fisher's exact test was used (ns, not significant); Scale bars: 5 μm.

The above results indicate that a sustained increase of medioapical contractility could drive loss of epithelial integrity. To further test this hypothesis, we used an optogenetic tool to locally stimulate constriction by light-dependent recruitment of a RhoGEF2-CRY2-mCherry to a PatJ-CIBN-GFP-CAAX fusion (Krueger et al., 2018). PatJ-CIBN-GFP-CAAX

is enriched in the apical side of follicle cells, where it recruits RhoGEF2-CRY2-mCherry from the cytoplasm upon excitation with the blue laser (Figure 5.7B). Live imaging shows that apical recruitment of RhoGEF2-CRY2 effectively induces apical myosin accumulation, while producing tissue deformation and the appearance of gaps next to dividing cells (Figure 5.7B and 5.7C and Movie 5.S11). Moreover, *in vivo* exposure of flies expressing this optogenetic system to 2h of blue light reproduces the phenotype of aPKC LARIAT, leading to a high frequency of egg chambers with epithelial ruptures (Figure 5.7D). Thus, increased apical contractility is sufficient to disrupt epithelial integrity in a proliferative epithelium, further supporting that aPKC protects epithelial integrity by balancing apical contractility.

DISCUSSION

Although polarity mutants are ubiquitously known to disrupt epithelial architecture (Halaoui et al., 2017; Harris and Peifer, 2007; Jung et al., 2019; Tanentzapf et al., 2000), deciphering the primary causative role of phenotypes demands temporally-controlled inactivation. Here, we show that transmission of light across the *Drosophila* abdomen enables non-invasive *in vivo* optogenetic interference with aPKC in the adult fly ovary. By complementing optogenetic clustering with the ability to selectively tune aPKC activity with chemical-genetics, we provide a detailed temporal analysis of how epithelial disorganization develops by the formation of epithelial gaps and multilayering. Fast and acute perturbation linked tissue phenotypes with the primary cellular effects caused by distinct levels of aPKC inactivation. In particular, we show epithelial gaps result from disrupting the role of aPKC in balancing apical contractility, and are only predominant for partial inactivation of aPKC, such as produced by low concentration of inhibitor or during the initial period of clustering. In contrast, multilayering predominates when aPKC is fully inactivated with higher concentration of the inhibitor or prolonged clustering. Optogenetic clustering of aPKC led to its inactivation, as evidenced by the impaired regulation of known substrates, Lgl and Mira. However, aPKC was only partially inactivated during the initial period of clustering, when it reproduces incomplete chemical inhibition of aPKC. This may result of the slow kinetics of aPKC trapping and mislocalization in optogenetic clusters. Partial aPKC inactivation resulted in an immediate increase in apical contractility that challenged tissue cohesion, but did not lead to immediate loss of apical-basal polarized organization. This finding is consistent with previous work showing that hypomorphic alleles normally produce gaps in the follicular epithelium but do not disrupt apical-basal polarity (Guilgur et al., 2012; Kim et al., 2009). Our results suggest that this is due to the higher threshold of aPKC inactivation

required to disrupt apical-basal polarity. This lower sensitivity of polarity could result from the presence of positive and double negative feedback loops that buffer fluctuations in activity (Ferrell, 2002; Fletcher et al., 2012; Goehring et al., 2011), and may be critical to enable a dynamic modulation of contractility by aPKC without impacting apical-basal polarity.

We show that acute inactivation of aPKC induces apical myosin accumulation with concomitant constriction. Importantly, chemical disruption of actomyosin-dependent forces or genetic downregulation of apical contractility rescue epithelial integrity upon aPKC inactivation, revealing that increased apical contractility drives epithelial gap formation upon partial aPKC inactivation. The apical pool of aPKC in follicle cells may therefore downregulate local actomyosin networks to coordinate the pulsatile behavior of actomyosin contractions as proposed for the embryonic amnioserosa (David et al., 2010; David et al., 2013). Interestingly, whereas inhibition of aPKC induces accumulation of myosin at the medioapical surface in follicle cells, in neuroepithelial tissue, the increase of myosin is more pronounced at junctions. Therefore, apical constriction of neuroepithelial cells may result of increased junctional tension as reported using loss of function analysis for aPKC (Ishiuchi and Takeichi, 2011; Matsuzawa et al., 2021; Warner and Longmore, 2009; Zihni et al., 2017). Hence, our work highlights that aPKC has a primary role as a negative regulator of apical constriction whose function is locally modulated in a tissue-specific manner. aPKC accumulation was also shown to downregulate apical contractility in the developing mammalian blastocyst, supporting that aPKC has ubiquitous ability to repressn cortical myosin accumulation (Maitre et al., 2016). The molecular nature of these functions has yet to be uncovered. Phosphorylation of ROCK by aPKC induces its cortical dissociation to downregulate junctional contractility in mammalian cells (Ishiuchi and Takeichi, 2011), but aPKC does not regulate equivalent sites in *Drosophila* Rok (Sidor et al., 2020). aPKC may also contribute to Rho inactivation or destabilization through p190RhoGAP or the E3 ligase Smurf (Wang et al., 2003; Zhang and Macara, 2008). Alternatively, other apical proteins regulated by aPKC and implicated in the regulation of apical contractility, such as Crumbs and Lulu2/Yurt (Biehler et al., 2021; Flores-Benitez and Knust, 2015; Letizia et al., 2011; Nakajima and Tanoue, 2011; Silver et al., 2019; Zihni et al., 2017), may integrate aPKC function in the maintenance of epithelial polarity with the regulation of apical actomyosin contractility.

This work also provides the first direct evidence that large epithelial rupture can arise by intercellular detachment during cell division. Upon acute aPKC inactivation, epithelial gaps form specifically in the proliferative stages of egg chamber development. Disruption of actomyosin-dependent forces restores epithelial integrity, which highlights that aPKC antagonizes apical contractility to balance apical forces between dividing and neighbour

cells and ensures cohesion during proliferation. Epithelial rupture next to dividing cells shows that cell division provides a weak spot primed for disruption upon increased mechanical stress in epithelia, likely due to reorganization of the actomyosin cortex during mitotic rounding (Ramkumar and Baum, 2016) and the need to remodel cell-cell adhesion (Aguilar-Aragon et al., 2020; Guillot and Lecuit, 2013; Higashi et al., 2016; Petridou et al., 2019; Ragkousi et al., 2017; Tepass and Hartenstein, 1994). In fact, reinforcement of junctional attachment to the cytoskeleton is necessary to prevent rupture during cell division in the *Drosophila* embryonic epithelium and mammalian cell culture (Manning et al., 2019; Monster et al., 2021). Our data indicates that sustained apical contractility in non-dividing cells generates extrinsic pulling forces that ultimately lead to detachment of dividing cells. Accordingly, optogenetic recruitment of RhoGEF2 to the apical surface increases apical myosin and disrupts epithelial integrity, mimicking aPKC inactivation.

Decreased myosin accumulation at the apical surface in mitotic cells even in the context of aPKC inactivation suggests that whereas aPKC breaks contractility during interphase, it is dispensable for reversion of apical contractility at mitotic entry. Recent findings show that reversion of apical constriction induces local relaxation of the apical surface and allows neighbouring interphasic cells to deform the apical side of mitotic cells (Godard et al., 2020; Ko et al., 2020). We show that the apical surface of mitotic cells further expands upon aPKC clustering, consistent with increased pulling forces exerted by neighbour cells. These extrinsic pulling forces are expected to amplify pushing forces exerted from the poles of the dividing cell (Gupta et al, 2021), while being spatially opposed by increased stiffness at the furrow region (Matzke et al., 2001) and ring constriction (Herszterg et al., 2013; Pinheiro et al., 2017). Consistent with this, we observed that gaps between cells normally appear next to the equatorial region of dividing cells and are often initiated during cytokinesis. Localized dilution or destabilization of adherens junctions next to the ingressing membrane (Founounou et al., 2013; Herszterg et al., 2013; Morais-de-Sa and Sunkel, 2013; Pinheiro et al., 2017) may also facilitate apical constriction-induced intercellular detachment

Interestingly, our analysis shows that epithelial gaps form almost exclusively at the dorsal/ventral regions of egg chambers The presence of gaps in this region correlates well with a tension gradient at the apical domain of the epithelium along the anterior-posterior axis with higher tension at equator and lower tension at the poles (Alegot et al., 2018; Finegan et al., 2019). The growing germline may also promote tissue rupture by compressing the epithelium, acting as an external source of stretching force (Balaji et al., 2019; Borreguero-Munoz et al., 2019; Wang and Riechmann, 2007). Moreover, increased tension likely builds in the follicular epithelium since shape changes necessary to accommodate global constriction at apical domain are physically constrained by the

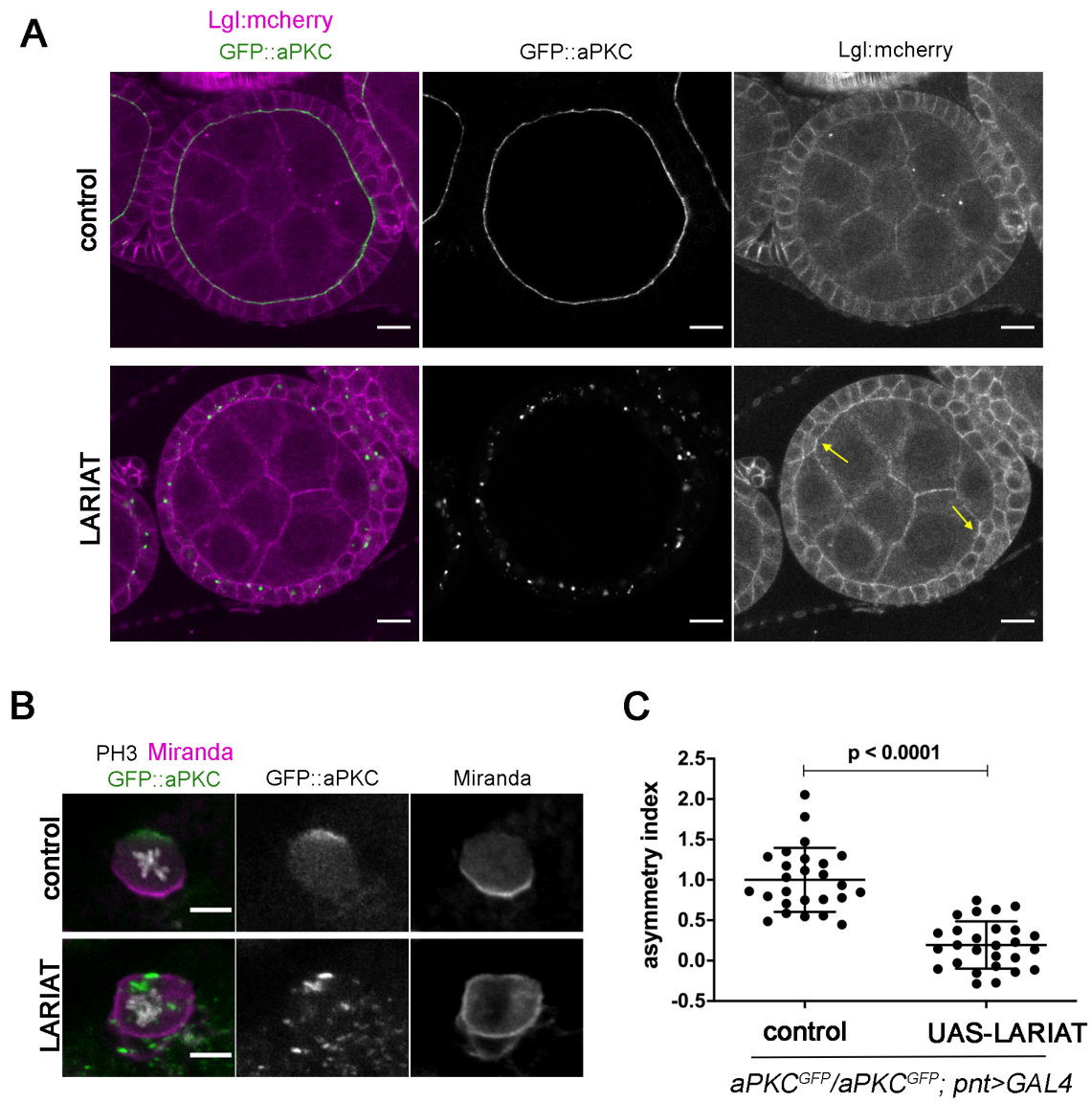
germline in one side, and a stiff basement membrane in the other (Crest et al., 2017). In contrast, the apical area of neuroepithelium cells constricts freely. This may release tension and reduce tissue rupture, which is only occasionally observed and much less dramatic in the neuroepithelium. On top of possible differences in the local response at junctional or medioapical levels, our findings further point towards the importance of physical boundaries and global mechanical context on the outcome of increased apical contractility (Ko et al., 2020).

Apical constriction is a morphogenetic process frequently used to bend or fold epithelia during development (Gilmour et al., 2017). The mitotic remodelling of the cytoskeleton is long known to prohibit simultaneous occurrence of cell division and morphogenetic processes that require apical constriction (Grosshans and Wieschaus, 2000; Mata et al., 2000; Seher and Leptin, 2000). Our work shows that apical constriction poses another challenge during proliferation by producing forces extrinsic to the mitotic cell that interfere with the ability to maintain cohesion at the dividing-neighbouring cell interface. In turn, cell division actively contributes to tissue morphogenesis by controlling tissue material properties (Campinho et al., 2013; Petridou et al., 2021; Petridou et al., 2019; Saadaoui et al., 2020), driving tissue shape change (Hoijman et al., 2015; Kondo and Hayashi, 2013) and cellular rearrangements (Firmino et al., 2016). Hence, our findings widen the importance of a strict control of the timing of apical constriction in proliferative tissues, so that cell division mediates growth and specific morphogenetic events without compromising epithelial integrity.

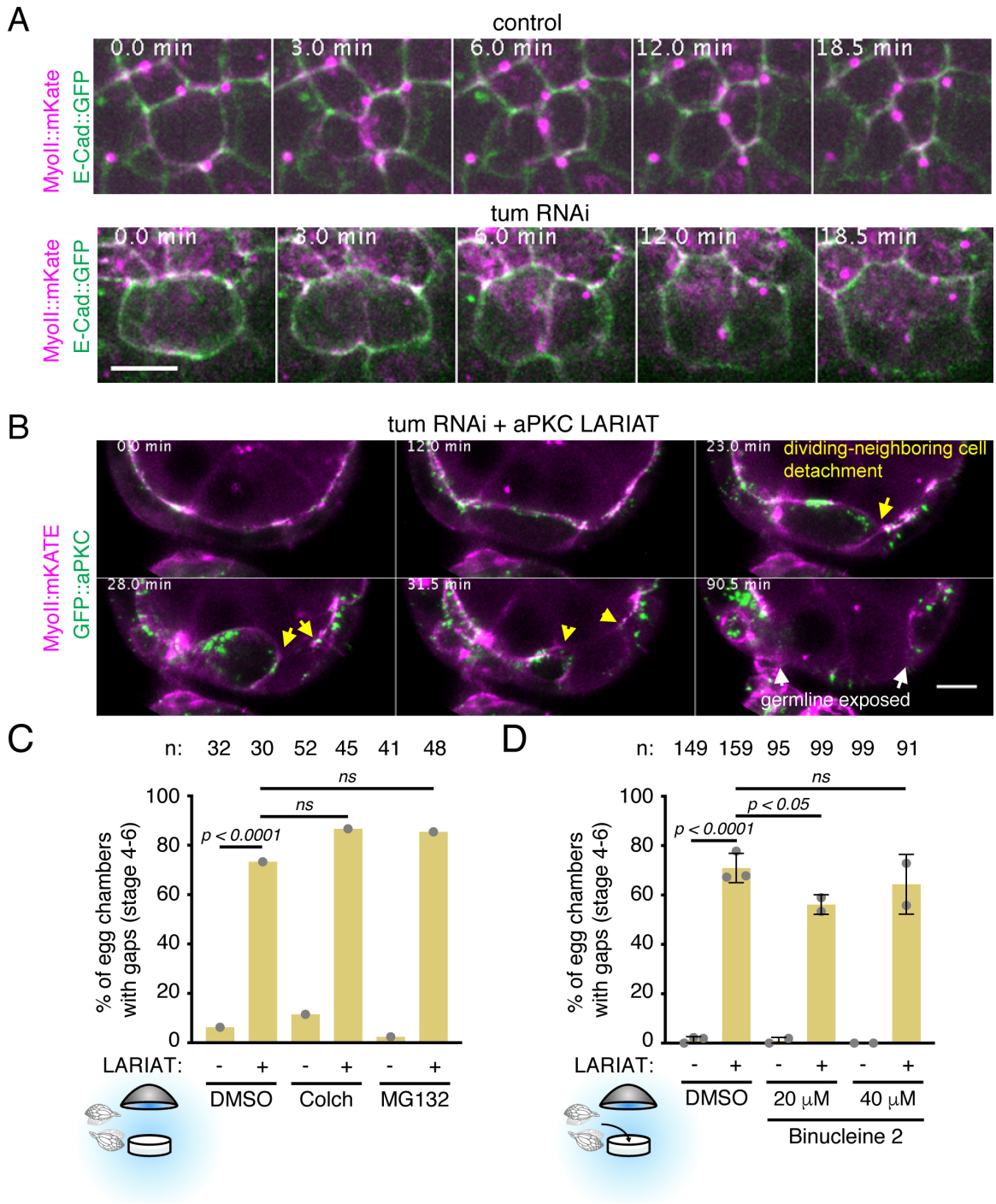
ACKNOWLEDGMENTS

We thank D. St Johnston, X. Wang, Y. Bellaiche and S. de Renzis and the Bloomington Drosophila stock center for *Drosophila*stocks. M.O. is part of the GABBA PhD program from the University of Porto and was supported by a fellowship from FCT (PD/BD/105746/2014). E.M.S. acknowledges FCT contract CEECIND/00622/2017. This work was funded by National Funds through FCT—Fundação para a Ciência e a Tecnologia, I.P., under the projects UIDB/04293/2020 and PTDC/BEX-BCM/0432/2014. This work also received funding from the project Norte-01-0145-FEDER-000029. We also acknowledge the support of the i3S Scientific Platform ALM, member of the national infrastructure PPBI - Portuguese Platform of Bioimaging (PPBI-POCI-01-0145-FEDER-022122).

SUPPLEMENTARY MATERIAL

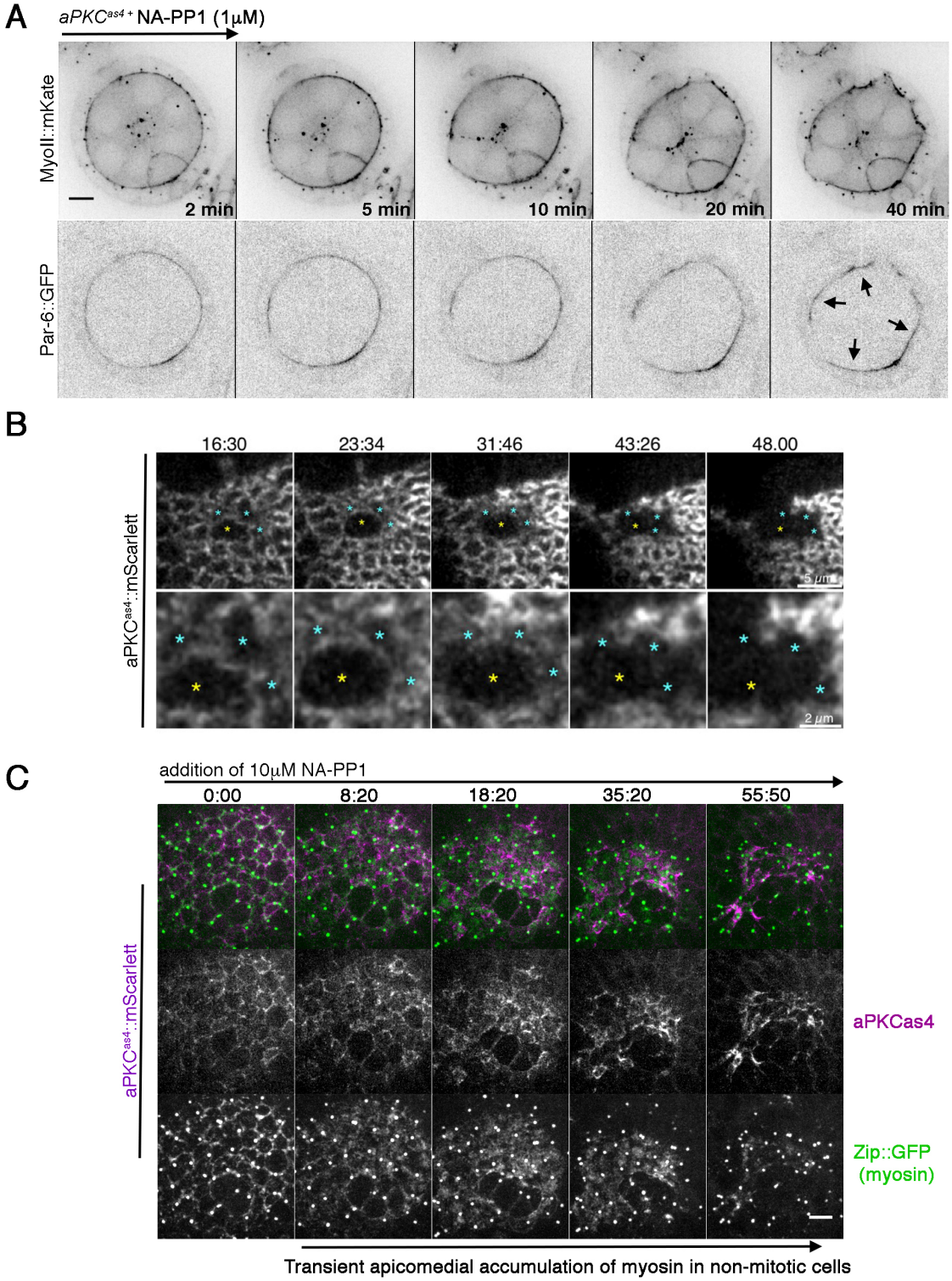


Supplementary Figure 5.S1 related to Figure 5.1. Optogenetic clustering disruptslocal release of aPKC substrates in the *Drosophila* follicular epithelium and neural stem cells. (A) Representative midsagittal images of control and LARIAT egg chambers from GFP::aPKC (green), Lgl::mCherry (magenta) flies exposed to blue light for 24 hours prior to fixation. Arrows point to apical Lgl-mCherry. **(B)** Representative images of control and LARIAT neuroblasts stained for Miranda (magenta) and pH3 to label mitotic cells (white). Exposure to blue light for 1 hour clustered GFP::aPKC and prevent apical release of Miranda (green). **(C)** Miranda asymmetry index along the cell cortex in control (n = 25 cells) and LARIAT neuroblasts (n = 27 cells) was normalized to control mean value. Graph shows mean ± SD values (p<0.0001, t-test). Scale bars: (A) 10 µm B) 5 µm



Supplementary Figure 5.S2 related to Figure 5.3. Cytokinesis completion is not required for tissue rupture upon aPKC inactivation. (A) Live imaging of cell division in follicle cell expressing MyoII(sqh)::mKate2 and E-cad::GFP in control egg chambers and upon Tum RNAi depletion. Tum-depleted cells start to constrict but fail cytokinesis (cytokinesis onset at min 0). **(B)** Time-lapse midsagittal images of the follicular epithelium expressing GFP::aPKC, MyoII(sqh)::mKate2x3 and LARIAT. Yellow arrows point to detachment of dividing cell from a neighbour cell; white arrow to exposed germline. **(C, D)** GFP::aPKC (green) control and LARIAT egg chambers were treated with (C) Colchicine (30 μM; depolymerize microtubules), MG132 (20 μM; block the proteasome) or (D) Binucleine-2 (20 μM or 40 μM; inhibit Aurora B) 15 minutes before light exposure for 2 hours *ex vivo*. Epithelial gaps were scored in stages 4 to 6. Graphs show mean ± SD; grey data points represent mean

value from independent experiments; n = total amount of egg chambers scored; Fisher's exact test was used (ns, not significant); Scale bars = (A) 5 μm (B) 10 μm



Supplementary Figure 5.S3 related to Figure 5.5. aPKC inhibition leads to increased apical myosin and tissue breaks in *Drosophila* epithelia. (A) Time-lapse midsagittal images of aPKC^{as4} egg chambers expressing MyoII(sqh)::mKate2 and Par6::GFP treated with 1NA-PP1 (1μM) at timepoint 0. Arrows indicate intact epithelium with apical Par6 and myosin II. **(B)** Time-lapse images of aPKC^{as4}::mScarlet shows dividing

(yellow asterisk) and non-dividing neighbour cells (blue asterisk) in the neuroepithelium treated with 10 μM 1NA-PP1 at timepoint 0. Loss of apical contacts marked up aPKC following a division occurred after 8/16 divisions in 9 epithelia. **(C)** Time-lapse surface images of aPKC^{as4}::mScarlet (magenta), MyoII(zip)::YFP (green) follicle cells treated with 10 μM 1NA-PP1 at timepoint 0 show transient apicomedial accumulation of myosin II. Scale bars: (A) 10 μm (B,C) 5 μm (B close up) 2 μm.

Supplementary Movie 5.S1 related to Figure 5.2. aPKC inactivation leads to fast and stereotyped tissue disorganization. Live imaging of egg chamber (midsagittal view) expressing GFP::aPKC (green), LARIAT, H2A::RFP (magenta) and stained with membrane marker (magenta). Imaging with 488nm laser triggered GFP::aPKC clustering from timepoint 0 onwards. Epithelial gaps appear at the dorsal and ventral side and multilayering at the posterior side. Right panel shows H2A::RFP and membrane marker. Stills in Figure 5.2A.

Supplementary Movie 5.S2 related to Figure 5.3. Epithelial gaps follow cell division upon aPKC inactivation. Live imaging of egg chamber (midsagittal view) expressing GFP::aPKC (green), LARIAT, MyoII(sqh)::mKate2x3 (magenta). Imaging with 488nm laser triggered GFP::aPKC clustering from timepoint 0 onwards. Right panel shows MyoII(sqh)::mKate2x3. Stills in Figure 5.3A.

Supplementary Movie 5.S3 related to Figure 5.3. Epithelial gaps form adjacent to dividing cells upon aPKC inhibition. Live imaging of egg chamber (surface view) expressing GFP::aPKC (green), LARIAT and stained with membrane marker (magenta). Imaging with 488nm laser triggered GFP::aPKC clustering from timepoint 0 onwards. Epithelial gap appears between dividing cells and their neighbours. Right panel shows membrane marker. Stills in Figure 5.3B.

Supplementary Movie 5.S4 related to Figure 5.3. Tissue disruption upon aPKC clustering depends on actomyosin-dependent forces. Live imaging of egg chamber (surface view) expressing GFP::aPKC (green), LARIAT, H2A::RFP (magenta) and stained with membrane marker (magenta). Actin was disrupted with Lat A (5 μg/mL). Imaging with 488nm laser triggered GFP::aPKC clustering from timepoint 0 onwards. Right panel shows H2A::RFP and membrane marker. Stills in Figure 5.3C.

Supplementary Movie 5.S5 related to Figure 5.4. Two sequencial time-lapse movies showing that Lgl::mCherry and E-cad::mKate maintain their asymmetric distribution during the initial period of aPKC clustering. Imaging with 488 nm laser triggered GFP::aPKC clustering from timepoint 0 onwards. Stills in Figure 5.4A.

Supplementary Movie 5.S6 related to Figure 5.4. aPKC inactivation induces cell-autonomous apical constriction. Live imaging of GFP::aPKC (green) follicular epithelial cells (surface view) with mosaic expression of LARIAT (marked by the presence of two copies of nlsRFP (bright magenta) and aPKC clustering). Imaging with 488 nm laser triggered GFP::aPKC clustering from timepoint 0 onwards. Right panel shows GFP::aPKC. Stills in Figure 5.4F.

Supplementary Movie 5.S7 related to Figure 5.5. aPKC inactivation leads to apical constriction in the Drosophila neuroepithelium. Live imaging of the neuroepithelium expressing aPKC^{as4}-mScarlet (magenta;

right panel) and MyoII(zip)::YFP (green; middle panel). aPKC^{as4} was inactivated with 10 μM 1NA-PP1 at timepoint 0. Stills in Figure S3B.

Supplementary Movie 5.S8 related to Figure 5.6. aPKC has a dynamic medioapical pool that accompanies cycles of myosin accumulation. Live imaging of GFP::aPKC (green; middle panel) and MyoII(sqh)::mKate2 (magenta; right panel) in the follicular epithelium (surface view). Stills in Figure 5.6B.

Supplementary Movie 5.S9 related to Figure 5.6. Myosin accumulates at the medioapical level upon optogenetic inactivation of aPKC. Live imaging of GFP::aPKC (green; right panel) and MyoII(sqh)::mKate2 (magenta; middle panel) in the follicular epithelium (surface view). Imaging with 488nm laser triggered GFP::aPKC clustering in the presence of LARIAT from timepoint 0 onwards. Stills in Figure 5.6C

Supplementary Movie 5.S10 related to Figure 5.6. aPKC inactivation leads to apical cell constriction and pulling on mitotic cells. Live imaging of GFP::aPKC (green) and E-cad-mKate2 (magenta; right panel) in the follicular epithelium (surface view). Imaging with 488nm laser triggered GFP::aPKC clustering in the presence of LARIAT from timepoint 0 onwards. Control cells did not express LARIAT (top panel). Actin was disrupted with LatA (bottom panel). Stills in Figure 5.6D.

Supplementary Movie 5.S11 related to Figure 5.7. Apical recruitment of RhoGEF2 induces tissue rupture next to dividing cells. Imaging with 488nm laser triggered RhoGEF2::CRY2::mCherry recruitment to apical PatJ::CIBN::pmGFP (green). Stills in Figure 5.7B.

CHAPTER 6

GENERAL DISCUSSION AND CONCLUSION

Adaptation of optogenetic clustering tools for protein inactivation to *Drosophila* S2 cells 142

Optogenetic inactivation reveals that aPKC downregulates apical contractility to preserve epithelial integrity 144

Epithelial gaps form by detachment between dividing and neighbour cells..... 147

Cell division has to be coordinated with other force-generating events in epithelia..... 149

Mechanical constraints likely dictate the phenotypic outcome of aPKC inactivation 150

Conclusion 152

To find out what happened in history is enough at the outset without trying too soon to make sure of the "why." I believe it is safer to leave the "why" alone until after one has not only gathered the facts but arranged them in sequence; to be exact, in sentences, paragraphs, and chapters. The very process of transforming a collection of personalities, dates, gun calibers, letters, and speeches into a narrative eventually forces the "why" to the surface. It will emerge of itself one fine day from the story of what happened. It will suddenly appear and tap one on the shoulder.

Barbara W. Tuchman (1981), *Practicing History: Selected Essays - In Search of History*, The Random House Publishing Group

Tissue architecture is essential for proper epithelial function (Hagios et al., 1998). In epithelia, apical-basal polarity controls the asymmetric organization of epithelial cell domains along an apical-basal axis and dictates the position of cell-cell junctions to create functional physiological barriers that compartmentalize multicellular organisms (Rodriguez-Boulan and Macara, 2014; St Johnston and Ahringer, 2010). Accordingly, loss of polarity has long been known to lead to defects in epithelial architecture, which are generally associated with developmental problems, epithelial dysfunction or disease (Martin-Belmonte and Perez-Moreno, 2011). Thus, apical-basal polarity organization in epithelia has to be robust to ensure epithelial function and integrity during development and homeostasis. Paradoxically, analysis of cell division in epithelial cells revealed that apical-basal polarity is partially remodelled during cell division: Par6, aPKC and Cdc42 extend along the lateral cortex to promote isotropic cortex assembly linked to mitotic cell rounding (Morais-de-Sa and Sunkel, 2013; Rosa et al., 2015; Ragkousi et al., 2017) and Lgl delocalizes from the basolateral domain to the cytoplasm to enable proper spindle orientation by Dlg (Bell et al., 2015; Carvalho et al., 2015; Saadaoui et a., 2014). This highlights a plastic behaviour of apical-basal polarity to accommodate the process of cell division and suggests that cell division poses a challenge to epithelial apical-basal organization. However, further understanding how apical-basal polarity contributes to epithelial architecture and cell division has been hampered by the lack of precise temporal control over protein function. Conventional available tools to induce loss of function through RNAi-mediated knockdown or gene knockout lead to generalized disruption of tissue architecture and are therefore not ideal to explore the interplay between apical-basal polarity and cell division and its impact on tissue architecture. In this work, I adapted optogenetic clustering tools for protein inactivation with high temporal control to a

Drosophila cell culture model system and explored the feasibility of targeting specific proteins during mitosis (Chapter 4). Furthermore, I used optogenetic clustering, adapted to the *Drosophila* organism by the X. Wang lab (Qin et al., 2017), to inactivate the main apical polarity kinase, aPKC, in a simple monolayered *Drosophila* epithelium (Chapter 5). Importantly, acute aPKC inactivation allowed us to directly capture for the first time how epithelial architecture is disrupted upon loss of aPKC activity and uncover that aPKC preserves epithelial integrity during proliferation by downregulating apical actomyosin contractility in non-dividing cells. Thus, this work contributes to our understanding of how epithelial architecture and integrity is maintained during proliferation.

ADAPTATION OF OPTOGENETIC CLUSTERING TOOLS FOR PROTEIN INACTIVATION TO *DROSOPHILA* S2 CELLS

To address the matter of temporal control over protein activity in experimental perturbation of apical-basal polarity, I used an optogenetic clustering tool – LARIAT. Optogenetic proteins can react to light stimuli within seconds and are, consequently, ideal for acute protein inactivation within the intended timeframe (Zhang and Cui, 2015). LARIAT had been previously developed in human cultured cells for protein inactivation through sequestration (Lee et al., 2014). Its ability to target GFP-tagged proteins through a GFP nanobody made it ideal for plug and play integration with the vast collection of available endogenously tagged GFP-proteins in the *Drosophila* system (Buszczak et al., 2007; Huang et al., 2009; Morin et al., 2001; Quinones-Coello et al., 2007). In this work, I adapted LARIAT to *Drosophila* S2 cells and established a working set of plasmids to target and cluster GFP-tagged proteins (Chapter 4). This increases the toolbox available in *Drosophila* S2 cells, a model system used for cell biology studies, screens and to complement studies in the *Drosophila* model organism (Afonso et al., 2014; Carvalho et al., 2015; Conde et al., 2013; Goshima et al., 2007; Jolly et al., 2016; Kwon et al., 2008; Moura et al., 2017; Moutinho-Pereira et al., 2013; Toret et al., 2014).

Protein targeting by LARIAT relies on the light-sensitive protein CRY2 fused to a GFP nanobody, which was found to co-localize with GFP-tagged target proteins, as previously described (Lee et al., 2014). Stimulation with blue light triggered clustering through CRY2 interaction with CIBN fused to a multimerization domain. Clustering was immediately visible within 1 minute after stimulation, confirming that the dynamics of optogenetic clustering by LARIAT were adequate for interfering with protein function within the timeframe of cell division. Additionally, we also tested the ability of CRY2 to cluster by

itself through oligomerization, which would obviate the need for CIBN and simplify the clustering tool. However, CRY2 was not found to cluster by itself in response to light, unlike in human cultured cells (Bugaj et al., 2013). Furthermore, the CRY2olig variant, previously described to have enhanced ability to oligomerize in human cells (Taslimi et al., 2014), was also found not to cluster in S2 cells, except in rare cells that expressed very high levels of CRY2olig (data not shown). This suggests that lack of CRY2 clustering in S2 cells may be related to differences in expression levels relative to previous studies.

LARIAT-mediated clustering inactivated the mitotic kinase Mps1 and partially reverted the mitotic delay caused by Mps1 overexpression in S2 cells. Furthermore, optogenetic clustering was shown to delocalize the polarity protein Lgl from the cortex. However, the success of optogenetic clustering was found to depend on the ratio of LARIAT levels to target protein, likely due to the inherent stoichiometry of the clustering process where GFP-tagged proteins that do not dimerize or oligomerize by themselves have to be targeted individually through binding to CRY2-V_HH in a 1:1 ratio for full sequestration. Initial tests to inactivate GFP-tagged proteins with LARIAT in the *Drosophila* follicular epithelium further confirmed this limitation. While LARIAT was able to cluster basolateral determinants Scrib, Lgl, Dlg, and Par1 endogenously tagged with GFP, it did not sequester and delocalize all GFP-tagged molecules for either of these proteins and long-term clustering did not reproduce known loss of function phenotypes for them (Appendix).

To build an alternative optogenetic inactivation tool, we coupled LARIAT-mediated optogenetic clustering to Trim21, a vertebrate E3 ubiquitin ligase that binds antibody-bound proteins and targets them for degradation within minutes of antibody injection (Clift et al., 2017). Trim21 had been seen to aggregate upon antibody injection, which suggested that antibodies induce oligomerization of Trim21 and trigger Trim21-mediated protein degradation. This suggested that Trim21 could be activated by LARIAT-mediated clustering. Direct fusion of Trim21 to CRY2 enabled Trim21 degradation in response to blue light in *Drosophila* S2 cells, confirming that clustering triggers Trim21 activity and integration of Trim21 with LARIAT is a viable strategy to build an optogenetic tool for protein degradation (Appendix). Such a tool could be easily deployed to target different proteins through coupling with a GFP-nanobody, and thus we developed OptoTrim as a potential addition to the repertoire of tools to trigger acute loss of function (briefly discussed in an appendix to this thesis; Zeng et al., 2021). Most alternative optogenetic strategies for protein inactivation rely on light-induced recruitment of inactivating proteins through optical dimerizers (Spiltoir and Tucker, 2019). Specific proteins have been engineered for photoinactivation through direct fusion with optogenetic domains (Wu et al., 2009; Zhou et al., 2017). However, this requires case-by-case identification of viable sites for protein fusion with an optogenetic domain, so that light stimulation triggers a conformational change

that propagates from the optogenetic domain to the target protein active site to control protein function. Although a computational pipeline for viable fusion site identification was recently published (Dagliyan et al., 2019; Dagliyan et al., 2016), this still requires individual protein engineering and validation. Recently, an optogenetic tool for protein degradation that relies on light to induce binding of LNX1 E3 ligase catalytic domain to specific target proteins was shown to trigger near complete protein degradation within 30 minutes (Deng et al., 2020). It would be interesting to compare how this strategy for protein degradation and OptoTrim perform *in vivo*.

CRY2olig had previously been used to detect protein-protein interactions *in vivo* in human cultured cells: CRY2olig was used to cluster a 'bait' protein and test for 'prey' protein colocalization as a readout for interaction (Taslimi et al., 2014). We confirmed that LARIAT-mediated clustering can also be used to detect protein-protein interactions live in single *Drosophila S2* cells (Chapter 4): we clustered GFP-aPKC and verified that Par6 co-clustered with full-length aPKC, but not with mutant aPKC lacking the Par6-interacting domain, showing that the detected interaction was specific (Hirano et al., 2005; Joberty et al., 2000; Suzuki et al., 2001). Optogenetic co-clustering assays are a simple method to complement biochemical assays and assess protein interactions in a physiological context in single cells with high temporal resolution. It should be noted that protein co-clustering does not show direct protein interaction, since, in principle, indirect interactors may also co-cluster. Therefore, optogenetic co-clustering cannot substitute further *in vitro* biochemical assays to study molecular interactions in detail. Nevertheless, LARIAT co-clustering provides an easy to use tool to directly test for protein interactions in cells. LARIAT has already been used in S2 cells to detect protein-protein interactions during mitosis (Cunha-Silva et al., 2020) and in the *Drosophila* follicular epithelium to assess basolateral polarity protein interactions in the basolateral domain (Ventura et al., 2020; Appendix). A recent pre-print also reports the use of LARIAT in *C. elegans* to study polarity protein interactions (Kroll et al., 2021).

OPTOGENETIC INACTIVATION REVEALS THAT APKC DOWNREGULATES APICAL CONTRACTILITY TO PRESERVE EPITHELIAL INTEGRITY

Apical-basal polarity is essential for epithelial architecture. Accordingly, loss of polarity proteins generally disrupts epithelial tissue organization and leads to failure in development (Bilder et al., 2000; Horne-Badovinac et al., 2001; Muller and Wieschaus, 1996; Rolls et al., 2003; Tepass et al., 1990). In particular, simple monolayered epithelia

become disorganized with different types of defects: masses of unpolarized cells can accumulate on top of each other with spurious ectopic accumulations of remaining apical or basolateral polarity proteins (multilayering; Bilder et al., 2000; Bilder et al., 2003; Horne-Badovinac et al., 2001; Tanentzapf et al., 2000; Tanentzapf and Tepass, 2003); cystic epithelia can form multiple ectopic lumens (Horne-Badovinac et al., 2001); and epithelia can lose their integrity (Guilgur et al., 2012; Horne-Badovinac et al., 2001; Kim et al., 2009; Muller and Wieschaus, 1996; Seidl et al., 2013; Tanentzapf et al., 2000). The emergence of these defects has been associated with 1) defective organization of epithelial domains along the apical-basal axis, which can lead to lack of adherens junctions formation at the *zonula adherens* and mispositioned cell-cell junctions; 2) defective control of proliferation, which can lead to overproliferation; 3) misoriented cell divisions along the apical-basal axis, which could lead to stratification or 4) failure of individual cells to integrate within the epithelium. However, although these mechanisms are based on detailed evidence of how apical-basal polarity proteins function at the molecular level and extensive characterization of defects upon loss or gain of function (Riga et al., 2020; Rodriguez-Boulan and Macara, 2014; St Johnston and Ahringer, 2010; Stephens et al., 2018), the exact cause of loss of epithelial architecture remains frequently uncertain, due to the complex interactions between apical-basal polarity and different aspects of epithelial cell biology that complicate analysis and due to lack of direct observation of how a polarized epithelium actually becomes disorganized. In this work, I combined optogenetic LARIAT clustering to inactivate aPKC acutely in the fully polarized *Drosophila* follicular epithelium to understand how aPKC preserves epithelial architecture and how an epithelium becomes disorganized upon its inactivation. This approach was complemented with a recently published aPKC^{as4} allele, sensitive to an ATP analog, that is therefore amenable to acute chemical inhibition (Hannaford et al., 2019). Surprisingly, acute aPKC inactivation disrupted epithelial architecture during proliferation by intercellular detachment of dividing and neighbour cells and revealed that aPKC preserves epithelial integrity by downregulating actomyosin contractility to balance forces in epithelia during proliferation.

LARIAT-mediated clustering of endogenously tagged GFP-aPKC led to aPKC inactivation in the follicular epithelium. Long-term clustering mimicked known defects in epithelial organization (Guilgur et al., 2012; Kim et al., 2009) – epithelial gaps and multilayering – and led to mislocalization of the known aPKC substrate – Lgl. Furthermore, aPKC clustering in *Drosophila* neuroblasts also led to mislocalization of another aPKC substrate – Miranda – further validating optogenetic clustering as a tool to inactivate aPKC in different tissues. However, during the initial stages of optogenetic aPKC clustering, apical-basal polarity was not affected and Lgl remained properly polarized at the basolateral domain and adherens junctions remained asymmetrically positioned. Furthermore, at this

stage of inactivation, epithelial gaps were the predominant defect in the follicular epithelium, similar to partial inactivation of aPKC^{as4} through chemical genetics with a low dose of ATP analog. This indicated that aPKC clustering initially leads to partial aPKC inactivation, possibly due to the kinetics of protein trapping in optogenetic clusters. Interestingly, it also showed that epithelial gaps are not directly caused by loss of apical-basal polarity. Consistent with this, hypomorphic aPKC alleles have been observed to cause epithelial gaps, but not loss of apical-basal polarity in the follicular epithelium (Guilgur et al., 2012; Kim et al., 2009). However, unlike previously proposed, our results suggest this is due to low levels of activity and not to kinase-independent functions. Maintenance of apical-basal polarity upon partial aPKC inactivation suggests that apical-basal polarity is indeed a robust system capable of withstanding fluctuations in individual protein activity. Furthermore, the higher sensitivity of apical contractility to aPKC levels makes sense from a physiological point of view, as it should enable local modulation of actomyosin through aPKC without compromising apical-basal polarity. Complete loss of apical-basal polarity upon full aPKC inactivation was found to lead predominantly to multilayering and no epithelial gaps, suggesting that loss of apical-basal polarity suppresses formation of epithelial gaps.

Finetuning aPKC activity allowed us to separate a role for aPKC in downregulating apical actomyosin independently of apical-basal polarity. Partial aPKC inactivation led to a striking increase in apical myosin II immediately upon inactivation, accompanied by apical constriction, showing that aPKC downregulates apical actomyosin. Importantly, downregulating actomyosin-dependent forces through actin depolymerization with LatA or expression of an inactive form of myosin II regulatory light chain (sqh^{A20A21}) rescued epithelial gaps, indicating that aPKC preserves epithelial integrity by downregulating apical actomyosin contractility. Furthermore, increasing apical contractility (sqh^{E20E21}) increased the incidence of epithelial gaps and triggering apical contractility through optogenetic recruitment of RhoGEF2 independently of apical-basal polarity was sufficient to phenocopy partial aPKC inactivation, showing that increased tension is sufficient to compromise epithelial integrity.

Actomyosin has been proposed to have intrinsically pulsatile behaviour that is coordinated by cycling Rho activity to drive morphogenetic events and balance external stresses in epithelia (Armon et al., 2018; Nishikawa et al., 2017). Apical actomyosin pulses in the follicular epithelium have been proposed to follow a gradient along the anterior posterior axis to shape the egg chamber (Alegot et al., 2018). Our results suggest that aPKC may regulate contractile pulses of actomyosin at the apical surface of the follicular epithelium, as was previously reported in the *Drosophila* amnioserosa during dorsal closure (David et al., 2010; David et al., 2013). Accordingly, aPKC was observed to co-localize with dynamic accumulations of myosin II at the apical surface and pulsatile behaviour was lost

upon aPKC inactivation. Thus aPKC may not only downregulate actomyosin globally, but also coordinate pulses at the apical surface. While in the amnioserosa this has been proposed to drive dorsal closure (David et al., 2010; David et al., 2013), we find that aPKC regulation of actomyosin contractility is essential to balance forces in the follicular epithelium and preserve epithelial integrity. In the neuroepithelium, aPKC inactivation also led to an increase in both apical and junctional myosin II concomitant with a reduction in apical surface area, suggesting that here apical constriction may also be driven by junctional contractility, consistent with previous observation in vertebrate cultured cells (Kishikawa et al., 2008; Ishiuchi et al., 2011, Zihni et al., 2017). aPKC has also been observed to downregulate apical actomyosin contractility during vertebrate gatrulation (Maitre et al., 2016), highlighting that regulation of apical actomyosin contractility is a conserved function of aPKC that can be used for different morphogenetic or homeostatic purposes.

Further studies are required to understand how aPKC downregulates actomyosin contractility at the apical surface. In vertebrate cells, aPKC was shown to directly phosphorylate ROCK to downregulate actomyosin contractility at adherens junctions (Nakajima and Tanoue, 2011). Additionally, vertebrate aPKCζ was shown to phosphorylate myosin IIB to slow down filament assembly (Even-Faitelson and Ravid, 2006). However, neither of these mechanisms appear to apply, at least in *Drosophila* (Sidor et al., 2020). Alternatively, aPKC may regulate actomyosin through Rho (Zhang and Macara, 2008) or indirectly through another polarity protein (Biehler et al., 2021; Hava et al., 2009; Majumder et al., 2012).

EPITHELIAL GAPS FORM BY DETACHMENT BETWEEN DIVIDING AND NEIGHBOUR CELLS

Live imaging upon partial aPKC inactivation enabled us to collect direct evidence for the first time of how epithelial gaps form. Strikingly, we observed that gaps formed through detachment between neighbour and dividing cells, showing that epithelial gaps appeared through tissue rupture rather than through failure of epithelial cells to integrate the epithelium, as was previously hypothesized (Tanentzapf et al., 2000). Furthermore, this observation suggests that dividing cells are weak spots for epithelial integrity. Importantly, during oogenesis, egg chambers progress from developmental stages where the follicular epithelium proliferates to naturally non-proliferative epithelial developmental stages, which allowed us to address the role of epithelial cell division. Strikingly, epithelial gaps were initially restricted to the proliferative stages and only appeared in non-proliferative stages

within a timeframe compatible with the natural progression of egg chambers to non-proliferative stages where aPKC had been inactivated during proliferative stages. This result reinforced cell division as a weak spot for epithelial integrity. Tissue rupture adjadecent to dividing cells suggests a local imbalance of forces that overcomes cell-cell adhesion.

During mitotic entry, the actomyosin cortex is remodelled to become isotropic and promote rounding up (Rosa et al., 2015; Sorce et al., 2015; Stewart 2010). Our data shows that during this process the increased apical actomyosin accumulation triggered by aPKC inactivation is reversed. A decrease in apical constriction at the apical domain concomitantly with mitotic rounding had been previously observed in the *Drosophila* embryo (Ko et al., 2020). Our results show that reversal of apical contractility upon mitotic entry is independent of aPKC. Interestingly, direct measurements of apical tension in ascidian blastomeres show that the apical surface relaxes during mitosis and becomes more compliant to deformation by neighbour cells (Godard et al., 2020). Accordingly, we observe that upon aPKC inactivation the apical surface area increases during mitosis, consistent with increased pulling forces exerted by neighbour cells on the dividing cells. This further supports that epithelial gaps appear by rupture adjacent to dividing cells due to excessive forces.

Generally, epithelial gaps formed adjacent to the ingressing furrow during cytokinesis, consistent with ring constriction during cytokinesis generating an inward pulling force that pulls on neighbour cells (Herszterg et al., 2013; Pinheiro et al., 2017). Epithelial cytokinesis involves an interplay between neighbour and individual cells with localized adherens junctions remodelling and neighbour cell deformation to accommodate the physical changes necessary to separate the two daughter cells and maintain epithelial architecture (Founounou et al., 2013; Guillot and Lecuit, 2013; Herszterg et al., 2013; Morais-de-Sa and Sunkel, 2013; Pinheiro et al., 2017). Importantly, adherens junctions were shown to be mechanically coupled to ring constriction during cytokinesis (Herszterg et al., 2013; Morais-de-Sa and Sunkel, 2013; Pinheiro et al., 2017), indicating that it pulls adherens junctions in the opposite direction than neighbour cells undergoing apical constriction do. Additionally, adherens junction remodelling during cell division may contribute to fragilize adhesion (Aguilar-Aragon et al., 2020; Founounou et al., 2013; Guillot and Lecuit, 2013; Herszterg et al., 2013; Morais-de-Sa and Sunkel, 2013; Pinheiro et al., 2017; Ragkousi et al., 2017).

Although epithelial gaps upon aPKC inactivation generally form next to ingressing cytokinetic rings, blocking cells in prometaphase, metaphase or blocking cytokinesis did not rescue epithelial gaps. This suggests epithelial tension is too great and epithelia break at other sites independently of cytokinesis. Interestingly, increasing tension in a Caco-2

epithelial monolayer with Calyculin-A revealed that tension was highest at tricellular junctions, suggesting they may be alternative rupture sites (Acharya et al., 2018).

Alltogether, our data strongly suggests that upon partial aPKC inactivation epithelial adhesions crack due to excessive opposite pulling forces at the site of contractile ring ingression.

CELL DIVISION HAS TO BE COORDINATED WITH OTHER FORCE-GENERATING EVENTS IN EPITHELIA

Our results indicate that epithelial cell division is a mechanical weak spot that can compromise epithelial integrity in the presence of excessive tension. Cell division is an important contributor to morphogenesis (Etournay et al., 2015; Guirao et al., 2015) that can actively contribute to modulate epithelial material properties (Petridou et al., 2021; Petridou et al., 2019; Saadaoui et al., 2020), dissipate tension (Campinho et al., 2013), promote cell rearrangements (Firmino et al., 2016), contribute to lumen expansion (Hoijman et al., 2015) and position epithelial folds (Tozluoglu et al., 2019). Interestingly, cell cycle and cell proliferation are known to have to be tightly regulated during embryo development (Farrell et al., 2012) and premature mitotic entry has been shown to interfere with gastrulation in *Drosophila* (Grosshans and Wieschaus, 2000; Mata et al., 2000; Seher and Leptin, 2000). During *Drosophila* gastrulation, the presumptive mesoderm constricts apically to form the ventral furrow and become internalized (Martin, 2020). This process is driven by pulsatile apical actomyosin contractions (Martin et al., 2009). Premature mitotic entry leads to failure in ventral furrow formation (Grosshans and Wieschaus, 2000; Mata et al., 2000; Seher and Leptin, 2000) due to reversal of apical constriction upon mitotic entry that disrupts the coordinated constriction in the presumptive mesoderm (Ko et al., 2020). Interestingly, ectopic induction of apical contractility in mitotic domains of the *Drosophila* embryo leads to epithelial folding of the contractile region likely due to relaxation-enabled deformation of neighbour mitotic domains (Ko et al., 2020). This further highlights the need to coordinate cell division with other morphogenetic events to ensure proper morphogenesis and epithelial tissue architecture. Accordingly, our work further highlights that apical constriction and cell division are incompatible events and suggests that the tension created by these two events can lead to intercellular detachment.

Our work indicates that epithelial gaps form adjacent to dividing cells due to excessive tissue tension. This suggests that mechanical forces have to be coordinated so that cell division does not compromise integrity. Our results show that aPKC downregulates

global tissue contractility for this purpose. Furthermore, they also highlight that dividing cells are mechanical weak spots in epithelia. Therefore, it is conceivable that local mechanisms exist to ensure that neighbouring cells do not impair cell division or cause dividing cells to detach from neighbouring cells through excessive pulling. A study using monolayer stress microscopy to map in-plane tension in MDCK cells found that tension decreases locally around prospective dividing cells 3 hours before mitotic entry (Uroz et al., 2018). In this study, tension decrease was shown to facilitate mitotic rounding up. However, it could serve additional purposes. Thus, further work is required to address how neighbouring cells are regulated so as not to interfere with cell division and whether aPKC also contributes to this force balance locally. Interestingly, mitotic cells tend to divide along the axis of highest tension along the tissue and thus the cytokinetic ring contracts perpendicular to it, which may contribute to balance cytokinesis forces (Bosveld et al., 2016; Campinho et al., 2013; Finegan et al., 2019; Lam et al., 2020). Furthermore, in vertebrate epithelia tight junctions can also help to balance excessive forces (Cartagena-Rivera et al., 2017; Hatte et al., 2018).

Our results highlight the need for mechanical coordination in epithelia and a role for aPKC in this process. Force balance by aPKC may also be relevant in the context of disease. Vertebrate aPKCι and aPKCζ have been found to function both as oncogenes and tumor suppressors in different contexts (Reina-Campos et al., 2019). Interestingly, a relationship between loss of tissue architecture, RhoA regulation and of loss of apical-basal polarity was identified in human breast lesions leading to carcinoma (Halaoui et al., 2017). Additionally, patients with inflamatory bowel disease have an increase in small epithelial gaps in the gut, which have been associated with aPKC downregulation and increased ROCK activity in polarized epithelial cells (Forteza et al., 2016; Kiesslich et al., 2007; Turcotte et al., 2013; Wald et al., 2011). These gaps are normally closed by neighbour epithelial cells in healthy individuals, however, this process may be impaired by downregulation of aPKC.

MECHANICAL CONSTRAINTS LIKELY DICTATE THE PHENOTYPIC OUTCOME OF aPKC INACTIVATION

Our results suggest a role for mechanical constraints in conditioning the end result of aPKC inactivation. Partial aPKC inactivation led to stereotypical architecture defects in the follicular epithelium: epithelial gaps formed in the dorsal-ventral region, while multilayering formed in the anterior and posterior regions. Furthermore, while partial aPKC

inactivation consistently led to epithelial gaps spanning several cell sizes in the follicular epithelium, in the neuroepithelium only minor perturbations of apical cell contacts were detected. This may be due to different mechanical constraints between both tissues. In egg chambers, the follicular epithelium encapsulates a growing germline cyst and is thus sandwiched between it and an external basement membrane (Wu et al., 2008). Partial aPKC inactivation triggers apical actomyosin contractility and concomitant apical constriction. However, the growing germline exerts outward pressure on the follicular epithelium (Wang and Riechmann, 2007), which we expect opposes constriction by the follicular epithelium. Accordingly, midsagital live imaging of the follicular epithelium upon aPKC inactivation shows changes in circularity, indicative of changes in forces at the apical surface, but no significant reduction of the total apical area of the follicular epithelium. This suggests that physical constraints keep the follicular epithelium stretched despite increased apical constriction, which should increase global tissue tension. Strikingly, epithelial gaps appear consistently at the dorsal-ventral region of the follicular epithelium, where tension is highest (Alegot et al., 2018; Finegan et al., 2019). This model suggests that epithelial gaps form due to increased tension imposed by mechanical constraints. On the other hand, we show that the neuroepithelium freely constricts its apical surface upon aPKC inactivation, which should release tension. Accordingly, no epithelial gaps significant in size were detected here. To test this model for gap formation, it would be interesting to inactivate aPKC in epithelia subjected to different mechanical constraints, such as the notum or the wing disc, and combine this with externally applied stretch forces to oppose apical constriction (Tozluoglu et al., 2019). Additionally, it is also possible that the concomitant accumulation of junctional actomyosin in the neuroepithelium upon aPKC inactivation may contribute to the difference in phenotype through regulation of adherens junction stability (Kale et al., 2018).

Our results show that while epithelial gaps form at the region with highest tension, multilayering occurs at the region with lowest tension and where epithelial cells are more crowded (Alegot et al., 2018; Finegan et al., 2019). Interestingly, in *Drosophila* tracheal placode invagination and vili formation in the mouse embryonic gut, epithelial cells invaginated upon cell division due to compression by the surrounding tissue and created a tissue fold (Freddo et al., 2016; Kondo and Hayashi, 2013). In these systems, increased compression has been proposed to cause the tissue to buckle upon cell division to relieve pressure. Although highly speculative, it is possible that increased tissue tension in the follicular epithelium upon aPKC inactivation leads to increased compression at the anterior and posterior domains. This could lead to an attempt of the tissue to buckle and invaginate that could be stopped by the presence of a rigid basement membrane (Chen et al., 2019, Tozluoglu and Mao 2020) and lead to cell internalization within the monolayer and beginning

of multilayering. Thus, it would be interesting to characterize better the extent to which the anterior and posterior domains are under compression and how cell division proceeds here.

Science […] never solves a problem without creating 10 more.
George Bernard Shaw in a toast to Albert Einstein

CONCLUSION

In this thesis, I adapted optogenetic tools for protein inactivation to the *Drosophila S2* cell culture system. Furthermore, I applied optogenetic clustering to inactivate the apical polarity kinase aPKC *in vivo* in a *Drosophila* epithelium and observe directly for the first time how an epithelial tissue becomes disorganized. This approach revealed that, surprisingly, loss of epithelial integrity in the follicular epithelium is a fast event triggered by force imbalances that break cell-cell adhesion without loss of apical-basal polarity. The results further show that partial aPKC inactivation does not cause immediate loss of apical-basal polarity, but rather upregulates apical contractility and constriction. Upregulation of apical contractility causes epithelial gaps between dividing and adjacent cells. Thus, this work uncovers a new role for aPKC in downregulating apical actomyosin contractility to balance forces in epithelia and preserve epithelial integrity during proliferation. This provides new insight into how forces in epithelia challenge epithelial integrity and how epithelia coordinate different force-generating events to maintain proper architecture and ensure epithelial functions.

REFERENCES

Abedrabbo, M., and Ravid, S. (2020). Scribble, Lgl1, and myosin II form a complex in vivo to promote directed cell migration. Mol Biol Cell *31*, 2234-2248.

Abrieu, A., Magnaghi-Jaulin, L., Kahana, J.A., Peter, M., Castro, A., Vigneron, S., Lorca, T., Cleveland, D.W., and Labbe, J.C. (2001). Mps1 is a kinetochore-associated kinase essential for the vertebrate mitotic checkpoint. Cell *106*, 83-93.

Acharya, B.R., Nestor-Bergmann, A., Liang, X., Gupta, S., Duszyc, K., Gauquelin, E., Gomez, G.A., Budnar, S., Marcq, P., Jensen, O.E*., et al.* (2018). A Mechanosensitive RhoA Pathway that Protects Epithelia against Acute Tensile Stress. Dev Cell *47*, 439-452 e436.

Acharya, B.R., Wu, S.K., Lieu, Z.Z., Parton, R.G., Grill, S.W., Bershadsky, A.D., Gomez, G.A., and Yap, A.S. (2017). Mammalian Diaphanous 1 Mediates a Pathway for E-cadherin to Stabilize Epithelial Barriers through Junctional Contractility. Cell Rep *18*, 2854-2867.

Achilleos, A., Wehman, A.M., and Nance, J. (2010). PAR-3 mediates the initial clustering and apical localization of junction and polarity proteins during *C. elegans* intestinal epithelial cell polarization. Development *137*, 1833-1842.

Adachi, M., Hamazaki, Y., Kobayashi, Y., Itoh, M., Tsukita, S., Furuse, M., and Tsukita, S. (2009). Similar and distinct properties of MUPP1 and Patj, two homologous PDZ domain-containing tight-junction proteins. Mol Cell Biol *29*, 2372-2389.

Adams, A.E., Johnson, D.I., Longnecker, R.M., Sloat, B.F., and Pringle, J.R. (1990). CDC42 and CDC43, two additional genes involved in budding and the establishment of cell polarity in the yeast Saccharomyces cerevisiae. J Cell Biol *111*, 131-142.

Afonso, O., Matos, I., and Maiato, H. (2014). Spatial control of the anaphase-telophase transition. Cell Cycle *13*, 2985-2986.

Agarwal, P., and Zaidel-Bar, R. (2019). Principles of Actomyosin Regulation In Vivo. Trends Cell Biol *29*, 150-163.

Aguilar-Aragon, M., Bonello, T.T., Bell, G.P., Fletcher, G.C., and Thompson, B.J. (2020). Adherens junction remodelling during mitotic rounding of pseudostratified epithelial cells. EMBO Rep *21*, e49700.

Aguilar-Aragon, M., Elbediwy, A., Foglizzo, V., Fletcher, G.C., Li, V.S.W., and Thompson, B.J. (2018). Pak1 Kinase Maintains Apical Membrane Identity in Epithelia. Cell Rep *22*, 1639-1646.

Aguilar-Aragon, M., Fletcher, G., and Thompson, B.J. (2020). The cytoskeletal motor proteins Dynein and MyoV direct apical transport of Crumbs. Dev Biol *459*, 126-137.

Ahmed, S.M., and Macara, I.G. (2017). The Par3 polarity protein is an exocyst receptor essential for mammary cell survival. Nat Commun *8*, 14867.

Albertson, R., Chabu, C., Sheehan, A., and Doe, C.Q. (2004). Scribble protein domain mapping reveals a multistep localization mechanism and domains necessary for establishing cortical polarity. J Cell Sci *117*, 6061-6070.

Alegot, H., Pouchin, P., Bardot, O., and Mirouse, V. (2018). Jak-Stat pathway induces Drosophila follicle elongation by a gradient of apical contractility. Elife *7*.

Almagor, L., Ufimtsev, I.S., Ayer, A., Li, J., and Weis, W.I. (2019). Structural insights into the aPKC regulatory switch mechanism of the human cell polarity protein lethal giant larvae 2. Proc Natl Acad Sci U S A *116*, 10804-10812.

Amano, M., Ito, M., Kimura, K., Fukata, Y., Chihara, K., Nakano, T., Matsuura, Y., and Kaibuchi, K. (1996). Phosphorylation and activation of myosin by Rho-associated kinase (Rho-kinase). J Biol Chem *271*, 20246-20249.

Angulo-Urarte, A., van der Wal, T., and Huveneers, S. (2020). Cell-cell junctions as sensors and transducers of mechanical forces. Biochim Biophys Acta Biomembr *1862*, 183316.

Armon, S., Bull, M.S., Aranda-Diaz, A., and Prakash, M. (2018). Ultrafast epithelial contractions provide insights into contraction speed limits and tissue integrity. Proc Natl Acad Sci U S A *115*, E10333-E10341.

Arnold, T.R., Stephenson, R.E., and Miller, A.L. (2017). Rho GTPases and actomyosin: Partners in regulating epithelial cell-cell junction structure and function. Exp Cell Res *358*, 20-30.

Aspenstrom, P. (2018). Activated Rho GTPases in Cancer-The Beginning of a New Paradigm. Int J Mol Sci *19*.

Assemat, E., Bazellieres, E., Pallesi-Pocachard, E., Le Bivic, A., and Massey-Harroche, D. (2008). Polarity complex proteins. Biochim Biophys Acta *1778*, 614-630.

Atwood, S.X., and Prehoda, K.E. (2009). aPKC phosphorylates Miranda to polarize fate determinants during neuroblast asymmetric cell division. Curr Biol *19*, 723-729.

Atwood, S.X., Chabu, C., Penkert, R.R., Doe, C.Q., and Prehoda, K.E. (2007). Cdc42 acts downstream of Bazooka to regulate neuroblast polarity through Par-6 aPKC. J Cell Sci *120*, 3200-3206.

Awadia, S., Huq, F., Arnold, T.R., Goicoechea, S.M., Sun, Y.J., Hou, T., Kreider-Letterman, G., Massimi, P., Banks, L., Fuentes, E.J.*, et al.* (2019). SGEF forms a complex with Scribble and Dlg1 and regulates epithelial junctions and contractility. J Cell Biol *218*, 2699-2725.

Azevedo, D., Antunes, M., Prag, S., Ma, X., Hacker, U., Brodland, G.W., Hutson, M.S., Solon, J., and Jacinto, A. (2011). DRhoGEF2 regulates cellular tension and cell pulsations in the Amnioserosa during *Drosophila* dorsal closure. PLoS ONE *6*, e23964.

Bachmann, A., Schneider, M., Theilenberg, E., Grawe, F., and Knust, E. (2001). *Drosophila* Stardust is a partner of Crumbs in the control of epithelial cell polarity. Nature *414*, 638-643.

Bai, X., Lee, P.-Y., Chen, C.-Y., Simmons, J.R., Nebenfuehr, B., Mitchell, D., Klebanow, L.R., Mattson, N., Sorensen Turpin, C.G., Chen, B.-C.*, et al.* (2018). Aurora B is required for programmed variations of cytokinesis during morphogenesis in the C. elegans embryo. bioRxiv, 319657.

Bailey, M.J., and Prehoda, K.E. (2015). Establishment of Par-Polarized Cortical Domains via Phosphoregulated Membrane Motifs. Dev Cell *35*, 199-210.

Baird, M.A., Billington, N., Wang, A., Adelstein, R.S., Sellers, J.R., Fischer, R.S., and Waterman, C.M. (2017). Local pulsatile contractions are an intrinsic property of the myosin 2A motor in the cortical cytoskeleton of adherent cells. Mol Biol Cell *28*, 240-251.

Bajur, A.T., Iyer, K.V., and Knust, E. (2019). Cytocortex-dependent dynamics of *Drosophila* Crumbs controls junctional stability and tension during germ band retraction. J Cell Sci *132*.

Baker, J., and Garrod, D. (1993). Epithelial cells retain junctions during mitosis. J Cell Sci *104 (Pt 2)*, 415-425.

Balaji, R., Weichselberger, V., and Classen, A.K. (2019). Response of Drosophila epithelial cell and tissue shape to external forces in vivo. Development *146*.

Balda, M.S., Whitney, J.A., Flores, C., Gonzalez, S., Cereijido, M., and Matter, K. (1996). Functional dissociation of paracellular permeability and transepithelial electrical resistance and disruption of the apical-basolateral intramembrane diffusion barrier by expression of a mutant tight junction membrane protein. J Cell Biol *134*, 1031-1049.

Balklava, Z., Pant, S., Fares, H., and Grant, B.D. (2007). Genome-wide analysis identifies a general requirement for polarity proteins in endocytic traffic. Nat Cell Biol *9*, 1066-1073.

Ballabio, A., and Bonifacino, J.S. (2020). Lysosomes as dynamic regulators of cell and organismal homeostasis. Nat Rev Mol Cell Biol *21*, 101-118.

Banerjee, S., Sousa, A.D., and Bhat, M.A. (2006). Organization and function of septate junctions: an evolutionary perspective. Cell Biochem Biophys *46*, 65-77.

Banks, L., Pim, D., and Thomas, M. (2012). Human tumour viruses and the deregulation of cell polarity in cancer. Nat Rev Cancer *12*, 877-886.

Basto, R., Lau, J., Vinogradova, T., Gardiol, A., Woods, C.G., Khodjakov, A., and Raff, J.W. (2006). Flies without centrioles. Cell *125*, 1375-1386.

Bastock, R., and St Johnston, D. (2008). *Drosophila* oogenesis. Curr Biol *18*, R1082-1087.

Baumgartner, S., Littleton, J.T., Broadie, K., Bhat, M.A., Harbecke, R., Lengyel, J.A., Chiquet-Ehrismann, R., Prokop, A., and Bellen, H.J. (1996). A *Drosophila* neurexin is required for septate junction and blood-nerve barrier formation and function. Cell *87*, 1059-1068.

Bayraktar, J., Zygmunt, D., and Carthew, R.W. (2006). Par-1 kinase establishes cell polarity and functions in Notch signaling in the *Drosophila* embryo. J Cell Sci *119*, 711-721.

Beach, J.R., Shao, L., Remmert, K., Li, D., Betzig, E., and Hammer, J.A., 3rd (2014). Nonmuscle myosin II isoforms coassemble in living cells. Curr Biol *24*, 1160-1166.

Behr, M., Riedel, D., and Schuh, R. (2003). The claudin-like megatrachea is essential in septate junctions for the epithelial barrier function in *Drosophila*. Dev Cell *5*, 611-620.

Belardi, B., Hamkins-Indik, T., Harris, A.R., Kim, J., Xu, K., and Fletcher, D.A. (2020). A Weak Link with Actin Organizes Tight Junctions to Control Epithelial Permeability. Dev Cell *54*, 792-804 e797.

Bell, G.P., Fletcher, G.C., Brain, R., and Thompson, B.J. (2015). Aurora kinases phosphorylate Lgl to induce mitotic spindle orientation in Drosophila epithelia. Curr Biol *25*, 61-68.

Benton, R., and St Johnston, D. (2003). A conserved oligomerization domain in *drosophila* Bazooka/PAR-3 is important for apical localization and epithelial polarity. Curr Biol *13*, 1330-1334.

Bergstralh, D.T., Lovegrove, H.E., and St Johnston, D. (2013). Discs large links spindle orientation to apical-basal polarity in Drosophila epithelia. Curr Biol *23*, 1707-1712.

Bergstralh, D.T., Lovegrove, H.E., and St Johnston, D. (2015). Lateral adhesion drives reintegration of misplaced cells into epithelial monolayers. Nat Cell Biol *17*, 1497-1503.

Bergstralh, D.T., Lovegrove, H.E., Kujawiak, I., Dawney, N.S., Zhu, J., Cooper, S., Zhang, R., and St Johnston, D. (2016). Pins is not required for spindle orientation in the Drosophila wing disc. Development *143*, 2573-2581.

Bernabe-Rubio, M., Andres, G., Casares-Arias, J., Fernandez-Barrera, J., Rangel, L., Reglero-Real, N., Gershlick, D.C., Fernandez, J.J., Millan, J., Correas, I.*, et al.* (2016). Novel role for the midbody in primary ciliogenesis by polarized epithelial cells. The Journal of cell biology *214*, 259-273.

Berns, N., Woichansky, I., Friedrichsen, S., Kraft, N., and Riechmann, V. (2014). A genome-scale in vivo RNAi analysis of epithelial development in Drosophila identifies new proliferation domains outside of the stem cell niche. J Cell Sci *127*, 2736-2748.

Betschinger, J., Mechtler, K., and Knoblich, J.A. (2003). The Par complex directs asymmetric cell division by phosphorylating the cytoskeletal protein Lgl. Nature *422*, 326-330.

Bettencourt-Dias, M., Giet, R., Sinka, R., Mazumdar, A., Lock, W.G., Balloux, F., Zafiropoulos, P.J., Yamaguchi, S., Winter, S., Carthew, R.W.*, et al.* (2004). Genome-wide survey of protein kinases required for cell cycle progression. Nature *432*, 980-987.

Biehler, C., Rothenberg, K.E., Jetté, A., Gaudé, H.-M., Fernandez-Gonzalez, R., and Laprise, P. (2021). Pak1 and PP2A antagonize aPKC function to support cortical tension induced by the Crumbs-Yurt complex. bioRxiv, 2021.01.05.425461

Bilder, D. (2004). Epithelial polarity and proliferation control: links from the *Drosophila* neoplastic tumor suppressors. Genes Dev *18*, 1909-1925.

Bilder, D., and Haigo, S.L. (2012). Expanding the morphogenetic repertoire: perspectives from the Drosophila egg. Dev Cell *22*, 12-23.

Bilder, D., and Perrimon, N. (2000). Localization of apical epithelial determinants by the basolateral PDZ protein Scribble. Nature *403*, 676-680.

Bilder, D., Li, M., and Perrimon, N. (2000). Cooperative regulation of cell polarity and growth by Drosophila tumor suppressors. Science *289*, 113-116.

Bilder, D., Schober, M., and Perrimon, N. (2003). Integrated activity of PDZ protein complexes regulates epithelial polarity. Nat Cell Biol *5*, 53-58.

Blanchoin, L., Amann, K.J., Higgs, H.N., Marchand, J.B., Kaiser, D.A., and Pollard, T.D. (2000). Direct observation of dendritic actin filament networks nucleated by Arp2/3 complex and WASP/Scar proteins. Nature *404*, 1007-1011.

Boeda, B., and Etienne-Manneville, S. (2015). Spectrin binding motifs regulate Scribble cortical dynamics and polarity function. Elife *4*.

Boettner, B., and Van Aelst, L. (2002). The role of Rho GTPases in disease development. Gene *286*, 155-174.

Bonello, T.T., and Peifer, M. (2019). Scribble: A master scaffold in polarity, adhesion, synaptogenesis, and proliferation. J Cell Biol *218*, 742-756.

Bonello, T.T., Choi, W., and Peifer, M. (2019). Scribble and Discs-large direct initial assembly and positioning of adherens junctions during the establishment of apical-basal polarity. Development *146*.

Borreguero-Munoz, N., Fletcher, G.C., Aguilar-Aragon, M., Elbediwy, A., Vincent-Mistiaen, Z.I., and Thompson, B.J. (2019). The Hippo pathway integrates PI3K-Akt signals with mechanical and polarity cues to control tissue growth. PLoS Biol *17*, e3000509.

Borrmann, C.M., Grund, C., Kuhn, C., Hofmann, I., Pieperhoff, S., and Franke, W.W. (2006). The area composita of adhering junctions connecting heart muscle cells of vertebrates. II. Colocalizations of desmosomal and fascia adhaerens molecules in the intercalated disk. Eur J Cell Biol *85*, 469-485.

Bos, J.L., Rehmann, H., and Wittinghofer, A. (2007). GEFs and GAPs: critical elements in the control of small G proteins. Cell *129*, 865-877.

Bosveld, F., Markova, O., Guirao, B., Martin, C., Wang, Z., Pierre, A., Balakireva, M., Gaugue, I., Ainslie, A., Christophorou, N.*, et al.* (2016). Epithelial tricellular junctions act as interphase cell shape sensors to orient mitosis. Nature *530*, 495-498.

Bourdages, K.G., Lacroix, B., Dorn, J.F., Descovich, C.P., and Maddox, A.S. (2014). Quantitative analysis of cytokinesis in situ during C. elegans postembryonic development. PLoS ONE *9*, e110689.

Brajenovic, M., Joberty, G., Kuster, B., Bouwmeester, T., and Drewes, G. (2004). Comprehensive proteomic analysis of human Par protein complexes reveals an interconnected protein network. J Biol Chem *279*, 12804-12811.

Brasch, J., Harrison, O.J., Honig, B., and Shapiro, L. (2012). Thinking outside the cell: how cadherins drive adhesion. Trends Cell Biol *22*, 299-310.

Bryant, D.M., Datta, A., Rodriguez-Fraticelli, A.E., Peranen, J., Martin-Belmonte, F., and Mostov, K.E. (2010). A molecular network for de novo generation of the apical surface and lumen. Nat Cell Biol *12*, 1035-1045.

Buckley, C.D., Tan, J., Anderson, K.L., Hanein, D., Volkmann, N., Weis, W.I., Nelson, W.J., and Dunn, A.R. (2014). Cell adhesion. The minimal cadherin-catenin complex binds to actin filaments under force. Science *346*, 1254211.

Buckley, C.E., Ren, X., Ward, L.C., Girdler, G.C., Araya, C., Green, M.J., Clark, B.S., Link, B.A., and Clarke, J.D. (2013). Mirror-symmetric microtubule assembly and cell interactions drive lumen formation in the zebrafish neural rod. EMBO J *32*, 30-44.

Bugaj, L.J., Choksi, A.T., Mesuda, C.K., Kane, R.S., and Schaffer, D.V. (2013). Optogenetic protein clustering and signaling activation in mammalian cells. Nat Methods *10*, 249-252.

Bunker, B.D., Nellimoottil, T.T., Boileau, R.M., Classen, A.K., and Bilder, D. (2015). The transcriptional response to tumorigenic polarity loss in *Drosophila*. Elife *4*.

Burute, M., Prioux, M., Blin, G., Truchet, S., Letort, G., Tseng, Q., Bessy, T., Lowell, S., Young, J., Filhol, O.*, et al.* (2017). Polarity Reversal by Centrosome Repositioning Primes Cell Scattering during Epithelial-to-Mesenchymal Transition. Dev Cell *40*, 168-184.

Buszczak, M., Paterno, S., Lighthouse, D., Bachman, J., Planck, J., Owen, S., Skora, A.D., Nystul, T.G., Ohlstein, B., Allen, A.*, et al.* (2007). The carnegie protein trap library: a versatile tool for Drosophila developmental studies. Genetics *175*, 1505-1531.

Butler, M.T., and Wallingford, J.B. (2017). Planar cell polarity in development and disease. Nat Rev Mol Cell Biol *18*, 375-388.

Bynum, W.F. (2008). The history of medicine: a very short introduction (Oxford: Oxford University Press).

Campanale, J.P., Sun, T.Y., and Montell, D.J. (2017). Development and dynamics of cell polarity at a glance. J Cell Sci *130*, 1201-1207.

Campbell, K., Knust, E., and Skaer, H. (2009). Crumbs stabilises epithelial polarity during tissue remodelling. J Cell Sci *122*, 2604-2612.

Campellone, K.G., and Welch, M.D. (2010). A nucleator arms race: cellular control of actin assembly. Nat Rev Mol Cell Biol *11*, 237-251.

Campinho, P., Behrndt, M., Ranft, J., Risler, T., Minc, N., and Heisenberg, C.P. (2013). Tension-oriented cell divisions limit anisotropic tissue tension in epithelial spreading during zebrafish epiboly. Nat Cell Biol *15*, 1405-1414.

Cao, H., Xu, R., Shi, Q., Zhang, D., Huang, J., and Hong, Y. (2017). FERM domain phosphorylation and endogenous 3'UTR are not essential for regulating the function and subcellular localization of polarity protein Crumbs. J Genet Genomics *44*, 409-412.

Carlsson, A.E. (2006). Stimulation of actin polymerization by filament severing. Biophys J *90*, 413-422.

Carroll, T.D., Langlands, A.J., Osborne, J.M., Newton, I.P., Appleton, P.L., and Nathke, I. (2017). Interkinetic nuclear migration and basal tethering facilitates post-mitotic daughter separation in intestinal organoids. J Cell Sci *130*, 3862-3877.

Cartagena-Rivera, A.X., Van Itallie, C.M., Anderson, J.M., and Chadwick, R.S. (2017). Apical surface supracellular mechanical properties in polarized epithelium using noninvasive acoustic force spectroscopy. Nat Commun *8*, 1030.

Carvalho, C.A., Moreira, S., Ventura, G., Sunkel, C.E., and Morais-de-Sa, E. (2015). Aurora A Triggers Lgl Cortical Release during Symmetric Division to Control Planar Spindle Orientation. Curr Biol *25*, 53-60.

Cetera, M., Lewellyn, L., and Horne-Badovinac, S. (2016). Cultivation and Live Imaging of Drosophila Ovaries. Methods Mol Biol *1478*, 215-226.

Chalmers, A.D., Pambos, M., Mason, J., Lang, S., Wylie, C., and Papalopulu, N. (2005). aPKC, Crumbs3 and Lgl2 control apicobasal polarity in early vertebrate development. Development *132*, 977-986.

Chandran, R., Kale, G., Philippe, J.M., Lecuit, T., and Mayor, S. (2021). Distinct actin-dependent nanoscale assemblies underlie the dynamic and hierarchical organization of E-cadherin. Curr Biol.

Charrier, L.E., Loie, E., and Laprise, P. (2015). Mouse Crumbs3 sustains epithelial tissue morphogenesis in vivo. Sci Rep *5*, 17699.

Chartier, F.J., Hardy, E.J., and Laprise, P. (2011). Crumbs controls epithelial integrity by inhibiting Rac1 and PI3K. J Cell Sci *124*, 3393-3398.

Chastney, M.R., Conway, J.R.W., and Ivaska, J. (2021). Integrin adhesion complexes. Curr Biol *31*, R536-R542.

Chen, B., Zheng, B., DeRan, M., Jarugumilli, G.K., Fu, J., Brooks, Y.S., and Wu, X. (2016). ZDHHC7-mediated S-palmitoylation of Scribble regulates cell polarity. Nat Chem Biol *12*, 686-693.

Chen, C.L., Gajewski, K.M., Hamaratoglu, F., Bossuyt, W., Sansores-Garcia, L., Tao, C., and Halder, G. (2010). The apical-basal cell polarity determinant Crumbs regulates Hippo signaling in *Drosophila*. Proc Natl Acad Sci U S A *107*, 15810-15815.

Chen, D.Y., Crest, J., Streichan, S.J., and Bilder, D. (2019). Extracellular matrix stiffness cues junctional remodeling for 3D tissue elongation. Nat Commun *10*, 3339.

Chen, J., Sayadian, A.C., Lowe, N., Lovegrove, H.E., and St Johnston, D. (2018). An alternative mode of epithelial polarity in the *Drosophila* midgut. PLoS Biol *16*, e3000041.

Chen, X., and Macara, I.G. (2005). Par-3 controls tight junction assembly through the Rac exchange factor Tiam1. Nat Cell Biol *7*, 262-269.

Chen, X., and Macara, I.G. (2006). Par-3 mediates the inhibition of LIM kinase 2 to regulate cofilin phosphorylation and tight junction assembly. J Cell Biol *172*, 671-678.

Cherfils, J., and Zeghouf, M. (2013). Regulation of small GTPases by GEFs, GAPs, and GDIs. Physiol Rev *93*, 269-309.

Chiou, J.G., Balasubramanian, M.K., and Lew, D.J. (2017). Cell Polarity in Yeast. Annu Rev Cell Dev Biol *33*, 77-101.

Choi, J., Troyanovsky, R.B., Indra, I., Mitchell, B.J., and Troyanovsky, S.M. (2019). Scribble, Erbin, and Lano redundantly regulate epithelial polarity and apical adhesion complex. J Cell Biol *218*, 2277-2293.

Christodoulou, N., and Skourides, P.A. (2015). Cell-Autonomous Ca(2+) Flashes Elicit Pulsed Contractions of an Apical Actin Network to Drive Apical Constriction during Neural Tube Closure. Cell Rep *13*, 2189-2202.

Chugh, P., and Paluch, E.K. (2018). The actin cortex at a glance. J Cell Sci *131*.

Citi, S. (2019). The mechanobiology of tight junctions. Biophys Rev *11*, 783-793.

Claret, S., Jouette, J., Benoit, B., Legent, K., and Guichet, A. (2014). PI(4,5)P2 produced by the PI4P5K SKTL controls apical size by tethering PAR-3 in *Drosophila* epithelial cells. Curr Biol *24*, 1071-1079.

Clift, D., McEwan, W.A., Labzin, L.I., Konieczny, V., Mogessie, B., James, L.C., and Schuh, M. (2017). A Method for the Acute and Rapid Degradation of Endogenous Proteins. Cell *171*, 1692-1706 e1618.

Conde, C., Osswald, M., Barbosa, J., Moutinho-Santos, T., Pinheiro, D., Guimaraes, S., Matos, I., Maiato, H., and Sunkel, C.E. (2013). *Drosophila* Polo regulates the spindle assembly checkpoint through Mps1-dependent BubR1 phosphorylation. EMBO J *32*, 1761-1777.

Coopman, P., and Djiane, A. (2016). Adherens Junction and E-Cadherin complex regulation by epithelial polarity. Cell Mol Life Sci *73*, 3535-3553.

Coravos, J.S., and Martin, A.C. (2016). Apical Sarcomere-like Actomyosin Contracts Nonmuscle *Drosophila* Epithelial Cells. Dev Cell *39*, 346-358.

Cox, R.T., Kirkpatrick, C., and Peifer, M. (1996). Armadillo is required for adherens junction assembly, cell polarity, and morphogenesis during *Drosophila* embryogenesis. J Cell Biol *134*, 133-148.

Craig, R., Smith, R., and Kendrick-Jones, J. (1983). Light-chain phosphorylation controls the conformation of vertebrate non-muscle and smooth muscle myosin molecules. Nature *302*, 436-439.

Crest, J., Diz-Munoz, A., Chen, D.Y., Fletcher, D.A., and Bilder, D. (2017). Organ sculpting by patterned extracellular matrix stiffness. Elife *6*.

Cunha-Silva, S., Osswald, M., Goemann, J., Barbosa, J., Santos, L.M., Resende, P., Bange, T., Ferras, C., Sunkel, C.E., and Conde, C. (2020). Mps1-mediated release of Mad1 from nuclear pores ensures the fidelity of chromosome segregation. J Cell Biol *219*.

D'Avino, P.P., Giansanti, M.G., and Petronczki, M. (2015). Cytokinesis in animal cells. Cold Spring Harb Perspect Biol *7*, a015834.

Dagliyan, O., Dokholyan, N.V., and Hahn, K.M. (2019). Engineering proteins for allosteric control by light or ligands. Nat Protoc *14*, 1863-1883.

Dagliyan, O., Tarnawski, M., Chu, P.H., Shirvanyants, D., Schlichting, I., Dokholyan, N.V., and Hahn, K.M. (2016). Engineering extrinsic disorder to control protein activity in living cells. Science *354*, 1441-1444.

Daniel, E., Daude, M., Kolotuev, I., Charish, K., Auld, V., and Le Borgne, R. (2018). Coordination of Septate Junctions Assembly and Completion of Cytokinesis in Proliferative Epithelial Tissues. Curr Biol *28*, 1380-1391 e1384.

Dauber, A., Golzio, C., Guenot, C., Jodelka, F.M., Kibaek, M., Kjaergaard, S., Leheup, B., Martinet, D., Nowaczyk, M.J., Rosenfeld, J.A.*, et al.* (2013). SCRIB and PUF60 are primary drivers of the multisystemic phenotypes of the 8q24.3 copy-number variant. Am J Hum Genet *93*, 798-811.

David, D.J., Tishkina, A., and Harris, T.J. (2010). The PAR complex regulates pulsed actomyosin contractions during amnioserosa apical constriction in *Drosophila*. Development *137*, 1645-1655.

David, D.J., Wang, Q., Feng, J.J., and Harris, T.J. (2013). Bazooka inhibits aPKC to limit antagonism of actomyosin networks during amnioserosa apical constriction. Development *140*, 4719-4729.

Dawes-Hoang, R.E., Parmar, K.M., Christiansen, A.E., Phelps, C.B., Brand, A.H., and Wieschaus, E.F. (2005). folded gastrulation, cell shape change and the control of myosin localization. Development *132*, 4165-4178.

de Vreede, G., Schoenfeld, J.D., Windler, S.L., Morrison, H., Lu, H., and Bilder, D. (2014). The Scribble module regulates retromer-dependent endocytic trafficking during epithelial polarization. Development *141*, 2796-2802.

Dehapiot, B., Clement, R., Alegot, H., Gazso-Gerhat, G., Philippe, J.M., and Lecuit, T. (2020). Assembly of a persistent apical actin network by the formin Frl/Fmnl tunes epithelial cell deformability. Nat Cell Biol *22*, 791-802.

Delva, E., Tucker, D.K., and Kowalczyk, A.P. (2009). The desmosome. Cold Spring Harb Perspect Biol *1*, a002543.

Deng, W., Bates, J.A., Wei, H., Bartoschek, M.D., Conradt, B., and Leonhardt, H. (2020). Tunable light and drug induced depletion of target proteins. Nat Commun *11*, 304.

Dettmer, J., and Friml, J. (2011). Cell polarity in plants: when two do the same, it is not the same. Curr Opin Cell Biol *23*, 686-696.

Devergne, O., Tsung, K., Barcelo, G., and Schupbach, T. (2014). Polarized deposition of basement membrane proteins depends on Phosphatidylinositol synthase and the levels of Phosphatidylinositol 4,5-bisphosphate. Proc Natl Acad Sci U S A *111*, 7689-7694.

Dias Gomes, M., and Iden, S. (2021). Orchestration of tissue-scale mechanics and fate decisions by polarity signalling. EMBO J, e106787.

Dias Gomes, M., Letzian, S., Saynisch, M., and Iden, S. (2019). Polarity signaling ensures epidermal homeostasis by coupling cellular mechanics and genomic integrity. Nat Commun *10*, 3362.

Diaz-Diaz, C., Baonza, G., and Martin-Belmonte, F. (2020). The vertebrate epithelial apical junctional complex: Dynamic interplay between Rho GTPase activity and cell polarization processes. Biochim Biophys Acta Biomembr *1862*, 183398.

Dickinson, D.J., Schwager, F., Pintard, L., Gotta, M., and Goldstein, B. (2017). A Single-Cell Biochemistry Approach Reveals PAR Complex Dynamics during Cell Polarization. Dev Cell *42*, 416-434 e411.

Diekmann, Y., and Pereira-Leal, J.B. (2013). Evolution of intracellular compartmentalization. Biochem J *449*, 319-331.

Doerflinger, H., Benton, R., Shulman, J.M., and St Johnston, D. (2003). The role of PAR-1 in regulating the polarised microtubule cytoskeleton in the *Drosophila* follicular epithelium. Development *130*, 3965-3975.

Doerflinger, H., Vogt, N., Torres, I.L., Mirouse, V., Koch, I., Nusslein-Volhard, C., and St Johnston, D. (2010). Bazooka is required for polarisation of the *Drosophila* anterior-posterior axis. Development *137*, 1765-1773.

Dong, W., Lu, J., Zhang, X., Wu, Y., Lettieri, K., Hammond, G.R., and Hong, Y. (2020). A polybasic domain in aPKC mediates Par6-dependent control of membrane targeting and kinase activity. J Cell Biol *219*.

Dong, W., Zhang, X., Liu, W., Chen, Y.J., Huang, J., Austin, E., Celotto, A.M., Jiang, W.Z., Palladino, M.J., Jiang, Y.*, et al.* (2015). A conserved polybasic domain mediates plasma membrane targeting of Lgl and its regulation by hypoxia. J Cell Biol *211*, 273-286.

Dorland, Y.L., and Huveneers, S. (2017). Cell-cell junctional mechanotransduction in endothelial remodeling. Cell Mol Life Sci *74*, 279-292.

Duan, L., Hope, J., Ong, Q., Lou, H.Y., Kim, N., McCarthy, C., Acero, V., Lin, M.Z., and Cui, B. (2017). Understanding CRY2 interactions for optical control of intracellular signaling. Nat Commun *8*, 547.

Duda, M., Kirkland, N.J., Khalilgharibi, N., Tozluoglu, M., Yuen, A.C., Carpi, N., Bove, A., Piel, M., Charras, G., Baum, B.*, et al.* (2019). Polarization of Myosin II Refines Tissue Material Properties to Buffer Mechanical Stress. Dev Cell *48*, 245-260 e247.

Durney, C.H., Harris, T.J.C., and Feng, J.J. (2018). Dynamics of PAR Proteins Explain the Oscillation and Ratcheting Mechanisms in Dorsal Closure. Biophys J *115*, 2230-2241.

Eaton, S., and Martin-Belmonte, F. (2014). Cargo sorting in the endocytic pathway: a key regulator of cell polarity and tissue dynamics. Cold Spring Harb Perspect Biol *6*, a016899.

Ebnet, K., Suzuki, A., Horikoshi, Y., Hirose, T., Meyer Zu Brickwedde, M.K., Ohno, S., and Vestweber, D. (2001). The cell polarity protein ASIP/PAR-3 directly associates with junctional adhesion molecule (JAM). EMBO J *20*, 3738-3748.

Eden, S., Rohatgi, R., Podtelejnikov, A.V., Mann, M., and Kirschner, M.W. (2002). Mechanism of regulation of WAVE1-induced actin nucleation by Rac1 and Nck. Nature *418*, 790-793.

Elbediwy, A., Vincent-Mistiaen, Z.I., and Thompson, B.J. (2016). YAP and TAZ in epithelial stem cells: A sensor for cell polarity, mechanical forces and tissue damage. Bioessays *38*, 644-653.

Elbediwy, A., Zhang, Y., Cobbaut, M., Riou, P., Tan, R.S., Roberts, S.K., Tynan, C., George, R., Kjaer, S., Martin-Fernandez, M.L.*, et al.* (2019). The Rho family GEF FARP2 is activated by aPKCiota to control tight junction formation and polarity. J Cell Sci *132*.

Ennomani, H., Letort, G., Guerin, C., Martiel, J.L., Cao, W., Nedelec, F., De La Cruz, E.M., Thery, M., and Blanchoin, L. (2016). Architecture and Connectivity Govern Actin Network Contractility. Curr Biol *26*, 616-626.

Erami, Z., Timpson, P., Yao, W., Zaidel-Bar, R., and Anderson, K.I. (2015). There are four dynamically and functionally distinct populations of E-cadherin in cell junctions. Biol Open *4*, 1481-1489.

Etienne-Manneville, S., and Hall, A. (2001). Integrin-mediated activation of Cdc42 controls cell polarity in migrating astrocytes through PKCzeta. Cell *106*, 489-498.

Etienne-Manneville, S., and Hall, A. (2002). Rho GTPases in cell biology. Nature *420*, 629-635.

Etournay, R., Popovic, M., Merkel, M., Nandi, A., Blasse, C., Aigouy, B., Brandl, H., Myers, G., Salbreux, G., Julicher, F.*, et al.* (2015). Interplay of cell dynamics and epithelial tension during morphogenesis of the Drosophila pupal wing. Elife *4*, e07090.

Even-Faitelson, L., and Ravid, S. (2006). PAK1 and aPKCzeta regulate myosin II-B phosphorylation: a novel signaling pathway regulating filament assembly. Mol Biol Cell *17*, 2869-2881.

Farquhar, M.G., and Palade, G.E. (1963). Junctional complexes in various epithelia. J Cell Biol *17*, 375-412.

Farrell, J.A., Shermoen, A.W., Yuan, K., and O'Farrell, P.H. (2012). Embryonic onset of late replication requires Cdc25 down-regulation. Genes Dev *26*, 714-725.

Fehon, R.G., McClatchey, A.I., and Bretscher, A. (2010). Organizing the cell cortex: the role of ERM proteins. Nat Rev Mol Cell Biol *11*, 276-287.

Feldman, J.L., and Priess, J.R. (2012). A role for the centrosome and PAR-3 in the hand-off of MTOC function during epithelial polarization. Curr Biol *22*, 575-582.

Feng, W., Wu, H., Chan, L.N., and Zhang, M. (2007). The Par-3 NTD adopts a PB1-like structure required for Par-3 oligomerization and membrane localization. EMBO J *26*, 2786-2796.

Feng, W., Wu, H., Chan, L.N., and Zhang, M. (2008). Par-3-mediated junctional localization of the lipid phosphatase PTEN is required for cell polarity establishment. J Biol Chem *283*, 23440-23449.

Fenix, A.M., Taneja, N., Buttler, C.A., Lewis, J., Van Engelenburg, S.B., Ohi, R., and Burnette, D.T. (2016). Expansion and concatenation of non-muscle myosin IIA filaments drive cellular contractile system formation during interphase and mitosis. Mol Biol Cell.

Ferrell, J.E., Jr. (2002). Self-perpetuating states in signal transduction: positive feedback, double-negative feedback and bistability. Curr Opin Cell Biol *14*, 140-148.

Fic, W., Bastock, R., Raimondi, F., Los, E., Inoue, Y., Gallop, J.L., Russell, R.B., and St Johnston, D. (2021). RhoGAP19D inhibits Cdc42 laterally to control epithelial cell shape and prevent invasion. J Cell Biol *220*.

Finegan, T.M., Na, D., Cammarota, C., Skeeters, A.V., Nadasi, T.J., Dawney, N.S., Fletcher, A.G., Oakes, P.W., and Bergstralh, D.T. (2019). Tissue tension and not interphase cell shape determines cell division orientation in the Drosophila follicular epithelium. EMBO J *38*.

Firmino, J., Rocancourt, D., Saadaoui, M., Moreau, C., and Gros, J. (2016). Cell Division Drives Epithelial Cell Rearrangements during Gastrulation in Chick. Dev Cell *36*, 249-261.

Fletcher, G.C., Lucas, E.P., Brain, R., Tournier, A., and Thompson, B.J. (2012). Positive feedback and mutual antagonism combine to polarize Crumbs in the *Drosophila* follicle cell epithelium. Curr Biol *22*, 1116-1122.

Flores-Benitez, D., and Knust, E. (2015). Crumbs is an essential regulator of cytoskeletal dynamics and cell-cell adhesion during dorsal closure in Drosophila. Elife *4*.

Flores-Benitez, D., and Knust, E. (2016). Dynamics of epithelial cell polarity in Drosophila: how to regulate the regulators? Curr Opin Cell Biol *42*, 13-21.

Fogg, V.C., Liu, C.J., and Margolis, B. (2005). Multiple regions of Crumbs3 are required for tight junction formation in MCF10A cells. J Cell Sci *118*, 2859-2869.

Fomicheva, M., Tross, E.M., and Macara, I.G. (2020). Polarity proteins in oncogenesis. Curr Opin Cell Biol *62*, 26-30.

Forteza, R., Figueroa, Y., Mashukova, A., Dulam, V., and Salas, P.J. (2016). Conditional knockout of polarity complex (atypical) PKCiota reveals an anti-inflammatory function mediated by NF-kappaB. Mol Biol Cell *27*, 2186-2197.

Founounou, N., Loyer, N., and Le Borgne, R. (2013). Septins Regulate the Contractility of the Actomyosin Ring to Enable Adherens Junction Remodeling during Cytokinesis of Epithelial Cells. Dev Cell *24*, 242-255.

Franco, M., and Carmena, A. (2019). Eph signaling controls mitotic spindle orientation and cell proliferation in neuroepithelial cells. J Cell Biol *218*, 1200-1217.

Franke, W.W. (2009). Discovering the molecular components of intercellular junctions--a historical view. Cold Spring Harb Perspect Biol *1*, a003061.

Franz, A., and Riechmann, V. (2010). Stepwise polarisation of the *Drosophila* follicular epithelium. Dev Biol *338*, 136-147.

Freddo, A.M., Shoffner, S.K., Shao, Y., Taniguchi, K., Grosse, A.S., Guysinger, M.N., Wang, S., Rudraraju, S., Margolis, B., Garikipati, K.*, et al.* (2016). Coordination of signaling and tissue mechanics during morphogenesis of murine intestinal villi: a role for mitotic cell rounding. Integr Biol (Camb) *8*, 918-928.

Fremont, S., and Echard, A. (2018). Membrane Traffic in the Late Steps of Cytokinesis. Curr Biol *28*, R458-R470.

Fricke, R., Gohl, C., Dharmalingam, E., Grevelhorster, A., Zahedi, B., Harden, N., Kessels, M., Qualmann, B., and Bogdan, S. (2009). *Drosophila* Cip4/Toca-1 integrates membrane trafficking and actin dynamics through WASP and SCAR/WAVE. Curr Biol *19*, 1429-1437.

Gamblin, C.L., Hardy, E.J., Chartier, F.J., Bisson, N., and Laprise, P. (2014). A bidirectional antagonism between aPKC and Yurt regulates epithelial cell polarity. J Cell Biol *204*, 487-495.

Gamblin, C.L., Parent-Prevost, F., Jacquet, K., Biehler, C., Jette, A., and Laprise, P. (2018). Oligomerization of the FERM-FA protein Yurt controls epithelial cell polarity. J Cell Biol *217*, 3853-3862.

Garcia De Las Bayonas, A., Philippe, J.M., Lellouch, A.C., and Lecuit, T. (2019). Distinct RhoGEFs Activate Apical and Junctional Contractility under Control of G Proteins during Epithelial Morphogenesis. Curr Biol *29*, 3370-3385 e3377.

Garcia-Mata, R., Boulter, E., and Burridge, K. (2011). The 'invisible hand': regulation of RHO GTPases by RHOGDIs. Nat Rev Mol Cell Biol *12*, 493-504.

Garcia, M.A., Nelson, W.J., and Chavez, N. (2018). Cell-Cell Junctions Organize Structural and Signaling Networks. Cold Spring Harb Perspect Biol *10*.

Gassama-Diagne, A., Yu, W., ter Beest, M., Martin-Belmonte, F., Kierbel, A., Engel, J., and Mostov, K. (2006). Phosphatidylinositol-3,4,5-trisphosphate regulates the formation of the basolateral plasma membrane in epithelial cells. Nat Cell Biol *8*, 963-970.

Gateff, E. (1978). The genetics and epigenetics of neoplasms in *Drosophila*. Biol Rev Camb Philos Soc *53*, 123-168.

Genova, J.L., and Fehon, R.G. (2003). Neuroglian, Gliotactin, and the Na+/K+ ATPase are essential for septate junction function in *Drosophila*. J Cell Biol *161*, 979-989.

Georgiou, M., Marinari, E., Burden, J., and Baum, B. (2008). Cdc42, Par6, and aPKC regulate Arp2/3-mediated endocytosis to control local adherens junction stability. Curr Biol *18*, 1631-1638.

Gerdes, J.M., Davis, E.E., and Katsanis, N. (2009). The vertebrate primary cilium in development, homeostasis, and disease. Cell *137*, 32-45.

Gilmour, D., Rembold, M., and Leptin, M. (2017). From morphogen to morphogenesis and back. Nature *541*, 311-320.

Glanc, M., Fendrych, M., and Friml, J. (2018). Mechanistic framework for cell-intrinsic re-establishment of PIN2 polarity after cell division. Nat Plants *4*, 1082-1088.

Godard, B.G., Dumollard, R., Munro, E., Chenevert, J., Hebras, C., McDougall, A., and Heisenberg, C.P. (2020). Apical Relaxation during Mitotic Rounding Promotes Tension-Oriented Cell Division. Dev Cell *55*, 695-706 e694.

Goehring, N.W., Trong, P.K., Bois, J.S., Chowdhury, D., Nicola, E.M., Hyman, A.A., and Grill, S.W. (2011). Polarization of PAR proteins by advective triggering of a pattern-forming system. Science *334*, 1137-1141.

Golub, O., Wee, B., Newman, R.A., Paterson, N.M., and Prehoda, K.E. (2017). Activation of Discs large by aPKC aligns the mitotic spindle to the polarity axis during asymmetric cell division. Elife *6*.

Goransson, O., Deak, M., Wullschleger, S., Morrice, N.A., Prescott, A.R., and Alessi, D.R. (2006). Regulation of the polarity kinases PAR-1/MARK by 14-3-3 interaction and phosphorylation. J Cell Sci *119*, 4059-4070.

Gorfinkiel, N. (2016). From actomyosin oscillations to tissue-level deformations. Dev Dyn *245*, 268-275.

Goshima, G., Wollman, R., Goodwin, S.S., Zhang, N., Scholey, J.M., Vale, R.D., and Stuurman, N. (2007). Genes required for mitotic spindle assembly in *Drosophila* S2 cells. Science *316*, 417-421.

Graybill, C., Wee, B., Atwood, S.X., and Prehoda, K.E. (2012). Partitioning-defective protein 6 (Par-6) activates atypical protein kinase C (aPKC) by pseudosubstrate displacement. J Biol Chem *287*, 21003-21011.

Green, K.J., Jaiganesh, A., and Broussard, J.A. (2019). Desmosomes: Essential contributors to an integrated intercellular junction network. F1000Res *8*.

Green, K.J., Roth-Carter, Q., Niessen, C.M., and Nichols, S.A. (2020). Tracing the Evolutionary Origin of Desmosomes. Curr Biol *30*, R535-R543.

Green, R.A., Paluch, E., and Oegema, K. (2012). Cytokinesis in Animal Cells. Annu Rev Cell Dev Biol *28*, 29-58.

Green, R.A., Paluch, E., and Oegema, K. (2012). Cytokinesis in animal cells. Annu Rev Cell Dev Biol *28*, 29-58.

Grifoni, D., Garoia, F., Bellosta, P., Parisi, F., De Biase, D., Collina, G., Strand, D., Cavicchi, S., and Pession, A. (2007). aPKCzeta cortical loading is associated with Lgl cytoplasmic release and tumor growth in *Drosophila* and human epithelia. Oncogene *26*, 5960-5965.

Grosshans, J., and Wieschaus, E. (2000). A genetic link between morphogenesis and cell division during formation of the ventral furrow in Drosophila. Cell *101*, 523-531.

Grzeschik, N.A., Parsons, L.M., Allott, M.L., Harvey, K.F., and Richardson, H.E. (2010). Lgl, aPKC, and Crumbs regulate the Salvador/Warts/Hippo pathway through two distinct mechanisms. Curr Biol *20*, 573-581.

Gubieda, A.G., Packer, J.R., Squires, I., Martin, J., and Rodriguez, J. (2020). Going with the flow: insights from Caenorhabditis elegans zygote polarization. Philos Trans R Soc Lond B Biol Sci *375*, 20190555.

Guglielmi, G., Barry, J.D., Huber, W., and De Renzis, S. (2015). An Optogenetic Method to Modulate Cell Contractility during Tissue Morphogenesis. Developmental cell *35*, 646-660.

Guglielmi, G., Falk, H.J., and De Renzis, S. (2016). Optogenetic Control of Protein Function: From Intracellular Processes to Tissue Morphogenesis. Trends Cell Biol *26*, 864-874.

Guilgur, L.G., Prudencio, P., Ferreira, T., Pimenta-Marques, A.R., and Martinho, R.G. (2012). *Drosophila* aPKC is required for mitotic spindle orientation during symmetric division of epithelial cells. Development *139*, 503-513.

Guillot, C., and Lecuit, T. (2013). Adhesion disengagement uncouples intrinsic and extrinsic forces to drive cytokinesis in epithelial tissues. Dev Cell *24*, 227-241.

Guillot, C., and Lecuit, T. (2013). Mechanics of epithelial tissue homeostasis and morphogenesis. Science (New York, NY) *340*, 1185-1189.

Guirao, B., Rigaud, S.U., Bosveld, F., Bailles, A., Lopez-Gay, J., Ishihara, S., Sugimura, K., Graner, F., and Bellaiche, Y. (2015). Unified quantitative characterization of epithelial tissue development. Elife *4*.

Gul, I.S., Hulpiau, P., Saeys, Y., and van Roy, F. (2017). Evolution and diversity of cadherins and catenins. Exp Cell Res *358*, 3-9.

Guntas, G., Hallett, R.A., Zimmerman, S.P., Williams, T., Yumerefendi, H., Bear, J.E., and Kuhlman, B. (2015). Engineering an improved light-induced dimer (iLID) for controlling the localization and activity of signaling proteins. Proc Natl Acad Sci U S A *112*, 112-117.

Guo, Z., Neilson, L.J., Zhong, H., Murray, P.S., Zanivan, S., and Zaidel-Bar, R. (2014). E-cadherin interactome complexity and robustness resolved by quantitative proteomics. Sci Signal *7*, rs7.

Gupta, T., and Schupbach, T. (2003). Cct1, a phosphatidylcholine biosynthesis enzyme, is required for Drosophila oogenesis and ovarian morphogenesis. Development *130*, 6075-6087.

Gupta, V.K., Nam, S., Yim, D., Camuglia, J., Martin, J.L., Sanders, E.N., O'Brien, L.E., Martin, A.C., Kim, T., Chaudhuri O. (2021). The nature of cell division forces in epithelial monolayers. J Cell Biol 220 (8): e202011106.

Hagios, C., Lochter, A., and Bissell, M.J. (1998). Tissue architecture: the ultimate regulator of epithelial function? Philos Trans R Soc Lond B Biol Sci *353*, 857-870.

Hakanen, J., Ruiz-Reig, N., and Tissir, F. (2019). Linking Cell Polarity to Cortical Development and Malformations. Front Cell Neurosci *13*, 244.

Halaoui, R., and McCaffrey, L. (2015). Rewiring cell polarity signaling in cancer. Oncogene *34*, 939-950.

Halaoui, R., Rejon, C., Chatterjee, S.J., Szymborski, J., Meterissian, S., Muller, W.J., Omeroglu, A., and McCaffrey, L. (2017). Progressive polarity loss and luminal collapse disrupt tissue organization in carcinoma. Genes Dev *31*, 1573-1587.

Hall, A. (1998). Rho GTPases and the actin cytoskeleton. Science *279*, 509-514.

Hall, A. (2012). Rho family GTPases. Biochem Soc Trans *40*, 1378-1382.

Hannaford, M., Loyer, N., Tonelli, F., Zoltner, M., and Januschke, J. (2019). A chemical-genetics approach to study the role of atypical Protein Kinase C in Drosophila. Development *146*.

Hannaford, M., Loyer, N., Tonelli, F., Zoltner, M., and Januschke, J. (2019). A chemical-genetics approach to study the role of atypical Protein Kinase C in Drosophila. Development *146*.

Hao, Y., Du, Q., Chen, X., Zheng, Z., Balsbaugh, J.L., Maitra, S., Shabanowitz, J., Hunt, D.F., and Macara, I.G. (2010). Par3 controls epithelial spindle orientation by aPKC-mediated phosphorylation of apical Pins. Curr Biol *20*, 1809-1818.

Harden, N., Ricos, M., Yee, K., Sanny, J., Langmann, C., Yu, H., Chia, W., and Lim, L. (2002). Drac1 and Crumbs participate in amnioserosa morphogenesis during dorsal closure in *Drosophila*. J Cell Sci *115*, 2119-2129.

Harris, T.J., and Peifer, M. (2004). Adherens junction-dependent and -independent steps in the establishment of epithelial cell polarity in *Drosophila*. J Cell Biol *167*, 135-147.

Harris, T.J., and Peifer, M. (2005). The positioning and segregation of apical cues during epithelial polarity establishment in *Drosophila*. J Cell Biol *170*, 813-823.

Harris, T.J., and Peifer, M. (2007). aPKC controls microtubule organization to balance adherens junction symmetry and planar polarity during development. Dev Cell *12*, 727-738.

Harris, T.J., and Tepass, U. (2010). Adherens junctions: from molecules to morphogenesis. Nat Rev Mol Cell Biol *11*, 502-514.

Harrison, O.J., Bahna, F., Katsamba, P.S., Jin, X., Brasch, J., Vendome, J., Ahlsen, G., Carroll, K.J., Price, S.R., Honig, B.*, et al.* (2010). Two-step adhesive binding by classical cadherins. Nat Struct Mol Biol *17*, 348-357.

Harrison, O.J., Jin, X., Hong, S., Bahna, F., Ahlsen, G., Brasch, J., Wu, Y., Vendome, J., Felsovalyi, K., Hampton, C.M.*, et al.* (2011). The extracellular architecture of adherens junctions revealed by crystal structures of type I cadherins. Structure *19*, 244-256.

Hartmann, J., Krueger, D., and De Renzis, S. (2020). Using optogenetics to tackle systems-level questions of multicellular morphogenesis. Curr Opin Cell Biol *66*, 19-27.

Haruta, T., Warrior, R., Yonemura, S., and Oda, H. (2010). The proximal half of the *Drosophila* E-cadherin extracellular region is dispensable for many cadherin-dependent events but required for ventral furrow formation. Genes Cells *15*, 193-208.

Hatte, G., Prigent, C., and Tassan, J.P. (2018). Tight junctions negatively regulate mechanical forces applied to adherens junctions in vertebrate epithelial tissue. J Cell Sci *131*.

Hatte, G., Prigent, C., and Tassan, J.P. (2018). Tight junctions negatively regulate mechanical forces applied to adherens junctions in vertebrate epithelial tissue. J Cell Sci *131*.

Hatzfeld, M., Keil, R., and Magin, T.M. (2017). Desmosomes and Intermediate Filaments: Their Consequences for Tissue Mechanics. Cold Spring Harb Perspect Biol *9*.

Hava, D., Forster, U., Matsuda, M., Cui, S., Link, B.A., Eichhorst, J., Wiesner, B., Chitnis, A., and Abdelilah-Seyfried, S. (2009). Apical membrane maturation and cellular rosette formation during morphogenesis of the zebrafish lateral line. J Cell Sci *122*, 687-695.

Hayase, J., Kamakura, S., Iwakiri, Y., Yamaguchi, Y., Izaki, T., Ito, T., and Sumimoto, H. (2013). The WD40 protein Morg1 facilitates Par6-aPKC binding to Crb3 for apical identity in epithelial cells. J Cell Biol *200*, 635-650.

Hayes, P., and Solon, J. (2017). *Drosophila* dorsal closure: An orchestra of forces to zip shut the embryo. Mech Dev *144*, 2-10.

He, L., Wang, X., Tang, H.L., and Montell, D.J. (2010). Tissue elongation requires oscillating contractions of a basal actomyosin network. Nat Cell Biol *12*, 1133-1142.

He, L., Wang, X., Tang, H.L., and Montell, D.J. (2010). Tissue elongation requires oscillating contractions of a basal actomyosin network. Nat Cell Biol *12*, 1133-1142.

Heck, B.W., and Devenport, D. (2017). Trans-endocytosis of Planar Cell Polarity Complexes during Cell Division. Curr Biol *27*, 3725-3733 e3724.

Heer, N.C., and Martin, A.C. (2017). Tension, contraction and tissue morphogenesis. Development *144*, 4249-4260.

Heigwer, F., Port, F., and Boutros, M. (2018). RNA Interference (RNAi) Screening in *Drosophila*. Genetics *208*, 853-874.

Heisenberg, C.-P., and Bellaiche, Y. (2013). Forces in tissue morphogenesis and patterning. Cell *153*, 948-962.

Hendrick, J., Franz-Wachtel, M., Moeller, Y., Schmid, S., Macek, B., and Olayioye, M.A. (2016). The polarity protein Scribble positions DLC3 at adherens junctions to regulate Rho signaling. J Cell Sci *129*, 3583-3596.

Henle, J. (1837). Symbolae ad anatomiam villorum intestinalium, imprimis eorum epithelii et vasorum lacteorum. Commentatio academica (Berolini: A. Hirschwald,), pp. vi, 37 pages.

Henle, J. (1841). Allgemeine Anatomie: Lehre von den Mischungs- und Formbestandtheilen des menschlichen Körpers (Leipzig: Verlag von Leopold Voss).

Heo, W.D., Inoue, T., Park, W.S., Kim, M.L., Park, B.O., Wandless, T.J., and Meyer, T. (2006). PI(3,4,5)P3 and PI(4,5)P2 lipids target proteins with polybasic clusters to the plasma membrane. Science *314*, 1458-1461.

Herbomel, G., Hatte, G., Roul, J., Padilla-Parra, S., Tassan, J.P., and Tramier, M. (2017). Actomyosin-generated tension on cadherin is similar between dividing and non-dividing epithelial cells in early Xenopus laevis embryos. Sci Rep *7*, 45058.

Herszterg, S., Leibfried, A., Bosveld, F., Martin, C., and Bellaiche, Y. (2013). Interplay between the dividing cell and its neighbors regulates adherens junction formation during cytokinesis in epithelial tissue. Dev Cell *24*, 256-270.

Herszterg, S., Pinheiro, D., and Bellaiche, Y. (2014). A multicellular view of cytokinesis in epithelial tissue. Trends Cell Biol *24*, 285-293.

Higashi, T., Arnold, T.R., Stephenson, R.E., Dinshaw, K.M., and Miller, A.L. (2016). Maintenance of the Epithelial Barrier and Remodeling of Cell-Cell Junctions during Cytokinesis. Curr Biol *26*, 1829-1842.

Hirano, Y., Yoshinaga, S., Takeya, R., Suzuki, N.N., Horiuchi, M., Kohjima, M., Sumimoto, H., and Inagaki, F. (2005). Structure of a cell polarity regulator, a complex between atypical PKC and Par6 PB1 domains. J Biol Chem *280*, 9653-9661.

Hirano, Y., Yoshinaga, S., Takeya, R., Suzuki, N.N., Horiuchi, M., Kohjima, M., Sumimoto, H., and Inagaki, F. (2005). Structure of a cell polarity regulator, a complex between atypical PKC and Par6 PB1 domains. J Biol Chem *280*, 9653-9661.

Hirose, T., Karasawa, M., Sugitani, Y., Fujisawa, M., Akimoto, K., Ohno, S., and Noda, T. (2006). PAR3 is essential for cyst-mediated epicardial development by establishing apical cortical domains. Development *133*, 1389-1398.

Hiruma, Y., Sacristan, C., Pachis, S.T., Adamopoulos, A., Kuijt, T., Ubbink, M., von Castelmur, E., Perrakis, A., and Kops, G.J. (2015). Competition between MPS1 and microtubules at kinetochores regulates spindle checkpoint signaling. Science *348*, 1264-1267.

Hodge, R.G., and Ridley, A.J. (2016). Regulating Rho GTPases and their regulators. Nat Rev Mol Cell Biol *17*, 496-510.

Hoege, C., and Hyman, A.A. (2013). Principles of PAR polarity in Caenorhabditis elegans embryos. Nat Rev Mol Cell Biol *14*, 315-322.

Hoijman, E., Rubbini, D., Colombelli, J., and Alsina, B. (2015). Mitotic cell rounding and epithelial thinning regulate lumen growth and shape. Nat Commun *6*, 7355.

Holly, R.W., and Prehoda, K.E. (2019). Phosphorylation of Par-3 by Atypical Protein Kinase C and Competition between Its Substrates. Dev Cell *49*, 678-679.

Holly, R.W., Jones, K., and Prehoda, K.E. (2020). A Conserved PDZ-Binding Motif in aPKC Interacts with Par-3 and Mediates Cortical Polarity. Curr Biol *30*, 893-898 e895.

Homem, C.C., and Peifer, M. (2008). Diaphanous regulates myosin and adherens junctions to control cell contractility and protrusive behavior during morphogenesis. Development *135*, 1005-1018.

Hong, S., Troyanovsky, R.B., and Troyanovsky, S.M. (2013). Binding to F-actin guides cadherin cluster assembly, stability, and movement. J Cell Biol *201*, 131-143.

Hong, Y. (2018). aPKC: the Kinase that Phosphorylates Cell Polarity. F1000Res *7*.

Hong, Y., Stronach, B., Perrimon, N., Jan, L.Y., and Jan, Y.N. (2001). *Drosophila* Stardust interacts with Crumbs to control polarity of epithelia but not neuroblasts. Nature *414*, 634-638.

Honig, B., and Shapiro, L. (2020). Adhesion Protein Structure, Molecular Affinities, and Principles of Cell-Cell Recognition. Cell *181*, 520-535.

Horikoshi, Y., Suzuki, A., Yamanaka, T., Sasaki, K., Mizuno, K., Sawada, H., Yonemura, S., and Ohno, S. (2009). Interaction between PAR-3 and the aPKC-PAR-6 complex is indispensable for apical domain development of epithelial cells. J Cell Sci *122*, 1595-1606.

Horne-Badovinac, S., Lin, D., Waldron, S., Schwarz, M., Mbamalu, G., Pawson, T., Jan, Y., Stainier, D.Y., and Abdelilah-Seyfried, S. (2001). Positional cloning of heart and soul reveals multiple roles for PKC lambda in zebrafish organogenesis. Curr Biol *11*, 1492-1502.

Horwitz, A.R. (2012). The origins of the molecular era of adhesion research. Nat Rev Mol Cell Biol *13*, 805-811.

Huang, J., Huang, L., Chen, Y.J., Austin, E., Devor, C.E., Roegiers, F., and Hong, Y. (2011). Differential regulation of adherens junction dynamics during apical-basal polarization. J Cell Sci *124*, 4001-4013.

Huang, J., Zhou, W., Dong, W., Watson, A.M., and Hong, Y. (2009). From the Cover: Directed, efficient, and versatile modifications of the Drosophila genome by genomic engineering. Proc Natl Acad Sci U S A *106*, 8284-8289.

Huang, J., Zhou, W., Dong, W., Watson, A.M., and Hong, Y. (2009). From the Cover: Directed, efficient, and versatile modifications of the Drosophila genome by genomic engineering. Proc Natl Acad Sci U S A *106*, 8284-8289.

Hung, T.J., and Kemphues, K.J. (1999). PAR-6 is a conserved PDZ domain-containing protein that colocalizes with PAR-3 in Caenorhabditis elegans embryos. Development *126*, 127-135.

Hurd, T.W., Fan, S., Liu, C.J., Kweon, H.K., Hakansson, K., and Margolis, B. (2003a). Phosphorylation-dependent binding of 14-3-3 to the polarity protein Par3 regulates cell polarity in mammalian epithelia. Curr Biol *13*, 2082-2090.

Hurd, T.W., Gao, L., Roh, M.H., Macara, I.G., and Margolis, B. (2003b). Direct interaction of two polarity complexes implicated in epithelial tight junction assembly. Nat Cell Biol *5*, 137-142.

Hurov, J.B., Watkins, J.L., and Piwnica-Worms, H. (2004). Atypical PKC phosphorylates PAR-1 kinases to regulate localization and activity. Curr Biol *14*, 736-741.

Hutterer, A., Betschinger, J., Petronczki, M., and Knoblich, J.A. (2004). Sequential roles of Cdc42, Par-6, aPKC, and Lgl in the establishment of epithelial polarity during *Drosophila* embryogenesis. Dev Cell *6*, 845-854.

Hyman, A.A., Weber, C.A., and Julicher, F. (2014). Liquid-liquid phase separation in biology. Annu Rev Cell Dev Biol *30*, 39-58.

Iden, S., Misselwitz, S., Peddibhotla, S.S., Tuncay, H., Rehder, D., Gerke, V., Robenek, H., Suzuki, A., and Ebnet, K. (2012). aPKC phosphorylates JAM-A at Ser285 to promote cell contact maturation and tight junction formation. J Cell Biol *196*, 623-639.

Iden, S., van Riel, W.E., Schafer, R., Song, J.Y., Hirose, T., Ohno, S., and Collard, J.G. (2012). Tumor type-dependent function of the par3 polarity protein in skin tumorigenesis. Cancer Cell *22*, 389-403.

Imai, F., Hirai, S., Akimoto, K., Koyama, H., Miyata, T., Ogawa, M., Noguchi, S., Sasaoka, T., Noda, T., and Ohno, S. (2006). Inactivation of aPKClambda results in the loss of adherens junctions in neuroepithelial cells without affecting neurogenesis in mouse neocortex. Development *133*, 1735-1744.

Inaba, M., and Yamashita, Y.M. (2012). Asymmetric stem cell division: precision for robustness. Cell Stem Cell *11*, 461-469.

Indra, I., Choi, J., Chen, C.S., Troyanovsky, R.B., Shapiro, L., Honig, B., and Troyanovsky, S.M. (2018). Spatial and temporal organization of cadherin in punctate adherens junctions. Proc Natl Acad Sci U S A *115*, E4406-E4415.

Indra, I., Troyanovsky, R.B., Shapiro, L., Honig, B., and Troyanovsky, S.M. (2020). Sensing Actin Dynamics through Adherens Junctions. Cell Rep *30*, 2820-2833 e2823.

Ishiuchi, T., and Takeichi, M. (2011). Willin and Par3 cooperatively regulate epithelial apical constriction through aPKC-mediated ROCK phosphorylation. Nat Cell Biol *13*, 860-866.

Itoh, M., Sasaki, H., Furuse, M., Ozaki, H., Kita, T., and Tsukita, S. (2001). Junctional adhesion molecule (JAM) binds to PAR-3: a possible mechanism for the recruitment of PAR-3 to tight junctions. J Cell Biol *154*, 491-497.

Izaddoost, S., Nam, S.C., Bhat, M.A., Bellen, H.J., and Choi, K.W. (2002). *Drosophila* Crumbs is a positional cue in photoreceptor adherens junctions and rhabdomeres. Nature *416*, 178-183.

Izquierdo, E., Quinkler, T., and De Renzis, S. (2018). Guided morphogenesis through optogenetic activation of Rho signalling during early Drosophila embryogenesis. Nat Commun *9*, 2366.

Izumi, Y., and Furuse, M. (2014). Molecular organization and function of invertebrate occluding junctions. Semin Cell Dev Biol *36*, 186-193.

Izumi, Y., Hirose, T., Tamai, Y., Hirai, S., Nagashima, Y., Fujimoto, T., Tabuse, Y., Kemphues, K.J., and Ohno, S. (1998). An atypical PKC directly associates and colocalizes at the epithelial tight junction with ASIP, a mammalian homologue of Caenorhabditis elegans polarity protein PAR-3. J Cell Biol *143*, 95-106.

Jaffe, A.B., and Hall, A. (2005). Rho GTPases: biochemistry and biology. Annu Rev Cell Dev Biol *21*, 247-269.

Jeanes, A., Gottardi, C.J., and Yap, A.S. (2008). Cadherins and cancer: how does cadherin dysfunction promote tumor progression? Oncogene *27*, 6920-6929.

Jelluma, N., Dansen, T.B., Sliedrecht, T., Kwiatkowski, N.P., and Kops, G.J. (2010). Release of Mps1 from kinetochores is crucial for timely anaphase onset. J Cell Biol *191*, 281-290.

Jenkins, G.W., and Tortora, G.J. (2013). Anatomy and physiology: from science to life (Hoboken, NJ : Wiley).

Ji, Z., Gao, H., and Yu, H. (2015). Kinetochore attachment sensed by competitive Mps1 and microtubule binding to Ndc80C. Science *348*, 1260-1264.

Jia, D., Xu, Q., Xie, Q., Mio, W., and Deng, W.M. (2016). Automatic stage identification of Drosophila egg chamber based on DAPI images. Sci Rep *6*, 18850.

Jiang, T., McKinley, R.F., McGill, M.A., Angers, S., and Harris, T.J. (2015). A Par-1-Par-3-Centrosome Cell Polarity Pathway and Its Tuning for Isotropic Cell Adhesion. Curr Biol *25*, 2701-2708.

Jin, X., Walker, M.A., Felsovalyi, K., Vendome, J., Bahna, F., Mannepalli, S., Cosmanescu, F., Ahlsen, G., Honig, B., and Shapiro, L. (2012). Crystal structures of *Drosophila* N-cadherin ectodomain regions reveal a widely used class of Ca(2)+-free interdomain linkers. Proc Natl Acad Sci U S A *109*, E127-134.

Jinguji, Y., and Ishikawa, H. (1992). Electron microscopic observations on the maintenance of the tight junction during cell division in the epithelium of the mouse small intestine. Cell Struct Funct *17*, 27-37.

Joberty, G., Petersen, C., Gao, L., and Macara, I.G. (2000). The cell-polarity protein Par6 links Par3 and atypical protein kinase C to Cdc42. Nat Cell Biol *2*, 531-539.

Johnson, H.E., and Toettcher, J.E. (2019). Signaling Dynamics Control Cell Fate in the Early Drosophila Embryo. Dev Cell *48*, 361-370 e363.

Johnston, C.A., Hirono, K., Prehoda, K.E., and Doe, C.Q. (2009). Identification of an Aurora-A/PinsLINKER/Dlg spindle orientation pathway using induced cell polarity in S2 cells. Cell *138*, 1150-1163.

Jolly, A.L., Luan, C.H., Dusel, B.E., Dunne, S.F., Winding, M., Dixit, V.J., Robins, C., Saluk, J.L., Logan, D.J., Carpenter, A.E.*, et al.* (2016). A Genome-wide RNAi Screen for Microtubule Bundle Formation and Lysosome Motility Regulation in Drosophila S2 Cells. Cell Rep *14*, 611-620.

Jones, M.C., Askari, J.A., Humphries, J.D., and Humphries, M.J. (2018). Cell adhesion is regulated by CDK1 during the cell cycle. J Cell Biol.

Jossin, Y., Lee, M., Klezovitch, O., Kon, E., Cossard, A., Lien, W.H., Fernandez, T.E., Cooper, J.A., and Vasioukhin, V. (2017). Llgl1 Connects Cell Polarity with Cell-Cell Adhesion in Embryonic Neural Stem Cells. Dev Cell *41*, 481-495 e485.

Jouette, J., Guichet, A., and Claret, S.B. (2019). Dynein-mediated transport and membrane trafficking control PAR3 polarised distribution. Elife *8*.

Jung, H.S., Komatsu, S., Ikebe, M., and Craig, R. (2008). Head-head and head-tail interaction: a general mechanism for switching off myosin II activity in cells. Mol Biol Cell *19*, 3234-3242.

Jung, H.Y., Fattet, L., Tsai, J.H., Kajimoto, T., Chang, Q., Newton, A.C., and Yang, J. (2019). Apical-basal polarity inhibits epithelial-mesenchymal transition and tumour metastasis by PAR-complex-mediated SNAI1 degradation. Nat Cell Biol *21*, 359-371.

Kale, G.R., Yang, X., Philippe, J.M., Mani, M., Lenne, P.F., and Lecuit, T. (2018). Distinct contributions of tensile and shear stress on E-cadherin levels during morphogenesis. Nat Commun *9*, 5021.

Kannan, N., and Tang, V.W. (2015). Synaptopodin couples epithelial contractility to alpha-actinin-4-dependent junction maturation. J Cell Biol *211*, 407-434.

Kasza, K.E., Farrell, D.L., and Zallen, J.A. (2014). Spatiotemporal control of epithelial remodeling by regulated myosin phosphorylation. Proc Natl Acad Sci U S A *111*, 11732-11737.

Kechagia, J.Z., Ivaska, J., and Roca-Cusachs, P. (2019). Integrins as biomechanical sensors of the microenvironment. Nat Rev Mol Cell Biol *20*, 457-473.

Kemphues, K.J., Kusch, M., and Wolf, N. (1988a). Maternal-effect lethal mutations on linkage group II of Caenorhabditis elegans. Genetics *120*, 977-986.

Kemphues, K.J., Priess, J.R., Morton, D.G., and Cheng, N.S. (1988b). Identification of genes required for cytoplasmic localization in early *C. elegans* embryos. Cell *52*, 311-320.

Kennedy, M.J., Hughes, R.M., Peteya, L.A., Schwartz, J.W., Ehlers, M.D., and Tucker, C.L. (2010). Rapid blue-light-mediated induction of protein interactions in living cells. Nat Methods *7*, 973-975.

Kerfeld, C.A., Aussignargues, C., Zarzycki, J., Cai, F., and Sutter, M. (2018). Bacterial microcompartments. Nat Rev Microbiol *16*, 277-290.

Kerridge, S., Munjal, A., Philippe, J.M., Jha, A., de las Bayonas, A.G., Saurin, A.J., and Lecuit, T. (2016). Modular activation of Rho1 by GPCR signalling imparts polarized myosin II activation during morphogenesis. Nat Cell Biol *18*, 261-270.

Khalilgharibi, N., Fouchard, J., Asadipour, N., Barrientos, R., Duda, M., Bonfanti, A., Yonis, A., Harris, A., Mosaffa, P., Fujita, Y.*, et al.* (2019). Stress relaxation in epithelial monolayers is controlled by the actomyosin cortex. Nat Phys *15*, 839-847.

Khoury, M.J., and Bilder, D. (2020). Distinct activities of Scrib module proteins organize epithelial polarity. Proc Natl Acad Sci U S A *117*, 11531-11540.

Kiesslich, R., Goetz, M., Angus, E.M., Hu, Q., Guan, Y., Potten, C., Allen, T., Neurath, M.F., Shroyer, N.F., Montrose, M.H.*, et al.* (2007). Identification of epithelial gaps in human small and large intestine by confocal endomicroscopy. Gastroenterology *133*, 1769-1778.

Kim, S., Gailite, I., Moussian, B., Luschnig, S., Goette, M., Fricke, K., Honemann-Capito, M., Grubmuller, H., and Wodarz, A. (2009). Kinase-activity-independent functions of atypical protein kinase C in *Drosophila*. J Cell Sci *122*, 3759-3771.

Kim, T.J., Zheng, S., Sun, J., Muhamed, I., Wu, J., Lei, L., Kong, X., Leckband, D.E., and Wang, Y. (2015). Dynamic visualization of alpha-catenin reveals rapid, reversible conformation switching between tension states. Curr Biol *25*, 218-224.

Kimura, K., Ito, M., Amano, M., Chihara, K., Fukata, Y., Nakafuku, M., Yamamori, B., Feng, J., Nakano, T., Okawa, K*., et al.* (1996). Regulation of myosin phosphatase by Rho and Rho-associated kinase (Rho-kinase). Science *273*, 245-248.

King, R.C. (1970). The meiotic behavior of the Drosophila oocyte. Int Rev Cytol *28*, 125-168.

Kinne-Saffran, E., and Kinne, R.K. (1994). Jacob Henle: the kidney and beyond. Am J Nephrol *14*, 355-360.

Kishikawa, M., Suzuki, A., and Ohno, S. (2008). aPKC enables development of zonula adherens by antagonizing centripetal contraction of the circumferential actomyosin cables. J Cell Sci *121*, 2481-2492.

Klebes, A., and Knust, E. (2000). A conserved motif in Crumbs is required for E-cadherin localisation and zonula adherens formation in *Drosophila*. Curr Biol *10*, 76-85.

Klinkert, K., Rocancourt, M., Houdusse, A., and Echard, A. (2016). Rab35 GTPase couples cell division with initiation of epithelial apico-basal polarity and lumen opening. Nat Commun *7*, 11166.

Klose, S., Flores-Benitez, D., Riedel, F., and Knust, E. (2013). Fosmid-based structure-function analysis reveals functionally distinct domains in the cytoplasmic domain of *Drosophila* crumbs. G3 (Bethesda) *3*, 153-165.

Knouse, K.A., Lopez, K.E., Bachofner, M., and Amon, A. (2018). Chromosome Segregation Fidelity in Epithelia Requires Tissue Architecture. Cell *175*, 200-211 e213.

Ko, C.S., Kalakuntla, P., and Martin, A.C. (2020). Apical Constriction Reversal upon Mitotic Entry Underlies Different Morphogenetic Outcomes of Cell Division. Mol Biol Cell *31*, 1663-1674.

Koch, L., Feicht, S., Sun, R., Sen, A., and Krahn, M.P. (2016). Domain-specific functions of Stardust in *Drosophila* embryonic development. R Soc Open Sci *3*, 160776.

Koenderink, G.H., and Paluch, E.K. (2018). Architecture shapes contractility in actomyosin networks. Curr Opin Cell Biol *50*, 79-85.

Kofron, M., Spagnuolo, A., Klymkowsky, M., Wylie, C., and Heasman, J. (1997). The roles of maternal alpha-catenin and plakoglobin in the early Xenopus embryo. Development *124*, 1553-1560.

Kolsch, V., Seher, T., Fernandez-Ballester, G.J., Serrano, L., and Leptin, M. (2007). Control of *Drosophila* gastrulation by apical localization of adherens junctions and RhoGEF2. Science *315*, 384-386.

Kondo, T., and Hayashi, S. (2013). Mitotic cell rounding accelerates epithelial invagination. Nature *494*, 125-129.

Korotkevich, E., Niwayama, R., Courtois, A., Friese, S., Berger, N., Buchholz, F., and Hiiragi, T. (2017). The Apical Domain Is Required and Sufficient for the First Lineage Segregation in the Mouse Embryo. Dev Cell *40*, 235-247 e237.

Kosodo, Y., Toida, K., Dubreuil, V., Alexandre, P., Schenk, J., Kiyokage, E., Attardo, A., Mora-Bermudez, F., Arii, T., Clarke, J.D*., et al.* (2008). Cytokinesis of neuroepithelial cells can divide their basal process before anaphase. Embo J *27*, 3151-3163.

Kovacs, E.M., Verma, S., Ali, R.G., Ratheesh, A., Hamilton, N.A., Akhmanova, A., and Yap, A.S. (2011). N-WASP regulates the epithelial junctional actin cytoskeleton through a non-canonical post-nucleation pathway. Nat Cell Biol *13*, 934-943.

Kozma, R., Ahmed, S., Best, A., and Lim, L. (1995). The Ras-related protein Cdc42Hs and bradykinin promote formation of peripheral actin microspikes and filopodia in Swiss 3T3 fibroblasts. Mol Cell Biol *15*, 1942-1952.

Krahn, M.P. (2020). Phospholipids of the Plasma Membrane - Regulators or Consequence of Cell Polarity? Front Cell Dev Biol *8*, 277.

Krahn, M.P., Buckers, J., Kastrup, L., and Wodarz, A. (2010a). Formation of a Bazooka-Stardust complex is essential for plasma membrane polarity in epithelia. J Cell Biol *190*, 751-760.

Krahn, M.P., Egger-Adam, D., and Wodarz, A. (2009). PP2A antagonizes phosphorylation of Bazooka by PAR-1 to control apical-basal polarity in dividing embryonic neuroblasts. Dev Cell *16*, 901-908.

Krahn, M.P., Klopfenstein, D.R., Fischer, N., and Wodarz, A. (2010b). Membrane targeting of Bazooka/PAR-3 is mediated by direct binding to phosphoinositide lipids. Curr Biol *20*, 636-642.

Kroll, J.R., Remmelzwaal, S., and Boxem, M. (2021). CeLINC, a fluorescence-based protein-protein interaction assay in C. elegans. bioRxiv, 2021.2006.2001.446599.

Krueger, D., Pallares Cartes, C., Makaske, T., and De Renzis, S. (2020). betaH-spectrin is required for ratcheting apical pulsatile constrictions during tissue invagination. EMBO Rep *21*, e49858.

Krueger, D., Tardivo, P., Nguyen, C., and De Renzis, S. (2018). Downregulation of basal myosin-II is required for cell shape changes and tissue invagination. EMBO J *37*.

Krummel, M.F., and Macara, I. (2006). Maintenance and modulation of T cell polarity. Nat Immunol *7*, 1143-1149.

Kuhn, S., and Geyer, M. (2014). Formins as effector proteins of Rho GTPases. Small GTPases *5*, e29513.

Kullmann, L., and Krahn, M.P. (2018). Redundant regulation of localization and protein stability of DmPar3. Cell Mol Life Sci *75*, 3269-3282.

Kunzelmann, S., Bottcher, R., Schmidts, I., and Forstemann, K. (2016). A Comprehensive Toolbox for Genome Editing in Cultured *Drosophila* melanogaster Cells. G3 (Bethesda) *6*, 1777-1785.

Kusakabe, M., and Nishida, E. (2004). The polarity-inducing kinase Par-1 controls Xenopus gastrulation in cooperation with 14-3-3 and aPKC. EMBO J *23*, 4190-4201.

Kwon, M., Godinho, S.A., Chandhok, N.S., Ganem, N.J., Azioune, A., Thery, M., and Pellman, D. (2008). Mechanisms to suppress multipolar divisions in cancer cells with extra centrosomes. Genes Dev *22*, 2189-2203.

Lam, M.S.Y., Lisica, A., Ramkumar, N., Hunter, G., Mao, Y., Charras, G., and Baum, B. (2020). Isotropic myosin-generated tissue tension is required for the dynamic orientation of the mitotic spindle. Mol Biol Cell *31*, 1370-1379.

Laprise, P., Beronja, S., Silva-Gagliardi, N.F., Pellikka, M., Jensen, A.M., McGlade, C.J., and Tepass, U. (2006). The FERM protein Yurt is a negative regulatory component of the Crumbs complex that controls epithelial polarity and apical membrane size. Dev Cell *11*, 363-374.

Laprise, P., Lau, K.M., Harris, K.P., Silva-Gagliardi, N.F., Paul, S.M., Beronja, S., Beitel, G.J., McGlade, C.J., and Tepass, U. (2009). Yurt, Coracle, Neurexin IV and the Na(+),K(+)-ATPase form a novel group of epithelial polarity proteins. Nature *459*, 1141-1145.

Laprise, P., Viel, A., and Rivard, N. (2004). Human homolog of disc-large is required for adherens junction assembly and differentiation of human intestinal epithelial cells. J Biol Chem *279*, 10157-10166.

Larue, L., Ohsugi, M., Hirchenhain, J., and Kemler, R. (1994). E-cadherin null mutant embryos fail to form a trophectoderm epithelium. Proc Natl Acad Sci U S A *91*, 8263-8267.

Lattner, J., Leng, W., Knust, E., Brankatschk, M., and Flores-Benitez, D. (2019). Crumbs organizes the transport machinery by regulating apical levels of PI(4,5)P2 in *Drosophila*. Elife *8*.

Lau, K., Tao, H., Liu, H., Wen, J., Sturgeon, K., Sorfazlian, N., Lazic, S., Burrows, J.T., Wong, M.D., Li, D.*, et al.* (2015). Anisotropic stress orients remodelling of mammalian limb bud ectoderm. Nat Cell Biol *17*, 569-579.

Lecuit, T., and Yap, A.S. (2015). E-cadherin junctions as active mechanical integrators in tissue dynamics. Nat Cell Biol *17*, 533-539.

Lecuit, T., Lenne, P.-F., and Munro, E. (2011). Force generation, transmission, and integration during cell and tissue morphogenesis. Annu Rev Cell Dev Biol *27*, 157-184.

Lee, S., Park, H., Kyung, T., Kim, N.Y., Kim, S., Kim, J., and Heo, W.D. (2014). Reversible protein inactivation by optogenetic trapping in cells. Nat Methods *11*, 633-636.

Leerberg, J.M., Gomez, G.A., Verma, S., Moussa, E.J., Wu, S.K., Priya, R., Hoffman, B.D., Grashoff, C., Schwartz, M.A., and Yap, A.S. (2014). Tension-sensitive actin assembly supports contractility at the epithelial zonula adherens. Curr Biol *24*, 1689-1699.

Legouis, R., Jaulin-Bastard, F., Schott, S., Navarro, C., Borg, J.P., and Labouesse, M. (2003). Basolateral targeting by leucine-rich repeat domains in epithelial cells. EMBO Rep *4*, 1096-1102.

Leibfried, A., Fricke, R., Morgan, M.J., Bogdan, S., and Bellaiche, Y. (2008). *Drosophila* Cip4 and WASp define a branch of the Cdc42-Par6-aPKC pathway regulating E-cadherin endocytosis. Curr Biol *18*, 1639-1648.

Lemmers, C., Michel, D., Lane-Guermonprez, L., Delgrossi, M.H., Medina, E., Arsanto, J.P., and Le Bivic, A. (2004). CRB3 binds directly to Par6 and regulates the morphogenesis of the tight junctions in mammalian epithelial cells. Mol Biol Cell *15*, 1324-1333.

Letizia, A., Ricardo, S., Moussian, B., Martin, N., and Llimargas, M. (2013). A functional role of the extracellular domain of Crumbs in cell architecture and apicobasal polarity. J Cell Sci *126*, 2157-2163.

Letizia, A., Sotillos, S., Campuzano, S., and Llimargas, M. (2011). Regulated Crb accumulation controls apical constriction and invagination in *Drosophila* tracheal cells. J Cell Sci *124*, 240-251.

Letort, G., Ennomani, H., Gressin, L., Thery, M., and Blanchoin, L. (2015). Dynamic reorganization of the actin cytoskeleton. F1000Res *4*.

Lewis, F.T., and Stöhr, P. (1913). A text-book of histology arranged upon an embryological basis (Philadelphia: P. Blakiston,), pp. xi, 539 pages.

Leys, S.P., and Riesgo, A. (2012). Epithelia, an evolutionary novelty of metazoans. J Exp Zool B Mol Dev Evol *318*, 438-447.

Li, C., Wen, A., Shen, B., Lu, J., Huang, Y., and Chang, Y. (2011a). FastCloning: a highly simplified, purification-free, sequence- and ligation-independent PCR cloning method. BMC Biotechnol *11*, 92.

Li, F., and Higgs, H.N. (2003). The mouse Formin mDia1 is a potent actin nucleation factor regulated by autoinhibition. Curr Biol *13*, 1335-1340.

Li, J., and Radice, G.L. (2010). A new perspective on intercalated disc organization: implications for heart disease. Dermatol Res Pract *2010*, 207835.

Li, J., Kim, H., Aceto, D.G., Hung, J., Aono, S., and Kemphues, K.J. (2010). Binding to PKC-3, but not to PAR-3 or to a conventional PDZ domain ligand, is required for PAR-6 function in *C. elegans*. Dev Biol *340*, 88-98.

Li, X., Wang, Q., Yu, X., Liu, H., Yang, H., Zhao, C., Liu, X., Tan, C., Klejnot, J., Zhong, D*., et al.* (2011b). Arabidopsis cryptochrome 2 (CRY2) functions by the photoactivation mechanism distinct from the tryptophan (trp) triad-dependent photoreduction. Proc Natl Acad Sci U S A *108*, 20844-20849.

Li, Y., Junge, J.A., Arnesano, C., Gross, G.G., Miner, J.H., Moats, R., Roberts, R.W., Arnold, D.B., and Fraser, S.E. (2018). Discs large 1 controls daughter-cell polarity after cytokinesis in vertebrate morphogenesis. Proc Natl Acad Sci USA *115*, E10859-E10868.

Li, Y., Wei, Z., Yan, Y., Wan, Q., Du, Q., and Zhang, M. (2014). Structure of Crumbs tail in complex with the PALS1 PDZ-SH3-GK tandem reveals a highly specific assembly mechanism for the apical Crumbs complex. Proc Natl Acad Sci U S A *111*, 17444-17449.

Li, Z., Wang, L., Hays, T.S., and Cai, Y. (2008). Dynein-mediated apical localization of crumbs transcripts is required for Crumbs activity in epithelial polarity. J Cell Biol *180*, 31-38.

Liem, R.K. (2016). Cytoskeletal Integrators: The Spectrin Superfamily. Cold Spring Harb Perspect Biol *8*.

Lin, D., Edwards, A.S., Fawcett, J.P., Mbamalu, G., Scott, J.D., and Pawson, T. (2000). A mammalian PAR-3-PAR-6 complex implicated in Cdc42/Rac1 and aPKC signalling and cell polarity. Nat Cell Biol *2*, 540-547.

Ling, C., Zheng, Y., Yin, F., Yu, J., Huang, J., Hong, Y., Wu, S., and Pan, D. (2010). The apical transmembrane protein Crumbs functions as a tumor suppressor that regulates Hippo signaling by binding to Expanded. Proc Natl Acad Sci U S A *107*, 10532-10537.

Liu, H., Wang, S., Hang, W., Gao, J., Zhang, W., Cheng, Z., Yang, C., He, J., Zhou, J., Chen, J*., et al.* (2018). LET-413/Erbin acts as a RAB-5 effector to promote RAB-10 activation during endocytic recycling. J Cell Biol *217*, 299-314.

Liu, Q., and Tucker, C.L. (2017). Engineering genetically-encoded tools for optogenetic control of protein activity. Curr Opin Chem Biol *40*, 17-23.

Lohia, M., Qin, Y., and Macara, I.G. (2012). The Scribble polarity protein stabilizes E-cadherin/p120-catenin binding and blocks retrieval of E-cadherin to the Golgi. PLoS ONE *7*, e51130.

Loie, E., Charrier, L.E., Sollier, K., Masson, J.Y., and Laprise, P. (2015). CRB3A Controls the Morphology and Cohesion of Cancer Cells through Ehm2/p114RhoGEF-Dependent Signaling. Mol Cell Biol *35*, 3423-3435.

Lu, J., Dong, W., Tao, Y., and Hong, Y. (2021). Electrostatic plasma membrane targeting contributes to Dlg function in cell polarity and tumorigenesis. Development *148*.

Lujan, P., Varsano, G., Rubio, T., Hennrich, M.L., Sachsenheimer, T., Galvez-Santisteban, M., Martin-Belmonte, F., Gavin, A.C., Brugger, B., and Kohn, M. (2016). PRL-3 disrupts epithelial architecture by altering the post-mitotic midbody position. J Cell Sci *129*, 4130-4142.

Ma, X., Kovacs, M., Conti, M.A., Wang, A., Zhang, Y., Sellers, J.R., and Adelstein, R.S. (2012). Nonmuscle myosin II exerts tension but does not translocate actin in vertebrate cytokinesis. Proc Natl Acad Sci U S A *109*, 4509-4514.

Machacek, M., Hodgson, L., Welch, C., Elliott, H., Pertz, O., Nalbant, P., Abell, A., Johnson, G.L., Hahn, K.M., and Danuser, G. (2009). Coordination of Rho GTPase activities during cell protrusion. Nature *461*, 99-103.

Maitre, J.L., Niwayama, R., Turlier, H., Nedelec, F., and Hiiragi, T. (2015). Pulsatile cell-autonomous contractility drives compaction in the mouse embryo. Nat Cell Biol *17*, 849-855.

Maitre, J.L., Turlier, H., Illukkumbura, R., Eismann, B., Niwayama, R., Nedelec, F., and Hiiragi, T. (2016). Asymmetric division of contractile domains couples cell positioning and fate specification. Nature *536*, 344-348.

Majumder, P., Aranjuez, G., Amick, J., and McDonald, J.A. (2012). Par-1 controls myosin-II activity through myosin phosphatase to regulate border cell migration. Curr Biol *22*, 363-372.

Makarova, O., Roh, M.H., Liu, C.J., Laurinec, S., and Margolis, B. (2003). Mammalian Crumbs3 is a small transmembrane protein linked to protein associated with Lin-7 (Pals1). Gene *302*, 21-29.

Mangan, A.J., Sietsema, D.V., Li, D., Moore, J.K., Citi, S., and Prekeris, R. (2016). Cingulin and actin mediate midbody-dependent apical lumen formation during polarization of epithelial cells. Nat Commun *7*, 12426.

Mangeol, P., Massey-Harroche, D., Richard, F., Lenne, P.-F., and Le Bivic, A. (2020). Super-resolution imaging uncovers the nanoscopic segregation of polarity proteins in epithelia. bioRxiv, 2020.2008.2012.248674.

Manning, A.J., and Rogers, S.L. (2014). The Fog signaling pathway: insights into signaling in morphogenesis. Dev Biol *394*, 6-14.

Manning, L., and Starz-Gaiano, M. (2015). Culturing Drosophila Egg Chambers and Investigating Developmental Processes Through Live Imaging. Methods Mol Biol *1328*, 73-88.

Manning, L.A., Perez-Vale, K.Z., Schaefer, K.N., Sewell, M.T., and Peifer, M. (2019). The *Drosophila* Afadin and ZO-1 homologues Canoe and Polychaetoid act in parallel to maintain epithelial integrity when challenged by adherens junction remodeling. Mol Biol Cell *30*, 1938-1960.

Margolis, B. (2018). The Crumbs3 Polarity Protein. Cold Spring Harb Perspect Biol *10*.

Margolis, B., and Borg, J.P. (2005). Apicobasal polarity complexes. J Cell Sci *118*, 5157-5159.

Marshall, W.F. (2020). Pattern Formation and Complexity in Single Cells. Curr Biol *30*, R544-R552.

Marston, D.J., Higgins, C.D., Peters, K.A., Cupp, T.D., Dickinson, D.J., Pani, A.M., Moore, R.P., Cox, A.H., Kiehart, D.P., and Goldstein, B. (2016). MRCK-1 Drives Apical Constriction in *C. elegans* by Linking Developmental Patterning to Force Generation. Curr Biol *26*, 2079-2089.

Martin-Belmonte, F., and Perez-Moreno, M. (2011). Epithelial cell polarity, stem cells and cancer. Nat Rev Cancer *12*, 23-38.

Martin-Belmonte, F., Gassama, A., Datta, A., Yu, W., Rescher, U., Gerke, V., and Mostov, K. (2007). PTEN-mediated apical segregation of phosphoinositides controls epithelial morphogenesis through Cdc42. Cell *128*, 383-397.

Martin, A.C. (2020). The Physical Mechanisms of Drosophila Gastrulation: Mesoderm and Endoderm Invagination. Genetics *214*, 543-560.

Martin, A.C., Gelbart, M., Fernandez-Gonzalez, R., Kaschube, M., and Wieschaus, E.F. (2010). Integration of contractile forces during tissue invagination. J Cell Biol *188*, 735-749.

Martin, A.C., Kaschube, M., and Wieschaus, E.F. (2009). Pulsed contractions of an actin-myosin network drive apical constriction. Nature *457*, 495-499.

Masedunskas, A., Sramkova, M., Parente, L., Sales, K.U., Amornphimoltham, P., Bugge, T.H., and Weigert, R. (2011). Role for the actomyosin complex in regulated exocytosis revealed by intravital microscopy. Proc Natl Acad Sci U S A *108*, 13552-13557.

Mashukova, A., Wald, F.A., and Salas, P.J. (2011). Tumor necrosis factor alpha and inflammation disrupt the polarity complex in intestinal epithelial cells by a posttranslational mechanism. Mol Cell Biol *31*, 756-765.

Mason, F.M., Tworoger, M., and Martin, A.C. (2013). Apical domain polarization localizes actin-myosin activity to drive ratchet-like apical constriction. Nat Cell Biol *15*, 926-936.

Mason, F.M., Xie, S., Vasquez, C.G., Tworoger, M., and Martin, A.C. (2016). RhoA GTPase inhibition organizes contraction during epithelial morphogenesis. J Cell Biol *214*, 603-617.

Mata, J., Curado, S., Ephrussi, A., and Rorth, P. (2000). Tribbles coordinates mitosis and morphogenesis in Drosophila by regulating string/CDC25 proteolysis. Cell *101*, 511-522.

Mathew, D., Gramates, L.S., Packard, M., Thomas, U., Bilder, D., Perrimon, N., Gorczyca, M., and Budnik, V. (2002). Recruitment of scribble to the synaptic scaffolding complex requires GUK-holder, a novel DLG binding protein. Curr Biol *12*, 531-539.

Matsuzawa, K., Ohga, H., Shigetomi, K., Shiiya, T., Hirashima, M., and Ikenouchi, J. (2021). MAGIs regulate aPKC to enable balanced distribution of intercellular tension for epithelial sheet homeostasis. Commun Biol *4*, 337.

Matzke, R., Jacobson, K., and Radmacher, M. (2001). Direct, high-resolution measurement of furrow stiffening during division of adherent cells. Nat Cell Biol *3*, 607-610.

Mayor, R., and Etienne-Manneville, S. (2016). The front and rear of collective cell migration. Nat Rev Mol Cell Biol *17*, 97-109.

McCaffrey, L.M., and Macara, I.G. (2012). Signaling pathways in cell polarity. Cold Spring Harb Perspect Biol *4*.

McCaffrey, L.M., Montalbano, J., Mihai, C., and Macara, I.G. (2012). Loss of the Par3 polarity protein promotes breast tumorigenesis and metastasis. Cancer Cell *22*, 601-614.

McCusker, D. (2020). Cellular self-organization: generating order from the abyss. Mol Biol Cell *31*, 143-148.

McGill, M.A., McKinley, R.F., and Harris, T.J. (2009). Independent cadherin-catenin and Bazooka clusters interact to assemble adherens junctions. J Cell Biol *185*, 787-796.

McGrath, J., Roy, P., and Perrin, B.J. (2017). Stereocilia morphogenesis and maintenance through regulation of actin stability. Semin Cell Dev Biol *65*, 88-95.

McKinley, K.L., Stuurman, N., Royer, L.A., Schartner, C., Castillo-Azofeifa, D., Delling, M., Klein, O.D., and Vale, R.D. (2018). Cellular aspect ratio and cell division mechanics underlie the patterning of cell progeny in diverse mammalian epithelia. Elife *7*.

McKinley, R.F., and Harris, T.J. (2012). Displacement of basolateral Bazooka/PAR-3 by regulated transport and dispersion during epithelial polarization in *Drosophila*. Mol Biol Cell *23*, 4465-4471.

Medina, E., Williams, J., Klipfell, E., Zarnescu, D., Thomas, G., and Le Bivic, A. (2002). Crumbs interacts with moesin and beta(Heavy)-spectrin in the apical membrane skeleton of *Drosophila*. J Cell Biol *158*, 941-951.

Mege, R.M., and Ishiyama, N. (2017). Integration of Cadherin Adhesion and Cytoskeleton at Adherens Junctions. Cold Spring Harb Perspect Biol *9*.

Mehalow, A.K., Kameya, S., Smith, R.S., Hawes, N.L., Denegre, J.M., Young, J.A., Bechtold, L., Haider, N.B., Tepass, U., Heckenlively, J.R.*, et al.* (2003). CRB1 is essential for external limiting membrane integrity and photoreceptor morphogenesis in the mammalian retina. Hum Mol Genet *12*, 2179-2189.

Mertens, A.E., Rygiel, T.P., Olivo, C., van der Kammen, R., and Collard, J.G. (2005). The Rac activator Tiam1 controls tight junction biogenesis in keratinocytes through binding to and activation of the Par polarity complex. J Cell Biol *170*, 1029-1037.

Mese, G., Richard, G., and White, T.W. (2007). Gap junctions: basic structure and function. J Invest Dermatol *127*, 2516-2524.

Metais, J.Y., Navarro, C., Santoni, M.J., Audebert, S., and Borg, J.P. (2005). hScrib interacts with ZO-2 at the cell-cell junctions of epithelial cells. FEBS Lett *579*, 3725-3730.

Miao, H., and Blankenship, J.T. (2020). The pulse of morphogenesis: actomyosin dynamics and regulation in epithelia. Development *147*.

Michel, D., Arsanto, J.P., Massey-Harroche, D., Beclin, C., Wijnholds, J., and Le Bivic, A. (2005). PATJ connects and stabilizes apical and lateral components of tight junctions in human intestinal cells. J Cell Sci *118*, 4049-4057.

Mishima, M., Kaitna, S., and Glotzer, M. (2002). Central spindle assembly and cytokinesis require a kinesin-like protein/RhoGAP complex with microtubule bundling activity. Dev Cell *2*, 41-54.

Mizuno, K., Suzuki, A., Hirose, T., Kitamura, K., Kutsuzawa, K., Futaki, M., Amano, Y., and Ohno, S. (2003). Self-association of PAR-3-mediated by the conserved N-terminal domain contributes to the development of epithelial tight junctions. J Biol Chem *278*, 31240-31250.

Monster, J.L., Donker, L., Vliem, M.J., Win, Z., Matthews, H.K., Cheah, J.S., Yamada, S., de Rooij, J., Baum, B., and Gloerich, M. (2021). An asymmetric junctional mechanoresponse coordinates mitotic rounding with epithelial integrity. J Cell Biol *220*.

Morais-de-Sa, E., and Sunkel, C. (2013). Adherens junctions determine the apical position of the midbody during follicular epithelial cell division. EMBO Rep *14*, 696-703.

Morais-de-Sa, E., Mirouse, V., and St Johnston, D. (2010). aPKC phosphorylation of Bazooka defines the apical/lateral border in *Drosophila* epithelial cells. Cell *141*, 509-523.

Morais-de-Sa, E., Mukherjee, A., Lowe, N., and St Johnston, D. (2014). Slmb antagonises the aPKC/Par-6 complex to control oocyte and epithelial polarity. Development *141*, 2984-2992.

Moreira, S., Osswald, M., Ventura, G., Goncalves, M., Sunkel, C.E., and Morais-de-Sa, E. (2019). PP1-Mediated Dephosphorylation of Lgl Controls Apical-basal Polarity. Cell Rep *26*, 293-301 e297.

Morgan, D.O. (2007). The Cell Cycle, 1st edn (New Scince Press).

Morin, X., Daneman, R., Zavortink, M., and Chia, W. (2001). A protein trap strategy to detect GFP-tagged proteins expressed from their endogenous loci in Drosophila. Proc Natl Acad Sci U S A *98*, 15050-15055.

Moura, M., Osswald, M., Leca, N., Barbosa, J., Pereira, A.J., Maiato, H., Sunkel, C.E., and Conde, C. (2017). Protein Phosphatase 1 inactivates Mps1 to ensure efficient Spindle Assembly Checkpoint silencing. Elife *6*.

Moutinho-Pereira, S., Matos, I., and Maiato, H. (2010). *Drosophila* S2 cells as a model system to investigate mitotic spindle dynamics, architecture, and function. Methods Cell Biol *97*, 243-257.

Moutinho-Pereira, S., Stuurman, N., Afonso, O., Hornsveld, M., Aguiar, P., Goshima, G., Vale, R.D., and Maiato, H. (2013). Genes involved in centrosome-independent mitotic spindle assembly in Drosophila S2 cells. Proc Natl Acad Sci U S A *110*, 19808-19813.

Muller, H.A., and Wieschaus, E. (1996). armadillo, bazooka, and stardust are critical for early stages in formation of the zonula adherens and maintenance of the polarized blastoderm epithelium in *Drosophila*. J Cell Biol *134*, 149-163.

Muller, P.M., Rademacher, J., Bagshaw, R.D., Wortmann, C., Barth, C., van Unen, J., Alp, K.M., Giudice, G., Eccles, R.L., Heinrich, L.E.*, et al.* (2020). Systems analysis of RhoGEF and RhoGAP regulatory proteins reveals spatially organized RAC1 signalling from integrin adhesions. Nat Cell Biol *22*, 498-511.

Munjal, A., and Lecuit, T. (2014). Actomyosin networks and tissue morphogenesis. Development *141*, 1789-1793.

Munjal, A., Philippe, J.M., Munro, E., and Lecuit, T. (2015). A self-organized biomechanical network drives shape changes during tissue morphogenesis. Nature *524*, 351-355.

Murat, D., Byrne, M., and Komeili, A. (2010). Cell biology of prokaryotic organelles. Cold Spring Harb Perspect Biol *2*, a000422.

Murdoch, J.N., Henderson, D.J., Doudney, K., Gaston-Massuet, C., Phillips, H.M., Paternotte, C., Arkell, R., Stanier, P., and Copp, A.J. (2003). Disruption of scribble (Scrb1) causes severe neural tube defects in the circletail mouse. Hum Mol Genet *12*, 87-98.

Nagafuchi, A., and Takeichi, M. (1988). Cell binding function of E-cadherin is regulated by the cytoplasmic domain. EMBO J *7*, 3679-3684.

Nagafuchi, A., Shirayoshi, Y., Okazaki, K., Yasuda, K., and Takeichi, M. (1987). Transformation of cell adhesion properties by exogenously introduced E-cadherin cDNA. Nature *329*, 341-343.

Nagai-Tamai, Y., Mizuno, K., Hirose, T., Suzuki, A., and Ohno, S. (2002). Regulated protein-protein interaction between aPKC and PAR-3 plays an essential role in the polarization of epithelial cells. Genes Cells *7*, 1161-1171.

Nagar, B., Overduin, M., Ikura, M., and Rini, J.M. (1996). Structural basis of calcium-induced E-cadherin rigidification and dimerization. Nature *380*, 360-364.

Nakajima, H., and Tanoue, T. (2010). Epithelial cell shape is regulated by Lulu proteins via myosin-II. J Cell Sci *123*, 555-566.

Nakajima, H., and Tanoue, T. (2011). Lulu2 regulates the circumferential actomyosin tensile system in epithelial cells through p114RhoGEF. J Cell Biol *195*, 245-261.

Nakajima, Y., Meyer, E.J., Kroesen, A., McKinney, S.A., and Gibson, M.C. (2013). Epithelial junctions maintain tissue architecture by directing planar spindle orientation. Nature *500*, 359-362.

Nakamura, M., Verboon, J.M., and Parkhurst, S.M. (2017). Prepatterning by RhoGEFs governs Rho GTPase spatiotemporal dynamics during wound repair. J Cell Biol *216*, 3959-3969.

Nam, S.C., and Choi, K.W. (2003). Interaction of Par-6 and Crumbs complexes is essential for photoreceptor morphogenesis in *Drosophila*. Development *130*, 4363-4372.

Navarro, C., Nola, S., Audebert, S., Santoni, M.J., Arsanto, J.P., Ginestier, C., Marchetto, S., Jacquemier, J., Isnardon, D., Le Bivic, A.*, et al.* (2005). Junctional recruitment of mammalian Scribble relies on E-cadherin engagement. Oncogene *24*, 4330-4339.

Nelson, K.S., Furuse, M., and Beitel, G.J. (2010). The *Drosophila* Claudin Kune-kune is required for septate junction organization and tracheal tube size control. Genetics *185*, 831-839.

Newman, S.A. (2016). 'Biogeneric' developmental processes: drivers of major transitions in animal evolution. Philos Trans R Soc Lond B Biol Sci *371*.

Newman, S.A. (2019). Inherency of Form and Function in Animal Development and Evolution. Front Physiol *10*, 702.

Ngok, S.P., Lin, W.H., and Anastasiadis, P.Z. (2014). Establishment of epithelial polarity--GEF who's minding the GAP? J Cell Sci *127*, 3205-3215.

Nguyen, M.K., Kim, C.Y., Kim, J.M., Park, B.O., Lee, S., Park, H., and Heo, W.D. (2016). Optogenetic oligomerization of Rab GTPases regulates intracellular membrane trafficking. Nat Chem Biol *12*, 431-436.

Niessen, M.T., Scott, J., Zielinski, J.G., Vorhagen, S., Sotiropoulou, P.A., Blanpain, C., Leitges, M., and Niessen, C.M. (2013). aPKClambda controls epidermal homeostasis and stem cell fate through regulation of division orientation. J Cell Biol *202*, 887-900.

Niklas, K.J., and Newman, S.A. (2020). The many roads to and from multicellularity. J Exp Bot *71*, 3247-3253.

Niklas, K.J., Wayne, R., Benitez, M., and Newman, S.A. (2019). Polarity, planes of cell division, and the evolution of plant multicellularity. Protoplasma *256*, 585-599.

Nikolaidou, K.K., and Barrett, K. (2004). A Rho GTPase signaling pathway is used reiteratively in epithelial folding and potentially selects the outcome of Rho activation. Curr Biol *14*, 1822-1826.

Nishiguchi, S., Yagi, A., Sakai, N., and Oda, H. (2016). Divergence of structural strategies for homophilic E-cadherin binding among bilaterians. J Cell Sci *129*, 3309-3319.

Nishikawa, M., Naganathan, S.R., Julicher, F., and Grill, S.W. (2017). Controlling contractile instabilities in the actomyosin cortex. Elife *6*.

Nobes, C.D., and Hall, A. (1995). Rho, rac, and cdc42 GTPases regulate the assembly of multimolecular focal complexes associated with actin stress fibers, lamellipodia, and filopodia. Cell *81*, 53-62.

Nunes de Almeida, F., Walther, R.F., Presse, M.T., Vlassaks, E., and Pichaud, F. (2019). Cdc42 defines apical identity and regulates epithelial morphogenesis by promoting apical recruitment of Par6-aPKC and Crumbs. Development *146*.

Nurse, P. (2020). What is life?: Understand biology in five steps.

Ohshiro, T., Yagami, T., Zhang, C., and Matsuzaki, F. (2000). Role of cortical tumour-suppressor proteins in asymmetric division of *Drosophila* neuroblast. Nature *408*, 593-596.

Oldenburg, J., van der Krogt, G., Twiss, F., Bongaarts, A., Habani, Y., Slotman, J.A., Houtsmuller, A., Huveneers, S., and de Rooij, J. (2015). VASP, zyxin and TES are tension-dependent members of Focal Adherens Junctions independent of the alpha-catenin-vinculin module. Sci Rep *5*, 17225.

Olivieri, D., Sykora, M.M., Sachidanandam, R., Mechtler, K., and Brennecke, J. (2010). An in vivo RNAi assay identifies major genetic and cellular requirements for primary piRNA biogenesis in Drosophila. EMBO J *29*, 3301-3317.

Ooshio, T., Fujita, N., Yamada, A., Sato, T., Kitagawa, Y., Okamoto, R., Nakata, S., Miki, A., Irie, K., and Takai, Y. (2007). Cooperative roles of Par-3 and afadin in the formation of adherens and tight junctions. J Cell Sci *120*, 2352-2365.

Ormo, M., Cubitt, A.B., Kallio, K., Gross, L.A., Tsien, R.Y., and Remington, S.J. (1996). Crystal structure of the Aequorea victoria green fluorescent protein. Science *273*, 1392-1395.

Osswald, M., and Morais-de-Sa, E. (2019). Dealing with apical-basal polarity and intercellular junctions: a multidimensional challenge for epithelial cell division. Curr Opin Cell Biol *60*, 75-83.

Otani, T., Ichii, T., Aono, S., and Takeichi, M. (2006). Cdc42 GEF Tuba regulates the junctional configuration of simple epithelial cells. J Cell Biol *175*, 135-146.

Otani, T., Nguyen, T.P., Tokuda, S., Sugihara, K., Sugawara, T., Furuse, K., Miura, T., Ebnet, K., and Furuse, M. (2019). Claudins and JAM-A coordinately regulate tight junction formation and epithelial polarity. J Cell Biol *218*, 3372-3396.

Otomo, T., Otomo, C., Tomchick, D.R., Machius, M., and Rosen, M.K. (2005). Structural basis of Rho GTPase-mediated activation of the formin mDia1. Mol Cell *18*, 273-281.

Ozawa, M., Baribault, H., and Kemler, R. (1989). The cytoplasmic domain of the cell adhesion molecule uvomorulin associates with three independent proteins structurally related in different species. EMBO J *8*, 1711-1717.

Pachis, S.T., and Kops, G. (2018). Leader of the SAC: molecular mechanisms of Mps1/TTK regulation in mitosis. Open Biol *8*.

Packard, A., Georgas, K., Michos, O., Riccio, P., Cebrian, C., Combes, A.N., Ju, A., Ferrer-Vaquer, A., Hadjantonakis, A.K., Zong, H.*, et al.* (2013). Luminal mitosis drives epithelial cell dispersal within the branching ureteric bud. Dev Cell *27*, 319-330.

Padmanabhan, A., Rao, M.V., Wu, Y., and Zaidel-Bar, R. (2015). Jack of all trades: functional modularity in the adherens junction. Curr Opin Cell Biol *36*, 32-40.

Pandey, R., Heidmann, S., and Lehner, C.F. (2005). Epithelial re-organization and dynamics of progression through mitosis in Drosophila separase complex mutants. J Cell Sci *118*, 733-742.

Pannekoek, W.J., de Rooij, J., and Gloerich, M. (2019). Force transduction by cadherin adhesions in morphogenesis. F1000Res *8*.

Pare, A.C., and Zallen, J.A. (2020). Cellular, molecular, and biophysical control of epithelial cell intercalation. Curr Top Dev Biol *136*, 167-193.

Park, H., Kim, N.Y., Lee, S., Kim, N., Kim, J., and Heo, W.D. (2017). Optogenetic protein clustering through fluorescent protein tagging and extension of CRY2. Nat Commun *8*, 30.

Pasakarnis, L., Frei, E., Caussinus, E., Affolter, M., and Brunner, D. (2016). Amnioserosa cell constriction but not epidermal actin cable tension autonomously drives dorsal closure. Nat Cell Biol *18*, 1161-1172.

Pellikka, M., Tanentzapf, G., Pinto, M., Smith, C., McGlade, C.J., Ready, D.F., and Tepass, U. (2002). Crumbs, the *Drosophila* homologue of human CRB1/RP12, is essential for photoreceptor morphogenesis. Nature *416*, 143-149.

Penalva, C., and Mirouse, V. (2012). Tissue-specific function of Patj in regulating the Crumbs complex and epithelial polarity. Development *139*, 4549-4554.

Peng, C.Y., Manning, L., Albertson, R., and Doe, C.Q. (2000). The tumour-suppressor genes lgl and dlg regulate basal protein targeting in *Drosophila* neuroblasts. Nature *408*, 596-600.

Penkert, R.R., DiVittorio, H.M., and Prehoda, K.E. (2004). Internal recognition through PDZ domain plasticity in the Par-6-Pals1 complex. Nat Struct Mol Biol *11*, 1122-1127.

Percipalle, P., and Visa, N. (2006). Molecular functions of nuclear actin in transcription. J Cell Biol *172*, 967-971.

Pertz, O. (2010). Spatio-temporal Rho GTPase signaling - where are we now? J Cell Sci *123*, 1841-1850.

Peters, N.C., and Berg, C.A. (2016). In Vitro Culturing and Live Imaging of Drosophila Egg Chambers: A History and Adaptable Method. Methods Mol Biol *1457*, 35-68.

Peterson, F.C., Penkert, R.R., Volkman, B.F., and Prehoda, K.E. (2004). Cdc42 regulates the Par-6 PDZ domain through an allosteric CRIB-PDZ transition. Mol Cell *13*, 665-676.

Petridou, N.I., Corominas-Murtra, B., Heisenberg, C.P., and Hannezo, E. (2021). Rigidity percolation uncovers a structural basis for embryonic tissue phase transitions. Cell *184*, 1914-1928 e1919.

Petridou, N.I., Grigolon, S., Salbreux, G., Hannezo, E., and Heisenberg, C.P. (2018). Fluidization-mediated tissue spreading by mitotic cell rounding and non-canonical Wnt signalling. Nat Cell Biol.

Petridou, N.I., Grigolon, S., Salbreux, G., Hannezo, E., and Heisenberg, C.P. (2019). Fluidization-mediated tissue spreading by mitotic cell rounding and non-canonical Wnt signalling. Nat Cell Biol *21*, 169-178.

Pichaud, F. (2018). PAR-Complex and Crumbs Function During Photoreceptor Morphogenesis and Retinal Degeneration. Front Cell Neurosci *12*, 90.

Pilot, F., Philippe, J.M., Lemmers, C., and Lecuit, T. (2006). Spatial control of actin organization at adherens junctions by a synaptotagmin-like protein Btsz. Nature *442*, 580-584.

Pinheiro, D., and Bellaiche, Y. (2018). Mechanical Force-Driven Adherens Junction Remodeling and Epithelial Dynamics. Dev Cell *47*, 3-19.

Pinheiro, D., Hannezo, E., Herszterg, S., Bosveld, F., Gaugue, I., Balakireva, M., Wang, Z., Cristo, I., Rigaud, S.U., Markova, O.*, et al.* (2017). Transmission of cytokinesis forces via E-cadherin dilution and actomyosin flows. Nature *545*, 103-107.

Pires, H.R., and Boxem, M. (2018). Mapping the Polarity Interactome. J Mol Biol *430*, 3521-3544.

Plant, P.J., Fawcett, J.P., Lin, D.C., Holdorf, A.D., Binns, K., Kulkarni, S., and Pawson, T. (2003). A polarity complex of mPar-6 and atypical PKC binds, phosphorylates and regulates mammalian Lgl. Nat Cell Biol *5*, 301-308.

Pokutta, S., Herrenknecht, K., Kemler, R., and Engel, J. (1994). Conformational changes of the recombinant extracellular domain of E-cadherin upon calcium binding. Eur J Biochem *223*, 1019-1026.

Pollarolo, G., Schulz, J.G., Munck, S., and Dotti, C.G. (2011). Cytokinesis remnants define first neuronal asymmetry in vivo. Nat Neurosci *14*, 1525-1533.

Pruliere, G., Cosson, J., Chevalier, S., Sardet, C., and Chenevert, J. (2011). Atypical protein kinase C controls sea urchin ciliogenesis. Mol Biol Cell *22*, 2042-2053.

Pruyne, D., Evangelista, M., Yang, C., Bi, E., Zigmond, S., Bretscher, A., and Boone, C. (2002). Role of formins in actin assembly: nucleation and barbed-end association. Science *297*, 612-615.

Pulido Companys, P., Norris, A., and Bischoff, M. (2020). Coordination of cytoskeletal dynamics and cell behaviour during *Drosophila* abdominal morphogenesis. J Cell Sci *133*.

Qin, X., Hannezo, E., Mangeat, T., Liu, C., Majumder, P., Liu, J., Choesmel-Cadamuro, V., McDonald, J.A., Liu, Y., Yi, B.*, et al.* (2018). A biochemical network controlling basal myosin oscillation. Nat Commun *9*, 1210.

Qin, X., Park, B.O., Liu, J., Chen, B., Choesmel-Cadamuro, V., Belguise, K., Heo, W.D., and Wang, X. (2017). Cell-matrix adhesion and cell-cell adhesion differentially control basal myosin oscillation and *Drosophila* egg chamber elongation. Nat Commun *8*, 14708.

Qin, Y., Capaldo, C., Gumbiner, B.M., and Macara, I.G. (2005). The mammalian Scribble polarity protein regulates epithelial cell adhesion and migration through E-cadherin. J Cell Biol *171*, 1061-1071.

Qin, Y., Meisen, W.H., Hao, Y., and Macara, I.G. (2010). Tuba, a Cdc42 GEF, is required for polarized spindle orientation during epithelial cyst formation. J Cell Biol *189*, 661-669.

Qiu, R.G., Abo, A., and Steven Martin, G. (2000). A human homolog of the *C. elegans* polarity determinant Par-6 links Rac and Cdc42 to PKCzeta signaling and cell transformation. Curr Biol *10*, 697-707.

Quan, J., and Tian, J. (2011). Circular polymerase extension cloning for high-throughput cloning of complex and combinatorial DNA libraries. Nat Protoc *6*, 242-251.

Quinones-Coello, A.T., Petrella, L.N., Ayers, K., Melillo, A., Mazzalupo, S., Hudson, A.M., Wang, S., Castiblanco, C., Buszczak, M., Hoskins, R.A.*, et al.* (2007). Exploring strategies for protein trapping in Drosophila. Genetics *175*, 1089-1104.

Ragkousi, K., and Gibson, M.C. (2014). Cell division and the maintenance of epithelial order. J Cell Biol *207*, 181-188.

Ragkousi, K., Marr, K., McKinney, S., Ellington, L., and Gibson, M.C. (2017). Cell-Cycle-Coupled Oscillations in Apical Polarity and Intercellular Contact Maintain Order in Embryonic Epithelia. Curr Biol *27*, 1381-1386.

Raman, R., Damle, I., Rote, R., Banerjee, S., Dingare, C., and Sonawane, M. (2016). aPKC regulates apical localization of Lgl to restrict elongation of microridges in developing zebrafish epidermis. Nat Commun *7*, 11643.

Raman, R., Pinto, C.S., and Sonawane, M. (2018). Polarized Organization of the Cytoskeleton: Regulation by Cell Polarity Proteins. J Mol Biol *430*, 3565-3584.

Ramanathan, S.P., Helenius, J., Stewart, M.P., Cattin, C.J., Hyman, A.A., and Muller, D.J. (2015). Cdk1-dependent mitotic enrichment of cortical myosin II promotes cell rounding against confinement. Nat Cell Biol *17*, 148-159.

Ramkumar, N., and Baum, B. (2016). Coupling changes in cell shape to chromosome segregation. Nat Rev Mol Cell Biol *17*, 511-521.

Ramkumar, N., Omelchenko, T., Silva-Gagliardi, N.F., McGlade, C.J., Wijnholds, J., and Anderson, K.V. (2016). Crumbs2 promotes cell ingression during the epithelial-to-mesenchymal transition at gastrulation. Nat Cell Biol *18*, 1281-1291.

Ratheesh, A., Gomez, G.A., Priya, R., Verma, S., Kovacs, E.M., Jiang, K., Brown, N.H., Akhmanova, A., Stehbens, S.J., and Yap, A.S. (2012). Centralspindlin and alpha-catenin regulate Rho signalling at the epithelial zonula adherens. Nat Cell Biol *14*, 818-828.

Rauzi, M., Lenne, P.F., and Lecuit, T. (2010). Planar polarized actomyosin contractile flows control epithelial junction remodelling. Nature *468*, 1110-1114.

Regala, R.P., Weems, C., Jamieson, L., Khoor, A., Edell, E.S., Lohse, C.M., and Fields, A.P. (2005). Atypical protein kinase C iota is an oncogene in human non-small cell lung cancer. Cancer Res *65*, 8905-8911.

Reina-Campos, M., Diaz-Meco, M.T., and Moscat, J. (2019). The Dual Roles of the Atypical Protein Kinase Cs in Cancer. Cancer Cell *36*, 218-235.

Renschler, F.A., Bruekner, S.R., Salomon, P.L., Mukherjee, A., Kullmann, L., Schutz-Stoffregen, M.C., Henzler, C., Pawson, T., Krahn, M.P., and Wiesner, S. (2018). Structural basis for the interaction between the cell polarity proteins Par3 and Par6. Sci Signal *11*.

Reymann, A.C., Boujemaa-Paterski, R., Martiel, J.L., Guerin, C., Cao, W., Chin, H.F., De La Cruz, E.M., Thery, M., and Blanchoin, L. (2012). Actin network architecture can determine myosin motor activity. Science *336*, 1310-1314.

Ribeiro, S.A., D'Ambrosio, M.V., and Vale, R.D. (2014). Induction of focal adhesions and motility in *Drosophila* S2 cells. Mol Biol Cell *25*, 3861-3869.

Rich, A., Fehon, R.G., and Glotzer, M. (2020). Rho1 activation recapitulates early gastrulation events in the ventral, but not dorsal, epithelium of *Drosophila* embryos. Elife *9*.

Ridley, A.J. (2015). Rho GTPase signalling in cell migration. Curr Opin Cell Biol *36*, 103-112.

Ridley, A.J., and Hall, A. (1992). The small GTP-binding protein rho regulates the assembly of focal adhesions and actin stress fibers in response to growth factors. Cell *70*, 389-399.

Ridley, A.J., Paterson, H.F., Johnston, C.L., Diekmann, D., and Hall, A. (1992). The small GTP-binding protein rac regulates growth factor-induced membrane ruffling. Cell *70*, 401-410.

Riga, A., Castiglioni, V.G., and Boxem, M. (2020). New insights into apical-basal polarization in epithelia. Curr Opin Cell Biol *62*, 1-8.

Rodriguez-Boulan, E., and Macara, I.G. (2014). Organization and execution of the epithelial polarity programme. Nature reviews Molecular cell biology *15*, 225-242.

Rodriguez, J., Peglion, F., Martin, J., Hubatsch, L., Reich, J., Hirani, N., Gubieda, A.G., Roffey, J., Fernandes, A.R., St Johnston, D.*, et al.* (2017). aPKC Cycles between Functionally Distinct PAR Protein Assemblies to Drive Cell Polarity. Dev Cell *42*, 400-415 e409.

Rogers, S.L., and Rogers, G.C. (2008). Culture of *Drosophila* S2 cells and their use for RNAi-mediated loss-of-function studies and immunofluorescence microscopy. Nat Protoc *3*, 606-611.

Roh-Johnson, M., Shemer, G., Higgins, C.D., McClellan, J.H., Werts, A.D., Tulu, U.S., Gao, L., Betzig, E., Kiehart, D.P., and Goldstein, B. (2012). Triggering a cell shape change by exploiting preexisting actomyosin contractions. Science *335*, 1232-1235.

Roh, M.H., Fan, S., Liu, C.J., and Margolis, B. (2003). The Crumbs3-Pals1 complex participates in the establishment of polarity in mammalian epithelial cells. J Cell Sci *116*, 2895-2906.

Roh, M.H., Makarova, O., Liu, C.J., Shin, K., Lee, S., Laurinec, S., Goyal, M., Wiggins, R., and Margolis, B. (2002). The Maguk protein, Pals1, functions as an adapter, linking mammalian homologues of Crumbs and Discs Lost. J Cell Biol *157*, 161-172.

Rohatgi, R., Ma, L., Miki, H., Lopez, M., Kirchhausen, T., Takenawa, T., and Kirschner, M.W. (1999). The interaction between N-WASP and the Arp2/3 complex links Cdc42-dependent signals to actin assembly. Cell *97*, 221-231.

Roignot, J., Peng, X., and Mostov, K. (2013). Polarity in mammalian epithelial morphogenesis. Cold Spring Harb Perspect Biol *5*.

Rolls, M.M., Albertson, R., Shih, H.P., Lee, C.Y., and Doe, C.Q. (2003). *Drosophila* aPKC regulates cell polarity and cell proliferation in neuroblasts and epithelia. J Cell Biol *163*, 1089-1098.

Roman-Fernandez, A., and Bryant, D.M. (2016). Complex Polarity: Building Multicellular Tissues Through Apical Membrane Traffic. Traffic *17*, 1244-1261.

Roper, K. (2012). Anisotropy of Crumbs and aPKC drives myosin cable assembly during tube formation. Dev Cell *23*, 939-953.

Roper, K. (2013). Supracellular actomyosin assemblies during development. Bioarchitecture *3*, 45-49.

Rosa, A., Vlassaks, E., Pichaud, F., and Baum, B. (2015). Ect2/Pbl acts via Rho and polarity proteins to direct the assembly of an isotropic actomyosin cortex upon mitotic entry. Dev Cell *32*, 604-616.

Rossman, K.L., Der, C.J., and Sondek, J. (2005). GEF means go: turning on RHO GTPases with guanine nucleotide-exchange factors. Nat Rev Mol Cell Biol *6*, 167-180.

Rost, B.R., Schneider-Warme, F., Schmitz, D., and Hegemann, P. (2017). Optogenetic Tools for Subcellular Applications in Neuroscience. Neuron *96*, 572-603.

Rothenberg, K.E., and Fernandez-Gonzalez, R. (2019). Forceful closure: cytoskeletal networks in embryonic wound repair. Mol Biol Cell *30*, 1353-1358.

Rothenberg, S.M., Mohapatra, G., Rivera, M.N., Winokur, D., Greninger, P., Nitta, M., Sadow, P.M., Sooriyakumar, G., Brannigan, B.W., Ulman, M.J*., et al.* (2010). A genome-wide screen for microdeletions reveals disruption of polarity complex genes in diverse human cancers. Cancer Res *70*, 2158-2164.

Ruysch, F. (1703). Thesaurus anatomicus tertius.

Saadaoui, M., Machicoane, M., di Pietro, F., Etoc, F., Echard, A., and Morin, X. (2014). Dlg1 controls planar spindle orientation in the neuroepithelium through direct interaction with LGN. The Journal of cell biology *206*, 707-717.

Saadaoui, M., Rocancourt, D., Roussel, J., Corson, F., and Gros, J. (2020). A tensile ring drives tissue flows to shape the gastrulating amniote embryo. Science *367*, 453-458.

Saito, Y., Desai, R.R., and Muthuswamy, S.K. (2018). Reinterpreting polarity and cancer: The changing landscape from tumor suppression to tumor promotion. Biochim Biophys Acta Rev Cancer *1869*, 103-116.

Salis, P., Payre, F., Valenti, P., Bazellieres, E., Le Bivic, A., and Mottola, G. (2017). Crumbs, Moesin and Yurt regulate junctional stability and dynamics for a proper morphogenesis of the *Drosophila* pupal wing epithelium. Sci Rep *7*, 16778.

Sanchez-Corrales, Y.E., Blanchard, G.B., and Roper, K. (2018). Radially patterned cell behaviours during tube budding from an epithelium. Elife *7*.

Sato, K., Watanabe, T., Wang, S., Kakeno, M., Matsuzawa, K., Matsui, T., Yokoi, K., Murase, K., Sugiyama, I., Ozawa, M*., et al.* (2011). Numb controls E-cadherin endocytosis through p120 catenin with aPKC. Mol Biol Cell *22*, 3103-3119.

Sauvanet, C., Wayt, J., Pelaseyed, T., and Bretscher, A. (2015). Structure, regulation, and functional diversity of microvilli on the apical domain of epithelial cells. Annu Rev Cell Dev Biol *31*, 593-621.

Sawyer, J.K., Harris, N.J., Slep, K.C., Gaul, U., and Peifer, M. (2009). The *Drosophila* afadin homologue Canoe regulates linkage of the actin cytoskeleton to adherens junctions during apical constriction. J Cell Biol *186*, 57-73.

Scarff, C.A., Carrington, G., Casas-Mao, D., Chalovich, J.M., Knight, P.J., Ranson, N.A., and Peckham, M. (2020). Structure of the shutdown state of myosin-2. Nature *588*, 515-520.

Schapira, M., Tyers, M., Torrent, M., and Arrowsmith, C.H. (2017). WD40 repeat domain proteins: a novel target class? Nat Rev Drug Discov *16*, 773-786.

Schindelin, J., Arganda-Carreras, I., Frise, E., Kaynig, V., Longair, M., Pietzsch, T., Preibisch, S., Rueden, C., Saalfeld, S., Schmid, B.*, et al.* (2012). Fiji: an open-source platform for biological-image analysis. Nat Methods *9*, 676-682.

Schleiden, M. (1838). Beitrage zur Phytogenesis. Archiv fur Anatomie, Physiologie und Wissenschaftliche Medicin.

Schluter, M.A., Pfarr, C.S., Pieczynski, J., Whiteman, E.L., Hurd, T.W., Fan, S., Liu, C.J., and Margolis, B. (2009). Trafficking of Crumbs3 during cytokinesis is crucial for lumen formation. Mol Biol Cell *20*, 4652-4663.

Schmoranzer, J., Fawcett, J.P., Segura, M., Tan, S., Vallee, R.B., Pawson, T., and Gundersen, G.G. (2009). Par3 and dynein associate to regulate local microtubule dynamics and centrosome orientation during migration. Curr Biol *19*, 1065-1074.

Schwann, T. (1839). Mikroskopische Untersuchungen über die Ubereinstimmung in der Struktur und dem Wachsthum der Thiere und Pflanzen.

Seher, T.C., and Leptin, M. (2000). Tribbles, a cell-cycle brake that coordinates proliferation and morphogenesis during Drosophila gastrulation. Curr Biol *10*, 623-629.

Seidl, S., Braun, U., Roos, N., Li, S., Ludtke, T.H., Kispert, A., and Leitges, M. (2013). Phenotypical analysis of atypical PKCs in vivo function display a compensatory system at mouse embryonic day 7.5. PLoS ONE *8*, e62756.

Sen, A., Nagy-Zsver-Vadas, Z., and Krahn, M.P. (2012). *Drosophila* PATJ supports adherens junction stability by modulating Myosin light chain activity. J Cell Biol *199*, 685-698.

Shahab, J., Tiwari, M.D., Honemann-Capito, M., Krahn, M.P., and Wodarz, A. (2015). Bazooka/PAR3 is dispensable for polarity in *Drosophila* follicular epithelial cells. Biol Open *4*, 528-541.

Shapiro, L., Fannon, A.M., Kwong, P.D., Thompson, A., Lehmann, M.S., Grubel, G., Legrand, J.F., Als-Nielsen, J., Colman, D.R., and Hendrickson, W.A. (1995). Structural basis of cell-cell adhesion by cadherins. Nature *374*, 327-337.

Sharifkhodaei, Z., Gilbert, M.M., and Auld, V.J. (2019). Scribble and Discs Large mediate tricellular junction formation. Development *146*.

Sherrard, K., Robin, F., Lemaire, P., and Munro, E. (2010). Sequential activation of apical and basolateral contractility drives ascidian endoderm invagination. Curr Biol *20*, 1499-1510.

Sherrard, K.M., and Fehon, R.G. (2015). The transmembrane protein Crumbs displays complex dynamics during follicular morphogenesis and is regulated competitively by Moesin and aPKC. Development *142*, 2226.

Shewan, A.M., Maddugoda, M., Kraemer, A., Stehbens, S.J., Verma, S., Kovacs, E.M., and Yap, A.S. (2005). Myosin 2 is a key Rho kinase target necessary for the local concentration of E-cadherin at cell-cell contacts. Mol Biol Cell *16*, 4531-4542.

Shin, K., Straight, S., and Margolis, B. (2005). PATJ regulates tight junction formation and polarity in mammalian epithelial cells. J Cell Biol *168*, 705-711.

Shivas, J.M., Morrison, H.A., Bilder, D., and Skop, A.R. (2010). Polarity and endocytosis: reciprocal regulation. Trends Cell Biol *20*, 445-452.

Sidor, C., Stevens, T.J., Jin, L., Boulanger, J., and Roper, K. (2020). Rho-Kinase Planar Polarization at Tissue Boundaries Depends on Phospho-regulation of Membrane Residence Time. Dev Cell *52*, 364-378 e367.

Siedlik, M.J., and Nelson, C.M. (2015). Regulation of tissue morphodynamics: an important role for actomyosin contractility. Curr Opin Genet Dev *32*, 80-85.

Silver, J.T., Wirtz-Peitz, F., Simoes, S., Pellikka, M., Yan, D., Binari, R., Nishimura, T., Li, Y., Harris, T.J.C., Perrimon, N*., et al.* (2019). Apical polarity proteins recruit the RhoGEF Cysts to promote junctional myosin assembly. J Cell Biol *218*, 3397-3414.

Silver, J.T., Wirtz-Peitz, F., Simoes, S., Pellikka, M., Yan, D., Binari, R., Nishimura, T., Li, Y., Harris, T.J.C., Perrimon, N*., et al.* (2019). Apical polarity proteins recruit the RhoGEF Cysts to promote junctional myosin assembly. J Cell Biol *218*, 3397-3414.

Simoes Sde, M., Blankenship, J.T., Weitz, O., Farrell, D.L., Tamada, M., Fernandez-Gonzalez, R., and Zallen, J.A. (2010). Rho-kinase directs Bazooka/Par-3 planar polarity during *Drosophila* axis elongation. Dev Cell *19*, 377-388.

Simoes, S., Oh, Y., Wang, M.F.Z., Fernandez-Gonzalez, R., and Tepass, U. (2017). Myosin II promotes the anisotropic loss of the apical domain during *Drosophila* neuroblast ingression. J Cell Biol *216*, 1387-1404.

Skau, C.T., and Waterman, C.M. (2015). Specification of Architecture and Function of Actin Structures by Actin Nucleation Factors. Annu Rev Biophys *44*, 285-310.

Skwarek, L.C., Windler, S.L., de Vreede, G., Rogers, G.C., and Bilder, D. (2014). The F-box protein Slmb restricts the activity of aPKC to polarize epithelial cells. Development *141*, 2978-2983.

Smurnyy, Y., Toms, A.V., Hickson, G.R., Eck, M.J., and Eggert, U.S. (2010). Binucleine 2, an isoform-specific inhibitor of Drosophila Aurora B kinase, provides insights into the mechanism of cytokinesis. ACS Chem Biol *5*, 1015-1020.

Solon, J., Kaya-Copur, A., Colombelli, J., and Brunner, D. (2009). Pulsed forces timed by a ratchet-like mechanism drive directed tissue movement during dorsal closure. Cell *137*, 1331-1342.

Sorce, B., Escobedo, C., Toyoda, Y., Stewart, M.P., Cattin, C.J., Newton, R., Banerjee, I., Stettler, A., Roska, B., Eaton, S*., et al.* (2015). Mitotic cells contract actomyosin cortex and generate pressure to round against or escape epithelial confinement. Nat Commun *6*, 8872.

Soriano, E.V., Ivanova, M.E., Fletcher, G., Riou, P., Knowles, P.P., Barnouin, K., Purkiss, A., Kostelecky, B., Saiu, P., Linch, M*., et al.* (2016). aPKC Inhibition by Par3 CR3 Flanking Regions Controls Substrate Access and Underpins Apical-Junctional Polarization. Dev Cell *38*, 384-398.

Sotillos, S., Diaz-Meco, M.T., Caminero, E., Moscat, J., and Campuzano, S. (2004). DaPKC-dependent phosphorylation of Crumbs is required for epithelial cell polarity in *Drosophila*. J Cell Biol *166*, 549-557.

Spadaro, D., Le, S., Laroche, T., Mean, I., Jond, L., Yan, J., and Citi, S. (2017). Tension-Dependent Stretching Activates ZO-1 to Control the Junctional Localization of Its Interactors. Curr Biol *27*, 3783-3795 e3788.

Spassky, N., and Meunier, A. (2017). The development and functions of multiciliated epithelia. Nat Rev Mol Cell Biol *18*, 423-436.

Spiltoir, J.I., and Tucker, C.L. (2019). Photodimerization systems for regulating protein-protein interactions with light. Curr Opin Struct Biol *57*, 1-8.

Spinelli, J.B., and Haigis, M.C. (2018). The multifaceted contributions of mitochondria to cellular metabolism. Nat Cell Biol *20*, 745-754.

St Johnston, D., and Ahringer, J. (2010). Cell polarity in eggs and epithelia: parallels and diversity. Cell *141*, 757-774.

Steinberg, S.F. (2008). Structural basis of protein kinase C isoform function. Physiol Rev *88*, 1341-1378.

Stephens, R., Lim, K., Portela, M., Kvansakul, M., Humbert, P.O., and Richardson, H.E. (2018). The Scribble Cell Polarity Module in the Regulation of Cell Signaling in Tissue Development and Tumorigenesis. J Mol Biol *430*, 3585-3612.

Stephenson, R.E., Higashi, T., Erofeev, I.S., Arnold, T.R., Leda, M., Goryachev, A.B., and Miller, A.L. (2019). Rho Flares Repair Local Tight Junction Leaks. Dev Cell *48*, 445-459 e445.

Stewart, M.P., Helenius, J., Toyoda, Y., Ramanathan, S.P., Muller, D.J., and Hyman, A.A. (2011). Hydrostatic pressure and the actomyosin cortex drive mitotic cell rounding. Nature *469*, 226-230.

Stoll, M., Corneliussen, B., Costello, C.M., Waetzig, G.H., Mellgard, B., Koch, W.A., Rosenstiel, P., Albrecht, M., Croucher, P.J., Seegert, D.*, et al.* (2004). Genetic variation in DLG5 is associated with inflammatory bowel disease. Nat Genet *36*, 476-480.

Straight, S.W., Shin, K., Fogg, V.C., Fan, S., Liu, C.J., Roh, M., and Margolis, B. (2004). Loss of PALS1 expression leads to tight junction and polarity defects. Mol Biol Cell *15*, 1981-1990.

Strand, D., Jakobs, R., Merdes, G., Neumann, B., Kalmes, A., Heid, H.W., Husmann, I., and Mechler, B.M. (1994). The *Drosophila* lethal(2)giant larvae tumor suppressor protein forms homo-oligomers and is associated with nonmuscle myosin II heavy chain. J Cell Biol *127*, 1361-1373.

Stricker, J., Falzone, T., and Gardel, M.L. (2010). Mechanics of the F-actin cytoskeleton. J Biomech *43*, 9-14.

Strickland, D., Lin, Y., Wagner, E., Hope, C.M., Zayner, J., Antoniou, C., Sosnick, T.R., Weiss, E.L., and Glotzer, M. (2012). TULIPs: tunable, light-controlled interacting protein tags for cell biology. Nat Methods *9*, 379-384.

Stucke, V.M., Sillje, H.H., Arnaud, L., and Nigg, E.A. (2002). Human Mps1 kinase is required for the spindle assembly checkpoint but not for centrosome duplication. EMBO J *21*, 1723-1732.

Sun, Z., Costell, M., and Fassler, R. (2019). Integrin activation by talin, kindlin and mechanical forces. Nat Cell Biol *21*, 25-31.

Suzuki, A., Hirata, M., Kamimura, K., Maniwa, R., Yamanaka, T., Mizuno, K., Kishikawa, M., Hirose, H., Amano, Y., Izumi, N.*, et al.* (2004). aPKC acts upstream of PAR-1b in both the establishment and maintenance of mammalian epithelial polarity. Curr Biol *14*, 1425-1435.

Suzuki, A., Yamanaka, T., Hirose, T., Manabe, N., Mizuno, K., Shimizu, M., Akimoto, K., Izumi, Y., Ohnishi, T., and Ohno, S. (2001). Atypical protein kinase C is involved in the evolutionarily conserved par protein complex and plays a critical role in establishing epithelia-specific junctional structures. J Cell Biol *152*, 1183-1196.

Suzuki, H., Nishizawa, T., Tani, K., Yamazaki, Y., Tamura, A., Ishitani, R., Dohmae, N., Tsukita, S., Nureki, O., and Fujiyoshi, Y. (2014). Crystal structure of a claudin provides insight into the architecture of tight junctions. Science *344*, 304-307.

Sweeton, D., Parks, S., Costa, M., and Wieschaus, E. (1991). Gastrulation in *Drosophila*: the formation of the ventral furrow and posterior midgut invaginations. Development *112*, 775-789.

Tabuse, Y., Izumi, Y., Piano, F., Kemphues, K.J., Miwa, J., and Ohno, S. (1998). Atypical protein kinase C cooperates with PAR-3 to establish embryonic polarity in Caenorhabditis elegans. Development *125*, 3607-3614.

Taguchi, K., Ishiuchi, T., and Takeichi, M. (2011). Mechanosensitive EPLIN-dependent remodeling of adherens junctions regulates epithelial reshaping. J Cell Biol *194*, 643-656.

Takeichi, M. (2014). Dynamic contacts: rearranging adherens junctions to drive epithelial remodelling. Nat Rev Mol Cell Biol *15*, 397-410.

Takekuni, K., Ikeda, W., Fujito, T., Morimoto, K., Takeuchi, M., Monden, M., and Takai, Y. (2003). Direct binding of cell polarity protein PAR-3 to cell-cell adhesion molecule nectin at neuroepithelial cells of developing mouse. J Biol Chem *278*, 5497-5500.

Tan, B., Yatim, S., Peng, S., Gunaratne, J., Hunziker, W., and Ludwig, A. (2020). The Mammalian Crumbs Complex Defines a Distinct Polarity Domain Apical of Epithelial Tight Junctions. Curr Biol *30*, 2791-2804 e2796.

Tan, I., Yong, J., Dong, J.M., Lim, L., and Leung, T. (2008). A tripartite complex containing MRCK modulates lamellar actomyosin retrograde flow. Cell *135*, 123-136.

Taneja, N., Fenix, A.M., Rathbun, L., Millis, B.A., Tyska, M.J., Hehnly, H., and Burnette, D.T. (2016). Focal adhesions control cleavage furrow shape and spindle tilt during mitosis. Sci Rep *6*, 29846.

Taneja, N., Rathbun, L., Hehnly, H., and Burnette, D.T. (2019). The balance between adhesion and contraction during cell division. Curr Opin Cell Biol *56*, 45-52.

Tanentzapf, G., and Tepass, U. (2003). Interactions between the crumbs, lethal giant larvae and bazooka pathways in epithelial polarization. Nat Cell Biol *5*, 46-52.

Tanentzapf, G., and Tepass, U. (2003). Interactions between the crumbs, lethal giant larvae and bazooka pathways in epithelial polarization. Nat Cell Biol *5*, 46-52.

Tanentzapf, G., Smith, C., McGlade, J., and Tepass, U. (2000). Apical, lateral, and basal polarization cues contribute to the development of the follicular epithelium during Drosophila oogenesis. J Cell Biol *151*, 891-904.

Taslimi, A., Vrana, J.D., Chen, D., Borinskaya, S., Mayer, B.J., Kennedy, M.J., and Tucker, C.L. (2014). An optimized optogenetic clustering tool for probing protein interaction and function. Nat Commun *5*, 4925.

Taslimi, A., Zoltowski, B., Miranda, J.G., Pathak, G.P., Hughes, R.M., and Tucker, C.L. (2016). Optimized second-generation CRY2-CIB dimerizers and photoactivatable Cre recombinase. Nat Chem Biol *12*, 425-430.

Taubenberger, A.V., Baum, B., and Matthews, H.K. (2020). The Mechanics of Mitotic Cell Rounding. Front Cell Dev Biol *8*, 687.

Tcherkezian, J., and Lamarche-Vane, N. (2007). Current knowledge of the large RhoGAP family of proteins. Biol Cell *99*, 67-86.

Tepass, U., and Hartenstein, V. (1994). The development of cellular junctions in the *Drosophila* embryo. Dev Biol *161*, 563-596.

Tepass, U., and Knust, E. (1990). Phenotypic and developmental analysis of mutations at thecrumbs locus, a gene required for the development of epithelia in*Drosophila* melanogaster. Rouxs Arch Dev Biol *199*, 189-206.

Tepass, U., Gruszynski-DeFeo, E., Haag, T.A., Omatyar, L., Torok, T., and Hartenstein, V. (1996). shotgun encodes *Drosophila* E-cadherin and is preferentially required during cell rearrangement in the neurectoderm and other morphogenetically active epithelia. Genes Dev *10*, 672-685.

Tepass, U., Theres, C., and Knust, E. (1990). crumbs encodes an EGF-like protein expressed on apical membranes of *Drosophila* epithelial cells and required for organization of epithelia. Cell *61*, 787-799.

Tepass, U., Theres, C., and Knust, E. (1990). crumbs encodes an EGF-like protein expressed on apical membranes of Drosophila epithelial cells and required for organization of epithelia. Cell *61*, 787-799.

Terry, S.J., Zihni, C., Elbediwy, A., Vitiello, E., Leefa Chong San, I.V., Balda, M.S., and Matter, K. (2011). Spatially restricted activation of RhoA signalling at epithelial junctions by p114RhoGEF drives junction formation and morphogenesis. Nat Cell Biol *13*, 159-166.

Thieleke-Matos, C., Osorio, D.S., Carvalho, A.X., and Morais-de-Sa, E. (2017). Emerging Mechanisms and Roles for Asymmetric Cytokinesis. Int Rev Cell Mol Biol *332*, 297-345.

Tischer, D., and Weiner, O.D. (2014). Illuminating cell signalling with optogenetic tools. Nat Rev Mol Cell Biol *15*, 551-558.

Toret, C.P., D'Ambrosio, M.V., Vale, R.D., Simon, M.A., and Nelson, W.J. (2014). A genome-wide screen identifies conserved protein hubs required for cadherin-mediated cell-cell adhesion. J Cell Biol *204*, 265-279.

Torres, M., Stoykova, A., Huber, O., Chowdhury, K., Bonaldo, P., Mansouri, A., Butz, S., Kemler, R., and Gruss, P. (1997). An alpha-E-catenin gene trap mutation defines its function in preimplantation development. Proc Natl Acad Sci U S A *94*, 901-906.

Totong, R., Achilleos, A., and Nance, J. (2007). PAR-6 is required for junction formation but not apicobasal polarization in *C. elegans* embryonic epithelial cells. Development *134*, 1259-1268.

Totsukawa, G., Yamakita, Y., Yamashiro, S., Hartshorne, D.J., Sasaki, Y., and Matsumura, F. (2000). Distinct roles of ROCK (Rho-kinase) and MLCK in spatial regulation of MLC phosphorylation for assembly of stress fibers and focal adhesions in 3T3 fibroblasts. J Cell Biol *150*, 797-806.

Tozluoglu, M., Duda, M., Kirkland, N.J., Barrientos, R., Burden, J.J., Munoz, J.J., and Mao, Y. (2019). Planar Differential Growth Rates Initiate Precise Fold Positions in Complex Epithelia. Dev Cell *51*, 299-312 e294.

Tozluoglu, M., and Mao, Y. (2020). On folding morphogenesis, a mechanical problem. Philos Trans R Soc Lond B Biol Sci *375*, 20190564.

Traweger, A., Wiggin, G., Taylor, L., Tate, S.A., Metalnikov, P., and Pawson, T. (2008). Protein phosphatase 1 regulates the phosphorylation state of the polarity scaffold Par-3. Proc Natl Acad Sci U S A *105*, 10402-10407.

Traweger, A., Wiggin, G., Taylor, L., Tate, S.A., Metalnikov, P., and Pawson, T. (2008). Protein phosphatase 1 regulates the phosphorylation state of the polarity scaffold Par-3. Proc Natl Acad Sci U S A *105*, 10402-10407.

Treuner-Lange, A., and Sogaard-Andersen, L. (2014). Regulation of cell polarity in bacteria. J Cell Biol *206*, 7-17.

Treyer, A., and Musch, A. (2013). Hepatocyte polarity. Compr Physiol *3*, 243-287.

Truong Quang, B.A., Mani, M., Markova, O., Lecuit, T., and Lenne, P.F. (2013). Principles of E-cadherin supramolecular organization in vivo. Curr Biol *23*, 2197-2207.

Tsukita, S., Tanaka, H., and Tamura, A. (2019). The Claudins: From Tight Junctions to Biological Systems. Trends Biochem Sci *44*, 141-152.

Turcotte, J.F., Kao, D., Mah, S.J., Claggett, B., Saltzman, J.R., Fedorak, R.N., and Liu, J.J. (2013). Breaks in the wall: increased gaps in the intestinal epithelium of irritable bowel syndrome patients identified by confocal laser endomicroscopy (with videos). Gastrointest Endosc *77*, 624-630.

Tyler, S. (2003). Epithelium--the primary building block for metazoan complexity. Integr Comp Biol *43*, 55-63.

Uemura, T., Oda, H., Kraut, R., Hayashi, S., Kotaoka, Y., and Takeichi, M. (1996). Zygotic *Drosophila* E-cadherin expression is required for processes of dynamic epithelial cell rearrangement in the *Drosophila* embryo. Genes Dev *10*, 659-671.

Uroz, M., Wistorf, S., Serra-Picamal, X., Conte, V., Sales-Pardo, M., Roca-Cusachs, P., Guimera, R., and Trepat, X. (2018). Regulation of cell cycle progression by cell-cell and cell-matrix forces. Nat Cell Biol *20*, 646-654.

Van Itallie, C.M., and Anderson, J.M. (2014). Architecture of tight junctions and principles of molecular composition. Semin Cell Dev Biol *36*, 157-165.

Van Itallie, C.M., Tietgens, A.J., Aponte, A., Fredriksson, K., Fanning, A.S., Gucek, M., and Anderson, J.M. (2014). Biotin ligase tagging identifies proteins proximal to E-cadherin, including lipoma preferred partner, a regulator of epithelial cell-cell and cell-substrate adhesion. J Cell Sci *127*, 885-895.

van, I.S.C.D., Agnetti, J., and Gassama-Diagne, A. (2020). Mechanisms behind the polarized distribution of lipids in epithelial cells. Biochim Biophys Acta Biomembr *1862*, 183145.

Vasioukhin, V. (2012). Adherens junctions and cancer. Subcell Biochem *60*, 379-414.

Vasquez, C.G., Heissler, S.M., Billington, N., Sellers, J.R., and Martin, A.C. (2016). Drosophila non-muscle myosin II motor activity determines the rate of tissue folding. Elife *5*.

Vasquez, C.G., Tworoger, M., and Martin, A.C. (2014). Dynamic myosin phosphorylation regulates contractile pulses and tissue integrity during epithelial morphogenesis. J Cell Biol *206*, 435-450.

Vendome, J., Posy, S., Jin, X., Bahna, F., Ahlsen, G., Shapiro, L., and Honig, B. (2011). Molecular design principles underlying beta-strand swapping in the adhesive dimerization of cadherins. Nat Struct Mol Biol *18*, 693-700.

Venkei, Z.G., and Yamashita, Y.M. (2018). Emerging mechanisms of asymmetric stem cell division. J Cell Biol *217*, 3785-3795.

Ventura, G., Moreira, S., Barros-Carvalho, A., Osswald, M., and Morais-de-Sa, E. (2020). Lgl cortical dynamics are independent of binding to the Scrib-Dlg complex but require Dlg-dependent restriction of aPKC. Development *147*.

Verboon, J.M., and Parkhurst, S.M. (2015). Rho family GTPase functions in *Drosophila* epithelial wound repair. Small GTPases *6*, 28-35.

Verma, S., Han, S.P., Michael, M., Gomez, G.A., Yang, Z., Teasdale, R.D., Ratheesh, A., Kovacs, E.M., Ali, R.G., and Yap, A.S. (2012). A WAVE2-Arp2/3 actin nucleator apparatus supports junctional tension at the epithelial zonula adherens. Mol Biol Cell *23*, 4601-4610.

Vicente-Manzanares, M., Ma, X., Adelstein, R.S., and Horwitz, A.R. (2009). Non-muscle myosin II takes centre stage in cell adhesion and migration. Nat Rev Mol Cell Biol *10*, 778-790.

Vorhagen, S., Kleefisch, D., Persa, O.D., Graband, A., Schwickert, A., Saynisch, M., Leitges, M., Niessen, C.M., and Iden, S. (2018). Shared and independent functions of aPKClambda and Par3 in skin tumorigenesis. Oncogene *37*, 5136-5146.

Wald, F.A., Forteza, R., Diwadkar-Watkins, R., Mashukova, A., Duncan, R., Abreu, M.T., and Salas, P.J. (2011). Aberrant expression of the polarity complex atypical PKC and non-muscle myosin IIA in active and inactive inflammatory bowel disease. Virchows Arch *459*, 331-338.

Wald, F.A., Oriolo, A.S., Mashukova, A., Fregien, N.L., Langshaw, A.H., and Salas, P.J. (2008). Atypical protein kinase C (iota) activates ezrin in the apical domain of intestinal epithelial cells. J Cell Sci *121*, 644-654.

Walther, R.F., and Pichaud, F. (2010). Crumbs/DaPKC-dependent apical exclusion of Bazooka promotes photoreceptor polarity remodeling. Curr Biol *20*, 1065-1074.

Walther, R.F., Burki, M., Pinal, N., Rogerson, C., and Pichaud, F. (2018). Rap1, Canoe and Mbt cooperate with Bazooka to promote zonula adherens assembly in the fly photoreceptor. J Cell Sci *131*.

Walther, R.F., Nunes de Almeida, F., Vlassaks, E., Burden, J.J., and Pichaud, F. (2016). Pak4 Is Required during Epithelial Polarity Remodeling through Regulating AJ Stability and Bazooka Retention at the ZA. Cell Rep *15*, 45-53.

Wang, H.R., Zhang, Y., Ozdamar, B., Ogunjimi, A.A., Alexandrova, E., Thomsen, G.H., and Wrana, J.L. (2003). Regulation of cell polarity and protrusion formation by targeting RhoA for degradation. Science *302*, 1775-1779.

Wang, Q., Hurd, T.W., and Margolis, B. (2004). Tight junction protein Par6 interacts with an evolutionarily conserved region in the amino terminus of PALS1/stardust. J Biol Chem *279*, 30715-30721.

Wang, T., Yanger, K., Stanger, B.Z., Cassio, D., and Bi, E. (2014). Cytokinesis defines a spatial landmark for hepatocyte polarization and apical lumen formation. J Cell Sci *127*, 2483-2492.

Wang, Y., and Riechmann, V. (2007). The role of the actomyosin cytoskeleton in coordination of tissue growth during Drosophila oogenesis. Curr Biol *17*, 1349-1355.

Wang, Y.C., Khan, Z., Kaschube, M., and Wieschaus, E.F. (2012). Differential positioning of adherens junctions is associated with initiation of epithelial folding. Nature *484*, 390-393.

Wang, Z., Bosveld, F., and Bellaiche, Y. (2018). Tricellular junction proteins promote disentanglement of daughter and neighbour cells during epithelial cytokinesis. J Cell Sci *131*.

Warner, S.J., and Longmore, G.D. (2009a). Cdc42 antagonizes Rho1 activity at adherens junctions to limit epithelial cell apical tension. J Cell Biol *187*, 119-133.

Warner, S.J., and Longmore, G.D. (2009b). Distinct functions for Rho1 in maintaining adherens junctions and apical tension in remodeling epithelia. J Cell Biol *185*, 1111-1125.

Warner, S.J., Yashiro, H., and Longmore, G.D. (2010). The Cdc42/Par6/aPKC polarity complex regulates apoptosis-induced compensatory proliferation in epithelia. Curr Biol *20*, 677-686.

Watanabe, N., Madaule, P., Reid, T., Ishizaki, T., Watanabe, G., Kakizuka, A., Saito, Y., Nakao, K., Jockusch, B.M., and Narumiya, S. (1997). p140mDia, a mammalian homolog of *Drosophila* diaphanous, is a target protein for Rho small GTPase and is a ligand for profilin. EMBO J *16*, 3044-3056.

Wei, S.Y., Escudero, L.M., Yu, F., Chang, L.H., Chen, L.Y., Ho, Y.H., Lin, C.M., Chou, C.S., Chia, W., Modolell, J.*, et al.* (2005). Echinoid is a component of adherens junctions that cooperates with DE-Cadherin to mediate cell adhesion. Dev Cell *8*, 493-504.

Wei, Z., Li, Y., Ye, F., and Zhang, M. (2015). Structural basis for the phosphorylation-regulated interaction between the cytoplasmic tail of cell polarity protein crumbs and the actin-binding protein moesin. J Biol Chem *290*, 11384-11392.

Weiss, E., and Winey, M. (1996). The Saccharomyces cerevisiae spindle pole body duplication gene MPS1 is part of a mitotic checkpoint. J Cell Biol *132*, 111-123.

Wells, C.D., Fawcett, J.P., Traweger, A., Yamanaka, Y., Goudreault, M., Elder, K., Kulkarni, S., Gish, G., Virag, C., Lim, C.*, et al.* (2006). A Rich1/Amot complex regulates the Cdc42 GTPase and apical-polarity proteins in epithelial cells. Cell *125*, 535-548.

Weng, M., and Wieschaus, E. (2017). Polarity protein Par3/Bazooka follows myosin-dependent junction repositioning. Dev Biol *422*, 125-134.

White, M.D., Zenker, J., Bissiere, S., and Plachta, N. (2017). How cells change shape and position in the early mammalian embryo. Curr Opin Cell Biol *44*, 7-13.

Whiteman, E.L., Fan, S., Harder, J.L., Walton, K.D., Liu, C.J., Soofi, A., Fogg, V.C., Hershenson, M.B., Dressler, G.R., Deutsch, G.H.*, et al.* (2014). Crumbs3 is essential for proper epithelial development and viability. Mol Cell Biol *34*, 43-56.

Whitney, D.S., Peterson, F.C., and Volkman, B.F. (2011). A conformational switch in the CRIB-PDZ module of Par-6. Structure *19*, 1711-1722.

Whitney, D.S., Peterson, F.C., Kittell, A.W., Egner, J.M., Prehoda, K.E., and Volkman, B.F. (2016). Binding of Crumbs to the Par-6 CRIB-PDZ Module Is Regulated by Cdc42. Biochemistry *55*, 1455-1461.

Wilson, D. (2009). Tissue. Lancet *374*, 109.

Wirtz-Peitz, F., Nishimura, T., and Knoblich, J.A. (2008). Linking cell cycle to asymmetric division: Aurora-A phosphorylates the Par complex to regulate Numb localization. Cell *135*, 161-173.

Wodarz, A., Hinz, U., Engelbert, M., and Knust, E. (1995). Expression of crumbs confers apical character on plasma membrane domains of ectodermal epithelia of *Drosophila*. Cell *82*, 67-76.

Wodarz, A., Ramrath, A., Grimm, A., and Knust, E. (2000). *Drosophila* atypical protein kinase C associates with Bazooka and controls polarity of epithelia and neuroblasts. J Cell Biol *150*, 1361-1374.

Wu, H., Feng, W., Chen, J., Chan, L.N., Huang, S., and Zhang, M. (2007). PDZ domains of Par-3 as potential phosphoinositide signaling integrators. Mol Cell *28*, 886-898.

Wu, J.Q., Guo, J.Y., Tang, W., Yang, C.S., Freel, C.D., Chen, C., Nairn, A.C., and Kornbluth, S. (2009). PP1-mediated dephosphorylation of phosphoproteins at mitotic exit is controlled by inhibitor-1 and PP1 phosphorylation. Nat Cell Biol *11*, 644-651.

Wu, V.M., Schulte, J., Hirschi, A., Tepass, U., and Beitel, G.J. (2004). Sinuous is a *Drosophila* claudin required for septate junction organization and epithelial tube size control. J Cell Biol *164*, 313-323.

Wu, X., Tanwar, P.S., and Raftery, L.A. (2008). Drosophila follicle cells: morphogenesis in an eggshell. Semin Cell Dev Biol *19*, 271-282.

Wu, Y., Jin, X., Harrison, O., Shapiro, L., Honig, B.H., and Ben-Shaul, A. (2010). Cooperativity between trans and cis interactions in cadherin-mediated junction formation. Proc Natl Acad Sci U S A *107*, 17592-17597.

Wu, Y., Kanchanawong, P., and Zaidel-Bar, R. (2015). Actin-delimited adhesion-independent clustering of E-cadherin forms the nanoscale building blocks of adherens junctions. Dev Cell *32*, 139-154.

Wu, Y.I., Frey, D., Lungu, O.I., Jaehrig, A., Schlichting, I., Kuhlman, B., and Hahn, K.M. (2009). A genetically encoded photoactivatable Rac controls the motility of living cells. Nature *461*, 104-108.

Xu, T., and Rubin, G.M. (1993). Analysis of genetic mosaics in developing and adult Drosophila tissues. Development *117*, 1223-1237.

Xue, B., Krishnamurthy, K., Allred, D.C., and Muthuswamy, S.K. (2013). Loss of Par3 promotes breast cancer metastasis by compromising cell-cell cohesion. Nat Cell Biol *15*, 189-200.

Yamanaka, T., Horikoshi, Y., Izumi, N., Suzuki, A., Mizuno, K., and Ohno, S. (2006). Lgl mediates apical domain disassembly by suppressing the PAR-3-aPKC-PAR-6 complex to orient apical membrane polarity. J Cell Sci *119*, 2107-2118.

Yamanaka, T., Horikoshi, Y., Sugiyama, Y., Ishiyama, C., Suzuki, A., Hirose, T., Iwamatsu, A., Shinohara, A., and Ohno, S. (2003). Mammalian Lgl forms a protein complex with PAR-6 and aPKC independently of PAR-3 to regulate epithelial cell polarity. Curr Biol *13*, 734-743.

Yamanaka, T., Horikoshi, Y., Suzuki, A., Sugiyama, Y., Kitamura, K., Maniwa, R., Nagai, Y., Yamashita, A., Hirose, T., Ishikawa, H.*, et al.* (2001). PAR-6 regulates aPKC activity in a novel way and mediates cell-cell contact-induced formation of the epithelial junctional complex. Genes Cells *6*, 721-731.

Yamashiro, S., Totsukawa, G., Yamakita, Y., Sasaki, Y., Madaule, P., Ishizaki, T., Narumiya, S., and Matsumura, F. (2003). Citron kinase, a Rho-dependent kinase, induces di-phosphorylation of regulatory light chain of myosin II. Mol Biol Cell *14*, 1745-1756.

Yamashita, K., Mizuno, K., Furukawa, K., Hirose, H., Sakurai, N., Masuda-Hirata, M., Amano, Y., Hirose, T., Suzuki, A., and Ohno, S. (2020). Phosphorylation and dephosphorylation of Ser852 and Ser889 control the clustering, localization and function of PAR3. J Cell Sci *133*.

Yamashita, Y.M., Yuan, H., Cheng, J., and Hunt, A.J. (2010). Polarity in stem cell division: asymmetric stem cell division in tissue homeostasis. Cold Spring Harb Perspect Biol *2*, a001313.

Yao, M., Qiu, W., Liu, R., Efremov, A.K., Cong, P., Seddiki, R., Payre, M., Lim, C.T., Ladoux, B., Mege, R.M.*, et al.* (2014). Force-dependent conformational switch of alpha-catenin controls vinculin binding. Nat Commun *5*, 4525.

Yap, A.S., Duszyc, K., and Viasnoff, V. (2018). Mechanosensing and Mechanotransduction at Cell-Cell Junctions. Cold Spring Harbor Perspectives in Biology *10*.

Yap, A.S., Gomez, G.A., and Parton, R.G. (2015). Adherens Junctions Revisualized: Organizing Cadherins as Nanoassemblies. Dev Cell *35*, 12-20.

Yoshida, C., and Takeichi, M. (1982). Teratocarcinoma cell adhesion: identification of a cell-surface protein involved in calcium-dependent cell aggregation. Cell *28*, 217-224.

Zaidel-Bar, R. (2013). Cadherin adhesome at a glance. J Cell Sci *126*, 373-378.

Zaidel-Bar, R., Zhenhuan, G., and Luxenburg, C. (2015). The contractome--a systems view of actomyosin contractility in non-muscle cells. J Cell Sci *128*, 2209-2217.

Zeitler, J., Hsu, C.P., Dionne, H., and Bilder, D. (2004). Domains controlling cell polarity and proliferation in the *Drosophila* tumor suppressor Scribble. J Cell Biol *167*, 1137-1146.

Zen, K., Yasui, K., Gen, Y., Dohi, O., Wakabayashi, N., Mitsufuji, S., Itoh, Y., Zen, Y., Nakanuma, Y., Taniwaki, M.*, et al.* (2009). Defective expression of polarity protein PAR-3 gene (PARD3) in esophageal squamous cell carcinoma. Oncogene *28*, 2910-2918.

Zenker, J., White, M.D., Gasnier, M., Alvarez, Y.D., Lim, H.Y.G., Bissiere, S., Biro, M., and Plachta, N. (2018). Expanding Actin Rings Zipper the Mouse Embryo for Blastocyst Formation. Cell *173*, 776-791 e717.

Zenker, J., White, M.D., Templin, R.M., Parton, R.G., Thorn-Seshold, O., Bissiere, S., and Plachta, N. (2017). A microtubule-organizing center directing intracellular transport in the early mouse embryo. Science *357*, 925-928.

Zhan, L., Rosenberg, A., Bergami, K.C., Yu, M., Xuan, Z., Jaffe, A.B., Allred, C., and Muthuswamy, S.K. (2008). Deregulation of scribble promotes mammary tumorigenesis and reveals a role for cell polarity in carcinoma. Cell *135*, 865-878.

Zhang, H., and Macara, I.G. (2008). The PAR-6 polarity protein regulates dendritic spine morphogenesis through p190 RhoGAP and the Rho GTPase. Dev Cell *14*, 216-226.

Zhang, H., Neimanis, S., Lopez-Garcia, L.A., Arencibia, J.M., Amon, S., Stroba, A., Zeuzem, S., Proschak, E., Stark, H., Bauer, A.F.*, et al.* (2014). Molecular mechanism of regulation of the atypical protein kinase C by N-terminal domains and an allosteric small compound. Chem Biol *21*, 754-765.

Zhang, K., and Cui, B. (2015). Optogenetic control of intracellular signaling pathways. Trends Biotechnol *33*, 92-100.

Zhang, Y., Wang, W., Chen, J., Zhang, K., Gao, F., Gao, B., Zhang, S., Dong, M., Besenbacher, F., Gong, W.*, et al.* (2013). Structural insights into the intrinsic self-assembly of Par-3 N-terminal domain. Structure *21*, 997-1006.

Zhou, X.X., Fan, L.Z., Li, P., Shen, K., and Lin, M.Z. (2017). Optical control of cell signaling by single-chain photoswitchable kinases. Science *355*, 836-842.

Zhu, J., Shang, Y., Wan, Q., Xia, Y., Chen, J., Du, Q., and Zhang, M. (2014). Phosphorylation-dependent interaction between tumor suppressors Dlg and Lgl. Cell Res *24*, 451-463.

Zihni, C., Mills, C., Matter, K., and Balda, M.S. (2016). Tight junctions: from simple barriers to multifunctional molecular gates. Nat Rev Mol Cell Biol *17*, 564-580.

Zihni, C., Munro, P.M., Elbediwy, A., Keep, N.H., Terry, S.J., Harris, J., Balda, M.S., and Matter, K. (2014). Dbl3 drives Cdc42 signaling at the apical margin to regulate junction position and apical differentiation. J Cell Biol *204*, 111-127.

Zihni, C., Vlassaks, E., Terry, S., Carlton, J., Leung, T.K.C., Olson, M., Pichaud, F., Balda, M.S., and Matter, K. (2017). An apical MRCK-driven morphogenetic pathway controls epithelial polarity. Nat Cell Biol *19*, 1049-1060.

APPENDIX

Contribution to additional publications 201

PP1-mediated dephosphorylation of Lgl controls apical-basal polarity 201

Lgl cortical dynamics are independent of binding to Dlg-Scrib complex but require Dlg dependent restriction of aPKC..... 203

Target-induced clustering activates Trim-Away of pathogens and proteins 206

References..... 207

CONTRIBUTION TO ADDITIONAL PUBLICATIONS

In the context of my thesis work, I also contributed to additional publications, which were not included in the main text. Here, I will contextualize these publications while giving an overview of my contribution.

PP1-mediated dephosphorylation of Lgl controls apical-basal polarity

Moreira S., Osswald M.*, Ventura G.*, Gonçalves M., Sunkel C.E., Morais-de-Sá E. (2019) *PP1-mediated dephosphorylation of Lgl controls apical-basal polarity.* Cell Reports 26(2):293-301. *Equal contributions.
doi.org/10.1016/j.celrep.2018.12.060

This publication is part of a PhD thesis entitled "Phosphoregulation of the *Drosophila* tumour suppressor Lgl during the cell cycle" by Sofia Moreira, submitted to Instituto de Ciências Biomédicas de Abel Salazar (ICBAS) at the University of Porto in 2019. It identifies PP1 phosphatase a major regulator of Lgl localization, which directly dephosphorylates Lgl to promote Lgl cortical recruitment. Experiments performed in the *Drosophila* follicular epithelium and *Drosophila S2* cells revealed that this event is particularly relevant to return cytoplasmic Lgl to the cortex during mitotic exit. This raised the question of whether Lgl accumulation at the cortex impacts the polarization of daughter cells.

As part of my thesis work, I developed an analysis pipeline to quantify the accumulation of polarity proteins at the new interface during mitotic exit. Live-imaging of the *Drosophila* follicular epithelium provides 3D stacks of epithelial cells dividing. Due to the round shape of *Drosophila* egg chambers and slight fluctuations in focal plane during image acquisition, the specific signal at the section of the membrane of interest is contained in multiple planes along the z-axis (Figure A1A bottom). We used previously published software – Epitools (Heller et al., 2016) – to extract fluorescence signal at the domain of interest and obtain a 2D projection with minimal noise (Figure A1A). Afterwards, fluorescence intensity at the interface of interest was quantified in FIJI (Schindelin et al., 2012) with a macro I wrote to extract signal intensity from manually tracked interfaces and normalize it to neighbour cell interfaces (Figure A1B).

Together with Sofia Moreira, I evaluated the impact of Lgl recruitment to the cortex on apical polarization at the new interface. I imaged apical determinant aPKC tagged with GFP expressed under control of its endogenous promoter. Acute loss of Lgl activity was triggered by shifting flies expressing a temperature-sensitive allele of Lgl – Lgl^{ts3} – to a

restrictive temperature. Sofia Moreira used the analysis pipeline described above to quantify the accumulation of aPKC at the new interface (data presented in Figure 4F of the respective publication). Impairment of Lgl with the temperature-sensitive allele decreased aPKC accumulation specifically at the apical domain of the new daughter cell interface.

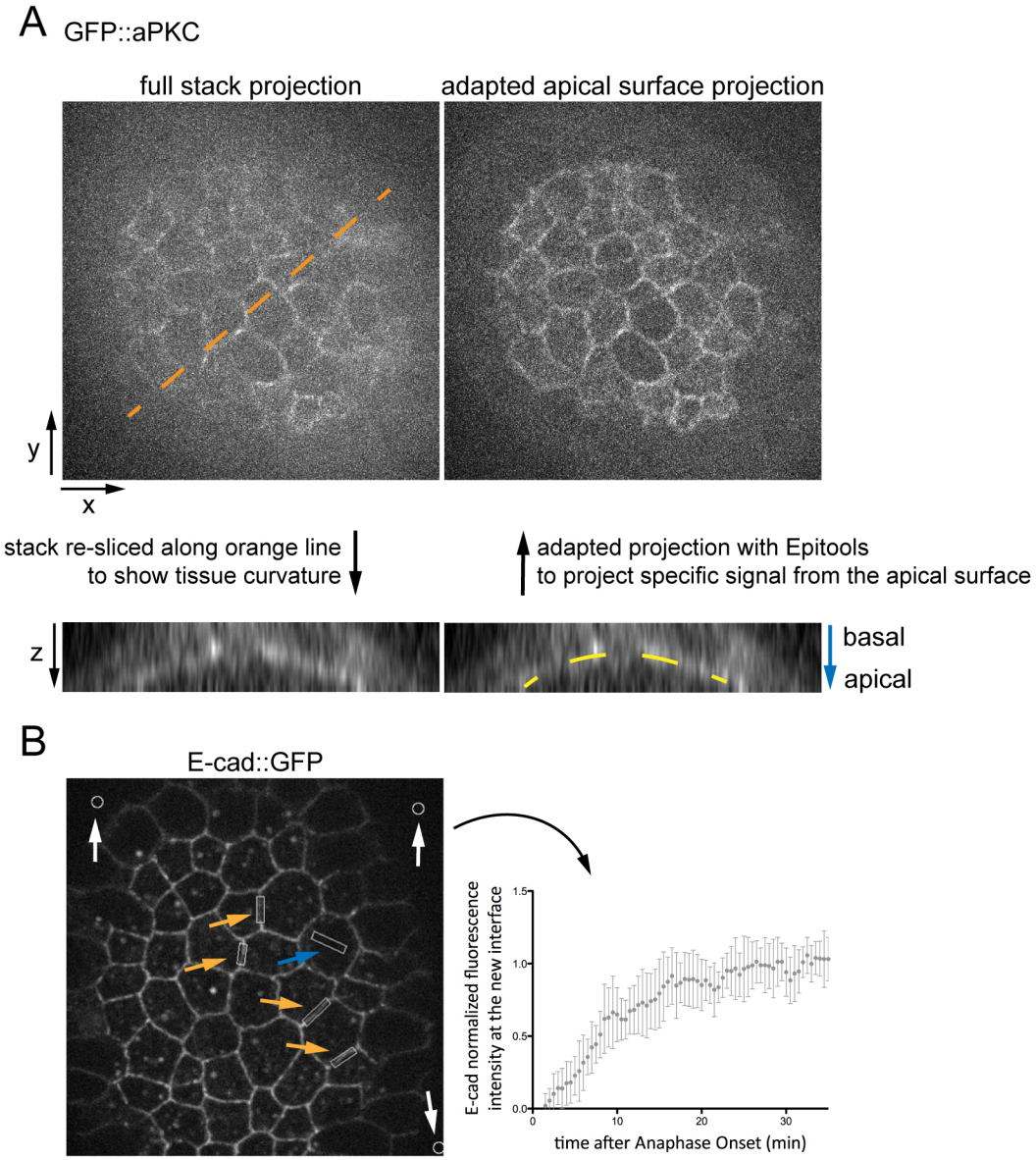


Figure A1. Quantification of protein accumulation at the new daughter cell interface in the follicular epithelium. (A) To quantify signal at the new cellular interface at mitotic exit, stacks at the surface of the egg chamber are collected. Representative frame for GFP::aPKC. Tissue curvature (visible in bottom images) prevents projection of individual planes for accurate fluorescent signal quantification at specific domains along the apical-basal axis. Adapted projection detects surface of interest (yellow line) and projects signal from this surface. Top images show the same GFP::aPKC z-stack projected with maximum signal intensity projection in FIJI or Epitools in Matlab. **(B)** New cellular interface (blue arrow), neighbour interfaces (orange arrow) and background (white arrow) are manually tracked as epithelial cells divide. Fluorescence intensity is extracted and analyzed with a FIJI

macro. Graph on the right shows example of analysis output for E-cad::GFP accumulation at the new interface formed between emerging daughter cells (n > 10 cells; graph shows mean ± SD).

Lgl cortical dynamics are independent of binding to Dlg-Scrib complex but require Dlg dependent restriction of aPKC

Ventura G., Moreira S., Barros-Carvalho A., Osswald M., Morais-de-Sá E. (2020) Lgl cortical dynamics are independent of binding to the Scrib-Dlg complex but require Dlg-dependent restriction of aPKC. Development 147:dev186593. doi.org/10.1242/dev.186593

This publication analyses the contribution of different factors to Lgl cortical localization through a combination of genetic, optogenetic and imaging approaches to evaluate protein localization, dynamic behaviour and protein interactions. It confirms membrane phospholipid PIP_2 as a major Lgl binding partner, responsible for localizing Lgl at the cortex. To evaluate its impact on Lgl dynamic behaviour, PIP_2 was depleted from the membrane through an optogenetic tool that controls 5'-phosphatase OCRL membrane recruitment and hereby triggers acute PIP_2 dephosphorylation (Guglielmi et al., 2015). During my initial work to implement optogenetic tools in the *Drosophila* follicular epithelium, I verified OCRL recruitment to the membrane and subsequent PIP_2 depletion and the effect on Lgl localization (data included in Figure 2C from the respective publication).

In this publication, aPKC is shown to be a major regulator of Lgl dynamic behaviour at the cortex through direct phosphorylation of Lgl, which decreases its ability to bind to membrane phospholipids (Dong et al., 2015). Interestingly, dynamic behaviour of Lgl at the basolateral cortex indicates that aPKC is not active in this domain and suggests that aPKC activity is restricted to apical side under normal circumstances. Restriction of aPKC is shown to depend on other basolateral determinants: Dlg and likely Scrib.

Together with André Carvalho, I tested the effect of LARIAT-mediated optogenetic clustering on different polarity proteins in the context of my thesis. LARIAT was expressed in the follicular epithelium and flies were exposed to blue light for two days to cluster endogenously tagged GFP-target proteins and verify if long-term clustering led to defects in epithelial architecture (Figure A2A). We verified that clustering of apical polarity determinants determinants aPKC and Par6 resulted in phenotypes consistent with loss of function (Kim et al., 2009; Wang and Riechmann, 2007), and which were further studied in chapter 5 of my thesis). Strikingly, clustering of basolateral polarity proteins, Lgl, Dlg and Scrib and Par1 (Figure A2C, D) significantly delocalized the targeted proteins, but was not sufficient to cause gross defects in epithelial organization, indicating that basolateral polarity

was not lost upon clustering (Bilder et al., 2000). However, clustering of basolateral proteins did promote their accumulation in clusters close to the apical membrane (Figure A2C, D). André Carvalho built on these initial observations to evaluate a potential interaction *in vivo* between different components of the Scrib module. We had previously shown that, in *Drosophila* S2 cells, LARIAT clustering could be used to test protein-protein interactions by evaluating the recruitment of potential interactors to clusters containing a GFP-tagged protein of interest (Chapter 4). Through a similar approach in the *Drosophila* follicular epithelium, André Carvalho detected an interaction between Dlg and Scrib, but not between either of these proteins and Lgl. Together, with data showing that Dlg is required for Lgl localization and dynamic behaviour only in the presence of aPKC, this indicated that contrary to previous models, Dlg (and Scrib) do not to regulate Lgl localization through direct interaction and formation of a complex, but rather by restricting aPKC activity.

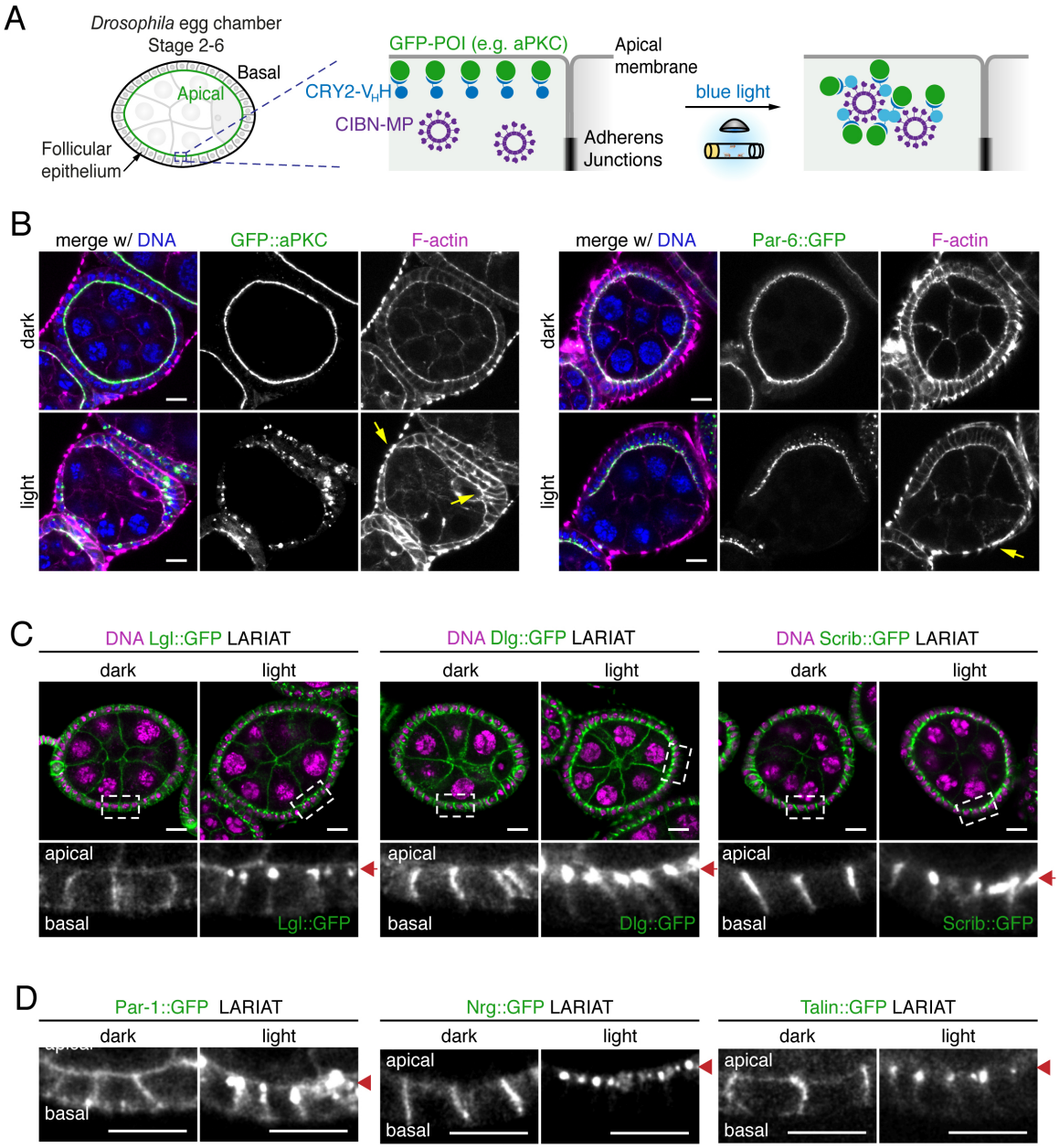


Figure A2. Optogenetic clustering of polarity proteins in the *Drosophila* follicular epithelium. (A) To test if LARIAT clustering can inactivate polarity proteins in the follicular epithelium, flies expressing LARIAT and endogenously tagged GFP-polarity proteins were exposed to blue light for 2 days to trigger clustering. LARIAT was expressed specifically in the follicular epithelium under regulation of *tj>Gal4* in all experiments except for Lgl panel in C and Par1 panel in D, where *GR1>Gal4* was used). Control flies were left in the dark for the same amount of time. After fixation, egg chambers were stained for DNA (DAPI, blue) and F-actin (Phalloidin, magenta). All polarity proteins clustered visibly. (B) GFP::aPKC and Par-6::GFP egg chambers had defects in epithelial organization consistent with loss of function: gaps in both and multilayering, as well, in GFP::aPKC egg chambers (yellow arrows). (C, D) Clustered basolateral polarity proteins accumulated in aggregates close to the apical surface (red arrowheads). No significant epithelial architecture defects were detected. Bottom panels in C show magnified boxed insets. D shows only representative images for the follicular epithelium. Scale bars: 10 μm.

Target-induced clustering activates Trim-Away of pathogens and proteins

Zeng J., Santos A.F., Mukadam A., Osswald M., Luptak J., Jacques D., Dickson C., Renner N., Johnson C., Vaysburd M., McEwan W. A., Morais-de-Sá E., Clift D., James L.C. (2021) Target-induced clustering activates Trim-Away of pathogens and proteins. Nat Struct Mol Biol. 28(3):278-289. doi.org/10.1038/s41594-021-00560-2

Our experiments to inactivate polarity proteins with LARIAT in the follicular epithelium confirmed that LARIAT is valuable to target apical polarity determinants aPKC and Par6 (Figure A2; Chapter 5). Furthermore, it was able to aggregate and delocalize several polarized proteins in the follicular epithelium, which proved to be useful to study protein interactions. However, LARIAT clustering was not sufficient to inactivate basolateral polarity determinants as evaluated by the absence of gross epithelial architecture defects (Figure A2C). An alternative strategy to trigger acute loss of function was needed, which led us to collaborate with Dean Clift and Leo James to develop OptoTrim.

Zeng *et al.,* addresses how tripartite motif-containing 21 (Trim21), an E3 ubiquin ligase, is activated upon target engagement and capitalizes on this information to expand the applications of Trim21 as a tool for acute protein degradation. Trim21 is a cytosolic protein that functions as part of the immune response in vertebrates (Ozato et al., 2008). Trim21 has a C-terminal domain capable of binding antibodies. Through this domain, Trim21 recognizes intracellular proteins or viruses coated with antibodies and targets them for destruction by the proteasome (Foss et al., 2019). Importantly for my purpose, Trim21 had recently been demonstrated to trigger target protein degradation with a half-life of 16.7 min and cause acute loss of function phenotypes (Clift et al., 2017). Injection of antibodies against specific endogenous proteins was shown to be sufficient to direct Trim21 against them in mammalian cultured cells and mouse oocytes. Thus, Trim21 was proposed as a new method for acute and targeted protein degradation named Trim-Away (Clift et al., 2017). Interestingly, time-lapse images in Clift *et al.,* 2017 showed considerable aggregation of Trim21-mCherry upon antibody injection, even when targeting cytosolic GFP. This suggested that Trim21 activity could depend on aggregation. Consequently, in collaboration with Dean Clift and Leo James, we decided to test if LARIAT could be used to cluster Trim21 and activate its ability to degrade proteins. As a proof of concept, I fused Trim21 directly to RFP-CRY2 (RFP-CRY2-Trim21) and co-transfected this new plasmid with CIBN-MP in *Drosophila* S2 cells to test for protein degradation live. Imaging with the 488nm laser triggered clustering of CRY2-Trim21 and subsequent decrease in RFP fluorescence intensity. This result indicated that clustering could trigger Trim21 degradation

and suggested that optogenetic control of Trim21 (OptoTrim) could be used as a tool for acute protein degradation with light. Filipa Santos then proceeded to characterize the kinetics of protein degradation to identify optimal OptoTrim variants, where Trim21 was combined with CRY2-based clustering modules through fusion to different protein domains. Furthermore, Filipa Santos developed CRY2-TRIM21 fusions with a GFP nanobody to recruit GFP-tagged proteins and validate that OptoTrim could target other proteins for degradation. This analysis also contributed to address how antibody engagement may trigger Trim21 activity and extended the potential of Trim-Away through combination with optogenetics.

References

Bilder, D., Li, M., and Perrimon, N. (2000). Cooperative regulation of cell polarity and growth by Drosophila tumor suppressors. Science 289, 113-116.

Clift, D., McEwan, W.A., Labzin, L.I., Konieczny, V., Mogessie, B., James, L.C., and Schuh, M. (2017). A Method for the Acute and Rapid Degradation of Endogenous Proteins. Cell 171, 1692-1706 e1618.

Dong, W., Zhang, X., Liu, W., Chen, Y.-j., Huang, J., Austin, E., Celotto, A.M., Jiang, W.Z., Palladino, M.J., Jiang, Y., et al. (2015). A conserved polybasic domain mediates plasma membrane targeting of Lgl and its regulation by hypoxia. J Cell Biol 211, 273-286.

Foss, S., Bottermann, M., Jonsson, A., Sandlie, I., James, L.C., and Andersen, J.T. (2019). TRIM21-From Intracellular Immunity to Therapy. Front Immunol 10, 2049.

Guglielmi, G., Barry, J.D., Huber, W., and De Renzis, S. (2015). An Optogenetic Method to Modulate Cell Contractility during Tissue Morphogenesis. Dev Cell 35, 646-660.

Heller, D., Hoppe, A., Restrepo, S., Gatti, L., Tournier, A.L., Tapon, N., Basler, K., and Mao, Y. (2016). EpiTools: An Open-Source Image Analysis Toolkit for Quantifying Epithelial Growth Dynamics. Dev Cell 36, 103-116.

Kim, S., Gailite, I., Moussian, B., Luschnig, S., Goette, M., Fricke, K., Honemann-Capito, M., Grubmuller, H., and Wodarz, A. (2009). Kinase-activity-independent functions of atypical protein kinase C in Drosophila. J Cell Sci 122, 3759-3771.

Ozato, K., Shin, D.M., Chang, T.H., and Morse, H.C., 3rd (2008). TRIM family proteins and their emerging roles in innate immunity. Nat Rev Immunol 8, 849-860.

Schindelin, J., Arganda-Carreras, I., Frise, E., Kaynig, V., Longair, M., Pietzsch, T., Preibisch, S., Rueden, C., Saalfeld, S., Schmid, B., et al. (2012). Fiji: an open-source platform for biological-image analysis. Nat Methods 9, 676-682.

Wang, Y., and Riechmann, V. (2007). The role of the actomyosin cytoskeleton in coordination of tissue growth during Drosophila oogenesis. Curr Biol 17, 1349-1355.